Optimised bacterial production and characterisation of natural antimicrobial peptides with potential application in agriculture

by

Johan Arnold Vosloo

Dissertation approved for the degree

Doctor of Philosophy (Biochemistry)

in the

Faculty of Science

at the

University of Stellenbosch

Promoter: Prof. Marina Rautenbach

Co-promoter: Prof. Jacky L. Snoep

Department of Biochemistry

University of Stellenbosch

March 2016

Declaration

I, ***Johan Arnold Vosloo*** hereby declare that the entirety of the work contained in this dissertation is my own original work, unless otherwise stated and acknowledged. I have not previously in its entirety or in part submitted it for obtaining any qualification at any university.

…… ……

Johan Arnold Vosloo Date

Summary

The use of chemical control agents to control microbial spoilage in agriculture has been compromised with the emergence of increasing microbial resistance, together with a shift in regulation toward pesticides with a lower intrinsic toxicity and lower environmental impact. This has instigated the search for alternate so-called green-biocides with a reduced environmental impact together with alternate modes of action to conventional chemical control agents to combat the trend of resistance development.

The antimicrobial peptides of focus in study may offer a potential solution. The tyrocidines and their analogues (Trcs) are a group of cyclodecapeptides [cyclo(D-Phe^{1}-L-Pro^{2}-L-(Phe^{3}/Trp^{3})-D-(Phe^{4}/Trp^{4})-L-Asn^{5}-L-Gln^{6}-L-(Tyr^{7}/Phe^{7}/Trp^{7})-L-Val^{8}-L-Orn^{9}-L-Leu^{10}] produced by the soil bacterium *Bacillus aneurinolyticus*. These cyclodecapeptides have shown potent antimicrobial activity toward a broad range of pathogens which affect the agricultural industries including Gram-positive bacteria as well as fungi. In addition to a rapid membrane lytic activity, they have alternate cellular targets that reduces the likelihood of resistance development. Increased antimicrobial activity toward different targets is achieved by different analogues which contain a variable primary structure mainly due to variation in aromatic amino acid content at residues 3, 4 and 7 in the cyclodecapeptides.

The first objective of this study was to elucidate the optimal conditions that would allow for the large scale production of target-specific subsets of these cyclodecapeptides that would enable their utilisation as green-biocides in the agricultural industry. Supplementation of defined ratios of Phe/Trp in the growth media shifted the cyclodecapeptide production profile to defined subsets of different analogues, as defined by changes in aromatic amino acids in their primary structures. Increased natural cyclodecapeptide production was achieved in excess of one gram per litre in flask cultures. Purification of culture extracts, either by manipulation of solubility of the cyclodecapeptides in solution or *via* column chromatography, achieved a peptide complex purity of >75% to utilise in agricultural applications. Further purification via high performance liquid chromatography yielded single peptides with purity >90%. The production and purification methodologies are of such a nature as to allow for future upscaling.

Investigation of the relationship between the structure and oligomerisation of the six major cyclodecapeptides produced in the different subsets under various Phe/Trp supplemented conditions revealed a relationship between increased hydrophobicity and the tendency to form dimeric structures, the proposed membrane active units. Increased higher order structure formation, however,

was dependent on intermediate hydrophobicity and dimerization. This coincided with structures of the tyrocidine A (Phe^3, Phe^4 and Tyr^7) and tyrocidine B (Trp^3, Phe^4 and Tyr^7) analogues. Furthermore, glucose disrupted higher order structures of analogues containing Phe^4 together with Tyr^7 or Phe^7. These properties correlated with increased antifungal activity toward *Aspergillus fumigatus*. Antifungal activity was found to be related to a balance in hydrophobicity and higher structure formation where interaction with hexose moieties in the target cell wall may play a role in the mode of action and possible pore formation in the target membrane. In contrast antibacterial activity toward *Bacillus subtilis* was found to be independent of dimerization and the variable characteristics of the different cyclodecapeptide analogues. Antibacterial activity was possibly more dependent on the conserved pentapeptide (VOLfP), as near equivalent activity was observed by 5 of the 6 analogues. Co-produced cyclodecapeptide pairs showed a propensity of forming heterodimers that mostly lead to additive antimicrobial activity. However, overt antagonism was observed in peptide combinations containing tryptocidines (Trp^7) which are not naturally produced in increased quantities, while synergism was observed in for the naturally produced combinations of TrcA:PhcA (Phe^3; Phe^4) and TrcA:TrcB (Phe^3; Phe^4, Tyr^7 and Trp^3; Phe^4, Tyr^7) toward the fungal target, and TrcA:TrcB and TrcB:TrcC (Phe^3; Trp^4, Tyr^7 and Trp^3; Trp^4, Tyr^7) toward the bacterial target. Characteristics of intermediate hydrophobicity and dimerization in peptide pairs again resulted in increased activity toward the fungal target. These peptide mixtures, specifically TrcA and TrcB, are naturally produced in high quantities, indicating an evolutionary advantage to the producer strain.

Formulation of the cyclodecapeptide mixtures in ethanol or dimethylformamide (DMF) revealed changes in oligomerisation, with reduced dimerization in ethanol relative to DMF. Furthermore, glucose and sucrose were observed to suppress antimicrobial activity when dissolved in ethanol, however, this was largely relieved when dissolved in DMF. The interaction of the cyclodecapeptides with sugar like moieties depended on a balance between the active conformation and target cell properties. Formulations of the natural peptide extract (Te) in 50% sucrose and DMF were found to be non-toxic towards toward adult bees and in field trials the Te-treated bees showed increased survival.

These cyclodecapeptides offer an alternate solution to conventional chemical agents to treat pathogens in the agricultural and food industries. Optimized formulation of these cyclodecapeptides would possibly enhance their potential. In order to harvest the potential of these cyclodecapeptides, a concerted effort must be made in future investigations to gain knowledge on their mode of action, toxicity and behaviour as mixtures.

Opsomming

Die gebruik van chemiese beheermiddels in landbou om mikrobiese bederf te beheer is onder druk deur toenemende mikrobiese weerstand en regulering van biosiedes ten gunste van dié met 'n laer intrinsieke toksisiteit en omgewingsimpak. Dit het die soektog na alternatiewe biosiede met 'n verminderde omgewingsimpak, naamlik die sogenaamde groen biosiede met alternatiewe werkingsmeganismes , as konvensionele chemiese biosiede, aangehelp om spesifiek om die tendens van toenemende weerstand te stuit.

Die antimikrobiese peptiede wat die fokus is hierdie studie kan 'n potensiële oplossing bied. Die tirosidiene en hul analoë is 'n groep sikloddekapeptiede [cyclo(D-Phe^{1}-L-Pro^{2}-L-(Phe^{3}/Trp^{3})-D-(Phe^{4}/Trp^{4})-L-Asn^{5}-L-Gln^{6}-L-(Tyr^{7}/Phe^{7}/Trp^{7})-L-Val^{8}-L-Orn^{9}-L-Leu^{10}] wat vervaardig word deur die grondbakterium *Bacillus aneurinolyticus*. Hierdie siklodekapeptiede het 'n kragtige antimikrobiese aktiwiteit teenoor 'n wye verskeidenheid van patogene wat 'n invloed het in die landbousektor het, spesifiek Gram-positiewe bakterieë en swamme. Benewens 'n vinnige litiese membraan aktiwiteit, het hulle alternatiewe sellulêre teikens wat die moontlikheid van weerstand verminder. Verhoogde antimikrobiese aktiwiteit teenoor spesifieke teikens deur die analoë met verskillende primêre strukture is hoofsaaklik te wyte aan variasie in aromatiese aminosuur identiteite van residue 3, 4 en 7 in die siklodekapeptiedes.

Die eerste doel van die studie was om die optimale kondisies te vind vir grootskaalse produksie van teiken-spesifieke subgroepe van hierdie siklodekapeptiede wat hul benutting as groen biosiede in die landboubedryf moontlik kon maak. Die byvoeging van 'n gedefinieerde ratio van Phe/Trp in die groei media verskuif die siklodekapeptiede produksieprofiel na gedefinieerde subgroepe van verskillende analoë, soos gedefinieer deur die veranderinge in aromatiese aminosure in residu-posisies 3, 4 en 7. Verhoogde natuurlike siklodekapeptiedproduksie van groter as een gram per liter in fles kulture kon bereik word. Suiwering van kultuurekstrakte, hetsy deur manipulasie van die siklodekapeptied oplosbaarheid of deur middel van kolomchromatografie, het 'n ekstrak suiwerheid van >75% peptiedkompleks gelewer vir aanwending in die landbousektor. Verdere suiwering via hoë doeltreffrendheid vloeistofchromatofrafie het enkel peptiede met >90% suiwerheid gelewer. Die produksie- en suiweringmetodes was ideaal vir toekomstige opskallering

Die ondersoek van ses verteenwoordigende peptiede, uit die verskillende subgroepe wat met verskillende Phe/Trp media aanvullings geproduseer is, het 'n verband tussen verhoogde hidrofobisiteit en die neiging om dimeriese strukture, die voorgestelde membraanaktiewe eenhede, onthul. Die verhoogde vorming van hoër orde dimeriese strukture was egter afhanklik van

intermediêre hidrofobisiteit, soos die van tirosidien A (Phe^3, Phe^4 en Tyr^7) en tirosidien B (Trp^3, Phe^4 en Tyr^7). Verder is gevind dat glukose hoër orde strukture van analoë met Phe^4 tesame met Tyr^7 of Phe^7 ontwrig. Hierdie eienskappe het met verhoogde antifungiese aktiwiteit teenoor *Aspergillus fumigatus* gekorreleer. Antifungiese aktiwiteit hou verband met 'n balans in hidrofobisiteit en die vorming van hoër strukture waar interaksie met heksoses in die teikenselwand 'n rol kan speel in die werkingsmeganisme en moontlike porieë wat vorm in die teikenmembraan. In teenstelling was die antibakteriese aktiwiteit met die *Bacillus subtilis* teiken onafhanklik van dimersasie en die veranderlike eienskappe van die verskillende sikliese dekapeptied analoë. Dit is moontlik afhanklik van die gekonserveerde pentapeptied (VOLfP), aangesien soortgelyke aktiwiteit gevind is vir vyf van die ses analoë. Die twee hoof siklodekapeptiede wat saam geproduseer word in subgroepe het geneig om heterodimere te vorm wat vir meeste peptiedpare tot additiewe antimikrobiese aktiwiteit. Daar is egter effense antagonisme waargeneem vir peptiedkombinasies wat triptosidiene (Trp^7) bevat wat nie natuurlik geproduseer word nie. Sinergisme is gevind vir die natuurlik geproduseerde peptiedkombinasies van TrcA:PhcA (Phe^3; Phe^4) en TrcA:TrcB (Phe^3; Phe^4, Tyr^7 en Trp^3; Phe^4, Tyr^7) teenoor die swam teiken, en TrcA:TrcB en TrcB:TrcC (Phe^3; Trp^4, Tyr^7 en Trp^3; Trp^4, Tyr^7) teenoor die bakteriële teiken. Die intermediêre hidrofobisiteit en dimerisasie is weer gevind vir aktiewe peptiedpare met die swam as teiken. Hierdie peptiedmengsels, spesifiek TrcA en TrcB word natuurlik geproduseer in groot hoeveelhede, wat dui op 'n evolusionêre voordeel vir die bakteriële produseerder.

Formulering van die peptiedmengsels in etanol of dimetielformamied (DMF) het verskille in oligomerisasie getoon, met minder dimeriese peptiedspesies in etanol as in DMF. Verder is gevind dat glukose en sukrose antimikrobiese aktiwiteit onderdruk met etanol in peptiedpreparaat, terwyl DMF in die peptiedoplossing die aktiwiteit hertel het. Die interaksie van die siklodekapeptiede met heksoses blyk afhanklik te wees van die balans tussen die aktiewe struktuur en teikensel eienskappe. Formulering van die natuurlike peptied ekstrak (Te) in 50% sukrose en DMF is gevind om nie giftig teenoor volwassene bye te wees nie en in veldproewe het die Te-behandelde bye tot verhoogde oorlewing gelei in sommige korwe.

Die siklodekapeptiede bied 'n natuurvriendelike alternatiewe oplossing vir konvensionele chemiese middels om bakteriële en swam patogene in die landbou- en voedselbedryf te behandel. Geoptimaliseerde formulering van hierdie siklodekapeptiede sal hul potensiaal verder kan uitbou. Ten einde die besondere potensiaal van die siklodekapeptiede ten volle te ontwikkel, moet 'n daadwerklike poging aangewend word in toekomstige ondersoeke om kennis te verkry oor hul manier van werking, toksisiteit, stabiliteit en gedrag as mengsels.

"*Carpe diem quam minimum credula postero*"

Seize the day, put very little trust in tomorrow

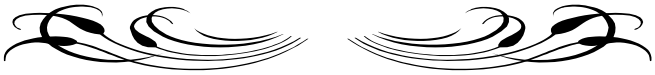

Acknowledgements

I would like to express my thanks and gratitude to the following people and institutions:

- Prof. Marina Rautenbach, my MSc supervisor and PhD promoter for the constant, support, motivation and guidance throughout my post-graduate studies, you have been my mentor and academic role model, this journey would have been a lot harder without you;
- Prof. Jacky Snoep for construction of the novel computational model for the tyrocidine production and invaluable assistance in preparation of my thesis;
- Ms. Gertrude Gerstner and Ms. Helba Bredell, BIOPEP Peptide Group laboratory managers and the BIOPEP colleagues for their support and companionship over the last few years;
- Dr. Marietjie Stander and staff of the Central Analytical Facilities (CAF) at Stellenbosch University for technical assistance;
- My parents for their love and all they have done for my brothers and I, making many scarifies to offer us the best opportunities in life that they possibly could;
- My brothers who are still with me and he who is no longer; for their love and experiences we have shared which have made me the person I am today;
- My granny Pat Vosloo, without your love and guidance as a child I may never have come to this academic achievement in my life;
- My aunt Rene Vosloo for always being there and lovingly supporting me;
- The Baker family, especially Vicky Baker for all the love and support over the last 10 years;
- My partner in life and mother of my child, Andrea Baker for all the years of loving support in all the good times as well as the hard, motivating me to always carry on;
- The National Research Foundation (NRF), Ernst & Ethel Eriksen trust and the BIOPEP Peptide Fund for funding which not only made it possible for me to complete this degree but also to grow as a scientist by attending international conferences.

Table of Contents

List of Abbreviations and Acronyms xii
PREFACE XVIII
Outputs of PhD study XX

CHAPTER 1 LITERATURE REVIEW: TYROCIDINES, ANTIMICROBIAL PEPTIDES WITH POTENTIAL APPLICATIONS IN AGRICULTURE AND INDUSTRY

1. 1 Introduction 1.1
1.2 Antimicrobial peptides 1.2
1.3 The tyrocidines 1.6
1.3.2 Structure of the tyrocidines 1.7
1.3.3 Non-ribosomal production of the tyrocidines 1.8
1.3.4 Tyrocidine production and control 1.12
1.3.5 Influence of the linear gramicidins in the tyrothricin complex 1.15
1.3.6 Toxicity of the tyrocidines in the tyrothricin complex 1.17
1.3.7 Tyrocidine targets and mode of action 1.18
1.3.8 Tyrocidine structure-activity relationships 1.19
1.4 References 1.22

CHAPTER 2 MANIPULATION OF THE TYROTHRICIN PRODUCTION PROFILE OF BACILLUS ANEURINOLYTICUS

VOSLOO JA, STANDER MA, LEUSSA A N-N, SPATHELF BM, RAUTENBACH M (2013) *Manipulation of the tyrothricin production profile of* Bacillus aneurinolyticus, Microbiology 159, 2200–2211; Supplementary data, 1-8

CHAPTER 3 A MODEL FOR INCORPORATION OF AROMATIC AMINO ACIDS IN THE THREE VARIABLE RESIDUE POSITIONS FOR THE DIFFERENT TYROCIDINES AND ANALOGUES

3.1 Introduction 3.1
3.2 Materials 3.3
3.3 Methods 3.3
3.3.1 Pre-culturing of the tyrothricin producer strain 3.3
3.3.2 Medium throughput deep well production of tyrothricin 3.4
3.3.3 ESMS and UPLC-MS analysis of tyrothricin extracts 3.4
3.3.4 Mathematical model analysis of the shift in the tyrocidine production profile 3.5
3.4 Results 3.7
3.3.1 Phe supplementation 3.7
3.4.2 Trp supplementation 3.8
3.4.3 Supplementation with a combination of Phe and Trp 3.8
3.4.4 Computational modelling of variability in residues in positions 3 and 4 ..... 3.10
3.4.5 Computational modelling of variability in residues in position 7 ..... 3.10
3.4.6 Direct comparison of variability in residues in position 3, 4 and 7 ..... 3.14
3.5 Discussion 3.14
3.6 Conclusions 3.18
3.7 Refrerences 3.18

CHAPTER 4 PRODUCTION AND PURIFICATION OF THE TYROCIDINES AND ANALOGUES

4.1 Introduction 4.1
4.2 Materials 4.3
4.3 Methods 4.4
4.3.1 Culturing of organisms 4.4
4.3.2 Selection of high tyrothricin producers 4.5
4.3.3 Tyrothricin production and extraction 4.5
4.3.4 Amino acid manipulated productions 4.6

4.3.5 Tyrothricin purification *4.7*
4.3.6 Antimicrobial activity assays *4.7*
4.3.7 Semi-preparative HPLC of extracts to purify single peptides *4.8*
4.3.8 ESMS and UPLC-MS analysis of tyrothricin extracts and purified peptides *4.9*
4.4 RESULTS AND DISCUSSION 4.10
4.4.1 Optimisation of tyrothricin production in different media compositions *4.10*
4.4.2 Evaluation of the growth and tyrothricin production in Media C *4.12*
4.4.3 Purification of the crude tyrothricin extract *4.18*
4.4.5 Characterization of Te for use in plant and bee studies *4.25*
4.4.6 Amino acid manipulated productions *4.28*
4.4.7 Purification and analyses of single peptides *4.31*
4.5 CONCLUSIONS 4.37
4.6 REFERENCES 4.38

CHAPTER 5 STRUCTURE AND OLIGOMERISATION RELATIONSHIPS OF THE SIX MAJOR CYCLODECAPEPTIDES PURIFIED FROM *BACILLUS ANEURINOLYTICUS* CULTURES

5.1 INTRODUCTION 5.1
5.2 MATERIALS AND METHODS 5.5
5.2.1 Materials and Reagents *5.5*
5.2.2 Detection of oligomerisation with ESMS *5.5*
5.2.3 Optical spectrometric analysis of the influence of different solvent environments on peptide structure *5.6*
5.2.4 Curve fitting and data analysis *5.6*
5.3 RESULTS AND DISCUSSION 5.7
5.3.1 Analysis of the cyclodecapeptides oligomerisation in aqueous and hydrophobic environments *5.7*
5.3.2 Influence of glucose on the cyclodecapeptides *5.21*
5.3 CONCLUSIONS 5.27
5.4 REFERENCES 5.28

CHAPTER 6 OLIGOMERISATION-ACTIVITY RELATIONSHIPS OF THE SINGLE AND COMBINATIONS OF THE SIX MAJOR CYCLODECAPEPTIDES PURIFIED FROM *BACILLUS ANEURINOLYTICUS* CULTURES

6.1 INTRODUCTION 6.1
6.2 MATERIALS AND METHODS 6.2
6.2.1 Materials and Reagents *6.2*
6.2.2 Detection of oligomerisation with ESMS *6.2*
6.2.3 Preparation of peptides for antimicrobial activity assays *6.3*
6.2.4 Antifungal activity assays *6.3*
6.2.5 Antibacterial activity assays *6.4*
6.2.6 Data analysis *6.4*
6.3 RESULTS 6.5
6.3.1 Formation of homo- and hetero-oligomers by the cyclodecapeptides *6.5*
6.3.2 Variability in antimicrobial activity of different cyclodecapeptides *6.7*
6.3.3 Activity of peptide mixtures *6.11*
6.4 DISCUSSION 6.17
6.5 CONCLUSION 6.20
6.5 REFERENCES 6.20

CHAPTER 7 FORMULATION OF TYROTHRICIN EXTRACTS AND *IN VIVO* TOXICITY TESTING TOWARD HONEY BEES

7. 1 INTRODUCTION 7.1
7. 2 MATERIALS AND METHODS 7.3
7.2.1 Materials and Reagents *7.3*
7.2.2 Preparation of peptide formulations for antimicrobial activity assays *7.5*
7.2.3 Antifungal activity assays toward Aspergillus fumigatus *7.5*
7.2.4 Antibacterial activity assays toward Bacillus subtilis *7.6*
7.2.5 Influence of different solvents and sugars on aggregation *7.6*

7.2.7 Toxicity toward insect cell lines *7.7*
7.2.8 Acute oral toxicity testing of tyrothricin toward adult honeybees *7.8*
7.2.9 Delayed toxicity testing and survival in hives after tyrothricin exposure *7.9*
7.2.10 Antibacterial activity assays toward foulbrood associated pathogens. *7.10*
7.2.11 Toxicity of tyrothricin peptides toward bee larvae *7.10*
7.2.12 Curing assays of Paenibacillus larvae infected bee larvae *7.11*
7.2.13 Antibacterial activity toward gut microbiota of honey bee larvae *7.12*
7.2.14 Data analysis *7.12*
7.3 RESULTS AND DISCUSSION 7.13
7.3.1 Influence of peptide formulation on aggregation *7.13*
7.3.2 Toxicity toward insect cell lines *7.17*
7.3.3 Antimicrobial activity of peptide formulations *7.18*
7.3.4 In vivo toxicity of the tyrothricin extract toward adult honey bees *7.22*
7.3.5 Survival in hives after tyrothricin exposure *7.24*
7.3.6 Toxicity testing of tyrothricin extract toward bee larvae *7.25*
7.3.7 Activity of peptide formulations toward honey bee pathogens causing foulbrood *7.26*
7.3.8 Assessment of the potential of tyrothricin to treat infected bee larvae *7.27*
7.3.9 Activity of tyrothricin extracts toward beneficial gut microbiota of honey bees and larvae *7.29*
7.4 CONCLUSIONS 7.30
7.5 REFERENCES 7.32

CHAPTER 8 CONCLUSIONS AND RECOMMENDATIONS FOR FUTURE STUDIES

8.1 INTRODUCTION 8.1
8.2 SUMMARY OF FINDINGS AND FUTURE WORK 8.1
8.2.1 Manipulation of the tyrothricin production profile *8.1*
8.2.2 Production and purification of the tyrocidines and analogues *8.3*
8.2.3 Structure and oligomerisation relationships of the six major cyclodecapeptides *8.4*
8.2.4 Oligomerisation-activity relationships of the six major cyclodecapeptides *8.6*
8.2.5 Formulation of tyrothricin extracts and in vivo toxicity testing toward honey bees *8.8*
8.3 LAST WORD 8.9
8.4 REFERENCES 8.9

List of Abbreviations and Acronyms

$[M+H]^+$	singly charged molecular ion
$[M+2H]^{2+}$	doubly charged molecular ion
aa	amino acid
A	adenylation domain
A	alanine
A	tyrocidine A
ACN	acetonitrile
Ala	alanine
AMP	adenosine monophosphate
A. mellifera	*Apis mellifera*
Arg	arginine
Asn	asparagine
ATCC	American type culture collection
ATP	adenosine triphosphate
a.u	arbitrary unit
B	tyrocidine B
B. aneurinolyticus	*Bacillus aneurinolyticus*
BHI	brain heart infusion
B. pumilus	*Bacillus pumilus*
B. subtilis	*Bacillus subtilis*
°C	degrees Celsius
C	condensation domain
C	tyrocidine C
C. albicans	*Candida albicans*
C. elegans	*Caenorhabditis elegans*
C. sepdonicum	*Corynebacterium sepdonicum*
CD	circular dichroism
CFU	colony forming units
CID	collision induced disassociation
cm	centimetre
Contam	contamination

CV	column volume
Cys	cystine
DiM	dimethoate
DLS	dynamic light scattering
DMEM	Dulbecco's modified Eagle's medium
DMF	N,N-Dimethylformamide
dO_2	dissolved oxygen concentration
DSM	German Collection of Microorganisms and Cell Cultures
E	epimerization domain
E. coli	*Escherichia coli*
EDTA	ethylenediaminetetraacetic acid
E. faecalis	*Enterococcus faecalis*
EtOH	ethanol
ESMS	electrospray mass spectrometry
f	D-phenylalanine
F	phenylalanine
fA	phenycidine A
Ff	tyrocidine A analogues
FIC	fractional inhibition concentration
FICI	fractional inhibition concentration index
FS	fluorescence spectroscopy
G	glycine
Glc	glucose
Gln	glutamine
Gly	glycine
Grm/s	linear gramicidin/s
GS	gramicidin S
GTP	Guanosine triphosphate
HCl	Hydrochloric acid
HPLC	high performance liquid chromatography
I	isoleucine
IC_{50}	peptide concentration leading to 50 % microbial growth inhibition
IC_{max}	peptide concentration leading to maximal microbial growth inhibition

Ile	isoleucine
IGA	isoleucine gramicidin A
IGB	isoleucine gramicidin B
IGC	isoleucine gramicidin C
K	lysine
K_2SO_4	potassium sulfate
K_M	enzyme affinity
l	D-leucine
L	leucine
LB	Luria Bertani
LBA	Luria Bertani agar
LC	liquid chromatography
LC_{50}	peptide concentration leading to 50% cytotoxicity
LCMS	liquid chromatography mass spectrometry
Leu	leucine
LMG	Belgian Co-ordinated Collection of Microorganisms
L. monocytogenes	*Listeria monocytogenes*
Lys	lysine
m/m	mass/mass
mM	millimolar
M	molar
M. luteus	*Micrococcus luteus*
MALDI	matrix-assisted laser desorption/ionization
MBC	minimal effective bactericidal concentration
mg	milligram
MIC	minimum inhibitory concentration
mL	millilitre
MOA	mode of action
M. plutonius	*Melissococcus plutonius*
M_r	molecular mass
MS	mass spectrometry
m/z	mass over charge ratio
NaCl	sodium chloride

N	Asparagine
n	extent of enzyme cooperativity
NCTC	national collection of type cultures
NDAs	non-disclosure agreements
ND	not determined
nm	nanometer
NMR	nuclear magnetic resonance
NRP	non-ribosomal peptides
ns	not significant
OD	optical density
Orn	ornithine
O	ornithine
P	Proline
P. alvei	*Paenibacillus alvei*
PBS	phosphate buffered saline
PCP	peptidyl carrier protein
PCR	polymerase chain reaction
PDA	potato dextrose agar plates
PDB	potato dextrose broth plates
P. falciparum	*Plasmodium falciparum*
PhcA	phenycidine A
$PhcA_1$	phenycidine A_1
PhcB	phenycidine B
PhcC	phenycidine C
Phc(s)	phenycidine(s)
Phe	phenylalanine
PI	phosphatidylinositol
PITC	phenylisothiocyanate
P. larvae	*Paenibacillus larvae*
PM	purification methodology
ppm	parts per million
Pro	proline
PTS	phosphotransferase system

Q	Glutamine
Q-TOF	quadrupole time of flight
R^2	coefficient of determination
RP-HPLC	reverse phase high performance liquid chromatography
RPM	revolutions per minute
R_t	retention time
SAR	structure activity relationship
SEM	standard error of the mean
Ser	serine
Sf_9	*Spodoptera frugiperda*
spp.	species in plural
sTrcAQ-O	synthetic tyrocidine A with a glutamine to ornithine substitution
Suc	sucrose
Tc	commercial tyrocidine
Tcn	tyrothricin
TE	thioestherase
Te	tyrocidine extract
TFA	trifluoroacetic acid
TFE	2,2,2-trifluoreoethanol
TG	Test Guideline
TGS	tryptone glucose and salts culture medium
Thr	threonine
TNM-FH	supplemented Grace's insect cell culture medium
TLC	thin layer chromatography
TOF	time of flight
TpcA	tryptocidine A
TpcB	tryptocidine B
$TpcB_1$	tryptocidine B_1
TpcC	tryptocidine C
$TpcC_1$	tryptocidine C_1
Tpc(s)	tryptocidine(s)
TrcA	tyrocidine A
$TrcA_1$	tyrocidine A_1

TrcB	tyrocidine B
$TrcB_1$	tyrocidine B_1
TrcC	tyrocidine C
$TrcC_1$	tyrocidine C_1
Trc(s)	tyrocidine(s)
Trp	tryptophan
TSA	tryptone soy agar
TSB	tryptone soy broth
Tyr	tyrosine
UPLC	ultra performance liquid chromatography
UV	ultraviolet
v	D-valine
V	valine
Val	valine
VGA	valine gramicidin A
VGB	valine gramicidin B
VGC	valine gramicidin C
VVM	volume per volume per minute
v/v	volume/volume
Vx_a	production rate
w	D-tryptophan
W	tryptophan
wA	tryptocidine A
wC	tryptocidine C
Wf	tyrocidine B analogues
Ww	tyrocidine C analogues
w/v	weight/volume
y	D-tyrosine
Y	tyrosine
µ	growth rate
µg	microgram
µL	microliter
µM	micromolar

Preface

The loss incurred due to microbial spoilage is a great concern to the agricultural and food industries. Microbial pathogens have typically been controlled through the use of chemical control agents and antibiotics. However, combination of emerging microbial resistance together with consumer opposition and regulation toward these chemical agents has instigated the need for so called green-biocides which have a reduced ecological impact together with lower potential for resistance development. The tyrocidines and their analogues, cyclic decapeptides produced by the soil bacterium *Bacillus aneurinolyticus,* show potential to serve as green-biocides. Potent antimicrobial activity toward bacterial and fungal pathogens which affect both the food and agricultural industries is achieved by different cyclodecapeptide analogues.

The objective of this study was the development and evaluation of the future potential of the cyclodecapeptides produced by *B. aneurinolyticus* to serve as green-biocides. In this thesis an overview is given in Chapter 1 of the challenges facing agricultural production due to microbial spoilage and resistance, as well as the potential of antimicrobial peptides, specifically the tyrocidines and analogues to address this problem. The optimal conditions allowing for future large scale production of target-specific subsets of these cyclodecapeptides and economical downstream purification of the peptide mixtures and single peptides is covered in Chapters 2-4. The produced cyclodecapeptide mixtures/formulations were investigated to elucidate some parameters which may allow for optimisation to target different agricultural and/or food related pathogens/problem organisms (Chapters 5 and 6). Initial formulation parameters were evaluated together with the relative safety of their application within an agricultural setting by determining their *in vivo* toxicity toward honey bees (Chapter 7). A Summary of the findings in each of the different chapters is presented together with proposed future work (Chapter 8). The experimental chapters of this thesis were written as independent units so as to enable future publication. In some chapters repetitions were unavoidable, every attempt was made to keep this to a minimum.

The first goal of this study was the increased natural production of these cyclodecapeptides to enabling their tailored application to target different pathogens in an agricultural environment. In order to achieve the goal of this study the following objectives were set:

- Manipulation of the natural cyclodecapeptide profile of *B. aneurinolyticus* to produce defined peptide subsets and single peptides. (Chapter 2).

- Construction of a computational model of cyclodecapeptide production by *B. aneurinolyticus* (Chapter 3).

- Optimise production and purification methodology of the tyrocidines and their analogues for future large scale production (Chapter 4).

The second goal was to characterise the peptides in order to facilitate formulation of the peptides for *in vivo* applications. In order to achieve the goal of this study the following objectives were set:

- Investigate the structure and oligomerisation relationships of the major cyclodecapeptide analogues produced in the different subsets (Chapter 5).

- Correlation of the oligomerisation characteristics of co-produced cyclodecapeptides with their antimicrobial activity toward two representative target organisms (Chapter 6).

- Formulation of the natural cyclodecapeptide extracts and investigation of their *in vivo* toxicity toward honey bees as representative non-target species (Chapter 7).

Outputs of PhD study

Oral and Poster presentations

- Vosloo, J. A. The production, isolation and activity of cyclic antibiotic peptides from tyrothricin by *Bacillus aneurinolyticus.* (2012) Biochemistry Forum, University of Stellenbosch, Oral presentation.
- Vosloo, J. A., De Beer, A., Rautenbach, M. (2012) Optimizing and manipulation of the natural production of cyclic antibiotic peptides directed against fungi, parasites and bacteria, SASBMB/FASBMB 2012 Conference, Drakensberg, South Africa, Poster presentation.
- Vosloo, J. A., Rautenbach, M. (2012) Optimizing and manipulation of the natural production of antimicrobial peptides directed against fungi, parasites and bacteria. 3rd International Conference on Antimicrobial Peptides (AMP2012) in Villeneuve D'AscQ, Lille, France.
- Vosloo, J. A. The production, isolation and activity of cyclic antibiotic peptides from tyrothricin by *Bacillus aneurinolyticus*. (2013) Biochemistry Forum, University of Stellenbosch, Oral presentation.
- Vosloo J. A., Snoep, J. L., Rautenbach, M. (2014) Manipulation of the tyrocidine and analogue production profile of *Brevibacillus parabrevis*: An in depth analysis reveals tryptophan supplementation results in a new subset of peptides, the tryptocidines. SASBMB 2014 Conference, Goudini, South Africa, Poster presentation.
- Vosloo J. A., Snoep, J. L., Rautenbach, M. (2015) Manipulation and modelling of the tyrocidine and tryptocidine profile of *Bacillus aneurinolyticus*. Gordon Research Conference: Antimicrobial Peptides, Renaissance Tuscany Il Ciocco, Lucca (Barga), Italy.
- Vosloo J. A., Allsopp, M., Tait, T., Troskie, A. M., and Rautenbach, M. (2015) Toxicity testing of the tyrocidines, cyclic antimicrobial peptides isolated from *Bacillus aneurinolyticus*, toward African honeybees, *Apis mellifera scutellata*. Gordon

Research Seminars: Antimicrobial Peptides, Renaissance Tuscany Il Ciocco, Lucca (Barga), Italy.

Patent

- Rautenbach, M., Troskie, A. M., De Beer, A., Vosloo, J. A. Antimicrobial peptide compositions for plants, WO/2013/150394 A1, PCT Patent filed on 22 February 2013, P2366CN00 China(TBA, 21/10/2014); P2366EP00 Europe (13717558.4, 22/09/2014); P2366IN00 India (1963/KOLNP/2014; 16/09/2014); P2366US00 United States (14380518, 22/08/2014); P2366ZA01South Africa (2014/06499; 04/09/2014)

Peer-reviewed research report

- Rautenbach, M., Vosloo J. A., van Rensburg, W. and Engelbrecht, Y. (2015) Natural antimicrobial peptides as green microbicides in agriculture: A proof of concept study on the tyrocidines from soil bacteria, Green Economy Research Report, Green Fund, Development Bank of Southern Africa, Midrand.

Peer-reviewed articles

- Vosloo J. A., Stander, M. A., Leussa, A. N., Spathelf, B. M., Rautenbach, M. (2013) Manipulation of the tyrothricin production profile of *Bacillus aneurinolyticus*, Microbiology, 159, 2200–2211
- Troskie, A. M., De Beer, A., Vosloo, J. A., Jacobs, K., Rautenbach, M. (2014) Inhibition of agronomically relevant fungal phytopathogens by tyrocidines, cyclic antimicrobial peptides isolated from *Bacillus aneurinolyticus*. Microbiology, 160, 2089–2101
- Troskie, A. M., Rautenbach M., Delattin, N., Vosloo, J. A., Dathe M., Cammue, B., Thevissen, K. (2014) Synergistic activity of the tyrocidines, antimicrobial cyclodecapeptides from *Bacillus aneurinolyticus*, with amphotericin B and caspofungin against *Candida albicans* biofilms. Antimicrobial Agents and Chemotherapy, 58, 3697–3707

Chapter 1
Literature review: Tyrocidines, antimicrobial peptides with potential applications in agriculture and industry

1.1 Introduction

The loss of production in the agricultural and food sector due to microbial disease and spoilage severely impacts productivity and global food security as a whole. Plant diseases or food spoilage caused by bacteria, fungi and viruses result in approximately 16% pre-harvest losses of global food production annually [1]. Postharvest losses of between 16 to 50% are not uncommon, particularly in developing countries [2]. The demand for food production and global food security is ever increasing with a growing human population and changing climatic conditions, a need clearly exists to increase available food resources. It has been estimated that in order to meet future global food demand in the year 2050 global food production will have to increase by 50% [2,3]. Efforts to increase food production on ever decreasing available agricultural land have encountered the problem of increased vulnerability of higher yielding plant varietals to pathogens [4].

Numerous microorganisms result in pre-harvest and postharvest spoilage of food products that may also be linked to food-borne pathogenic outbreaks in humans. These range from bacteria such as *Erwinia amylovora* responsible for causing fire blight and black soft rot in various types of fruit and vegetables [5,6]. Bacterial species such as *Corynebacterium michiganeses*, *C. sepdonicum*, *Xanthomonas campestris* and numerous genres of the *Pseudomonas* species lead to fruit and vegetable spoilage by causing various forms of spots, rot and blight [5]. Furthermore, numerous fungi such as those of the order *Pucciniales*, which cause Rust, result in severe losses in cereal production [4]. While *Botrytis cinerea*, *B. allii* and *Rhizoctonia solani* represent but a few fungal species responsible for large pre and postharvest losses in vegetable and fruit production [3,4,6]. Further food spoilage may occur due to contamination with food-borne pathogens such as *Listeria monocytogenes*, *Escherichia coli* and *Salmonella* [7]. Food-borne diseases cause further reductions in the available food resources as well as posing a serious health and economic concern by causing diarrheal diseases. These could be life threatening, particularly in immunocompromised individuals [7-10].

Through the use of chemical pesticides and antibiotics such as oxyteracyclin and streptomycin to control many of these pathogens as well as improved agricultural practises, food production has been doubled over the last four decades [6,11,12]. The emergence of multiple drug resistant pathogens [7,12], and a shift in regulation toward pesticides with a lower intrinsic toxicity and lower environmental impact has, however, driven the search for alternative pesticides [1,11]. The use of antibiotics in the agricultural industry has been implicated in the resistance development of multiple drug resistant human pathogens through the horizontal transfer of resistant genes between different bacterial genres [1,12]. Increased social awareness has resulted in the banning of other plant pesticides due to the negative environmental impact that arises as a consequence of their use [6]. A significant reduction in the available number of pesticides able to treat pathogenic microbial infections in plants has resulted, limiting the ability to combat plant pathogens that affect numerous plant species of significant food and economic importance [1,13]. A need therefore exists to develop novel so called green-biocides with a reduced ecological impact and alternate mode of action.

1.2 Antimicrobial peptides

Antimicrobial peptides may be a solution to the resistance and environmental problem. Antimicrobial peptides are found throughout the prokaryotic and eukaryotic kingdoms [14,15], and show a broad range of activity toward Gram-positive and Gram-negative bacteria, fungi and viruses [9,16-21]. They are an alternate class of antimicrobial agents which have a novel mechanism of action and alternate cellular targets compared to conventional antibiotics [15,20,22,23].

Antimicrobial peptides typically contain an amphipathic secondary structure within which hydrophobic and cationic residues are spatially separated from one another [14]. This characteristic allows antimicrobial peptides to associate with hydrophobic membrane structures and cause disruptions to the membrane and/or cellular processes, consequently leading to cell death [9,14,18,24]. A number of these antimicrobial peptides contain a net positive charge which allows them to show selective toxicity toward the more negatively charged bacterial cell membrane, allowing them to be discriminated from the neutral membranes of plants and animals. Furthermore, their rapid membranolytic activity reduces the likelihood of the development of resistance [14].

Consequently the antimicrobial peptides show potential in the development of an novel class of therapeutic agents to treat resistant strains of pathogenic microorganisms, or to serve as green-biocides and preservatives [9,15,19,23,25]. This has set off the impetus to elucidate the precise mode of action, as well as the bioactivity of the antimicrobial peptides [15,16,18,21,23,24,26-30], including the tyrocidines (Trcs) [9,19,20,31,32], the antimicrobial peptides of interest in this project.

Antimicrobial peptides consist of a wide variety of different molecules, with more than 880 known natural peptides [14,15,18,33]. These have been broadly grouped into six different categories in a review by Epand and Vogel [24]. These include: linear peptides which form amphipathic and hydrophobic α-helices, cyclic β-sheet peptides, peptides containing unique amino acids, cyclic peptides containing thio-ether groups known as lantibiotics, peptaibols and macrocyclic knotted peptides consisting of lipopeptides that contain amino alcohols on the terminal ends [15,24]. Of these groups considerably the largest amount of attention has been focused on the α-helical peptides. This includes peptides such as the magainins which are derived from the skin of the African clawed frog *Xenopus laevis* [34] and alamethicin derived from the *Trichoderma viride* fungus [15,35].

A number of mechanisms of action have been proposed for these α-helical peptides which centre on their interaction and insertion into model membranes to form pores. One model is the barrel-stave model, whereby individual peptides bind and insert themselves through the membrane bilayer, without changing the phospholipid head group orientation to from pores and recruit additional peptides to increase the pore size [17,18,30,36]. The second being the toroidal pore model, where the peptide molecules bind and accumulate on the membrane surface in a parallel orientation until a certain critical concentration is reached when the peptides insert themselves perpendicularly into the membrane, remaining associated with the phospholipid head groups, resulting in disruption in both phospholipid head group orientation and membrane permeabilization [17,18,29,30,37]. However, both of these models have been disputed with flaws indicated in both of them [17,24]. Other models propose that the peptides carpet the membranes and cause vesicles to form [29,38] or aggregate within the membranes causing disruption [18,39]. Recently it has been proposed that some peptides lead to phase separation of lipids [40] or lipid demixing [41,42], without permeabilising membranes but leading to membrane dysfunction in terms of supporting protein functionality.

Newer evidence has come to light proposing that membrane binding may only be part of the picture. Some antimicrobial peptides may bind to the membrane only as a means to enter the cell and then act on intracellular targets thereby causing cell death by means other than cell lysis or other membrane disruptions [9,16,16,24]. Moreover, the importance of peptide concentration has been highlighted by in a review by Hancock and Rozek [18]. Most experiments that deal with the elucidation of the mechanism of action of antimicrobial peptides are done with model membranes and high peptide concentrations resulting in an erroneous and unnatural point of view being created. It is proposed that high peptide concentrations together with model membranes fail to capture the true nature and heterogeneity of biological membranes, as well as the true range of activities of the antimicrobial peptides [18].

Most antimicrobial peptides may have a more subtle effect than previously thought. The majority of experiments are performed with concentrations well in excess of the minimal effective bactericidal concentration (MBC) where most antimicrobial peptides breakdown the cytoplasmic membrane integrity [33]. Antimicrobial peptides such as indolicidin and bactenecin have been shown to not disrupt the membrane potential at their MBC yet still cause cell death [16-18,43,44]. It has been proposed that antimicrobial peptides may target the cytoplasmic membrane at high concentrations, but also have a preferred intracellular or membrane target as well as other secondary targets at lower concentrations [14,30,43,44]. These multiple targets of antimicrobial peptides has ensured they maintain their potency despite being evolutionally conserved throughout the biosphere [16,21]. Characteristics such as these make antimicrobial peptides attractive candidates for the development of novel antimicrobial agents.

Considerably less is known about the mechanism of action of the β-sheet peptides which includes; loloatins [45,46], defensins [47], the Trcs and their structurally related streptocidines [48,49] and gramicidin S (GS) [23]. The amphipathic β-type secondary structures of these peptides allows them to interact with bacterial membranes and cause cell lysis [31,32,47,50], yet specificity and activity is due to a fine balance between amphipathicity and positive charge [26]. Increasing the size and hydrophobicity of GS analogues is show to increase both their activity as well as inherent haemolytic toxicity. The addition of positively charged residues to these larger structure, however, maintained their activity and concomitantly increased specificity toward the negatively charged bacterial

membrane while decreasing haemolytic toxicity [27,51-53]. Similarly, the introduction of a positive charge to the structures of three diverse peptides namely the α-helical indolicidin [54] and maganin2 [55], as well as the β-peptide lactoferricin B [56] resulted in increased activity and reduced haemolytic toxicity [26]. Furthermore, modifications of the structure of GS with D-amino acids leads to the disruption of the formation of β-sheet type structure which are proposed to be the active structure in their membranolytic activity. These modifications, however, resulted in increased antimicrobial activity suggesting that GS has other intracellular targets in addition to the cell membrane [15,53,57]. The latter correlates with the reported interaction of GS with various intracellular targets such as carbohydrates [58] and enzymes of certain metabolic pathways [59].

Manipulation of the native structures of the antimicrobial peptides by the introduction of positively charged residues has been used to increase their specificities for microbial membranes of numerous peptides including: GS [51-53,57], indolicidin [54], maganin 2 [55], lactoferricin B [56], as well as tyrocidine A [60,61]. This approach aims to reduce the inherent haemolytic toxicity of these peptides and concomitantly increase their therapeutic index. Ultimately the goal is the development of novel chemotherapeutic agents for treatment of pathogenic infections in humans and other mammalians.

We, however, propose to use naturally produced Trcs and their analogues as a preventative measure aimed at agricultural applications and food bio-security. The losses in agricultural food production due to pathogenic spoilage of numerous crops of not only dietary but also economic importance severely effects social well-being of the human population [2,4]. This is of particular concern in third world countries where many individuals survive by subsistence farming, thus crop losses may potentially cause famine as well as financial hardship. Infections with food-borne pathogens and their associated negative effect due to food spoilage and morbidity may be prevented by pre-treatment of food stuffs or crops with antimicrobial peptides [9].

The potential of antimicrobial peptides as bio-control agents has been recognised. Agricultural research related to the use of microbial producers of antimicrobial peptides as bio-control agents was already in progress in the middle of the last century [62]. The natural abundance of antimicrobial peptides throughout all biospheres [14,63,64] led to them to be often considered as one of the most natural ways of maintaining a balanced ecosystem [62].

The successfully protection of plants from typically fungal, as well bacterial pathogens, using microorganisms as natural bio-control agents has in many instances been achieved using bacteria which produce antimicrobial peptides in natural soil and water bodies [65-76]. The cyclic structure of many these naturally produces antimicrobial peptides makes them more resistant to degradation allowing them sufficient time to target slow growing fungal pathogens, while still remaining biodegradable to their basic amino acid building blocks which may serve as nutrients to plants [77].

The current increase in resistance of pathogens to conventional chemical control agents [7,12]; together with increased awareness of the negative ecological impact of chemical control agents [6], has driven the impetus of renewed interest in the use of natural bio-control as a means to curb the losses due to microbial spoilage and diseases in plants [66,69,72]. Different strains of the soil bacterium *Bacillus subtilis* have been shown to protect plants from phytopathogenic fungal pathogens through the production of a broad range of different cyclic β-sheet antimicrobial peptides including: iturin [70,75,76], iturin A and surfactin [65,78].The lipopeptide surfactin and fengycin are also shown to protect plant by inducing systemic resistance [74]. The bacterial producer of the antimicrobial peptide GS, which has a primary structure of 50% analogy to the Trcs, has also been shown to protect plants and their fruit from fungal pathogens [67,68,73]. Moreover, GS as well as the bacterial producer is shown to have a broad antibacterial activity [79] which would also allow for protection against a broader range of pathogens.

The use of the bacterial producers of cyclic-antimicrobial peptides as bio-control agents thus shows significant promise. However, this approach has some limitation with regard to the range of applications where it is applicable, as well as the inherent unpredictability related to the growth and antimicrobial peptide production by microbes within an agricultural or industrial application. An alternate approach taken in this project entailed the increased production of the Trcs within a controlled environment, thereby increasing the control and scope of their application.

1.3 The tyrocidines

The Trcs and the cyclodecapeptide analogues have so far shown promising antimicrobial activity toward numerous pathogenic microorganisms which cause food spoilage and disease

including: the Gram positive bacteria *L. monocytogenes* [20,80], as well as a multitude of pre- and postharvest fungi such as: *Botrytis cinerea*, *Fusarium* spp and *Penicillium* spp [81-84]; while also including the human malaria parasite *Plasmodium falciparum* [19]. All of which directly or indirectly result in extensive morbidity and mortality in developing countries such as those of Southern Africa.

The Trcs, as well as their structural analogues the tryptocidines and phenycidines, are isolated from the tyrothricin (Tcn) peptide complex which is primarily produced during the late logarithmic growth phase by the soil bacterium *Bacillus aneurinolyticus*, previously known as *Bacillus brevis* [9,85-87]. The Tcn complex is composed of two fractions, the first being a neutral fraction consisting of linear pentadecapeptides known as the gramicidins (Grms) and the second being a basic fraction consisting of cyclic decapeptides, namely the Trcs and analogues [25].

Despite being discovered 10 years after penicillin, Tcn was the first antibiotic to be used in clinical practices, yet due to its haemolytic toxicity [88] use was limited to topical applications [89-92]. They have also been proven safe for oral consumption [86,93-96] and as such have been extensively utilised as the active ingredient in throat lozenges containing 1 mg Tcn under the trade name of Tyrozets® [97]. Tcn has also been used to successfully treat ulcers in the eye [98]. However, due to the perceived toxicity of the Trcs in the Tcn complex [95,96,99-101], attention has largely been focused on the β-lactam antibiotics as chemotherapeutic agents.

1.3.1 Structure of the tyrocidines

Investigations into the structure of the Trcs and their analogues have indicated that they are cationic antimicrobial peptides containing a fairly conserved cyclic decapeptide structure (Fig. 1.1), with variations mainly at positions three and four (Phe and Trp), seven (aromatic residues) and nine (ornithine, Orn or Lys) [9,25,32].This variability accounts for 24 of the 28 Trcs previously characterised by Tang *et al*. [25]. The last four are formed due to variability at position eight (Val, Leu and Ile) [25] (Table 1.1). This variability indicates that there are possibly 72 different Trcs; hence there may be a large number of as yet uncharacterised Trcs.

The structure of tyrocidine A has been determined to form a two stranded antiparallel β-sheet structure connected by a type II β-turn on the one end and slightly distorted type I β-turn on

the other end of the molecule [50,102-106]. The structure is stabilised by the formation of four intramolecular hydrogen bonds, as well as hydrophobic interactions between some of the side chains to yield an amphipathic curved structure [105]. Despite some variation in primary structure, particularity with regard to aromatic amino acid identity, the basic backbone structure is proposed to generally be conserved among the different Trc analogues [107]. The Trcs are proposed to oligomerize into higher ordered structures which associate with cell membranes, causing loss of structural integrity [9,20,32,50,105,106], as well as targeting alternate intracellular targets [108,109], both of which result in cell death [19,20,20,80,82].

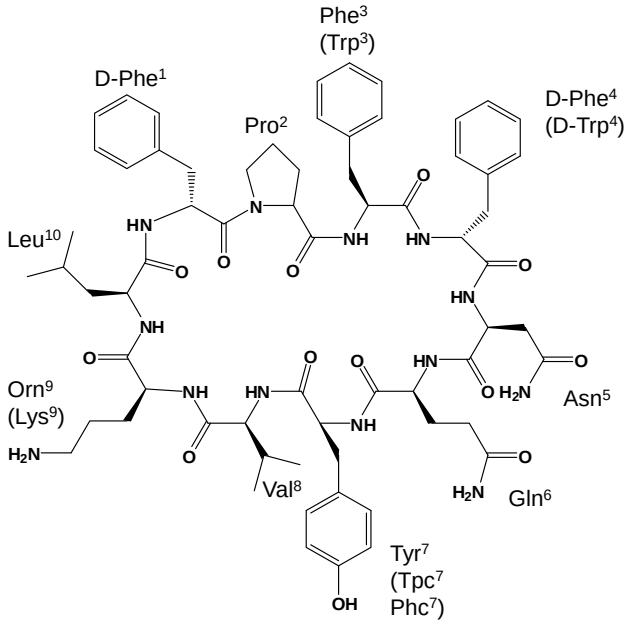

Figure 1.1 Primary structure of tyrocidine A exemplifying the cyclic decapeptide structure of the Trcs and their analogues. Residues are referred to using standard three letter amino acid abbreviations with Orn representing ornithine. Residues are numbered according to their order of incorporation during biological synthesis, with variable amino acids represented in brackets. The tyrocidine analogues are formed when residue 7 is substituted by either phenylalanine or tryptophan to produce the phenycidines or tryptocidines respectively. Adapted from Tang [25].

1.3.2 Non-ribosomal production of the tyrocidines

The Trcs and their analogues are cyclic non-ribosomal peptides (NRP) produced by a series of multi-domain enzymatic peptide synthetases (TycA, TycB and TycC). These are not encoded for by a single gene but by the 39.5kb tyrocidine biosynthesis operon containing the genes *tycA*, *tycB* and t*ycC*, as well as *tycD*, *tycE* and *tycF* [110]. Through data base searches the two genes *tycD* and *tycE*, which show 36% sequence identity, are suggested to encode for two ABC transporters. Due to the observed function of similar proteins in *Proteus mirabilis*

[111], the proteins these genes encode for are putatively suggested to be responsible for resistance of the producer strain to the Trcs by actively transporting them out of the cell [110]. While *tycF* is proposed to encode for a putative thioesterase as it shares 34% identity with the thioesterase of the GS operon [110,112] (Fig. 1.2).

Table 1.1 Summary of the different Trcs and analogous previously isolated and characterised from Tcn [25].

No	Identity	Abbreviations	Sequence [a]	Monoisotopic Molecular mass	Abundance [b]
1	-	-	VKLfP(L/I)fNQY	1249.7	<1
2	Phenycidine A [c]	PhcA	VOLfPFfNQF	1253.8	2.8
3	Tyrocidine A	TrcA	VOLfPFfNQY	1269.7	81
4	Tyrocidine A_1	$TrcA_1$	VKLfPFfNQY	1283.7	36
5	Tyrocidine E [d]	TrcE	VOLfPFyNQY	1285.7	<1
6	Tyrocidine E' [d]	TrcE'	VOLfPYfNQY	1285.7	2.0
7	Tryptocidine A	TpcA	VOLfPFfNQW	1292.7	14
8	Phenycidine B [d]	PhcB	VOLfPWfNQF	1292.7	3.4
9	Tyrocidine E_1	$TrcE_1$	VKLfPYfNQY	1299.7	1.0
10	Tyrocidine E_1	$TrcE_1$	VKLfPFyNQY	1299.7	<1
11	Tyrocidine B	TrcB	VOLfPWfNQY	1308.7	100
12	Tyrocidine B' [d]	TrcB'	VOLfPFwNQY	1308.7	13
13	Tyrocidine B_1	$TrcB_1$	VKLfPFwNQFY	1322.7	40
14	Tyrocidine B_1	$TrcB_1$	VKLfPWfNQFY	1322.7	5.3
15	-	-	(L/I)OLfPWfNQY	1322.7	1.7
16	Tyrocidine D [cd]	TrcD	VOLfPYwNQY	1324.7	1.9
17	-	-	VOLfP(L/I)fNQY	1325.7	1.1
18	Tryptocidine B	TpcB	VOLfPWfNQW	1331.7	24
19	-	-	VOLfPF(?)NQY	1336.7	4.1
20	-	-	(L/I)KLfPWfNQY	1336.7	2.4
21	Tyrocidine D_1	$TrcD_1$	VKLfPYwNQY	1338.7	1.6
22	Tryptocidine B_1	$TpcB_1$	VOLfPWfNQW	1345.7	12
23	Tyrocidine C	TrcC	VOLfPWwNQY	1347.7	92
24	-	-	VKLfPF(?)NQY	1350.7	8.6
25	Tyrocidine C_1	$TrcC_1$	VKLfPWwNQY	1361.7	28
26	-	-	VOLyPWwNQY	1363.7	<1
27	Tryptocidine C	TpcC	VOLfPWwNQW	1370.7	21
28	Tryptocidine C_1	$TpcC_1$	VKLfPWwNQW	1384.7	2.1

[a] Conventional one letter abbreviations used for amino acid sequences as obtained from Tang *et al.* [25] with O representing ornithine and lower case representing D-amino acids
[b] Expressed relative to that observed for tyrocidine B
[c] Renamed from tyrocidine E [25]
[d] Named by the BIOPEP group [9]

The three Trc peptide synthetases, TycA, TycB and TycC are composed of one, three and six modules respectively, correlating with the number and order of the amino acids each

incorporates into the Trc polypeptide chain [110]. Each of these modules is divided into a number of catalytic domains which is responsible for a specific step in the recognition, activation and addition of a single amino acid residue to the Trc polypeptide chain [113-115]. In the process a linear molecule is constructed through the tethering of intermediates to successive enzymatic modules. Ultimately the process culminates with the cyclization of the linear molecule by a carboxy-terminal thioesterase (TE) domain of the final enzymatic module [110,116,117] (Fig. 1.3).

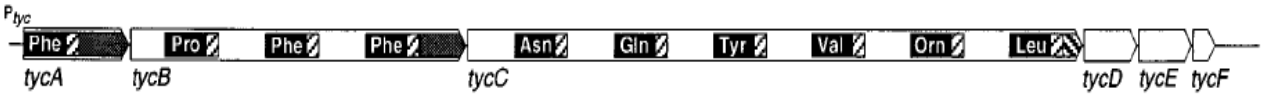

Figure 1.2 Entire tyrocidine biosynthesis operon composed of genes *tycA* to *tycF*, as well as the respective amino acids incorporated by each module in the backbone structure of tyrocidine A. As obtained from Mootz and Marahiel [110].

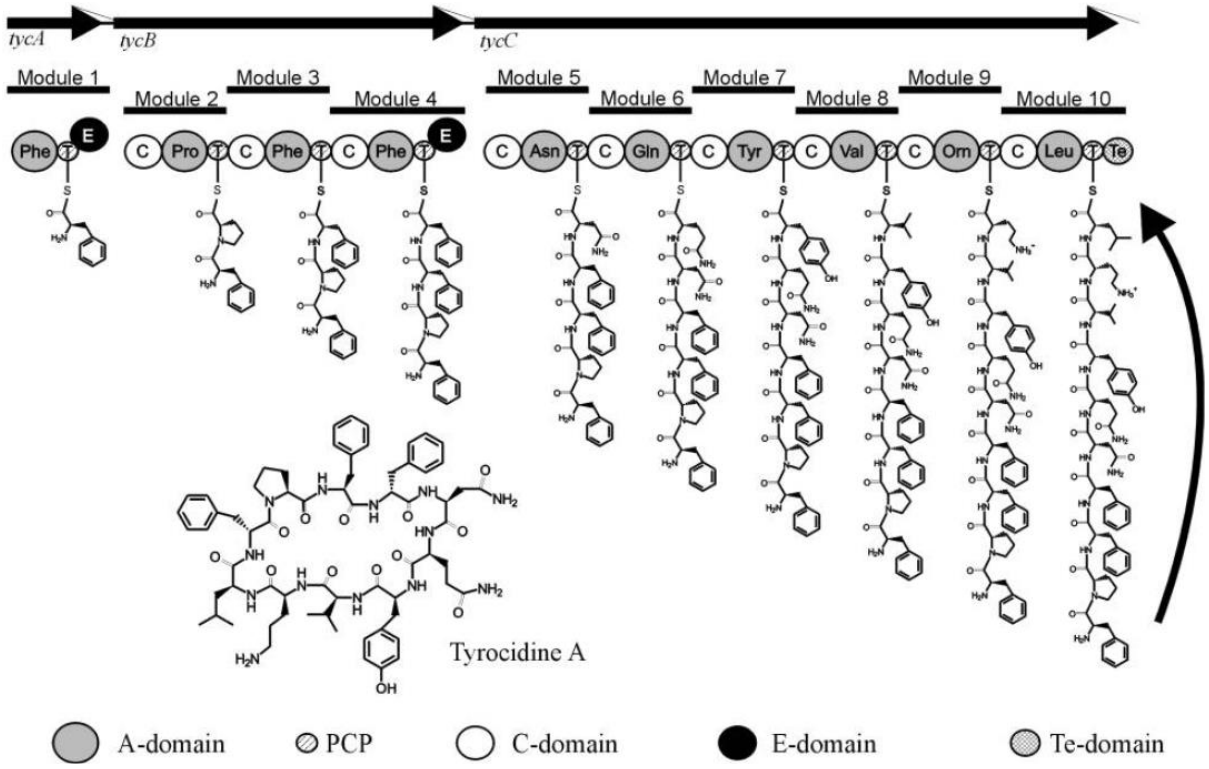

Figure 1.3 Process of tyrocidine synthesis [117]. The three genes *tycA*, *tycB* and *tycC* encode for the three multi-domain peptide synthetases TycA, TycB and TycC which incorporate one, three and six amino acids respectively. The number of amino acids incorporated coinciding with the number of modules of each synthetase. Modification of the bound amino acid residues by epimerization occurs at module one and four, where the epimerization by module one serves as an initiation of polypeptide synthesis. Figure from Linne *et al.* [113].

The first step at every module is the binding of a specific amino acid residue within the binding pocket of an adenylation (A) domain [118] and activation using ATP to form an aminoacyl-AMP anhydride [110,115,119]. The activated amino acid is then transferred to a 4'-phosphopantetheine moiety which is covalently bound to a highly conserved serine residue of a peptidyl carrier protein (PCP) to form a high energy thiol bond on the C-terminal of the amino acid [113,119]. The PCP then functions like a swinging arm, similar to fatty acid synthesis, to transport the activated amino acid to a highly specific downstream condensation (C) domain [115,119]. Peptide bond formation is catalysed by the latter C domain through the nucleophilic attack of the α-amino group of the new amino acid residue with the thio-esterified α-carboxy group on the 4'-phosphopantetheine moiety of the upstream module containing the initial amino acid [120]. This results in growth of the polypeptide chain on the α-carboxy terminal as the growing polypeptide chain is transferred from one module to the next by each subsequent PCP [110,115,121] (Fig. 1.4).

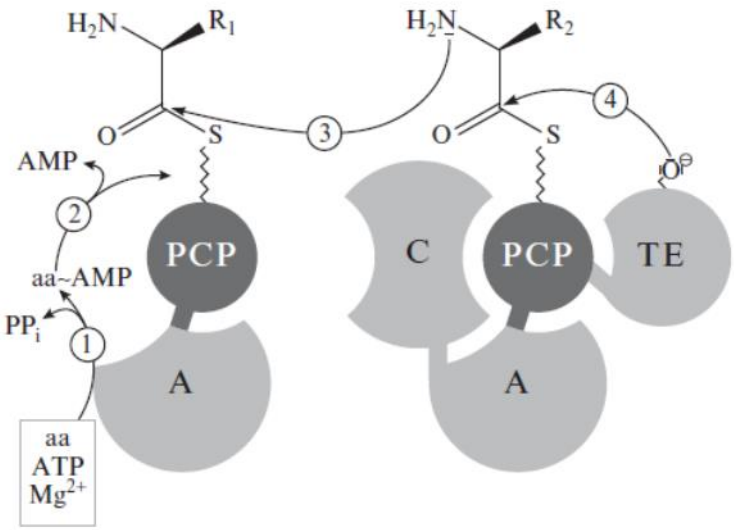

Figure 1.4 Mechanism of polypeptide elongation by the various domains of the nonribosomal peptide synthetases. (1) Amino acid (aa) selection and activation by the Adenylation (A) domain using ATP. (2) Transfer of the aminoacyl-AMP anhydride to a 4'-phosphopantetheine moiety which is covalently bound to a highly conserved serine residue of a peptidyl carrier protein (PCP) to form a high energy thio-ester bond on the C-terminal of the amino acid. (3) Nucleophilic attack and consequent transfer of the growing polypeptide to the N-terminal of the downstream PCP bound amino acid, catalysed by the Condensation (C) domain. (4) Transfer of the full length polypeptide chain to the thioesterase (TE) domain from the final PCP and consequent product release. Figure from Marahiel and Essen [120].

The first module of the, TycA peptide synthetase, however, does not contain a C domain and is known as the initiation module [122]. TycA is responsible for the binding of L-Phe, the first amino acid residue, and its conversion to D-Phe via an Epimerization (E) domain [113,114,121,123]. The D-Phe isomer is then transferred by the PCP to the C domain on TycB and thus initiates product formation [113]. All of the subsequent modules contain a C domain and are referred to as elongation modules which are dependent on the first module for the initiation of product formation [122]. Further amino acid epimerization is performed by the E domain containing module 4, which is situated within the non-ribosomal peptide synthesis assembly line and merely adds the modified residue to the growing polypeptide chain [113,114].

Ultimately Trc synthesis culminates when the polypeptide chain reaches the final PCP and is transferred to a TE domain on the C-terminal of TycC. The TE domain then catalyses the transfer of the full-length polypeptide chain to its active site serine residue where it causes head to tail cyclization of the Trc molecule. Consequently the fully formed peptide is released from the non-ribosomal peptide synthetase machinery [114,115] (Fig. 1.4).

1.3.3 Tyrocidine production and control

The Trcs and Grms antimicrobial peptides are maximally produced after the vegetative growth phase, particularly during the early stationary phase [124-126]. The precise function of the antimicrobial peptides in the producer organism remains to be elucidated. Numerous authors have, however, proposed that the antimicrobial peptides may play a role in the process of sporulation [124,127-136] in addition to their antimicrobial action which provides a competitive advantage to the producer strain [126].

This is based on the fact that when the producer strain was grown in a nitrogen deficient medium the addition of Trc was observed to induce sporulation [130,131,134,135]. Furthermore, the Trcs were observed to interact with DNA and inhibit RNA transcription [136-138], which is then reversed by the Grms [135,136,139,140]. The expression and production of the Trcs was observed to occur before that of Grms. After the production of the Trcs certain proteases were expressed which together with products of the protease digestion of casein peptide induced high levels of Grm production [124,129]. Grm then interacts with the σ subunit of RNA polymerase and inhibited the transcription of some genes [127], while

its interaction with the Trcs promotes the transcription of other genes [134,135]. The Trcs and Grms are proposed to act as cell cycle regulators through the timeous activation or repression of the expression of certain genes during the stationary growth phase and induction of sporulation [128,130,134]. However, the evidence in literature is ambiguous as others have reported the ability of the producer strain to produce viable spores and sporulate in the absence of Trc production [141].

The development of newer molecular techniques and an understanding of the genetic level of control of sporulation, as well as antimicrobial production have altered this perception. It would now seem that the previously mentioned relationship may possibly be an artefact of the greater genetic control. Both sporulation and antimicrobial production are induced under conditions where the producer is placed under metabolic stress such as nitrogen deficiency or oxygen limitation [108] or other forms of nutritional stress [142]. Initial work on Tcn production by Stokes and Woodward [143] found that Tcn production could be induced in stationary cultures, but not in submerged aerated cultures grown in media containing complex nitrogen sources. While Seddon and Fynn [108] reported a slower growth rate and increased Tcn production under conditions with low oxygen concentrations. Moreover, higher concentrations of Trc within the concentration range observed at the end of exponential growth were reported to inhibit NADH oxidase activity and consequently the electron transport chain [108]. These data all indicate the presence of some form of regulatory system which is activated and causes the expression of secondary growth phase genes, including the tyrocidine biosynthesis operon, under conditions of metabolic stress.

Many of these genes that are activated at the onset of the stationary growth phase and that result in sporulation are under control of the SpoOA-AbrB regulatory circuit [144-148]. During the exponential growth phase the expression of many secondary growth phase and sporulation related genes are blocked by the binding of the 10.7 kDa AbrB protein to their promoter sequences [144,149-151]. However, upon receiving a metabolic stress signal a series of reactions known as the phosphorelay are activated which convert the un-phosphorylated SpoOA transcriptional repressor to a phosphorylated transcriptional activator. Although the precise nature of the signal is unknown, the first step in the pathway is the autophosphorylation of the KinA or KinB proteins, which then transfer the phosphate molecule to a second messenger SpoOF. A further two phosphotransfer reactions cause the transfer of the phosphate molecule to SpoOB and finally SpoOA [142,146,148,150]. The

phosphorylated SpoOA then activates numerous genes associated with the stationary growth phase and sporulation by binding to the promoter sequence of the *abrB* gene. Thereby relieving repression of genes by the AbrB protein such as *tycA*, the first gene of the tyrocidine operon [142,144,147,152] (Fig. 1.5).

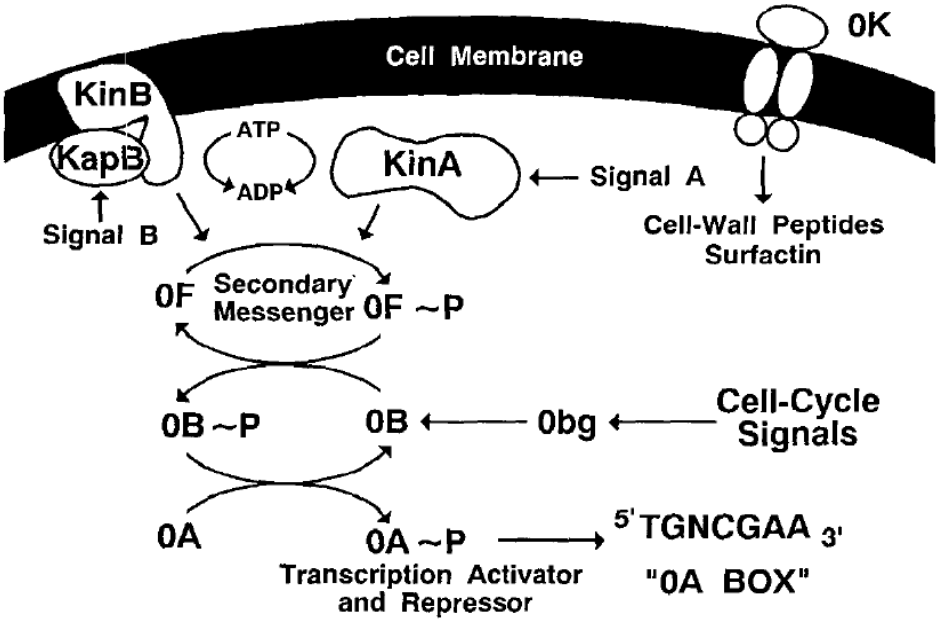

Figure 1.5 Phosphorelay cascade of reactions responsible for the phosphorylation of SpoOA and activation of the genes controlled by the SpoOA-AbrB regulatory system. Autophosphorylation of KinA and/or KinB serves as the first step of the phosphorelay, the signal for which, however, is unknown. The phosphate molecule is then transferred *via* three transfer reactions: to firstly the second messenger SpoOF (OF), then to SpoOB (OB) and finally to SpoOA (OA). The phosphorylated SpoOA then activates the transcription of various genes related to the secondary growth phase and sporulation. Phosphorylated SpoOA binds to the OA box within the promoter of the *abr* gene and inhibits its transcription thereby relieving the repression of genes by the AbrB protein such the tyrocidine biosynthesis operon [148,150,155]. Cell cycle signal may further influence the phosphorelay at SpoOB via the GTP-binding protein Ibg [148]. Figure from Hoch [148].

Much of the knowledge gained about the control of sporulation as well as those controlling Trc expression were elucidated in *B. subtilis* as many of the necessary tools used to study genetic control in *Bacillus* are available in this species.[153] Using a *tycA-lacZ* fusion protein Marahiel *et al.* [153] demonstrated that the expression of the tyrocidine biosynthesis operon is under the solitary control of the AbrB protein. While other sporulation specific genes such as *spoVG* and *aprE* may be subject to additional levels of control as they maintained their post-exponential phase induction in *abrB* mutants [150,153-155]. This control may be related to an additional regulatory role of the SpoOA protein aside from its interaction with AbrB as

spoOA abrB double mutants are unable to sporulate [149,153]. Moreover *spoOA abrB* double mutants are observed by Marahiel *et al.* [153] to result in seven fold higher levels of constitutive expression of *tycA-lacZ* fusion protein relative to wild-type cells [153,154].

Taken together it is evident that antimicrobial peptide production is closely linked to sporulation and other post exponential growth phase events. The antimicrobial peptides may have a secondary function as cell cycle regulators during the post-exponential phase of growth. However, control of their production, as well as sporulation, occurs on a genetic level *via* the same SpoOA-AbrB regulatory circuit which is triggered by environmental changes [149,152]. Furthermore, the AbrB protein may be but one of the factors involved in the regulation of antimicrobial production, other factors relating to SpoOA may play an additional role to regulate antimicrobial production in addition to binding AbrB. Nonetheless, with some understanding of the internal processes controlling natural Trc production in *B. aneurinolyticus*, some valuable insight is garnered which may allow for the manipulation of the culturing conditions of the producer organism to naturally increase Trc production.

The previously stated potential of the Trcs to act as green-biocides targeting a range of industrially relevant pathogens, as well as isoform variable activity clearly indicate the necessity for the elucidation of the conditions that allow for the maximal production of the different Trc analogues produced by *B. aneurinolyticus* [25] (refer to Table 1.1). The conditions that govern Trc production by *B. aneurinolyticus* in relation to nitrogen and carbon nutrition [143,156,157], including urea supplementation [158], principally in submerged aerated cultures performed in fermentor vessels has been reported in literature. Increased Tcn production has largely been achieved in stationary cultures using complex nitrogen sources from tryptone or vegetable waste [159]. These studies have essentially focused on total Tcn production and not the identity of the specific antimicrobial peptides produced. For the Trcs to reach their true potential and application as green-biocides, increased production of selected Trc analogues or subsets of peptides needs to be achieved to target specific pathogens.

1.3.4 Influence of the linear gramicidins in the tyrothricin complex

The influence of the co-produced Grms on the activity and formulation of the previously mentioned Trc formulations will also need to be considered. As secondary metabolites these

peptides (Grms) are also produced after the logarithmic growth phase together with other gene products under the control of the SpoOA-AbrB regulatory circuit [144-148]. The Grms are NRP that are produced by four independent multi-domain peptide synthetases LgrA, LgrB, LgrC and LgrD which catalyse the incorporation of two, four, six, and four amino acid residues respectively into the final polypeptide structure. These peptide synthetases are encoded for by the gramicidin biosynthesis operon containing four large open reading frames which correspond with the four peptide synthetases [160]. The final structure of which is composed of a linear chain of 15 alternating hydrophobic L- and D-amino acid residues that are the result of seven E domains found on alternating synthetases. The first residue is formylated by a proposed N-formyltransferase domain situated on the N-terminal of the first module of the initial peptide synthetase, LgrA. Synthesis of the linear gramicidin polypeptide follows the same principals as described for the non-ribosomal synthesis of the Trcs barring that the last module of LgrD contains a reductase domain (R domain) on the C-terminal instead of TE domain found in Trc biosynthesis, which is responsible for product release [160]. Through the process of releasing the synthesised polypeptide chain the R domain converts a C-terminal Gly residue incorporated by the final module of LgrD into an aldehyde intermediate which is finally reduced by an aldoreductase LgrE *via* a NADPH-dependent reaction to a C-terminal ethanolamine [161].

This yields the Grms with the primary sequence fomyl-L-X^1-L-Gly^2-L-Ala^3-D-Leu^4-L-Ala^5-D-Val^6-L-Val^7-D-Val^8-L-Trp^9-D-Leu^{10}-L-X^{11}-D-Leu^{12}-L-Trp^{13}-D-Leu^{14}-L-Trp^{15}-ethanolamine [162]. Variable position L-X^1 is predominantly occupied by L-Val, however, in approximately 5% of the cases it may also be occupied by L-Ile. While the variable position L-X^{11} is predominantly occupied by L-Trp to yield the A analogue, it may also be occupied by either L-Phe or L-Tyr to yield either the B or C analogues respectively [163-166]. The linear gramicidins form a β-helix secondary structure with side chains of the amino acid residues pointing outwards [167,168]. The latter structures form homodimers that permeabilize membrane structures [167] resulting in high antibacterial activity [109,169,170] through the formation of ion channels which allow the rapid leakage of singly charged cations [167].

The high membrane activity of the Grms, however, has also been attributed to the increased toxicity of the Tcn peptide complex [88,95,96,171]. They have also been found to antagonise the antimicrobial activity of the Trcs [31]. Hence, their contribution to the Tcn extracts needs

to be considered relative to the additional purification steps required to remove them from the Trcs in the different applications of the Trcs as green-biocides.

1.3.5 Toxicity of the tyrocidines in the tyrothricin complex

Hand-in-hand with the potent membranolytic activity of the Trcs, toxicity has also been reported for the Trcs, particularly in the Tcn complex which also contains the Grms. Haemolytic toxicity has been reported for the Trcs and Grms both in the Tcn complex and separated into the two fractions [96,99-101,171,172]. The haemolytic activity of the Trcs is initially more rapid. It is, however, inhibited after a short period by some undefined component of the red blood cells, leading to them being considerably less toxic than the Grms [88,101]. Similarly, increased toxicity of Grms is reported when applied intraperitoneally in mice and rats [95,96]. Some discrepancy exists in the reported leukocytic toxicity and intravenous application where the Trcs are reported to be more toxic [95], however, this may be due to decreased solubility of the Grms.

The Tcn peptides have been safely utilised when applied topically [89-92] and has typically been effective at treating ulcers of the skin in humans or cutaneous infections [98,173-177]. Toxicity is, however, reported when applied to open wounds, which has been attributed to the haemolytic action of these peptides [95,171]. The relative safety of the Tcn peptides has also been demonstrated when taken orally in mammals [93,96,97,178,179]. Oral dosages as high as 1000 mg per kg body mass were not toxic to mice and rats [96]. While a maximum tolerated tyrothricin dosage of 0.8 mg per mouse was found after being successively fed three times a day for 10 days [94].

Some authors have reported successful attempts at treating microbial infections in mice by oral administration of Tcn [86,94]. In other instances it was only able to slow down the rate of infection of pathogens which typically invade the upper gastro intestinal tract [94]. The use of Tcn to treat microbial infections by oral administration has largely been unsuccessful, despite high *in vitro* activity of the Tcn peptides toward the microbial targets [93,95]. Moreover, Tcn was found to be ineffective at treating infections away from the gastrointestinal tract when taken orally [94]. Taken together with the fact that mice orally treated with tyrothricin were observed to show no change in their intestinal microbiota [93,95], it would indicate the Tcn

peptides are not absorbed by the body and may be degraded and/or inactivated within the mammalian gastrointestinal tract.

1.3.6 Tyrocidine targets and mode of action

The antimicrobial activity of the Trcs, as with many other antimicrobial peptides, has largely been attributed to their ability to interact with hydrophobic cell membrane [31] causing permeabilization [180] and ultimately cell lysis [170]. The Trcs have been shown to associate into dimeric structures of increased amphipathicity which are stabilised by both hydrogen bonding and hydrophobic interactions [105,106] to form an arrow head like conformation [105].

The Trcs, particularly at higher concentrations, are known to aggregate into higher order structures [9,181-185]. Consequently, the Trcs are suggested to oligomerize to form pore/channel like structures similar to those found in analogous GS [186] and other β-sheet peptides [187]. The dimeric unit of the Trcs has been shown to integrate into the surface layers of model membrane structures [105]. It has been suggested these may be the initial seeding units in the formation of pore/channel like structures within membrane targets [106]. However, due to the distinct curvature of the dimerised structures, the possibility of linking them into extended sheet-like structures is questioned [105]. At present the exact nature of how the Trcs cause membrane permeabilization, which leads to loss of integrity and cell lysis, remains unknown.

Interaction of the Trcs with membrane structures occurs through a combination of hydrophobic interactions, Hydrogen bonding as well as ionic interactions [80]. While antifungal activity relied on cell wall binding as one of it possible targets as well as the cell membrane [81,82]. More subtle, non-lytic modes of antimicrobial action have also been suggested [19,20,82,188], these too would also depend on some form of initial membrane interaction and translocation to the intracellular space or contact with membrane bound enzymes. Antiplasmodial activity by the Trcs toward the malaria parasite occurs by targeting an alternate cellular target such as the food vacuole [188], as well as additional targets which may include a cell cycle regulator [19]. Moreover, the Trcs are shown to disrupt glucose metabolism in Gram-positive bacteria [99,109]. The Trcs therefore have additional targets other than just the cell membrane.

Considering the Trcs are known to bind DNA within the producer organism [137-139] and inhibit transcription *in vitro* [189], it is hypothesized that the Trcs may function through the inhibition of transcription and/or replication in addition to their membranolytic action [31]. This hypothesis of multiple cellular targets in addition to the cell membrane is supported by the possibility of multiple modes of action when targeting of different fungal pathogens [81,82]. Although calcium was observed to retard the cell wall/membrane antifungal activity of the Trcs, it brings to the fore disruption of other internal processes, including hyphal elongation to induce hyperbranching in the fungal pathogens thereby disrupting fungal growth [82]. Consequently, the Trc group are shown to not only consist of a range of different analogues, they also display multiple modes of action with variable targets, thereby reducing the likelihood of the development of resistant mutants.

1.3.7 Tyrocidine structure-activity relationships

Optimal antimicrobial activity of the Trcs toward different pathogens has been found to be related to both properties of the different target cell together with those of the different Trc analogues [9,19,20,80,82,188]. Differences in the primary structures of the Trcs, particularly those related to identity of the cationic residue at position 9 or variable aromatic amino acids at positions 3, 4 and 7 (refer to Fig. 1.1), lead to a variation in lipophilicity, side-chain surface area and mass-over-charge ratio which affect the activity of the peptides. These variations may cause changes to the conformation adopted by the different Trc analogues, altering the nature of their interaction with the target cells and thus influence antimicrobial activity.

Analysis of the structure activity relationship (SAR) of the six major Trcs toward Gram-positive bacterium *L. monocytogenes* found they displayed similar lytic activity, but differed in their ability to cause growth inhibition [20]. Growth inhibition and therefore activity was found to be dependent on both the variable aromatic residues. Increased antibacterial activity was observed by the more polar analogues containing Trp^3 [20], while some correlation was observed for preference for Orn^9 rather that Lys^9 the variable cationic residue [80]. An investigation of the SAR of the Trcs, using an extended library of both natural and synthetic analogues by Leussa and Rautenbach [80], reported increased activity of a TrcA analogue containing a trimelylated Orn, indicating that the character of the cationic residue may play a major role in activity. These differences in antimicrobial activity could be because of differences in dimerization which are the proposed amphipathic active unit required for

antibacterial activity [105,106]. However, the membrane interaction by the cationic residue in relation to activity also determined by the properties of the target cell structure [80]. Increased antimicrobial activity of cationic antimicrobial peptides has largely been attributed to membrane binding and insertion of hydrophobic residues which are specially separated from cationic residues [14,24].

The selectivity of natural antimicrobial peptides has been attributed to their positive charge causing preferential binding to the more negatively charged prokaryotic membrane structures [26]. One approach to increase the antimicrobial activity of the Trcs and related peptides such as GS while also decreasing their inherent haemolytic toxicity has entailed the manipulation of their native structures to alter their amphipathicity as well as increase positive charge [32,51-53,57,60,61,117,189,190]. This approach has largely been achieved through manipulation of the backbone structure of the TrcA analogue in the case of the Trcs. Qin *et al.* [60] reported increased activity toward *B. subtilis* while reducing haemolytic toxicity with synthetic TrcA analogue containing increased positive charge originating from a Glu^6 to Orn^6 substitution (sTrcAQ-O). Similarly, Marques *et al.* [32] reported two to eight fold increased antibacterial activity toward a range of Gram-positive bacteria by TrcA analogues containing increased positive charge by inclusion of Lys at position 6, similar to the sTrcAQ-O. Furthermore, through the substitution of $D\text{-}Phe^4$ by $D\text{-}Lys^4$ an analogue containing three cationic residues was created, inducing activity toward Gram-negative bacteria [32]. Substitution of only $D\text{-}Phe^4$ with a cationic D-amino acid is reported by Kohli et *al.* [117] to increase selectivity, despite displaying decreased activity toward Gram-positive bacteria relative to the native TrcA. These analogues also displayed some activity toward Gram-negative bacteria not observed by the natural Trcs. [117].

Marques *et al* [32] reported a loss of antibacterial activity when amphipathicity of the structure was disrupted by substitution of hydrophobic pentafluorophenlyl residues on opposite sides of TrcA structure at positions 3 and 7. However, activity is regained when the substitution was only done at one of the two positions at a time. Similarly, increased antibacterial activity toward Gram-positive and Gram-negative bacteria is observed when Lys is included at positions 6 and/or 4 together with pentafluorophenlyl residue at position 3 [32]. Substitution of position 3 with Val is reported to result in a reduction in antimicrobial activity combined with reduced inhibition of active transport and transcription *in vitro* [189].

Leussa and Rautenbach [80] reported decreased antilisterial activity by sTrcAQ-O analogue in contrast to increased activity reported by Qin *et al.* [60] toward *B. subtilis.* Differences in antimicrobial activity are attributed to changes in the target cell structure [80]. The changes in antimicrobial activity observed with the synthetic analogues exemplify the importance of an amphipathic structure [32]. As exemplified by Danders *et.al* [189], increasing hydrophobicity may not necessarily correlate with increased activity, as was also reported by Marques *et al* [32]. Similarly, increase in positive charge did not necessarily result in increased antibacterial activity.

Increased antimicrobial activity would depend on a balance between the differences in target cell structures as well as properties of the different Trcs originating from changes in their primary structures. A balance therefore exists between the strength of the membrane interaction and antimicrobial activity [80] which differs according to the target cell properties. This indicate a role in the placement of the different residues in higher order conformation adopted by the cyclodecapeptides [105,106].

Rautenbach *et al.* [19] found the more hydrophobic tyrocidine A, containing two Phe residues in the variable aromatic dipeptide moiety, to be most active against the human malaria parasite *Plasmodium falciparum* [19]. Further investigation of the antiplasmodial activity of an extended library of the Trc analogues by Leussa [188], in contrast found the more hydrophilic TpcC analogue (containing Trp as variable aromatic residues, Table 1.1) to also have increased activity. These differences in activity of these analogues are attributed to a difference in the non-lytic mode of action toward the malaria parasite occurs by targeting an alternate cellular target such as the plasmodial food vacuole [188].

Antifungal activity on the other hand was observed to be greatest with all the Trc analogues containing a Tyr residue at position 7 [81,82]. It would therefore seem apparent that the broad range of different natural Trcs that are produced enables the targeting of a multitude of different pathogens. Maximal activity toward different pathogens would consequently be achieved when increased amounts of selected analogues were present to target specific pathogens; most likely due to varying modes of antimicrobial action.

1.4 References

1. Montesinos, E. and Bardaji, E. (2008) Synthetic antimicrobial peptides as agricultural pesticides for plant-disease control. Chem. Biodivers. **5**, 1225-1237
2. Chakraborty, S. and Newton, A. C. (2011) Climate change, plant diseases and food security: An overview. Plant Pathol. **60**, 2-14
3. Spadaro, D. and Gullino, M. L. (2004) State of the art and future prospects of the biological control of postharvest fruit diseases. Int. J. Food Microbiol. **91**, 185-194
4. Oerke, E. C. (2006) Crop losses to pests. J. Agric. Sci. **144**, 31-43
5. Tournas, V. (2005) Spoilage of vegetable crops by bacteria and fungi and related health hazards. Crit. Rev. Microbiol. **31**, 33-44
6. Vidaver, A. M. (2002) Uses of antimicrobials in plant agriculture. Clin. Infect. Dis. **34**, S107-10
7. White, D. G., Zhao, S., Simjee, S., Wagner, D. D. and McDermott, P. F. (2002) Antimicrobial resistance of foodborne pathogens. Microb. Infect. **4**, 405-412.
8. Tauxe, R. V. (2002) Emerging foodborne pathogens. Int. J. Food Microbiol. **78**, 31-41
9. Spathelf, B. M. (2010) Qualitative structure-activity relationships of the major tyrocidines, cyclic decapeptides from *Bacillus aneurinolyticus*. Stellenbosch University, Department of Biochemistry, Stellenbosch, South Africa. **PhD. Thesis**, http://hdl.handle.net/10019.1/4001
10. Gandhi, M. and Chikindas, M. L. (2007) *Listeria*: A foodborne pathogen that knows how to survive. Int. J. Food Microbiol. **113**, 1-15
11. Agrios, G. N. (2005) Plant pathology. Fifth edition. Elsevier Academic. Press, London, UK.
12. McManus, P. S., Stockwell, V. O., Sundin, G. W. and Jones, A. L. (2002) Antibiotic use in plant agriculture. Annu. Rev. Phytopathol. **40**, 443-465
13. Montesinos, E. (2007) Antimicrobial peptides and plant disease control. FEMS Microbiol. Lett. **270**, 1-11
14. Zasloff, M. (2002) Antimicrobial peptides of multicellular organisms. Nature. **415**, 389-395
15. Bradshaw, J. P. (2003) Cationic antimicrobial peptides: Issues for potential clinical use. BioDrugs. **17**, 233-240
16. Hancock, R. E. W. (2001) Cationic peptides: Effectors in innate immunity and novel antimicrobials. Lancet Infect. Dis. **1**, 156-164
17. Hancock, R. E. W. and Chapple, D. S. (1999) Peptide antibiotics. Antimicrob. Agents Chemother. **43**, 1317
18. Hancock, R. E. W. and Rozek, A. (2002) Role of membranes in the activities of antimicrobial cationic peptides. FEMS Microbiol. Lett. **206**, 143-149
19. Rautenbach, M., Vlok, N. M., Stander, M. and Hoppe, H. C. (2007) Inhibition of malaria parasite blood stages by tyrocidines, membrane-active cyclic peptide antibiotics from *Bacillus brevis*. Biochim. Biophys. Acta. **1768**, 1488-1497

20. Spathelf, B. M. and Rautenbach, M. (2009) Anti-listerial activity and structure-activity relationships of the six major tyrocidines, cyclic decapeptides from *Bacillus aneurinolyticus*. Bioorg. Med. Chem. **17**, 5541-5548

21. Zasloff, M. (2000) Reconstructing one of nature's designs. Trends Pharmacol. Sci. **21**, 236-238

22. Fernandez-Lopez, S., Kim, H. S., Choi, E. C., Delgado, M., Granja, J. R., Khasanov, A., Kraehenbuehl, K., Long, G., Weinberger, D. A. and Wilcoxen, K. M. (2001) Antibacterial agents based on the cyclic D, L-α-peptide architecture. Nature. **412**, 452-455

23. Mogi, T. and Kita, K. (2009) Gramicidin S and polymyxins: The revival of cationic cyclic peptide antibiotics. Cell Mol. life Sci. **66**, 3821-3826

24. Epand, R. M. and Vogel, H. J. (1999) Diversity of antimicrobial peptides and their mechanisms of action. Biochim. Biophys. Acta. **1462**, 11-28

25. Tang. X.J., Thibault. P., Boyd. R.K. (1992) Characterization of the tyrocidine and gramicidin fractions of the tyrothricin complex from *Bacillus brevis* using liquid chromatography and mass spectrometry. Int. J. Mass Spectrom. Ion Processes. **122**, 153-179

26. Hwang, P. M. and Vogel, H. J. (1998) Structure-function relationships of antimicrobial peptides. Biochem. Cell Biol. **76**, 235-246

27. Lee, D. L. and Hodges, R. S. (2003) Structure–activity relationships of de novo designed cyclic antimicrobial peptides based on gramicidin S. Biopolymers. **71**, 28-48

28. Prenner, E. J., Lewis, R. N. A. H. and McElhaney, R. N. (1999) The interaction of the antimicrobial peptide gramicidin S with lipid bilayer model and biological membranes. Biochim. Biophys. Acta. **1462**, 201-221

29. Shai, Y. (1999) Mechanism of the binding, insertion and destabilization of phospholipid bilayer membranes by α-helical antimicrobial and cell non-selective membrane-lytic peptides. BBA-Biomembranes. **1462**, 55–70

30. Zhao, H. (2003) Mode of action of antimicrobial peptides. University of Helsinki. **Phd. Thesis**

31. Aranda, F. J. and de Kruijff, B. (1988) Interrelationships between tyrocidine and gramicidin A′ in their interaction with phospholipids in model membranes. Biochim. Biophys. Acta. **937**, 195-203

32. Marques, M. A., Citron, D. M. and Wang, C. C. (2007) Development of tyrocidine A analogues with improved antibacterial activity. Bioorg. Med. Chem. **15**, 6667-6677

33. Brogden, K. A. (2005) Antimicrobial peptides: Pore formers or metabolic inhibitors in bacteria? Nat. Rev. Microbiol. **3**, 238-250

34. Zasloff, M. (1987) Magainins, a class of antimicrobial peptides from *Xenopus* skin: Isolation, characterization of two active forms, and partial cDNA sequence of a precursor. Proc. Natl. Acad. Sci. U. S. A. **84**, 5449-5453

35. Jaworski, A., Kirschbaum, J. and Brückner, H. (1999) Structures of trichovirins II, peptaibol antibiotics from the mold *Trichoderma viride* NRRL 5243. J. Pept. Sci. **5**, 341-351

36. Hancock, R. E. W., Falla, T. and Brown, M. (1995) Cationic bactericidal peptides. Adv. Microb. Physiol. **37**, 135-175

37. Shai, Y. (1995) Molecular recognition between membrane-spanning polypeptides. Trends Biochem. Sci. **20**, 460-464

38. Shai, Y. and Oren, Z. (2001) From "carpet" mechanism to de-novo designed diastereomeric cell-selective antimicrobial peptides. Peptides. **22**, 1629-1641

39. Fjell, C. D., Hiss, J. A., Hancock, R. E. W. and Schneider, G. (2012) Designing antimicrobial peptides: Form follows function. Nat Rev Drug Discov. **11**, 37-51

40. Wenzel, M., Chiriac, A. I., Otto, A., Zweytick, D., May, C., Schumacher, C., Gust, R., Albada, H. B., Penkova, M., Kramer, U., Erdmann, R., Metzler-Nolte, N., Straus, S. K., Bremer, E., Becher, D., Brotz-Oesterhelt, H., Sahl, H. G. and Bandow, J. E. (2014) Small cationic antimicrobial peptides delocalize peripheral membrane proteins. Proc. Natl. Acad. Sci. **111**, E1409-18

41. Scheinpflug, K., Krylova, O., Nikolenko, H., Thurm, C. and Dathe, M. (2015) Evidence for a novel mechanism of antimicrobial action of a cyclic R-,W-rich hexapeptide. PLoS One. **10**, e0125056

42. Arouri, A., Dathe, M. and Blume, A. (2009) Peptide induced demixing in PG/PE lipid mixtures: A mechanism for the specificity of antimicrobial peptides towards bacterial membranes? BBA-Biomembranes. **1788**, 650-659

43. Wu, M., Maier, E., Benz, R. and Hancock, R. E. W. (1999) Mechanism of interaction of different classes of cationic antimicrobial peptides with planar bilayers and with the cytoplasmic membrane of *Escherichia coli*. Biochemistry **38**, 7235-7242

44. Wu, M. and Hancock, R. E. W. (1999) Interaction of the cyclic antimicrobial cationic peptide bactenecin with the outer and cytoplasmic membrane. J. Biol. Chem. **274**, 29

45. Gerard, J. M., Haden, P., Kelly, M. T. and Andersen, R. J. (1999) Loloatins A−D, cyclic decapeptide antibiotics produced in culture by a tropical marine bacterium. J. Nat. Prod. **62**, 80-85

46. Gerard, J., Haden, P., Kelly, M. T. and Andersen, R. J. (1996) Loloatin B, a cyclic decapeptide antibiotic produced in culture by a tropical marine bacterium. Tetrahedron Lett. **37**, 7201-7204

47. Cornet, B., Bonmatin, J., Hetru, C., Hoffmann, J. A., Ptak, M. and Vovelle, F. (1995) Refined three-dimensional solution structure of insect defensin A. Structure. **3**, 435-448

48. Gebhardt, K., Pukall, R. and Fiedler, H. P. (2001) Streptocidins A-D, novel cyclic decapeptide antibiotics produced by *Streptomyces* sp. tu 6071. I. Taxonomy, fermentation, isolation and biological activities. J. Antibiot. **54**, 428-433

49. Holtzel, A., Jack, R. W., Nicholson, G. J., Jung, G., Gebhardt, K., Fiedler, H. P. and Sussmuth, R. D. (2001) Streptocidins A-D, novel cyclic decapeptide antibiotics produced by *Streptomyces* sp. tu 6071. II. Structure elucidation. J. Antibiot. **54**, 434-440

50. Gibbons, W. A., Beyer, C. F., Dadok, J., Sprecher, R. F. and Wyssbrod, H. R. (1975) Studies of individual amino acid residues of the decapeptide tyrocidine A by proton

double-resonance difference spectroscopy in the correlation mode. Biochemistry. **14**, 420-429

51. Jelokhani-Niaraki, M., Prenner, E. J., Kay, C. M., McElhaney, R. N. and Hodges, R. S. (2002) Conformation and interaction of the cyclic cationic antimicrobial peptides in lipid bilayers. J. Pept. Sci. **60**, 23-36

52. Jelokhani-Niaraki, M., Prenner, E. J., Kay, C. M., McElhaney, R. N., Hodges, R. S. and Kondejewski, L. H. (2001) Conformation and other biophysical properties of cyclic antimicrobial peptides in aqueous solutions. J. Pept. Sci. **58**, 293-306

53. Kondejewski, L. H., Farmer, S. W., Wishart, D. S., Kay, C. M., Hancock, R. E. W. and Hodges, R. S. (1996) Modulation of structure and antibacterial and haemolytic activity by ring size in cyclic gramicidin S analogues. J. Biol. Chem. **271**, 25261

54. Falla, T. J. (1997) Improved activity of a synthetic indolicidin analogue. Antimicrob. Agents Chemother. **41**, 771-775

55. Matsuzaki, K., Sugishita, K., Harada, M., Fujii, N. and Miyajima, K. (1997) Interactions of an antimicrobial peptide, magainin 2, with outer and inner membranes of gram-negative bacteria. Biochim. Biophys. Acta. **1327**, 119-130

56. Kang, J., Lee, M., Kim, K. and Hahm, K. (1996) Structure-biological activity relationships of 11-residue highly basic peptide segment of bovine lactoferrin. Int. J. Pept. Protein Res. **48**, 357-363

57. Jelokhani-Niaraki, M. (2009) Effect of ring size on conformation and biological activity of cyclic cationic antimicrobial peptides. J. Med. Chem. **52**, 2090

58. Niidome, T., Murakami, H., Kawazoe, M., Hatakeyama, T., Kobashigawa, Y., Matsushita, M., Kumaki, Y., Demura, M., Nitta, K. and Aoyagi, H. (2001) Carbohydrate recognition of gramicidin S analogues in aqueous medium. Bioorg. Med. Chem. Lett. **11**, 1893-1896

59. Mogi, T., Ui, H., Shiomi, K., Omura, S. and Kita, K. (2008) Gramicidin S identified as a potent inhibitor for cytochrome bd-type quinol oxidase. FEBS Lett. **582**, 2299-2302

60. Qin, C., Zhong, X., Bu, X., Ng, N. L. J. and Guo, Z. (2003) Dissociation of antibacterial and haemolytic activities of an amphipathic peptide antibiotic. J. Med. Chem. **46**, 4830-4833

61. Qin, C., Bu, X., Wu, X. and Guo, Z. (2003) A chemical approach to generate molecular diversity based on the scaffold of cyclic decapeptide antibiotic tyrocidine A. J. Comb. Chem. **5**, 353-355

62. Waksman, S. A. (1945) Microbial antagonisms and antibiotic substances. Soil Sci. **59**, 482

63. Hancock, R. E. W. and Lehrer, R. (1998) Cationic peptides: A new source of antibiotics. Trends Biotechnol. **16**, 82-88

64. Rautenbach, M. and Hastings, J. (1999) Cationic peptides with antimicrobial activity: The new generation of antibiotics? Chimica oggi. **17**, 81-89

65. Asaka, O. and Shoda, M. (1996) Biocontrol of *Rhizoctonia solani* damping-off of tomato with *Bacillus subtilis* RB14. Appl. Environ. Microbiol. **62**, 4081-4085

66. Bashan, Y. (1998) Inoculants of plant growth-promoting bacteria for use in agriculture. Biotechnol. Adv. **16**, 729-770

67. Chandel, S., Allan, E. J. and Woodward, S. (2010) Biological control of *Fusarium oxysporum* f. sp. *lycopersici* on tomato by *Brevibacillus brevis*. J. Phytopathol. **158**, 470-478

68. Che, J., Liu, B., Ruan, C., Tang, J. and Huang, D. (2015) Biocontrol of *Lasiodiplodia theobromae*, which causes black spot disease of harvested wax apple fruit, using a strain of *Brevibacillus brevis* FJAT-0809-GLX. Crop Prot. **67**, 178-183

69. Compant, S., Duffy, B., Nowak, J., Clement, C. and Barka, E. A. (2005) Use of plant growth-promoting bacteria for biocontrol of plant diseases: Principles, mechanisms of action, and future prospects. Appl. Environ. Microbiol. **71**, 4951-4959

70. Gueldner, R. C., Reilly, C. C., Pusey, P. L., Costello, C. E., Arrendale, R. F., Cox, R. H., Himmelsbach, D. S., Crumley, F. G. and Cutler, H. G. (1988) Isolation and identification of iturins as antifungal peptides in biological control of peach brown rot with *Bacillus subtilis*. J. Agric. Food Chem. **36**, 366-370

71. Gutiérrez-Mañero, F. J., Ramos-Solano, B., Probanza, A., Mehouachi, J., R Tadeo, F. and Talon, M. (2001) The plant-growth-promoting rhizobacteria *Bacillus pumilus* and *Bacillus licheniformis* produce high amounts of physiologically active gibberellins. Physiol. Plantarum. **111**, 206-211

72. Hayat, R., Ali, S., Amara, U., Khalid, R. and Ahmed, I. (2010) Soil beneficial bacteria and their role in plant growth promotion: A review. Ann. Microbiol. **60**, 579-598

73. Joo, H. J., Kim, H., Kim, L., Lee, S., Ryu, J. and Lee, T. (2015) A *Brevibacillus* sp. antagonistic to mycotoxigenic *fusarium* spp. Biol. Control. **87**, 64-70

74. Ongena, M., Jourdan, E., Adam, A., Paquot, M., Brans, A., Joris, B., Arpigny, J. and Thonart, P. (2007) Surfactin and fengycin lipopeptides of *Bacillus subtilis* as elicitors of induced systemic resistance in plants. Environ. Microbiol. **9**, 1084-1090

75. Pusey, P. L. (1989) Use of *Bacillus subtilis* and related organisms as biofungicides. Pestic. Sci. **27**, 133-140

76. Pusey, P. and Wilson, C. (1984) Postharvest biological control of stone fruit brown rot by *Bacillus subtilis*. Plant Dis. **68**, 753-756

77. Jones, D. (1999) Amino acid biodegradation and its potential effects on organic nitrogen capture by plants. Soil Biol. Biochem. **31**, 613-622

78. Hiraoka, H., Asaka, O., Ano, T. and Shoda, M. (1992) Characterization of *Bacillus subtilis* RB14, coproducer of peptide antibiotics iturin A and surfactin. J. Gen. Appl. Microbiol. **38**, 635-640

79. Kondejewski, L. H., Wishart, D. S., Hancock, R. E. W. and Hodges, R. S. (1996) Gramicidin S is active against Gram-positive and Gram-negative bacteria. Int. J. Pept. Protein Res. **47**, 460-466

80. Leussa, A. N. and Rautenbach, M. (2014) Detailed SAR and PCA of the tyrocidines and analogues towards leucocin A-Sensitive and leucocin A-Resistant *Listeria monocytogenes*. Chem. Biol. Drug Des. **84**, 543-557

81. Troskie, A. M. (2014) Tyrocidines, cyclic decapeptides produced by soil bacilli, as potent inhibitors of fungal pathogens. Stellenbosch University, Department of Biochemistry, Stellenbosch, South Africa. **PhD. Thesis**, http://hdl.handle.net/10019.1/86162

82. Troskie, A. M., de Beer, A., Vosloo, J. A., Jacobs, K. and Rautenbach, M. (2014) Inhibition of agronomically relevant fungal phytopathogens by tyrocidines, cyclic antimicrobial peptides isolated from *Bacillus aneurinolyticus*. Microbiology. **160**, 2089-20101

83. Troskie, A. M., Rautenbach, M., Delattin, N., Vosloo, J. A., Dathe, M., Cammue, B. P. and Thevissen, K. (2014) Synergistic activity of the tyrocidines, antimicrobial cyclodecapeptides from *Bacillus aneurinolyticus*, with amphotericin B and caspofungin against *Candida albicans* biofilms. Antimicrob. Agents Chemother. **58**, 3697-3707

84. Rautenbach, M., Troskie, A. M., De Beer, A. and Vosloo, J. A. (2013) Antimicrobial peptide formulations for plants. WO/2013/150394 A1, P2366CN00 China (TBA, 21/10/2014); P2366EP00 Europe (13717558.4, 22/09/2014); P2366IN00 India (1963/KOLNP/2014; 16/09/2014); P2366US00 United States (14380518, 22/08/2014); P2366ZA01 South Africa (2014/06499; 04/09/2014)

85. Hotchkiss, R. D. and Dubos, R. J. (1941) The isolation of bactericidal substances from cultures of *Bacillus brevis*. J. Biol. Chem. **141**, 155-162

86. Dubos, R. J. and Cattaneo, C. (1939) Studies on a bactericidal agent extracted from a soil *Bacillus*: III. Preparation and activity of a protein-free fraction. J. Exp. Med. **70**, 249-256

87. Fujikawa, K., Suzuki, T. and Kurahashi, K. (1968) Biosynthesis of tyrocidine by a cell-free enzyme system of *Bacillus brevis* ATCC 8185: I. Preparation of partially purified enzyme system and its properties. Biochim. Biophys. Acta. **161**, 232-246

88. Dimick, K. P. (1951) The haemolytic action of gramicidin and tyrocidine. Proc. Soc. Exp. Biol. Med. **78**, 782-784

89. Henderson, J. (1946) The status of tyrothricin as an antibiotic agent for topical application. J. Am. Pharm. Assoc. **35**, 141-147

90. Goldman, L., Feldman, M. D. and Altemeier, W. A. (1948) Contact dermatitis from topical tyrothricin and associated with polyvalent hypersensitivity to various Antibiotics1. J. Invest. Dermatol. **11**, 243-244

91. Wigger-Alberti, W., Stauss-Grabo, M., Grigo, K., Atiye, S., Williams, R. and Korting, H. C. (2013) Efficacy of a tyrothricin-containing wound gel in an abrasive wound model for superficial wounds. Skin Pharmacol. Physiol. **26**, 52-56.

92. Rankin, L. (1944) The use of tyrothricin in the treatment of ulcers of the skin. The American Journal of Surgery. **65**, 391-392

93. Weinstein, L. and Rammelkamp, C. H. (1941) A study of the effect of gramicidin administered by the oral route. Exp. Biol. Med. **48**, 147-149

94. Kolmer, J. A. and Rule, A. M. (1946) Toxicity and therapeutic activity of tyrothricin by oral administration. Proc. Soc. Exp. Biol. Med. **63**, 315-317

95. Rammelkamp, C. H. and Weinstein, L. (1942) Toxic effects of tyrothricin, gramicidin and tyrocidine. J. Infect. Dis. **71**, 166-173

96. Robinson, H. J. and Molitor, H. (1942) Some toxicological and pharmacological properties of gramicidin, tyrocidine and tyrothricin. J. Pharmacol. Exp. Ther. **74**, 75-82

97. Kagan, G., Huddlestone, L. and Wolstencroft, P. (1982) Two lozenges containing benzocaine assessed in the relief of sore throat. J. Int. Med. Res. **10**, 443-446

98. Bloomfield, S. (1944) The use of tyrothricin, a bacterial extract, in the treatment of marginal ulcers of the cornea. Am. J. Ophthalmol. **27**, 500-504

99. Dubos, R. J. and Hotchkiss, R. D. (1941) The production of bactericidal substances by aerobic sporulating *Bacilli*. J. Exp. Med. **73**, 629-640

100. Herrell, W. E. and Heilman, D. (1943) Tissue culture studies on the cytotoxicity of bactericidal agents: I. Effects of gramicidin, tyrocidine and penicillin on cultures of mammalian lymph node. Am. J. Med. Sci. **205**, 157-162

101. Mann, F. C., Heilman, D. and Herrell, W. E. (1943) Effect of serum on haemolysis by gramicidin and tyrocidine. Exp. Biol. Med. **52**, 31-33

102. Kuo, M. and Gibbons, W. A. (1979) Total assignments, including four aromatic residues, and sequence confirmation of the decapeptide tyrocidine A using difference double resonance. Qualitative nuclear overhauser effect criteria for beta turn and antiparallel beta-pleated sheet conformations. J. Biol. Chem. **254**, 6278-6287

103. Kuo, M. and Gibbons, W. A. (1979) Determination of individual side-chain conformations, tertiary conformations, and molecular topography of tyrocidine A from scalar coupling constants and chemical shifts. Biochemistry. **18**, 5855-5867

104. Kuo, M. and Gibbons, W. (1980) Nuclear overhauser effect and cross-relaxation rate determinations of dihedral and transannular interproton distances in the decapeptide tyrocidine A. Biophys. J. **32**, 807-836

105. Loll, P. J., Upton, E. C., Nahoum, V., Economou, N. J. and Cocklin, S. (2014) The high resolution structure of tyrocidine A reveals an amphipathic dimer. BBA-Biomembranes. **1838**, 1199-1207

106. Munyuki, G., Jackson, G. E., Venter, G. A., Kövér, K. E., Szilágyi, L., Rautenbach, M., Spathelf, B. M., Bhattacharya, B. and van der Spoel, D. (2013) β-Sheet structures and dimer models of the two major tyrocidines, antimicrobial peptides from *Bacillus aneurinolyticus*. Biochemistry. **52**, 7798-7806

107. Laiken, S., Printz, M. and Craig, L. C. (1969) Circular dichroism of the tyrocidines and gramicidin S-A. J. Biol. Chem. **244**, 4454-4457

108. Seddon, B. and Fynn, G. (1973) Energetics of growth in a tyrothricin-producing strain of *Bacillus brevis*. Microbiology. **74**, 305-314

109. Dubos, R. J., Hotchkiss, R. D. and Coburn, A. F. (1942) The effect of gramicidin and tyrocidine on bacterial metabolism. J. Biol. Chem. **146**, 421-426

110. Mootz, H. D. and Marahiel, M. A. (1997) The tyrocidine biosynthesis operon of *Bacillus brevis*: Complete nucleotide sequence and biochemical characterization of functional internal adenylation domains. J. Bacteriol. **179**, 6843

111. Gaisser, S. and Hughes, C. (1997) A locus coding for putative non-ribosomal peptide/polyketide synthase functions is mutated in a swarming-defective *Proteus mirabilis* strain. Mol. Gen. Genet. **253**, 415-427

112. Kratzschmar, J., Krause, M. and Marahiel, M. A. (1989) Gramicidin S biosynthesis operon containing the structural genes grsA and grsB has an open reading frame encoding a protein homologous to fatty acid thioesterases. J. Bacteriol. **171**, 5422-5429

113. Linne, U., Stein, D. B., Mootz, H. D. and Marahiel, M. A. (2003) Systematic and quantitative analysis of protein− protein recognition between nonribosomal peptide synthetases investigated in the tyrocidine biosynthetic template. Biochemistry. **42**, 5114-5124

114. Kopp, F. and Marahiel, M. A. (2007) Macrocyclization strategies in polyketide and nonribosomal peptide biosynthesis. Nat. Prod. Rep. **24**, 735-749

115. Marahiel, M. A. (2009) Working outside the protein-synthesis rules: Insights into non-ribosomal peptide synthesis. J. Pept. Sci. **15**, 799-807

116. Trauger, J. W., Kohli, R. M., Mootz, H. D., Marahiel, M. A. and Walsh, C. T. (2000) Peptide cyclization catalysed by the thioesterase domain of tyrocidine synthetase. Nature. **407**, 215-218

117. Kohli, R. M., Walsh, C. T. and Burkart, M. D. (2002) Biomimetic synthesis and optimization of cyclic peptide antibiotics. Nature. **418**, 658-661

118. Conti, E., Stachelhaus, T., Marahiel, M. A. and Brick, P. (1997) Structural basis for the activation of phenylalanine in the non-ribosomal biosynthesis of gramicidin S. EMBO J. **16**, 4174-4183

119. Mootz, H. D., Schwarzer, D. and Marahiel, M. A. (2002) Ways of assembling complex natural products on modular nonribosomal peptide synthetases. Chembiochem. **3**, 490-504

120. Marahiel, M. A. and Essen, L. O. (2009) Nonribosomal peptide synthetases: Mechanistic and structural aspects of essential domains. Meth. Enzymol. **458**, 337-351

121. Lipmann, F. (1973) Nonribosomal polypeptide synthesis on polyenzyme templates. Acc. Chem. Res. **6**, 361-367

122. Linne, U. and Marahiel, M. A. (2000) Control of directionality in nonribosomal peptide synthesis: Role of the condensation domain in preventing misinitiation and timing of epimerization. Biochemistry. **39**, 10439-10447

123. Lipmann, F., Gevers, W., Kleinkauf, H. and Roskoski, R.,Jr. (1971) Polypeptide synthesis on protein templates: The enzymatic synthesis of gramicidin S and tyrocidine. Adv. Enzymol. Relat. Areas Mol. Biol. **35**, 1-34

124. Oyama, M. and Kubota, K. (1993) Induction of antibiotic production by protease in *Bacillus brevis* (ATCC 8185). J. Biochem. **113**, 637

125. Oyama, M. and Kubota, K. (1990) Suppression of tyrocidine production by purine nucleotides and related substances in *Bacillus brevis*. FEMS Microbiol. Lett. **66**, 277-279

126. Katz, E. and Demain, A. L. (1977) The peptide antibiotics of *Bacillus*: Chemistry, biogenesis, and possible functions. Bacteriol. Rev. **41**, 449-474

127. Fisher, R. and Blumenthal, T. (1982) An interaction between gramicidin and the sigma subunit of RNA polymerase. Proc. Natl. Acad. Sci. U. S. A. **79**, 1045-1048

128. Hodgson, B. (1971) Possible roles for antibiotics and other biologically active peptides at specific stages during sporulation of *Bacillaceae.* J. Theor. Biol. **30**, 111-119

129. Nakai, T., Yamauchi, D. and Kubota, K. (2005) Enhancement of linear gramicidin expression from *Bacillus brevis* ATCC 8185 by casein peptide. Biosci. Biotechnol. Biochem. **69**, 700-704

130. Pschorn, W., Paulus, H., Hansen, J. and Ristow, H. (1982) Induction of sporulation in *Bacillus brevis*. 2. Dependence on the presence of the peptide antibiotics tyrocidine and linear gramicidin. Eur. J. Biochem. **129**, 403-407

131. Ristow, H., Pschorn, W., Hansen, J. and Winkel, U. (1979) Induction of sporulation in *Bacillus brevis* by peptide antibiotics. Nature. **280**, 165-166

132. Ristow, H., Schazschneider, B., Bauer, K. and Kleinkauf, H. (1975) Tyrocidine and the linear gramicidin: Do these peptide antibiotics play an antagonistic regulative role in sporulation? Biochim Biophys Acta. **390**, 246-252

133. Ristow, H., Schazschneider, B. and Kleinkauf, H. (1975) Effects of the peptide antibiotics tyrocidine and the linear gramicidin on RNA synthesis and sporulation of *Bacillus brevis*. Biochem. Biophys. Res. Commun. **63**, 1085-1092

134. Ristow, H. and Paulus, H. (1982) Induction of sporulation in *Bacillus brevis*. Eur. J. Biochem. **129**, 395-401.

135. Federn, H. and Ristow, H. (1987) The GTP pool in *Bacillus brevis* and its significance for sporulation. Eur. J. Biochem. **165**, 223-227

136. Hansen, J., Pschorn, W. and Ristow, H. (1982) Functions of the peptide antibiotics tyrocidine and gramicidin. Eur. J. Biochem. **126**, 279-284

137. Schazschneider, B., Ristow , H. and Kleinkauf, H. (1974) Interaction between the antibiotic tyrocidine and DNA *in vitro*. Nature. **249**, 757-759

138. Bohg, A. and Ristow, H. (1987) Tyrocidine-induced modulation of the DNA conformation in *Bacillus brevis*. Eur. J. Biochem. **170**, 253-258

139. Bohg, A. and Ristow, H. (1986) DNA- supercoiling is affected *in vitro* by the peptide antibiotics tyrocidine and gramicidin. Eur. J. Biochem. **160**, 587-591

140. Chakraborty, T., Hansen, J., Ristow, H. and Schazschneider, B. (1978) The DNA· tyrocidine complex and its dissociation in the presence of gramicidin D. Eur. J. Biochem. **90**, 261-270

141. Symons, D. C. and Hodgson, B. (1982) Isolation and properties of *Bacillus brevis* mutants unable to produce tyrocidine. J. Bacteriol. **151**, 580-590

142. Trach, K., Burbulys, D., Strauch, M., Wu, J., Dhillon, N., Jonas, R., Hanstein, C., Kallio, P., Perego, M., Bird, T., Spiegelman, G., Fogher, C. and Hoch, J. A. (1991) Control of the initiation of sporulation in *Bacillus subtilis* by a phosphorelay. Res. Microbiol. **142**, 815-823

143. Stokes, J. L. and Woodward, C. R. (1943) Formation of tyrothricin in submerged cultures of *Bacillus brevis*. J. Bacteriol. **46**, 83-88

144. Strauch, M. A., Spiegelman, G. B., Perego, M., Johnson, W. C., Burbulys, D. and Hoch, J. A. (1989) The transition state transcription regulator abrB of *Bacillus subtilis* is a DNA binding protein. EMBO J. **8**, 1615-1621

145. Strauch, M. A. and Hoch, J. A. (1993) Transition-state regulators: Sentinels of *Bacillus subtilis* post-exponential gene expression. Mol. Microbiol. **7**, 337-342

146. Strauch, M. A. (1995) AbrB modulates expression and catabolite repression of a *Bacillus subtilis* ribose transport operon. J. Bacteriol. **177**, 6727-6731

147. Strauch, M. A. (1993) Regulation of *Bacillus subtilis* gene expression during the transition from exponential growth to stationary phase. Prog. Nucleic Acid Res. Mol. Biol. **46**, 123-123

148. Hoch, J. A. (1993) Regulation of the phosphorelay and the initiation of sporulation in *Bacillus subtilis*. Annu. Rev. Microbiol. **47**, 441-465

149. Robertson, J. B., Gocht, M., Marahiel, M. A. and Zuber, P. (1989) AbrB, a regulator of gene expression in *Bacillus*, interacts with the transcription initiation regions of a sporulation gene and an antibiotic biosynthesis gene. Proc. Natl. Acad. Sci. **86**, 8457-8461

150. Fürbass, R., Gocht, M., Zuber, P. and Marahiel, M. A. (1991) Interaction of AbrB, a transcriptional regulator from *Bacillus subtilis* with the promoters of the transition state-activated genes tycA and spoVG. Mol. Gen. Genet. **225**, 347-354

151. Perego, M., Spiegelman, G. B. and Hoch, J. A. (1988) Structure of the gene for the transition state regulator, abrB: Regulator synthesis is controlled by the spo0A sporulation gene in *Bacillus subtilis*. Mol. Microbiol. **2**, 689-699

152. Zuber, P. and Losick, R. (1987) Role of AbrB in Spo0A-and Spo0B-dependent utilization of a sporulation promoter in *Bacillus subtilis*. J. Bacteriol. **169**, 2223-2230

153. Marahiel, M., Zuber, P., Czekay, G. and Losick, R. (1987) Identification of the promoter for a peptide antibiotic biosynthesis gene from *Bacillus brevis* and its regulation in *Bacillus subtilis*. J. Bacteriol. **169**, 2215-2222

154. Marahiel, M. A., Nakano, M. M. and Zuber, P. (1993) Regulation of peptide antibiotic production in *Bacillus*. Mol. Microbiol. **7**, 631-636

155. Fürbaβ, R. and Marahiel, M. A. (1991) Mutant analysis of interaction of the *Bacillus subtilis* transcription regulator AbrB with the antibiotic biosynthesis gene tycA. FEBS Lett. **287**, 153-156

156. Appleby, J., Knowles, E., Mcallister, R., Pearson, J. and White, T. (1947) The production of tyrothricin by submerged culture of *Bacillus brevis* in synthetic media. J. Gen. Microbiol. **1**, 145-157

157. Appleby, J., Knowles, E., Pearson, J. and White, T. (1947) A preliminary study of the formation, assay and stability of tyrothricin. J. Gen. Microbiol. **1**, 137-144

158. Baron, A. L. (1949) Preparation of tyrothricin. USA patent office. **2482832**

159. Lewis, J., Dimick, K. P. and Feustel, I. (1945) Production of tyrothricin in cultures of *Bacillus brevis*. Ind. Eng. Chem. Res. **37**, 996-1004

160. Kessler, N., Schuhmann, H., Morneweg, S., Linne, U. and Marahiel, M. A. (2004) The linear pentadecapeptide gramicidin is assembled by four multimodular nonribosomal peptide synthetases that comprise 16 modules with 56 catalytic domains. J. Biol. Chem. **279**, 7413-7419

161. Schracke, N., Linne, U., Mahlert, C. and Marahiel, M. A. (2005) Synthesis of linear gramicidin requires the cooperation of two independent reductases. Biochemistry **44**, 8507-8513

162. Sarges, R. and Witkop, B. (1964) Gramicidin A. IV. Primary sequence of valine and isoleucine gramicidin A. J. Am. Chem. Soc. **86**, 1862-1863

163. Sarges, R. and Witkop, B. (1965) Gramicidin A. V. The structure of valine-and isoleucine-gramicidin A. J. Am. Chem. Soc. **87**, 2011-2020

164. Sarges, R. and Witkop, B. (1965) Gramicidin A. VI. The synthesis of valine-and isoleucine-gramicidin A. J. Am. Chem. Soc. **87**, 2020-2027

165. Sarges, R. and Witkop, B. (1965) Gramicidin. VII. The structure of valine-and isoleucine-gramicidin B. J. Am. Chem. Soc. **87**, 2027-2030

166. Sarges, R. and Witkop, B. (1965) Gramicidin. VIII. The structure of valine-and isoleucine-gramicidin C. Biochemistry **4**, 2491-2494

167. Weinstein, S., Wallace, B. A., Morrow, J. S. and Veatch, W. R. (1980) Conformation of the gramicidin A transmembrane channel: A ^{13}C nuclear magnetic resonance study of ^{13}C-enriched gramicidin in phosphatidylcholine vesicles. J. Mol. Biol. **143**, 1-19.

168. Smart, O. S., Goodfellow, J. M. and Wallace, B. A. (1993) The pore dimensions of gramicidin A. Biophys. J. **65**, 2455-2460

169. Dubos, R. J. and Hotchkiss, R. (1942) Origin, nature and properties of gramicidin and tyrocidine. Trans. Coll. Physicians Phila. **10**, 11-19

170. Dubos, R. J. (1939) Studies on a bactericidal agent extracted from a soil *Bacillus*: I. Preparation of the agent. Its activity *in vitro*. J. Exp. Med. **70**, 1-10

171. Rammelkamp, C. H. and Weinstein, L. (1941) Haemolytic effect of tyrothricin. Exp. Biol. Med. **48**, 211-214

172. Herrell, W. E. and Heilman, D. (1941) Experimental and clinical studies on gramicidin. J. Clin. Invest. **20**, 583-591

173. Foley, E. and Lee, S. (1946) Tyrothricin in cutaneous infections. Arch. Derm. Syphilol. **53**, 291-291

174. Tulloch, L. G. (1954) Nasal carriage in staphylococcal skin infections. Br. Med. J. **2**, 912-913

175. Anderson, H. E. (1946) Tyrothricin in cutaneous infections. Arch Derm Syphilol. **53**, 20-25

176. Bayerl, C. and Volp, A. (2004) Tyrothricin powder in the treatment of cutaneous lesions. Pharmazie. **59**, 864-868

177. Franks, A. G., Dobes, W. L. and Jones, J. (1946) Tyrothricin in the treatment of diseases of the skin. Arch. Derm. Syphilol. **53**, 498-502

178. Richards, R. M. E. and Xing, D. K. (1993) *In vitro* evaluation of the antimicrobial activities of selected lozenges. J. Pharm. Sci. **82**, 1218-1220

179. Dubos, R. J. (1939) Studies on a bactericidal agent extracted from a soil *Bacillus*: II. Protective effect of the bactericidal agent against experimental pneumococcus infections in mice. J. Exp. Med. **70**, 11-17

180. Goodall, M. C. (1970) Structural effects in the action of antibiotics on the ion permeability of lipid bilayers. I. Tyrocidine B. BBA-Biomembranes. **203**, 28-33.

181. Eyeghe-Bickong, H. (2011) Role of surfactin from *Bacillus subtilis* in protection against antimicrobial peptides produced by *Bacillus* species. Stellenbosch University. **Phd. Thesis**, http://hdl.handle.net/10019.1/6773

182. Ruttenberg, M. A., King, T. P. and Craig, L. C. (1965) The use of the tyrocidines for the study of conformation and aggregation behaviour. J. Am. Chem. Soc. **87**, 4196-4198

183. Stern, A., Gibbons, W. A. and Craig, L. C. (1969) Effect of association on the nuclear magnetic resonance spectra of tyrocidine B. J. Am. Chem. Soc. **91**, 2794-2796

184. Ruttenberg, M. A., King, T. P. and Craig, L. C. (1966) The chemistry of tyrocidine. VII. Studies on association behaviour and implications regarding conformation. Biochemistry. **5**, 2857-2864

185. Williams Jr, R. C., Yphantis, D. A. and Craig, L. C. (1972) Noncovalent association of tyrocidine B. Biochemistry. **11**, 70-77

186. Llamas-Saiz, A. L., Grotenbreg, G. M., Overhand, M. and van Raaij, M. J. (2007) Double-stranded helical twisted β-sheet channels in crystals of gramicidin S grown in the presence of trifluoroacetic and hydrochloric acids. Acta Crystallographica Section D: Biological Crystallography. **63**, 401-407

187. Yount, N. Y. and Yeaman, M. R. (2005) Immunocontinuum: Perspectives in antimicrobial peptide mechanisms of action and resistance. Protein Peptide Lett. **12**, 49-67

188. Leussa, N. A. (2014) Characterisation of small cyclic peptides with antilisterial and antimalarial activity. Stellenbosch University, Department of Biochemistry, Stellenbosch, South Africa. **PhD. Thesis**, http://hdl.handle.net/10019.1/86161

189. Danders, W., Marahiel, M. A., Krause, M., Kosui, N., Kato, T., Izumiya, N. and Kleinkauf, H. (1982) Antibacterial action of gramicidin S and tyrocidines in relation to active transport, *in vitro* transcription, and spore outgrowth. Antimicrob. Agents Chemother. **22**, 785-790

190. Joo, S. H., Xiao, Q., Ling, Y., Gopishetty, B. and Pei, D. (2006) High-throughput sequence determination of cyclic peptide library members by partial edman degradation/mass spectrometry. J. Am. Chem. Soc. **128**, 13000-13009

Chapter 2

Manipulation of the tyrothricin production profile of *Bacillus aneurinolyticus*

This chapter has been published in *Microbiology* Volume 159, October 2013, Pages 2200-2211; first author J. A Vosloo (principal investigator of experimental work, data analysis and writing of article as first author), M. A Stander (development of ultra-performance chromatography methodology together with M. Rautenbach), A. N. N. Leussa (initial development of high-throughput-assay), B. M Spathelf (MS-MS sequencing of six of the ten tyrocidine analogues) and M. Rautenbach (study supervisor and communicating author; co-writer and editing, critical evaluation of the study and data analysis). This article appears as published together with supplementary data as Chapter 2 to form part of this thesis.

Microbiology (2013), **159**, 2200–2211 **DOI** 10.1099/mic.0.068734-0

Manipulation of the tyrothricin production profile of *Bacillus aneurinolyticus*

Johan Arnold Vosloo,[1] Marietjie A. Stander,[2] Adrienne N.-N. Leussa,[1] Barbara M. Spathelf[1] and Marina Rautenbach[1]

[1]BIOPEP Peptide Group, Department of Biochemistry, Stellenbosch University, Private Bag X1, Matieland 7602, South Africa

[2]Department of Biochemistry and LCMS-Central Analytical Facility, Science Faculty, Stellenbosch University, Private Bag X1, Matieland 7602, South Africa

Correspondence
Marina Rautenbach
mra@sun.ac.za

A group of non-ribosomally produced antimicrobial peptides, the tyrocidines from the tyrothricin complex, have potential as antimicrobial agents in both medicine and industry. Previous work by our group illustrated that the more polar tyrocidines rich in Trp residues in their structure were more active toward Gram-positive bacteria, while the more non-polar tyrocidines rich in Phe residues had greater activity toward *Plasmodium falciparum*, one of the major causative pathogens of malaria in humans. Our group also found that the tyrocidines have pronounced antifungal activity, dictated by the primary sequence of the tyrocidine. By simply manipulating the Phe or Trp concentration in the culture medium of the tyrothricin producer, *Bacillus aneurinolyticus* ATCC 10068, we were able to modulate the production of subsets of tyrocidines, thereby tailoring the tyrothricin complex to target specific pathogens. We optimized the tailored tyrothricin production using a novel, small-scale, high-throughput deep 96-well plate culturing method followed by analyses of the peptide mixtures using ultra-performance liquid chromatography linked to mass spectrometry. We were able to gradually shift the production profile of the tyrocidines and analogues, as well as the gramicidins between two extremes in terms of peptide subsets and peptide hydrophobicity. This study demonstrated that tyrothricin peptide subsets with targeted activity can be efficiently produced by simple manipulation of the aromatic amino acid profile of the culture medium.

Received 19 April 2013
Accepted 19 August 2013

INTRODUCTION

Since the advent of antimicrobial use, there has been a progressive increase in drug resistance toward conventional antibiotics. This has instigated the search for an alternative class of antimicrobial agents with novel mechanisms of action and rare resistance (Brown & Wright, 2005). Antimicrobial peptides are potential candidates with membrane-linked mechanisms of action as well as possible cellular targets (Brown & Wright, 2005). Their rapid membranolytic activity reduces the likelihood of resistant mutants developing. Furthermore, reduced toxicities of the antimicrobial peptides through greater selectivity toward the more negatively charged bacterial cell membrane allow them to discriminate between pathogen targets and the neutral membranes of plants and animals (Javadpour *et al.*, 1996; Matsuzaki *et al.*, 1991, 1995; Qin *et al.*, 2003). Consequently, antimicrobial peptides show potential in the development of therapeutic agents to treat resistant strains of pathogenic micro-organisms or to serve as bio-pesticides and preservatives (Brul & Coote, 1999; Cleveland *et al.*, 2001; Keymanesh *et al.*, 2009).

A major limitation to the large-scale use of antimicrobial peptides has been the cost and efficiency of their production (Bradshaw, 2003; Gordon *et al.*, 2005; Marr *et al.*, 2006; Yeaman & Yount, 2003). Automated chemical synthesis to produce antimicrobial peptides remains very costly (Hancock & Lehrer, 1998; Hancock & Sahl, 2006; Marr *et al.*, 2006), while use of transgenic organisms for the production of antimicrobial peptides, either directly (De Bolle *et al.*, 1996; François *et al.*, 2002; Yarus *et al.*, 1996) or as fusion proteins (Lee *et al.*, 2000; Li, 2011; Moon *et al.*, 2007), is limited to ribosomally produced antimicrobial peptides. Our attention has turned to a group of non-ribosomal antimicrobial peptides, the tyrocidines, which in the tyrothricin complex were the first antibiotics in clinical use (Dubos & Cattaneo, 1939; Dubos, 1939), although their use was limited to topical applications due to observed haemolytic toxicity (Rammelkamp & Weinstein, 1942;

Abbreviations: GS, gramicidin S; LC, liquid chromatography; Phc, phenycidine; Tpc, tryptocidine; Trc, tyrocidine; UPLC, ultra-performance liquid chromatography; VGA, Val-gramicidin A.

Supplementary material is available with the online version of this paper.

Rankin, 1944; Robinson & Molitor, 1942). The production of non-ribosomal peptides such as the tyrocidines by recombinant technology is, however, much more challenging. The vast majority of the work on the synthesis of non-ribosomal peptides has arguably been done on the peptide surfactin, a promising biosurfactant (Arima *et al.*, 1968; Desai & Banat, 1997) and antimicrobial lipopeptide produced by *Bacillus subtilis* (Hiraoka *et al.*, 1992; Huang *et al.*, 2011; Sandrin *et al.*, 1990). Efforts to increase surfactin production have included the alteration of growth medium composition, environmental factors, product removal (Cooper *et al.*, 1981; Ohno *et al.*, 1995; Sheppard & Mulligan, 1987) and the addition of carriers to the growth medium (Drouin & Cooper, 1992; Yeh *et al.*, 2005). Genetic manipulation of *B. subtilis* has shown some success via the induction of random mutations (Gong *et al.*, 2009; Liu *et al.*, 2006; Mulligan *et al.*, 1989) as well as recombinant technology (Ohno *et al.*, 1992).

The peptides in the tyrothricin complex, the basic tyrocidines and neutral gramicidins (Dubos & Hotchkiss, 1941; Hotchkiss & Dubos, 1941; Tang *et al.* 1992) (refer to Table 1), are produced by a series of multi-domain enzymic peptide synthetases that are encoded by the tyrocidine biosynthesis operon (Mootz & Marahiel, 1997) or gramicidin biosynthesis operon, respectively (Kessler *et al.*, 2004). Most of the understanding of the genetic control of tyrocidine production has been garnered from expression systems in *B. subtilis* (Marahiel *et al.*, 1987; Mootz & Marahiel, 1997), as the tyrocidine producer strain *Bacillus aneurinolyticus*, previously known as *Bacillus brevis* (Dubos, 1939), has been found to be genetically less accessible (Marahiel *et al.*, 1987). Whilst a truncated dipeptide version of the tyrocidines has been produced successfully in *Escherichia coli* through the recombinant expression of the first two modules of the tyrocidine biosynthesis operon (Gruenewald *et al.*, 2004), the synthesis of a complete tyrocidine peptide in a recombinant organism is yet to be achieved.

Employing recombinant technology to improve tyrothricin production may not be necessary, as high natural production of tyrothricin has been achieved by several investigators (Appleby *et al.*, 1947a, b; Baron, 1949; Lewis *et al.*, 1945; Stokes & Woodward, 1943), including our group. The tyrocidines, as well as their structural analogues the tryptocidines and phenycidines (Table 1), are produced primarily during the late exponential growth phase by *B. aneurinolyticus* (Dubos & Hotchkiss, 1941; Dubos & Cattaneo, 1939; Dubos, 1939; Hotchkiss & Dubos, 1941). The conditions that govern tyrocidine production by *B. aneurinolyticus* relate to nitrogen, such as urea (Baron, 1949) and amino acid (Mach & Tatum, 1964; Ruttenberg & Mach, 1966; Stokes & Woodward, 1943) supplementation, and carbon nutrition (Stokes & Woodward, 1943). Whilst shifts in tyrothricin production have been reported in the literature (Mach & Tatum, 1964; Ruttenberg & Mach, 1966), the exact nature and control of this shift in antimicrobial production remain to be elucidated. Furthermore, Stokes & Woodward (1943) have reported an inhibition of tyrothricin production with the supplementation of certain amino acids to the culture medium. These studies have largely focused on total tyrothricin production and not the identity of the specific antimicrobial peptides produced.

These cationic tyrocidines and their analogues in the tyrothricin complex have a fairly conserved cyclic decapeptide structure (Table 1), containing one pentapeptide repeat of gramicidin S (GS) (Paladini & Craig, 1954; Ruttenberg *et al.*, 1965). Variations are mainly in the variable pentapeptide moiety at the aromatic dipeptide unit containing Trp and/or Phe or at the third variable aromatic residue (generally Tyr) (King & Craig, 1955a, b; Mach & Tatum, 1964; Paladini & Craig, 1954; Ruttenberg & Mach, 1966; Ruttenberg *et al.*, 1965; Tang *et al.* 1992). However, despite the conserved structures of the tyrocidines, it has been found that specific tyrocidines were more active against certain pathogens. The more polar Trc B and C (Table 1), containing either Phe and Trp or two Trp residues in the aromatic dipeptide moiety, respectively, are more active against Gram-positive bacteria (Spathelf & Rautenbach, 2009). The more non-polar Trc A, containing two Phe residues, is most active against the human malaria parasite *Plasmodium falciparum* 3D7 (Rautenbach *et al.*, 2007). Our group also found that the tyrocidines have pronounced antifungal activity, dictated by the primary sequence (Rautenbach *et al.*, 2013). Whilst previous results on the major tyrocidines are promising, this clearly accentuated the need to elucidate the conditions that would allow for the maximal production of the different coproduced tyrocidines and analogues described previously by Tang *et al.* (1992).

The aim of our study was to elucidate the optimal amino acid supplementation for the manipulation of tyrothricin production by *B. aneurinolyticus* ATCC 10068 to produce pathogen-specific tailored tyrocidine subsets or to produce extracts that could ease the downstream purification of single peptides. We supplemented culture media with selected amino acids central to the production and variability of the different tyrocidines and analogues. A small-scale high-throughput culturing methodology was developed to vary the culture medium concentrations of certain amino acids central to tyrocidine and gramicidin production by the *B. aneurinolyticus* ATCC 10068 producer strain. The peptide mixtures produced were then analysed using ultra-performance liquid chromatography (UPLC) linked to ES-MS to reveal the antimicrobial production profile of the producer strain as affected by the specific ratio of certain key amino acids in the culture media.

METHODS

Materials and reagents. *B. aneurinolyticus* ATCC 10068 was obtained from the American Type Culture Collection. *Micrococcus luteus* NCTC 8340 was obtained from the UK National Collection of Type Cultures. Deep 96-well plates, tryptone, yeast extract, peptone,

Table 1. Summary of identity, sequence and UPLC-MS data of the major peptides investigated in tyrothricin extracts from *B. aneurinolyticus* ATCC 10068

High-resolution MS data (error <5 p.p.m.) are given for both the $[M+2H]^{2+}$ monoisotopic molecular ion and calculated experimental monoisotopic M_r.

Peptide	Abbreviation	Sequence	UPLC retention time (min)	Major *m/z* detected*	M_r experimental*,† (M_r theoretical)*
Tyrocidine A analogues (*Ff*)					
Phenycidine A‡,§	Phc A	Cyclo-(fP*Ff*NQ*F*VOL)	10.97	627.8367	1253.6578 (1253.6579)
Tyrocidine A	Trc A	Cyclo-(fP*Ff*NQ*Y*VOL)	10.56	635.8347	1269.6538 (1269.6546)
Tyrocidine A_1	Trc A_1	Cyclo-(fP*Ff*NQ*Y*VKL)	10.39	642.8423	1283.6690 (1283.6703)
Tryptocidine A	Tpc A	Cyclo-(fP*Ff*NQ*W*VOL)	11.13	647.3443	1292.6730 (1292.6706)
Tyrocidine B analogues (*Wf*)					
Tyrocidine B	Trc B	Cyclo-(fP*Wf*NQ*Y*VOL)	9.46	655.3398	1308.6640 (1308.6655)
Tyrocidine B_1	Trc B_1	Cyclo-(fP*Wf*NQ*Y*VKL)	9.26	662.3489	1322.6822 (1322.6812)
Tryptocidine B	Tpc B	Cyclo-(fP*Wf*NQ*W*VOL)	9.82	666.8477	1331.6798 (1331.6815)
Tyrocidine C analogues (*Ww*)					
Tyrocidine C	Trc C	Cyclo-(fP*Ww*NQ*Y*VOL)	8.65	674.8451	1347.6746 (1347.6764)
Tyrocidine C_1	Trc C_1	Cyclo-(fP*Ww*NQ*Y*VKL)	8.60	681.8536	1361.6916 (1361.6921)
Tryptocidine C‡	Tpc C	Cyclo-(fP*Ww*NQ*W*VOL)	9.07	686.3535	1370.6914 (1370.6924)
Linear gramicidin					
Val-gramicidin A	VGA	¶HCO-*V*GAlAvVvWl*W*lWlW-$NHCH_2CH_2OH$#	11.00	941.5469	1881.0782 (1881.0783)

Standard one-letter abbreviations for amino residues are used; O, ornithine. D-residues are shown in lower case and variable residues are shown in italics. Sequence data obtained from Tang *et al.* (1992) and identities were confirmed in our own MS-MS studies [refer to Tables S2–S11 and Spathelf (2010)].

*Monoisotopic *m/z*; M_r.

†Experimental M_r calculated using the following equation: $M_r=(m/z\times 2)-2\times 1.007825$.

‡Phc A and Tpc C previously known as tyrocidine E and D, respectively (Tang *et al.* 1992).

§Named in this study due to the Tyr^7 to Phe^7 modification.

¶N-terminal residue formylated (HCO).

#C-terminal residue blocked by ethanolamine ($NHCH_2CH_2OH$).

glucose, agar, HCl tryptone soy broth (TSB), LB broth, and the L-amino acids Lys and Arg were from Merck. The L-amino acids Cys, Phe, Tyr and Trp were from Sigma-Aldrich. Sterilization of media was achieved by filtration using either a 0.22 µm sterile bottle top filtration system from Whatman Klari-Flex or sterile syringes and 0.20 µm to 25 mm syringe filters from Lasec (Cape Town, South Africa). GS and a commercially obtained tyrothricin extract (Sigma) were used as positive controls in the antibacterial activity assays. Acetonitrile (HPLC grade, far-UV cut-off) was from Romil. Acquity UPLC BEH C_{18} (1.7 µm particle size, 2.1 mm × 100 mm) UPLC columns and Nova-Pak C_{18} (5 µm particle size, 60 Å pore size 150 mm × 3.9 mm) analytical HPLC columns were supplied by Waters-Millipore. Analytical-grade water was prepared by filtering water from a reverse osmosis plant through a Millipore-Q water purification system.

Pre-culturing of the producer strain. Single colonies of the *B. aneurinolyticus* ATCC 10068 producer strain were obtained from freezer stocks by culturing using normal sterile techniques on pre-culture plates (5.0 g peptone, 2.5 g yeast extract, 1.0 g glucose and 1.0 g skimmed milk powder, 15 g agar in 1.0 l water). Single colonies were selected and incubated while shaking at 220 r.p.m. for 24 h at 37 °C in Falcon tubes containing 5 ml TGS (tryptone, glucose and inorganic salts) culture media (Lewis *et al.*, 1945). Amino acid composition of the tryptone in TGS medium was determined by HPLC using the Pico-Tag method (Bidlingmeyer *et al.*, 1984) (Table S1, available in *Microbiology* Online).

Analysis of growth rates of *B. aneurinolyticus* ATCC 10068. A dilution series of single amino acids (Phe and Trp) ranging from 2.75

to 27.5 mM was performed in quintuplicate (n=5) in sterile flat-bottom microtitre plates. A pre-culture of *B. aneurinolyticus* was diluted four times into the wells of the microtitre plates using TGS culture media with or without supplemented amino acids at different concentrations. The inoculated plates were incubated at 37 °C and growth was monitored spectrophotometrically (595 nm) every hour for a period of 16 h using a Bio-Rad microtitre plate reader.

Analysis of effect of amino acids supplementation on tyrothricin yield. Concentrations of 5.5, 16.5 and 27.5 mM of amino acids (Phe, Trp, Tyr, Cys, Lys and Arg) were prepared. Triplicate sterile dilutions of the respective amino acids concentrations were performed using TGS culture medium, and the dilutions were inoculated with a pre-culture of *B. aneurinolyticus* and incubated for 10 days at 37 °C. They were then centrifuged for 5 min at 4500 ***g***, and the cell pellet freeze-dried and weighed. Tyrothricin was then extracted using 50 % acetonitrile, and freeze-dried for determination of crude yield and activity against *M. luteus*.

Antibacterial activity assays. *M. luteus* NCTC 8340 was cultured on LB broth to an OD_{620} of ~0.8 and then subcultured in TSB and grown to an OD_{620} of 0.6 for use in dose–response assays. The microtitre broth dilution method described by du Toit & Rautenbach (2000) and Lehrer *et al.* (1991) was used to test the antimicrobial activity of the peptides. Stock solutions (10 ×) of the analytically weighed tyrothricin extracts and commercial tyrocidine were prepared in 15 % ethanol (v/v) and diluted with media in order to determine activity over a concentration range of 0.8–200 μg ml^{-1}. All cultures were grown for 16 h at 37 °C in the presence of 1.5 % ethanol (v/v) to compensate for the effect of ethanol in the peptide samples. Growth was measured at 595 nm. The MIC was determined as the first dilution where no growth was detected.

High-throughput deep-well production of tyrothricin. A fourfold dilution of pre-cultured *B. aneurinolyticus* was prepared using TGS culture medium. Aliquots of 10 μl were pipetted into sterile deep 96-well plates containing 500 μl per well of TGS culture medium supplemented with quadruplicate dilutions (2.75–27.5 mM) of amino acids (Phe, Trp, Tyr, Cys, Lys and Arg). These microtitre plates were subsequently covered and incubated for 96 h at 37 °C.

The cultures in the deep-well plates were then acidified with HCl to pH 4.7 and allowed to stand at room temperature for 24 h. The deep-well plates were subsequently centrifuged for 60 min at 2200 ***g***. The pellet in each well was resuspended in 200 μl of 100 % acetonitrile and sonicated for 15 min. A further 200 μl of analytical-grade water was then added to each well and the microtitre plate was sonicated for a further 15 min followed by centrifugation for 30 min at 2200 ***g***. Thereafter, the respective extracts were pooled in analytically weighed vials and freeze-dried to allow for analytical determination of extract mass and analysis by UPLC linked to ES-MS.

ES-MS and UPLC-MS analysis of tyrothricin extracts. ES-MS was performed using a Waters Quadrupole Time-of-Flight Synapt G2. Samples were dissolved in 50 % (v/v) acetonitrile to 10.0 mg ml^{-1}, centrifuged at 8600 ***g*** for 10 min to remove particulates and then diluted to 1.00 mg ml^{-1} using analytical-grade water. Injections of 3 μl samples were introduced via a Waters Acquity UPLC into a Z-spray electrospray ionization source in positive mode for direct mass analysis. The peptide identities were confirmed with high-resolution MS (Table 1) and sequences via collision-induced dissociation (Tables S2–S11). For UPLC analysis, 3 μl samples were separated on an Acquity UPLC BEH C_{18} column at a flow rate of 0.450 ml min^{-1} using a 0.1 % trifluoroacetic acid (A) to acetonitrile (B) gradient (100 % A from 0 to 0.5 min for loading, gradient was from 0 to 58 % B from 0.5 to 12 min and then 58 to 90 % B from 12 to 13 min, column wash was at 90 % B from 13 to 13.5 min, reconditioning was done from 10 to 100 % A from 13.5 to 14 min and then 100 % A from 14 to 17 min). Analytes were subjected to a capillary voltage of 3.0 kV and cone voltages of 15 V at a temperature of 120 °C at the source. Data acquisition was performed by scanning the second analyser (MS_2) through the mass/charge ratio (m/z) range of 400–2000. Data were then analysed using TARGETLYNX 4.1 (MASSLYNX mass spectrometry software; Waters).

HPLC analysis of peptide extracts. Extracts obtained in 50 % acetonitrile (1 mg ml^{-1}, 10 μl injection) were analysed by reverse-phase HPLC using methodology described previously by Rautenbach *et al.* (2007).

RESULTS

Effect of amino acids supplementation on the growth and tyrothricin production of *B. aneurinolyticus* ATCC 10068

Having established the effects of certain key amino acids on the growth and antimicrobial peptide production of the producer strain, the ability of Phe and Trp, as well as selected amino acids (Tyr, Cys, Lys and Arg), to manipulate antimicrobial production was evaluated. Only supplementation of Phe and Trp had an effect on the tyrothricin production profile; however, these amino acids had a negative impact of the initial growth (primary growth phase) of *B. aneurinolyticus* ATCC 10068 when compared with growth in normal TGS medium (Table 2, Fig. 1). A secondary growth phase (diauxie) was observed in cultures where the growth medium was supplemented with Phe and Trp (Fig. 1, Table 2). The pronounced inhibitory effect of Trp supplementation on the initial growth was concentration dependent, as is evident from the delayed growth of the producer strain with increasing concentrations of Trp (Table 2). This effect, however, was overcome as increased biomass was observed after 96 h (results not shown), which was sustained during the 10 days of culturing (Table 2, Fig. 1). In contrast, supplementation with Phe initially only had a slight dampening effect on the growth of the producer strain (Fig. 1). After 96 h (results not shown) and 10 days (Table 2), increased biomass was obtained at the higher Phe concentrations.

The relative antibacterial activity of the extracts obtained from the cultures supplemented with increased amino acid concentrations was generally less than that of the commercial tyrothricin extract, as well as that of non-supplemented control. However, the 5.5 mM Phe and Trp, as well as 16.5 mM Phe, supplementation yielded high-activity extracts, whilst the 27.5 mM Phe- and other two Trp-supplemented cultures showed large decreases in activity despite an increase in the extract masses (Table 2).

Manipulation of antimicrobial production of *B. aneurinolyticus*

Using the novel, small-scale, high-throughput, deep 96-well plate culturing method the producer strain was

Table 2. Effect of supplementation of growth medium of *B. aneurinolyticus* with either Phe or Trp compared with the non-supplemented growth control

Condition (mM Phe or Trp)	Lag time (h)	First growth rate ± SEM (μ) (n=5)*	Second growth rate ± SEM (μ) (n=5)*	Per cent growth after 16 h ± SEM (n=5)†	Dry cell mass (g l^{-1})‡ (n=2)	Extract mass (g l^{-1})‡ (n=2)	Per cent IU ± SEM§ (MIC) (n=12)
Growth control	5	0.92 ± 0.02	–	100 ± 6.6	6.91 ± 0.29	2.29 ± 0.01	102 ± 2 (6.25)
Phe							
2.75	5	0.89 ± 0.03	0.32 ± 0.02	91.9 ± 3.5	–	–	–
4	5	0.85 ± 0.01	0.23 ± 0.03	160 ± 28	–	–	–
5.5	5	0.82 ± 0.03	0.22 ± 0.03	198 ± 30	6.14 ± 1.91	2.18 ± 0.36	91 ± 3 (3.125)
11	5	0.83 ± 0.02	0.22 ± 0.03	206 ± 34	–	–	–
16.5	5	0.78 ± 0.02	0.15 ± 0.03	178 ± 33	10.1 ± 0.41	2.85 ± 0.06	99 ± 3 (6.25)
22	6	0.79 ± 0.02	0.15 ± 0.02	136 ± 28	–	–	–
27.5	6	0.75 ± 0.01	0.15 ± 0.01	100 ± 6.0	10.6 ± 0.57	2.19 ± 0.16	69 ± 10 (12.5)
Trp							
2.75	6	0.75 ± 0.02	0.24 ± 0.04	57.5 ± 1.8	–	–	–
4	7	0.62 ± 0.02	0.24 ± 0.04	49.0 ± 2.4	–	–	–
5.5	7	0.59 ± 0.01	0.25 ± 0.02	48.8 ± 4.6	7.20 ± 3.45	2.10 ± 0.48	89 ± 5 (6.25)
11	8	0.46 ± 0.02	0.14 ± 0.01	46.2 ± 2.2	–	–	–
16.5	8	0.39 ± 0.01	0.13 ± 0.01	38.3 ± 1.1	7.95 ± 2.14	2.73 ± 0.68	62 ± 12 (12.5)
22	12	0.33 ± 0.02	0.13 ± 0.01	23.7 ± 0.3	–	–	–
27.5	14	0.09 ± 0.01	–	9.10 ± 0.1	7.96 ± 1.38	2.90 ± 0.58	10 ± 3 (25.0)

*Growth rate (μ) was determined as the $\Delta \ln OD_{595}/\Delta$ time during the exponential growth phase over 16 h.
†As determined from OD_{595} of culture after 16 h at 37 °C; calculated in terms of growth controls.
‡Determined after 10 days of cultivation at 37 °C.
§Per cent inhibition units (IU) defined as the percentage of the activity against *M. luteus* in terms of the MIC of commercial tyrothricin at 6.25 μg ml^{-1} (mean of 12 determinations).

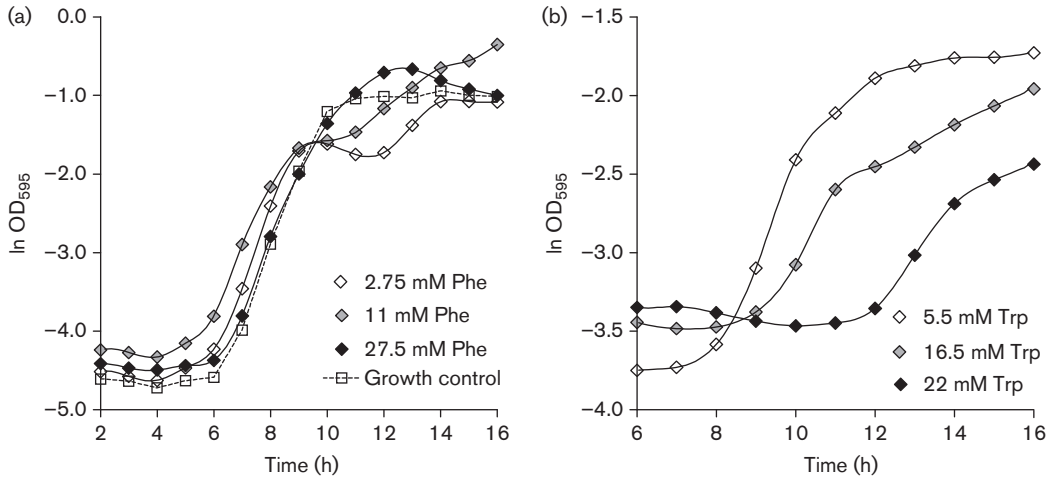

Fig. 1. Growth curves of *B. aneurinolyticus* in cultures supplemented with different concentrations of Phe (a) and Trp (b) showing pronounced diauxie. Each time point is the mean of quintuplicate determinations.

cultured in culture medium supplemented with the selected L-amino acids. The extracts obtained by growing *B. aneurinolyticus* ATCC 10068 in the TGS medium or L-amino acid-supplemented TGS medium were analysed by analytical HPLC and UPLC-MS (Fig. 2). In TGS medium the Trc A and B analogues (*Ff* and *Wf*) and Orn variants dominated the tyrothricin profile, whilst the Trc C analogue (*Ww*), Lys variants from the tyrocidine group and VGA from the gramicidin group were also observed in appreciable, but lower amounts (Table 1). The Orn variant-dominated production profile was found, regardless of amino acid supplementation. Moreover, the addition of Lys (or Arg) to culture medium did not shift the production profile towards the Lys-containing peptides (results not shown). We did not detect the Lys variants of Tpc A or Tpc C and detected only trace amounts of the Lys variants of Phc A and Tpc B, as well as the Ile variant of gramicidin A and Val-gramicidin B within the extracts. This result may possibly be accounted for when considering the endogenous low levels of the Lys variants and minor gramicidins, as well as the low solubility of gramicidins in polar solvents such as water (Hotchkiss & Dubos, 1941) and 50 % acetonitrile as used in the extraction and UPLC-MS methodology. Due to the extremely low amounts of these and other rare peptides in the extracts, we focused our analyses on the 10 major tyrocidines and analogues, and VGA as representative of the gramicidins, in our global analyses of the tyrothricin production profile.

From all the amino acids tested, only Phe- or Trp-supplemented cultures significantly altered the antimicrobial production profile of the producer strain relative to the non-supplemented control (Fig. 3). According to the amino acid analyses of tryptone used in our media, the TGS medium contained 3.4 mM Phe and 1 mM Trp in free form, and 1.9 mM Phe and 0.2 mM Trp in the less-available peptide/protein form (Table S1). A complete shift of the antimicrobial peptide production profiles occurred at the pivotal supplement concentrations of 5.5 mM Phe (total 10.8 mM Phe in medium) and 11 mM Trp (total 12.2 mM Trp in medium) (Fig. 4). Phe supplementation shifted the antimicrobial production profile toward the production of the Trc A analogues (denoted *Ff*), while VGA production was concomitantly inhibited with increasing concentrations of Phe (Fig. 4a). This correlated with the antibacterial activity of the 10 day extracts, as at the supplementation concentration of 5.5 mM Phe, the extract yielded an MIC of 3.125 μg ml^{-1}, a higher activity than the growth control extract and commercial tyrothricin. However, at the highest Phe concentration of 27.5 mM, a reduction in activity was observed (fourfold increase in the MIC), as well as a decrease in activity units. In contrast, Trp supplementation shifted the antimicrobial production profile towards the production of the Trc C analogues (denoted *Ww*), as well as increasing VGA production (Fig. 4b). Trp supplementation led to a reduction in antimicrobial activity with increased Trp concentrations. The 5.5 mM Trp-supplemented culture extract yielded a MIC of 6.25 μg ml^{-1} equivalent to that of both the controls. However, the MIC doubled with the extracts from 16.5 and 27.5 mM Trp supplementation, correlating with the reduced activity units of 62 % and 10 %, respectively (Table 2).

Having established the effect on the antimicrobial production profile of the producer strain through supplementation of the growth media with both Phe and Trp alone, the effect of supplementation with different combinations of Phe and Trp was evaluated. The concentration of supplemented Phe was varied from 2.75 to 27.5 mM, together with fixed concentrations of Trp of 5.5, 11 or 16.5 mM, respectively (Fig. 5). Supplementation with a combination of Phe together with Trp led to a shift in the antimicrobial peptide production profile toward predominantly the Trc B

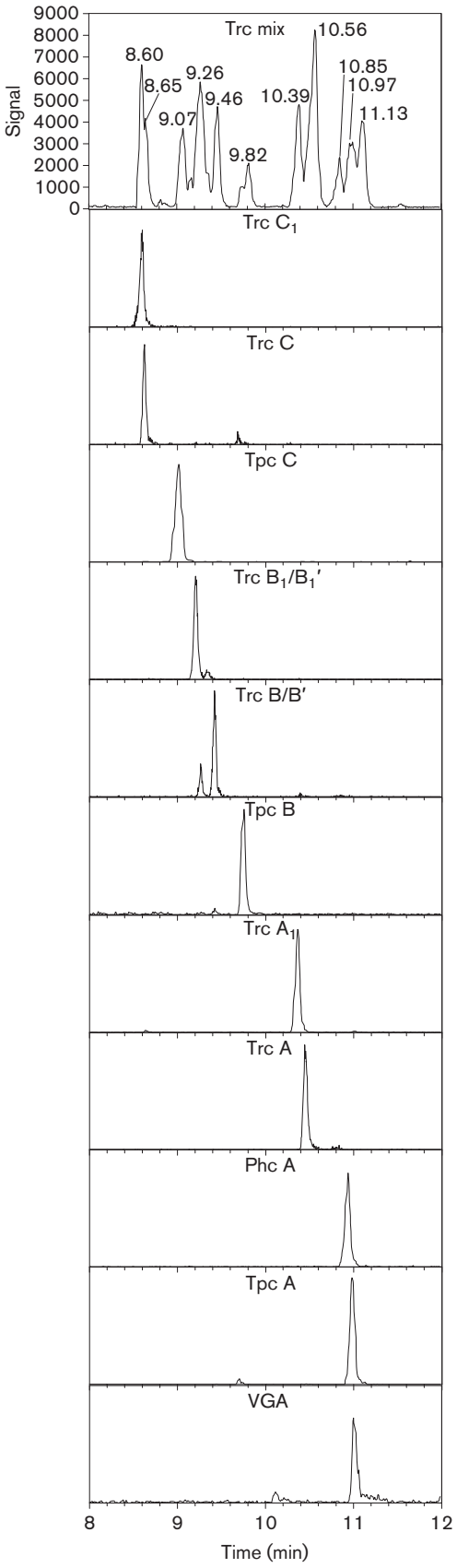

Fig. 2. UPLC-MS chromatograms depicting the separation of a mixture of the different tyrocidines, their analogues and VGA in this study. The retention time for each of the peaks is given in the top figure and the *y*-axis depicts the ES-MS signal. The small fronting Trc B peak and trailing Trc B_1 peak are the minor Trc B/B_1 analogues with an inverted aromatic dipeptide unit (Trc B′ and B_1′, respectively). Details of the primary structures are given in Table 1.

analogues. A supplement concentration of 5.5 mM Trp led to domination of the *Ww* subset, with the *Ww* to *Wf* analogue shift observed with addition of 2.5 mM Phe, *Wf* to *Ff* at 11 mM Phe, and only at 27.5 mM Phe did the *Ff* subset equal the *Ww* subset (Fig. 5a). As expected, these shifts in antimicrobial peptide subset production only occurred at much higher concentrations of Phe when higher Trp concentrations were supplemented in the media (Fig. 5b, c).

When all the Trp and Phe supplementation data and total concentrations of these amino acids in the media were considered in combined graphs (Fig. 6a, b), the production trends again showed that ~75 % Phe (<0.2 Trp : Phe) was needed for *Ff* > *Ww* and >80 % Phe was needed for *Ff* > *Wf*. The *Wf* subset was sensitive to the Phe and Trp contribution and dominated only in the narrow 60–80 % Phe concentration range (Fig. 6). Conversely, a >40 % Trp contribution or a ratio of Trp : Phe >0.8 led to the dominance of the Trc C analogues (*Ww*), at the expense of both the Trc A (*Ff*) and B (*Wf*) analogues (Fig. 6). VGA production increased initially, following the Trc C analogue increase, but then the VGA concentration remained relatively constant with increasing Trp contribution (results not shown).

DISCUSSION

Two key amino acids (Phe and Trp) had a major effect on the growth and total tyrothricin production. The diauxic growth observed in the cultures supplemented with amino acids is similar to that observed by Vandamme & Demain (1976) in *B. brevis* ATCC 9999, the GS producer strain. They found *B. brevis* initially grew at the expense of amino acids supplemented in the growth medium; only after a diauxic lag was the available carbon source utilized and antimicrobial peptide production initiated.

The initial lag in the growth of the cultures supplemented with Trp which was far less evident in the Phe-supplemented cultures may possibly be due to the toxic effects of Trp, which were overcome over an extended growth period. Stokes & Woodward (1943) reported an inhibition of tyrothricin production in submerged, aerated cultures supplemented with 0.5 % (w/v) of Trp, which equated to a molar concentration of 24.5 mM. In the present study, biomass production was initially lower, but this was overcome after 96 h of culturing where biomass and extract masses were similar to that of the control after

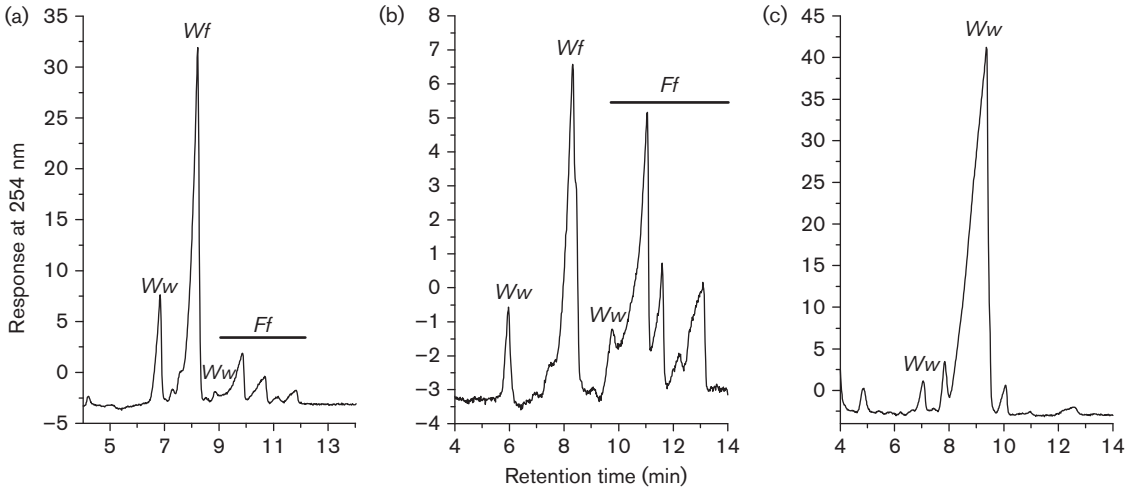

Fig. 3. Analytical HPLC chromatograms visualized at 254 nm depicting the peptide production profiles of the extracts obtained from cultures of *B. aneurinolyticus* ATCC 10068 grown in non-supplemented medium (a) or altered by supplementation of the medium with 5.5 mM Phe (b) or 5.5 mM Trp (c).

the culmination of the culturing period at 10 days (Table 2). However, if the antimicrobial activity determined in the 27.5 mM Trp extract is considered, our results correlate well with those of Stokes & Woodward (1943). In contrast, the antimicrobial activity in the extracts of all the Phe-supplemented cultures was particularly high, directly correlating with the good biomass yields.

Analysis of the tyrothricin extracts by UPLC-MS revealed only Phe and Trp supplementation significantly altered the tyrothricin production profile *B. aneurinolyticus*. These results are similar to those of Demain & Matteo (1976) who found that Phe did not stimulate growth, but it did stimulate GS production in *B. brevis* ATCC 9999 by acting as a precursor for the initiation module, which is similar to the module for tyrocidine initiation. In contrast, we found Phe supplementation stimulated growth and also production of *Ff* tyrocidine subsets more than the linear gramicidins (i.e. VGA) in *B. aneurinolyticus* (Table 2, refer to Fig. 4). In the non-supplemented culture medium the

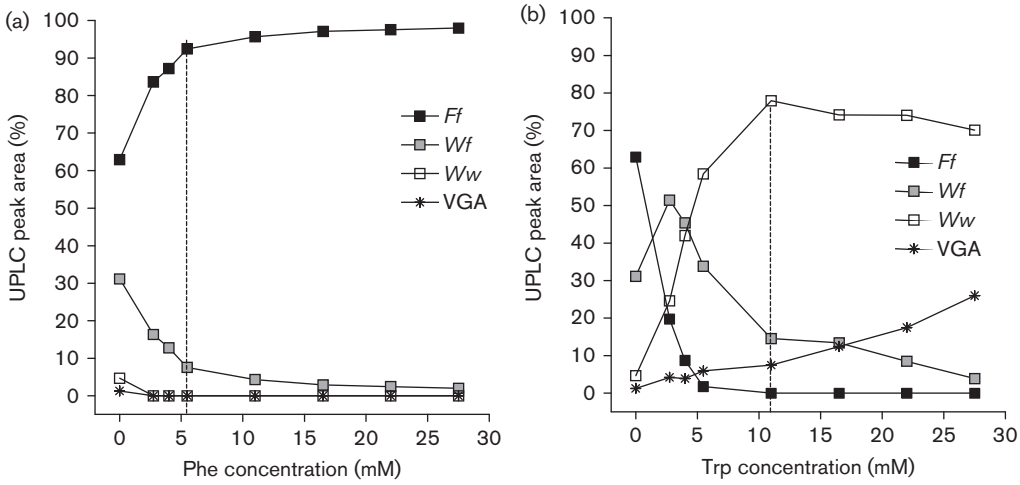

Fig. 4. Peptide production profiles of the extracts obtained from cultures of *B. aneurinolyticus* ATCC 10068 grown in medium supplemented with 2.75–27.5 mM of either: (a) Phe, resulting in predominantly the production of the Trc A analogues (*Ff*), or (b) Trp, resulting in predominantly the production of the Trc C analogues (*Ww*) together with VGA, relative to the non-supplemented control. The contribution of each analogue was calculated as a percentage of the sum of the total UPLC peak areas observed for the different peptides. The dotted lines show the pivotal Phe or Trp concentrations where one peptide subset dominated in the tyrothricin extract.

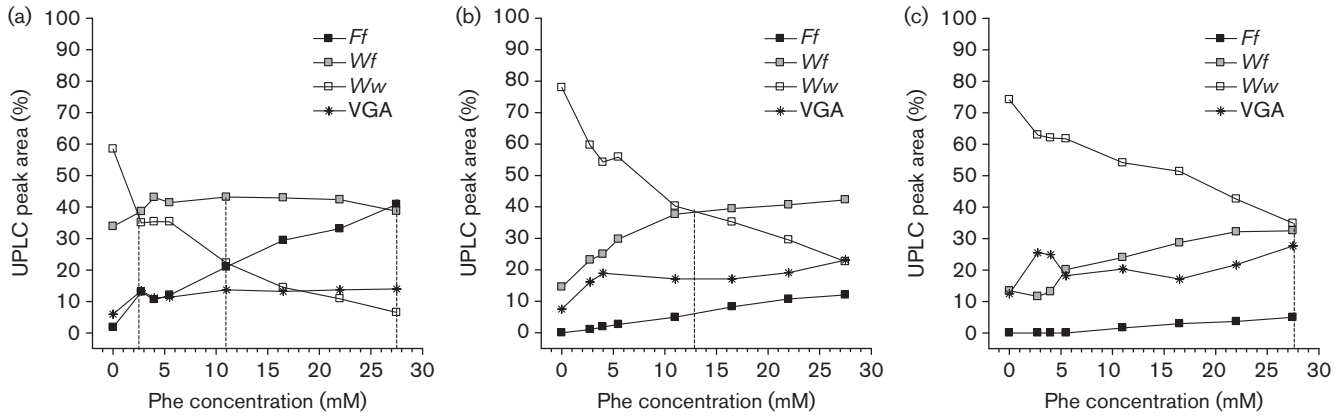

Fig. 5. Peptide production profiles of the extracts obtained from cultures of *B. aneurinolyticus* ATCC 10068 grown in medium supplemented with 2.75–27.5 mM Phe together with either: (a) 5.5, (b) 11 or (c) 16.5 mM Trp; relative to the non-supplemented control. The contribution of each analogue was calculated as a percentage of the sum of the total UPLC peak areas observed for the different peptides. The dotted lines show the Phe concentration that led to production change from one peptide subset to another.

producer strain predominantly produced Trc A and B analogues as well as low levels of VGA. Supplementation of the growth medium with either Trp or Phe above the pivotal concentrations of 5.5 and 11 mM, respectively, shifted the antimicrobial production profile between two extremes of the Phe-containing peptides and Trp-containing peptides (Fig. 4). In general, Phe supplementation shifted the production towards peptides with high Phe content and Phe in position 4 of the tyrocidine structure (*Ff*, Trc A and analogues). Phe supplementation suppressed not only the production of the Trc B and C analogues, but also that of VGA. This shift is beneficial as we found purification of Trc A analogues to be quite difficult in the presence of gramicidins. In contrast, Trp supplementation enhanced the production of the Trc C analogues (Trp in position 4), similar to what was observed

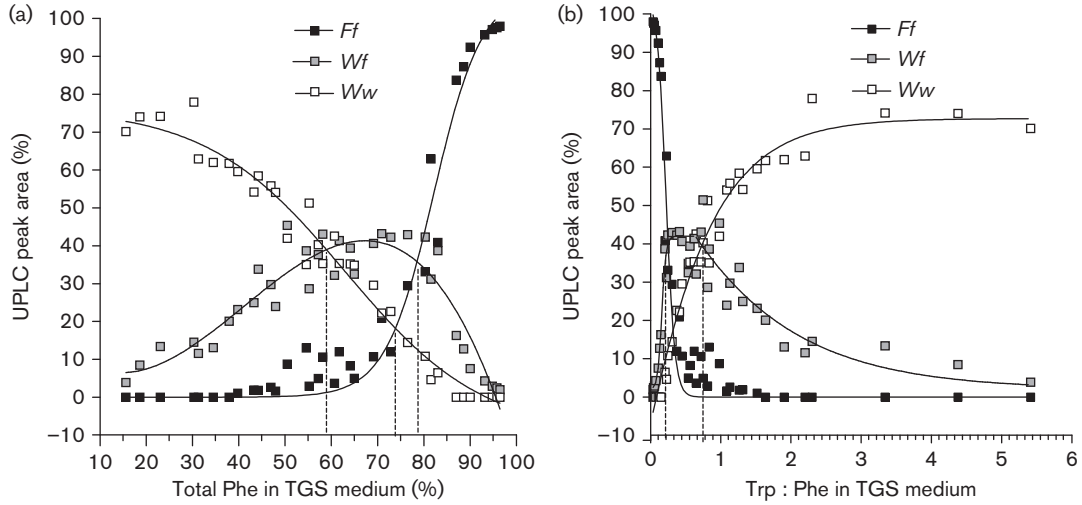

Fig. 6. General trends of tyrocidine production as related to the per cent total Phe (molar content) in the TGS medium (including tryptone contribution) (a) and consequent Trp : Phe ratio (total Trp and Phe) in the TGS medium (b). The dotted lines show the per cent Phe (molar content) and major Trp : Phe ratio for production change from one peptide subset to another. All the UPLC-derived production data from Figs 4 and 5 were plotted. The best trend line fits were sigmoidal curves with $R^2>0.97$ for all (two opposing sigmoidal curves were fitted to *Wf* in b), except for *Wf* in (a) where only a third-order polynomial could be fitted.

by Ruttenberg & Mach (1966), but also the production of gramicidin A, which also contains a Trp in the variable aromatic residue position (Figs 2, 3 and 4).

Supplementation of both Trp and Phe led to a major loss in the peptides with high Phe content at >20 % Trp in supplement, and peptides with both Trp and Phe in their structure (*Wf*, Trc B analogues) increased as the Trp : Phe ratio approached 1 : 1 (Fig. 6b). The supplementation of 5.5 mM Trp to the culture medium gave an ~55 % molar content of Trp, and hence both the *Ww* and *Wf* subsets were produced. Further Trp concentration increase to >60 % Trp led predominantly to the production of the C analogues (*Ww*) together with the Trp-rich VGA (Figs 5c and 6a). These studies also clarify the predominance of Trc A (*Ff*) and B analogues (*Wf*) produced by *B. aneurinolyticus* in the non-supplemented TGS culture medium. The only source of amino acids in the non-supplemented TGS medium is from the trypsin-digested casein in the tryptone added to the media. From the amino acid analysis of the tryptone it was calculated that there was >80 % free Phe molar content in terms of total Trp + Phe concentration in the non-supplemented medium and hence production of the *Ff* subset (Trc A analogues) predominates, with some *Wf* subset production. The latter is most probably due to the availability of ~100 % free Trp versus 64 % free Phe.

These peptide subset shifts are probably due to a balance between the aromatic amino acid affinity of the peptide synthetases and increased availability of Phe or Trp. Mootz & Marahiel (1997) found the adenylation domain of the related tyrocidine producer strain *B. aneurinolyticus* ATCC 8185, responsible for incorporation of either Phe or Trp at position 4, had an affinity approximately fivefold higher for Trp (Mootz & Marahiel, 1997). Therefore, the proportion of each of the antimicrobial peptides produced due to the incorporation of the variable residues was dependent not only on amino acid availability within the growth media (Ruttenberg & Mach, 1966) and subsequent transport into the cells, but also on the affinity of the peptide synthetases for the respective residues (Mootz & Marahiel, 1997).

Knowledge of the identity of the different antimicrobial peptides produced under the different conditions also explained the variation in antibacterial activity of our different extracts (Table 2). Increased Trp supplementation led to not only an increase in the production of the Trc C analogues (*Ww*), but also that of VGA (Fig. 4b). Aranda & de Kruijff (1988) reported the disruption of model membranes by the tyrocidines to be antagonized by VGA. Hence, increased VGA production, particularly in the 16.5 and 27.5 mM Trp-supplemented cultures, accounts for the significant loss in activity observed with increasing Trp supplementation (Table 2).

When considering the Phe-supplemented cultures, both the 5.5 and 16.5 mM Phe extracts showed potent activity that may relate to an optimal *Ff* to *Wf* tyrocidine combination and very low VGA in the extracts. However, there was a drop in the extract mass as well as activity with supplementation of 27.5 mM Phe (Table 2). Spathelf & Rautenbach (2009) reported that the Trc B analogues (*Wf*) had greater antibacterial activity than the Trc A analogues (*Ff*). Therefore, the observed loss in activity may possibly be accounted for when considering the shift in antimicrobial production away from the production of a combination of the Trc A (*Ff*) and B (*Wf*) analogues at lower concentrations of Phe, toward the sole production of the Trc A analogues at increased Phe concentrations. The drop in extract mass observed at the increased Phe concentration could be due to growth inhibition at high amino acid concentrations or aggregation of the hydrophobic *Ff* peptides at high concentrations leading to loss during extraction. However, these hypotheses remain to be investigated, as well as possible interactions between the different tyrocidine analogues and VGA, which may affect their activity in extracts.

CONCLUSION

Our studies showed that the availability of the aromatic amino acids, Phe and Trp, had a major role in the highly controlled antimicrobial peptide production profile of *B. aneurinolyticus* ATCC 10068. We have also demonstrated clearly that selected analogues could be produced by simply changing the availability and ratios of Phe and Trp within the culture medium. From these studies it is possible to design large-scale production cultures to produce tailored antimicrobial peptide complexes such as the Trc B and C analogues targeting Gram-positive bacteria (Spathelf & Rautenbach, 2009), and Trc A analogues targeting the human malaria parasite, *P. falciparum* (Rautenbach *et al.*, 2007).

REFERENCES

Appleby, J. C., Knowles, E., Pearson, J. & White, T. (1947a). A preliminary study of the formation, assay and stability of tyrothricin. *J Gen Microbiol* **1**, 137–144.

Appleby, J. C., Knowles, E., Mcallister, R., Pearson, J. & White, T. (1947b). The production of tyrothricin by submerged culture of *Bacillus brevis* in synthetic media. *J Gen Microbiol* **1**, 145–157.

Aranda, F. J. & de Kruijff, B. (1988). Interrelationships between tyrocidine and gramicidin A′ in their interaction with phospholipids in model membranes. *Biochim Biophys Acta* **937**, 195–203.

Arima, K., Kakinuma, A. & Tamura, G. (1968). Surfactin, a crystalline peptidelipid surfactant produced by *Bacillus subtilis*: isolation, characterization and its inhibition of fibrin clot formation. *Biochem Biophys Res Commun* **31**, 488–494.

Baron, A. L. (1949). Preparation of tyrothricin. US Patent 2482832.

Bidlingmeyer, B. A., Cohen, S. A. & Tarvin, T. L. (1984). Rapid analysis of amino acids using pre-column derivatization. *J Chromatogr A* **336**, 93–104.

Bradshaw, J. P. (2003). Cationic antimicrobial peptides: issues for potential clinical use. *BioDrugs* **17**, 233–240.

Brown, E. D. & Wright, G. D. (2005). New targets and screening approaches in antimicrobial drug discovery. *Chem Rev* **105**, 759–774.

Brul, S. & Coote, P. (1999). Preservative agents in foods. Mode of action and microbial resistance mechanisms. *Int J Food Microbiol* **50**, 1–17.

Cleveland, J., Montville, T. J., Nes, I. F. & Chikindas, M. L. (2001). Bacteriocins: safe, natural antimicrobials for food preservation. *Int J Food Microbiol* **71**, 1–20.

Cooper, D. G., Macdonald, C. R., Duff, S. J. & Kosaric, N. (1981). Enhanced production of surfactin from *Bacillus subtilis* by continuous product removal and metal cation additions. *Appl Environ Microbiol* **42**, 408–412.

De Bolle, M. F., Osborn, R. W., Goderis, I. J., Noe, L., Acland, D., Hart, C. A., Torrekens, S., Van Leuven, F. & Broekaert, W. F. (1996). Antimicrobial peptides from *Mirabilis jalapa* and *Amaranthus caudatus*: expression, processing, localization and biological activity in transgenic tobacco. *Plant Mol Biol* **31**, 993–1008.

Demain, A. L. & Matteo, C. C. (1976). Phenylalanine stimulation of gramicidin S formation. *Antimicrob Agents Chemother* **9**, 1000–1003.

Desai, J. D. & Banat, I. M. (1997). Microbial production of surfactants and their commercial potential. *Microbiol Mol Biol Rev* **61**, 47–64.

Drouin, C. M. & Cooper, D. G. (1992). Biosurfactants and aqueous two-phase fermentation. *Biotechnol Bioeng* **40**, 86–90.

du Toit, E. A. & Rautenbach, M. (2000). A sensitive standardised micro-gel well diffusion assay for the determination of antimicrobial activity. *J Microbiol Methods* **42**, 159–165.

Dubos, R. J. (1939). Studies on a bactericidal agent extracted from a soil bacillus: I. preparation of the agent. Its activity in vitro. *J Exp Med* **70**, 1–10.

Dubos, R. J. & Cattaneo, C. (1939). Studies on a bactericidal agent extracted from a soil bacillus: III. Preparation and activity of a protein-free fraction. *J Exp Med* **70**, 249–256.

Dubos, R. J. & Hotchkiss, R. D. (1941). The production of bactericidal substances by aerobic sporulating bacilli. *J Exp Med* **73**, 629–640.

François, I. E. J. A., De Bolle, M. F. C., Dwyer, G., Goderis, I. J. W. M., Woutors, P. F. J., Verhaert, P. D., Proost, P., Schaaper, W. M. M., Cammue, B. P. A. & Broekaert, W. F. (2002). Transgenic expression in Arabidopsis of a polyprotein construct leading to production of two different antimicrobial proteins. *Plant Physiol* **128**, 1346–1358.

Gong, G., Zheng, Z., Chen, H., Yuan, C., Wang, P., Yao, L. & Yu, Z. (2009). Enhanced production of surfactin by *Bacillus subtilis* E8 mutant obtained by ion beam implantation. *Food Technol Biotechnol* **47**, 27–31.

Gordon, Y. J., Romanowski, E. G. & McDermott, A. M. (2005). A review of antimicrobial peptides and their therapeutic potential as anti-infective drugs. *Curr Eye Res* **30**, 505–515.

Gruenewald, S., Mootz, H. D., Stehmeier, P. & Stachelhaus, T. (2004). *In vivo* production of artificial nonribosomal peptide products in the heterologous host *Escherichia coli*. *Appl Environ Microbiol* **70**, 3282–3291.

Hancock, R. E. W. & Lehrer, R. (1998). Cationic peptides: a new source of antibiotics. *Trends Biotechnol* **16**, 82–88.

Hancock, R. E. W. & Sahl, H. G. (2006). Antimicrobial and host-defense peptides as new anti-infective therapeutic strategies. *Nat Biotechnol* **24**, 1551–1557.

Hiraoka, H., Asaka, O., Ano, T. & Shoda, M. (1992). Characterization of *Bacillus subtilis* RB14, coproducer of peptide antibiotics iturin A and surfactin. *J Gen Appl Microbiol* **38**, 635–640.

Hotchkiss, R. D. & Dubos, R. J. (1941). The isolation of bactericidal substances from cultures of *Bacillus brevis*. *J Biol Chem* **141**, 155.

Huang, X., Suo, J. & Cui, Y. (2011). Optimization of antimicrobial activity of surfactin and polylysine against *Salmonella enteritidis* in milk evaluated by a response surface methodology. *Foodborne Pathog Dis* **8**, 439–443.

Javadpour, M. M., Juban, M. M., Lo, W. C., Bishop, S. M., Alberty, J. B., Cowell, S. M., Becker, C. L. & McLaughlin, M. L. (1996). De novo antimicrobial peptides with low mammalian cell toxicity. *J Med Chem* **39**, 3107–3113.

Kessler, N., Schuhmann, H., Morneweg, S., Linne, U. & Marahiel, M. A. (2004). The linear pentadecapeptide gramicidin is assembled by four multimodular nonribosomal peptide synthetases that comprise 16 modules with 56 catalytic domains. *J Biol Chem* **279**, 7413–7419.

Keymanesh, K., Soltani, S. & Sardari, S. (2009). Application of antimicrobial peptides in agriculture and food industry. *World J Microbiol Biotechnol* **25**, 933–944.

King, T. P. & Craig, L. C. (1955a). The chemistry of tyrocidine. IV. Purification and characterization of tyrocidine B. *J Am Chem Soc* **77**, 6624–6627.

King, T. P. & Craig, L. C. (1955b). The chemistry of tyrocidine. V. The amino acid sequence of tyrocidine B. *J Am Chem Soc* **77**, 6627–6631.

Lee, J. H., Kim, J. H., Hwang, S. W., Lee, W. J., Yoon, H. K., Lee, H. S. & Hong, S. S. (2000). High-level expression of antimicrobial peptide mediated by a fusion partner reinforcing formation of inclusion bodies. *Biochem Biophys Res Commun* **277**, 575–580.

Lehrer, R. I., Rosenman, M., Harwig, S. S. S. L., Jackson, R. & Eisenhauer, P. (1991). Ultrasensitive assays for endogenous antimicrobial polypeptides. *J Immunol Methods* **137**, 167–173.

Lewis, J., Dimick, K. P. & Feustel, I. (1945). Production of tyrothricin in cultures of *Bacillus brevis*. *Ind Eng Chem Res* **37**, 996–1004.

Li, Y. (2011). Recombinant production of antimicrobial peptides in *Escherichia coli*: a review. *Protein Expr Purif* **80**, 260–267.

Liu, Q., Yuan, H., Wang, J., Gong, G., Zhou, W., Fan, Y., Wang, L., Yao, J. & Yu, Z. (2006). A mutant of *Bacillus subtilis* with high-producing surfactin by ion beam implantation. *Plasma Sci Technol* **8**, 491–496.

Mach, B. & Tatum, E. L. (1964). Environmental control of amino acid substitutions in the biosynthesis of the antibiotic polypeptide tyrocidine. *Proc Natl Acad Sci U S A* **52**, 876–884.

Marahiel, M. A., Zuber, P., Czekay, G. & Losick, R. (1987). Identification of the promoter for a peptide antibiotic biosynthesis gene from *Bacillus brevis* and its regulation in *Bacillus subtilis*. *J Bacteriol* **169**, 2215–2222.

Marr, A. K., Gooderham, W. J. & Hancock, R. E. (2006). Antibacterial peptides for therapeutic use: obstacles and realistic outlook. *Curr Opin Pharmacol* **6**, 468–472.

Matsuzaki, K., Harada, M., Funakoshi, S., Fujii, N. & Miyajima, K. (1991). Physicochemical determinants for the interactions of magainins 1 and 2 with acidic lipid bilayers. *Biochim Biophys Acta* **1063**, 162–170.

Matsuzaki, K., Sugishita, K., Fujii, N. & Miyajima, K. (1995). Molecular basis for membrane selectivity of an antimicrobial peptide, magainin 2. *Biochemistry* **34**, 3423–3429.

Moon, W. J., Hwang, D. K., Park, E. J., Kim, Y. M. & Chae, Y. K. (2007). Recombinant expression, isotope labeling, refolding, and purification of an antimicrobial peptide, piscidin. *Protein Expr Purif* **51**, 141–146.

Mootz, H. D. & Marahiel, M. A. (1997). The tyrocidine biosynthesis operon of *Bacillus brevis*: complete nucleotide sequence and biochemical characterization of functional internal adenylation domains. *J Bacteriol* **179**, 6843–6850.

Mulligan, C. N., Chow, T. Y.-K. & Gibbs, B. F. (1989). Enhanced biosurfactant production by a mutant *Bacillus subtilis* strain. *Appl Microbiol Biotechnol* **31**, 486–489.

Ohno, A., Ano, T. & Shoda, M. (1992). Production of a lipopeptide antibiotic surfactin with recombinant *Bacillus subtilis*. *Biotechnol Lett* **14**, 1165–1168.

Ohno, A., Ano, T. & Shoda, M. (1995). Production of a lipopeptide antibiotic, surfactin, by recombinant *Bacillus subtilis* in solid state fermentation. *Biotechnol Bioeng* **47**, 209–214.

Paladini, A. & Craig, L. C. (1954). The chemistry of tyrocidine. III. The structure of tyrocidine A. *J Am Chem Soc* **76**, 688–692.

Qin, C., Zhong, X., Bu, X., Ng, N. L. J. & Guo, Z. (2003). Dissociation of antibacterial and hemolytic activities of an amphipathic peptide antibiotic. *J Med Chem* **46**, 4830–4833.

Rammelkamp, C. H. & Weinstein, L. (1942). Toxic effects of tyrothricin, gramicidin and tyrocidine. *J Infect Dis* **71**, 166–173.

Rankin, L. (1944). The use of tyrothricin in the treatment of ulcers of the skin. *Am J Surg* **65**, 391–392.

Rautenbach, M., Vlok, N. M., Stander, M. & Hoppe, H. C. (2007). Inhibition of malaria parasite blood stages by tyrocidines, membrane-active cyclic peptide antibiotics from *Bacillus brevis*. *Biochim Biophys Acta* **1768**, 1488–1497.

Rautenbach M., Troskie A. M., De Beer A. & Vosloo J. A. (2013). Antimicrobial peptide formulations for plants. PCT Patent PCT/IB 2013/051457.

Robinson, H. J. & Molitor, H. (1942). Some toxicological and pharmacological properties of gramicidin, tyrocidine and tyrothricin. *J Pharmacol Exp Ther* **74**, 75–82.

Ruttenberg, M. A. & Mach, B. (1966). Studies on amino acid substitution in the biosynthesis of the antibiotic polypeptide tyrocidine. *Biochemistry* **5**, 2864–2869.

Ruttenberg, M. A., King, T. P. & Craig, L. C. (1965). The chemistry of tyrocidine. VI. The amino acid sequence of tyrocidine C. *Biochemistry* **4**, 11–18.

Sandrin, C., Peypoux, F. & Michel, G. (1990). Coproduction of surfactin and iturin A, lipopeptides with surfactant and antifungal properties, by *Bacillus subtilis*. *Biotechnol Appl Biochem* **12**, 370–375.

Sheppard, J. D. & Mulligan, C. N. (1987). The production of surfactin by *Bacillus subtilis* grown on peat hydrolysate. *Appl Microbiol Biotechnol* **27**, 110–116.

Spathelf, B. M. (2010). *Qualitative structure-activity relationships of the major tyrocidines, cyclic decapeptides from* Bacillus aneurinolyticus. PhD thesis, Stellenbosch University, Department of Biochemistry, Stellenbosch, South Africa.

Spathelf, B. M. & Rautenbach, M. (2009). Anti-listerial activity and structure-activity relationships of the six major tyrocidines, cyclic decapeptides from *Bacillus aneurinolyticus*. *Bioorg Med Chem* **17**, 5541–5548.

Stokes, J. L. & Woodward, C. R. (1943). Formation of tyrothricin in submerged cultures of *Bacillus brevis*. *J Bacteriol* **46**, 83–88.

Tang, X. J., Thibault, P. & Boyd, R. K. (1992). Characterization of the tyrocidine and gramicidine fractions of the tyrothricin complex from *Bacillus brevis* using liquid chromatography and mass spectrometry. *Int J Mass Spectrom Ion Process* **122**, 153–179.

Vandamme, E. J. & Demain, A. L. (1976). Nutrition of *Bacillus brevis* ATCC 9999, the producer of gramicidin S. *Antimicrob Agents Chemother* **10**, 265–273.

Yarus, S., Rosen, J. M., Cole, A. M. & Diamond, G. (1996). Production of active bovine tracheal antimicrobial peptide in milk of transgenic mice. *Proc Natl Acad Sci U S A* **93**, 14118–14121.

Yeaman, M. R. & Yount, N. Y. (2003). Mechanisms of antimicrobial peptide action and resistance. *Pharmacol Rev* **55**, 27–55.

Yeh, M. S., Wei, Y. H. & Chang, J. S. (2005). Enhanced production of surfactin from *Bacillus subtilis* by addition of solid carriers. *Biotechnol Prog* **21**, 1329–1334.

Edited by: J. Stülke

Manipulation of the tyrothricin production profile of *Bacillus aneurinolyticus*

Johan Arnold Vosloo, Marietjie A. Stander, Adrienne N.-N. Leussa,
Barbara M. Spathelf and Marina Rautenbach*

*Communicating author: mra@sun.ac.za

SUPPLEMENTARY DATA

METHODS

Amino acid analysis of tryptone

Vacuum-dried samples of 1.5% tryptone in water were analysed for amino acid composition after a shortened 1 hour gaseous phase hydrochloric acid hydrolysis (6M HCl, 1% phenol, 150°C) or 24 hour liquid hydrolysis using methane sulfonic acid (4M MSA, 0.2% tryptamine) at 110°C (Cohen *et al.*. Pico-Tag® manual)**.** Amino acid analyses were done via HPLC using a pre-column derivatisation of samples with phenylisothiocyanate (PITC), according to the Pico-Tag® method (Bidlingmeyer *et al.*1984, Cohen *et al.*. Pico-Tag® manual).

ESMS sequencing of peptides

MS-MS sequencing of the six major tyrocidines (Trc A, A_1, B, B_1, C, and C_1) and TrpC were performed using a Waters Q-TOF Ultima mass spectrometer fitted with an electrospray ionisation source. Capillary voltage was 3.5 kV with the source temperature and cone voltage set at 100 ºC and 35 V, respectively. MS-MS analyses were performed by injecting 30 µL of peptide solution (100 µg/mL in acetonitrile/ water, 1:1, *v/v*) into the mass spectrometer and subjecting the selected molecular species to decomposition at collision energy of 40 eV. Data was collected in MS_2 through m/z = 100-1999.

For sequence analysis of TpcA, TpcB and PhcA we utilised a Waters Q-TOF Synapt mass spectrometer fitted with a Z-spray electrospray ionisation source. Capillary voltage was 3.5 kV with the source temperature and cone voltage was set at 120 ºC and 15 V, respectively. MS–MS analyses were performed by injecting 2 µL peptide solution (200 µg/mL in acetonitrile/water, 1:1, *v/v*) was introduced into spectrometer via a Waters Acquity UPLC™. CID of selected molecular ions was performed with collision energy of argon gas at a gas pressure of 10-15 psi in MS_2 with the collision energy ramp from 15 to 60 eV. The second analyzer was scanned from m/z = 40 to 1400. Fragment ions are named according to the principal established by Roepstorff and Fohlmann (1984), as revised by Biemann and Martin (1988).

RESULTS

Amino acid composition of tryptone used in culture medium

Table S1 Amino acid concentrations of the 1.5% tryptone used in culture medium in comparison with literature values obtained for 1.5% casein. The tryptone amino acid concentrations are the average of 3-8 determinations.

Amino acid	Casein: total [Amino acid] ±SEM (mM)[$]	Tryptone: total [amino acid] ±SEM (mM)	Tryptone: free [amino acid] ± SEM (mM)
Alanine	5.5 ± 0.2	5.5 ± 0.1	2.6 ± 0.2
Arginine	3.5 ± 0.1	3.2 ± 0.1	3.4 ± 0.2
Aspartic acid	8.4 ± 0.2	7.1 ± 0.1	0.6 ± 0.05
Cystine	0.5 ± 0.1	ND	0.7 ± 0.1
Glutamic acid	22.5 ± 0.6	17.3 ± 0.3	2.2 ± 0.1
Glycine	4.5 ± 0.6	4.9 ± 0.05	1.0 ± 0.1
Histidine	3.1 ± 0.1	2.3 ± 0.1	0.5 ± 0.04
Isoleucine	6.9 ± 0.1	6.4 ± 0.2	1.8 ± 0.2
Leucine	10.9 ± 0.2	10.4 ± 0.3	7.3 ± 0.4
Lysine	8.5 ± 0.2	9.8 ± 0.1	9.3 ± 0.7
Methionine	3.0 ± 0.1	2.8 ± 0.1	1.6 ± 0.2
Phenylalanine	4.8 ± 0.2	5.3 ± 0.1	3.4 ± 0.2
Proline	15.3 ± 0.2	13.1 ± 0.2	0.5 ± 0.01
Serine	9.1 ± 0.3	8.0 ± 0.2*	1.5 ± 0.2
Threonine	6.1 ± 0.3	4.6 ± 0.1*	1.5 ± 0.1
Tryptophan	1.0 ± 0.1	1.2 ± 0.1	1.0 ± 0.1
Tyrosine	5.5 ± 0.2	3.1 ± 0.4*	0.8 ± 0.1
Valine	9.1 ± 0.1	7.8 ± 0.3	2.6 ± 0.4

[$] Literature values from Gordon *et al.* (1949); Sundararajan & Sarma (1957); Ellinger & Boyne (1965)

* Corrected respectively for 17% (Ser), 13% (Thr) and 11% (Tyr) loss during hydrolysis.

ND, not determined

MS-MS sequencing of tyrocidines and analogues in this study

Table S2 Summary of fragment assignment of the major product ions generated by CID of the *m/z*=1270.7 molecular ion of tyrocidine A

m/z observed	Proposed ring opening	Proposed fragment type	*m/z* calculated	Sequence
1270.67	-	$[M+H]^+$	1270.66	cyclo($P^2F^3f^4N^5Q^6Y^7V^8O^9L^{10}f^1$)
1105.60	Phe^1-Pro^2	b_9 -NH_3	1105.56	$P^2F^3f^4N^5Q^6Y^7V^8O^9L^{10}$
1010.54	Phe^1-Pro^2	b_8	1010.51	$P^2F^3f^4N^5Q^6Y^7V^8O^9$
896.45	Phe^1-Pro^2	b_7	896.43	$P^2F^3f^4N^5Q^6Y^7V^8$
797.35	Phe^1-Pro^2	b_6	797.36	$P^2F^3f^4N^5Q^6Y^7$
634.31	Phe^1-Pro^2	b_5	634.30	$P^2F^3f^4N^5Q^6$
506.25	Phe^1-Pro^2	b_4	506.24	$P^2F^3f^4N^5$
406.18	any	Internal fragment	406.17	$N^5Q^6Y^7$
392.21	Phe^1-Pro^2	b_3	392.20	$P^2F^3f^4$
390.18	any	Internal fragment	390.18	$f^4N^5Q^6$
245.14	Phe^1-Pro^2	b_2	245.13	P^2F^3
243.15	any	Internal fragment	243.11	N^5Q^6
217.14	Phe^1-Pro^2	a_2	217.12	P^2F^3
115.09	Val^8-Orn^9	b_1	115.09	O^9

Table S3 Summary of fragment assignment of the major product ions generated by CID of the *m/z*=1284.7 molecular ion of tyrocidine A_1

m/z observed	Proposed ring opening	Proposed fragment type	*m/z* calculated	Sequence
1284.69	-	$[M+H]^+$	1284.68	cyclo($P^2F^3f^4N^5Q^6Y^7V^8K^9L^{10}f^1$)
1137.63	Phe^1-Pro^2	b_9	1137.61	$P^2F^3f^4N^5Q^6Y^7V^8K^9L^{10}$
1024.54	Phe^1-Pro^2	b_8	1024.53	$P^2F^3f^4N^5Q^6Y^7V^8K^9$
896.46	Phe^1-Pro^2	b_7	896.43	$P^2F^3f^4N^5Q^6Y^7V^8$
797.36	Phe^1-Pro^2	b_6	797.36	$P^2F^3f^4N^5Q^6Y^7$
634.31	Phe^1-Pro^2	b_5	634.30	$P^2F^3f^4N^5Q^6$
506.25	Phe^1-Pro^2	b_4	506.24	$P^2F^3f^4N^5$
406.18	any	Internal fragment	406.17	$N^5Q^6Y^7$
392.21	Phe^1-Pro^2	b_3	392.20	$P^2F^3f^4$
390.19	any	Internal fragment	390.18	$f^4N^5Q^6$
364.20	Phe^1-Pro^2	a_3	364.19	$P^2F^3f^4$
245.14	Phe^1-Pro^2	b_2	245.13	P^2F^3
243.15	any	Internal fragment	243.11	N^5Q^6
217.14	Phe^1-Pro^2	a_2	217.12	P^2F^3
120.09	any	Internal fragment-CO	120.07	f^1 or F^3 or f^4

Table S4 Summary of fragment assignment of the major product ions generated by CID of the *m/z*=1309.7 molecular ion of tyrocidine B

m/z observed	Proposed ring opening	Proposed fragment type	*m/z* calculated	Sequence
1309.69	-	$[M+H]^+$	1309.67	cyclo($P^2W^3f^4N^5Q^6Y^7V^8O^9L^{10}f^1$)
1144.62	Phe^1-Pro^2	b_9 -NH_3	1145.60	$P^2W^3f^4N^5Q^6Y^7V^8O^9L^{10}$
1049.53	Phe^1-Pro^2	b_8	1049.52	$P^2W^3f^4N^5Q^6Y^7V^8O^9$
935.47	Phe^1-Pro^2	b_7	935.44	$P^2W^3f^4N^5Q^6Y^7V^8$
836.37	Phe^1-Pro^2	b_6	836.37	$P^2W^3f^4N^5Q^6Y^7$
673.33	Phe^1-Pro^2	b_5	673.31	$P^2W^3f^4N^5Q^6$
545.27	Phe^1-Pro^2	b_4	545.25	$P^2W^3f^4N^5$
431.22	Phe^1-Pro^2	b_3	431.21	$P^2W^3f^4$
406.18	any	Internal fragment	406.17	$N^5Q^6Y^7$
390.19	any	Internal fragment	390.18	$f^4N^5Q^6$
284.14	Phe^1-Pro^2	b_2	284.14	P^2W^3
256.15	Phe^1-Pro^2	a_2	256.13	P^2W^3
243.12	any	Internal fragment	243.11	N^5Q^6
159.10	any	Internal fragment-CO	159.08	W^3

Table S5 Summary of fragment assignment of the major product ions generated by CID of the *m/z*=1323.7 molecular ion of tyrocidine B_1

m/z observed	Proposed ring opening	Proposed fragment type	*m/z* calculated	Sequence
1323.72	-	$[M+H]^+$	1323.69	cyclo($P^2W^3f^4N^5Q^6Y^7V^8K^9L^{10}f^1$)
1176.62	Phe^1-Pro^2	b_9	1176.62	$P^2W^3f^4N^5Q^6Y^7V^8K^9L^{10}$
1063.56	Phe^1-Pro^2	b_8	1063.54	$P^2W^3f^4N^5Q^6Y^7V^8K^9$
935.44	Phe^1-Pro^2	b_7	935.44	$P^2W^3f^4N^5Q^6Y^7V^8$
836.37	Phe^1-Pro^2	b_6	836.37	$P^2W^3f^4N^5Q^6Y^7$
673.33	Phe^1-Pro^2	b_5	673.31	$P^2W^3f^4N^5Q^6$
545.26	Phe^1-Pro^2	b_4	545.25	$P^2W^3f^4N^5$
431.22	Phe^1-Pro^2	b_3	431.21	$P^2W^3f^4$
406.18	any	Internal fragment	406.17	$N^5Q^6Y^7$
390.19	any	Internal fragment	390.18	$f^4N^5Q^6$
284.15	Phe^1-Pro^2	b_2	284.14	P^2W^3
256.15	Phe^1-Pro^2	a_2	256.13	P^2W^3
243.12	any	Internal fragment	243.11	N^5Q^6

Table S5 Summary of fragment assignment of the major product ions generated by CID of the *m/z*=1348.7 molecular ion of tyrocidine C

***m/z* observed**	**Proposed ring opening**	**Proposed fragment type**	***m/z* calculated**	**Sequence**
1348.63	-	$[M+H]^+$	1348.68	cyclo($P^2W^3w^4N^5Q^6Y^7V^8O^9L^{10}f^1$)
1184.61	Phe^1-Pro^2	b_9 -NH_3	1184.61	$P^2W^3w^4N^5Q^6Y^7V^8O^9L^{10}$
1088.51	Phe^1-Pro^2	b_8	1088.53	$P^2W^3w^4N^5Q^6Y^7V^8O^9$
957.41	Phe^1-Pro^2	b_7 -NH_3	957.45	$P^2W^3w^4N^5Q^6Y^7V^8$
875.38	Phe^1-Pro^2	b_6	875.38	$P^2W^3w^4N^5Q^6Y^7$
844.43	Val^8-Orn^9	b_6	844.45	$O^9L^{10}F^1P^2W^3w^4$
712.31	Phe^1-Pro^2	b_5	712.32	$P^2W^3w^4N^5Q^6$
584.25	Phe^1-Pro^2	b_4	584.26	$P^2W^3w^4N^5$
470.21	Phe^1-Pro^2	b_3	470.22	$P^2W^3w^4$
406.17	any	Internal fragment	406.17	$N^5Q^6Y^7$
284.14	Phe^1-Pro^2	b_2	284.14	P^2W^3
256.14	Phe^1-Pro^2	a_2	256.13	P^2W^3
243.10	any	Internal fragment	243.11	N^5Q^6

Table S6 Summary of fragment assignment of the major product ions generated by CID of the *m/z*=1362.7 molecular ion of tyrocidine C_1

***m/z* observed**	**Proposed ring opening**	**Proposed fragment type**	***m/z* calculated**	**Sequence**
1362.73	-	$[M+H]^+$	1362.68	cyclo($f^1P^2W^3w^4N^5Q^6Y^7V^8K^9L^{10}$)
1198.65	Phe^1-Pro^2	b_9 -NH_3	1198.62	$P^2W^3w^4N^5Q^6Y^7V^8K^9L^{10}$
1102.58	Phe^1-Pro^2	b_8	1102.55	$P^2W^3w^4N^5Q^6Y^7V^8K^9$
974.49	Phe^1-Pro^2	b_7	974.45	$P^2W^3w^4N^5Q^6Y^7V^8$
858.51	Phe^1-Pro^2	b_6 -NH_3	858.38	$P^2W^3w^4N^5Q^6Y^7$
712.33	Phe^1-Pro^2	b_5	712.32	$P^2W^3w^4N^5Q^6$
584.29	Phe^1-Pro^2	b_4	584.26	$P^2W^3w^4N^5$
470.23	Phe^1-Pro^2	b_3	470.22	$P^2W^3w^4$
406.19	any	Internal fragment	406.17	$N^5Q^6Y^7$
284.15	Phe^1-Pro^2	b_2	284.14	P^2W^3
256.10	Phe^1-Pro^2	a_2	256.13	P^2W^3
243.10	any	Internal fragment	243.11	N^5Q^6

Table S7 Summary of fragment assignment of the major product ions generated by CID of *m/z*=627.3 molecular ion of tryptocidine A

m/z observed	Proposed ring opening	Proposed fragment type	*m/z* calculated	Sequence
647.34	-	$[M+2H]^{2+}$	647.34	cyclo($f^1P^2F^3f^4N^5Q^6W^7V^8O^9L^{10}$)
1194.60	Val^8-Orn^9	b_9	1194.61	$O^9L^{10}f^1P^2F^3f^4N^5Q^6W^7$
1033.53	Phe^1-Pro^2	b_8	1033.53	$P^2F^3f^4N^5Q^6W^7V^8O$
1008.53	Val^8-Orn^9	b_8	1008.53	$O^9L^{10}f^1P^2F^3f^4N^5Q^6$
820.41	Phe^1-Pro^2	b_6	820.38	$P^2F^3f^4N^5Q^6W$
634.30	Phe^1-Pro^2	b_5	634.30	$P^2F^3f^4N^5Q^6$
619.36	Val^8-Orn^9	b_5	619.36	$O^9L^{10}f^1P^2F^3$
506.24	Phe^1-Pro^2	b_4	506.24	$P^2F^3f^4N^5$
392.20	Phe^1-Pro^2 any	b_3; Internal fragment	392.20	$P^2F^3f^4$ $f^1P^2F^3$
245.13	Phe^1-Pro^2 any	b_2 Internal fragment	245.13	P^2F^3 f^2P^2
228.14	Val^8-Orn^9	b_2	228.17	O^9L^{10}
115.09	Val^8-Orn^9	b_1	115.09	O^9

Table S8 Summary of fragment assignment of the major product ions generated by CID of *m/z*=666.9 molecular ion of tryptocidine B

m/z observed	Proposed ring opening	Proposed fragment type	*m/z* calculated	Sequence
666.80	-	$[M+2H]^{2+}$	666.85	cyclo($f^1P^2W^3f^4N^5Q^6W^7V^8O^9L^{10}$)
1233.62	Val^8-Orn^9	b_9	1233.62	$O^9L^{10}f^1P^2W^3f^4N^5Q^6W^7$
1047.54	Val^8-Orn^9	b_8	1247.54	$O^9L^{10}f^1P^2W^3f^4N^5Q^6$
859.40	Phe^1-Pro^2	b_6	859.39	$P^2W^3f^4N^5Q^6W^7$
805.42	Val^8-Orn^9	b_6	805.44	$O^9L^{10}f^1P^2W^3f^4$
673.32	Phe^1-Pro^2	b_5	673.31	$P^2W^3f^4N^5Q^6$
545.20	Phe^1-Pro^2	b_4	545.25	$P^2W^3f^4N^5$
472.31	Val^8-Orn^9	b_4	472.29	$O^9L^{10}f^1P^2$
431.18	Phe^1-Pro^2 any	b_3 internal fragment	431.21	$P^2W^3f^4$ $f^1P^2W^3$
375.25	Val^8-Orn^9	b_3	375.24	$O^9L^{10}f^1$
284.14	Phe^1-Pro^2	b_2	284.14	P^2W^3
115.08	Val^8-Orn^9	b_1	115.08	O^9

Table S9 Summary of fragment assignment of the major product ions generated by CID of *m/z*=1371.7 molecular ion of tryptocidine C

m/z observed	Proposed ring opening	Proposed fragment type	*m/z* calculated	Sequence
1371.70	-	$[M+H]^+$	1371.67	cyclo($f^1P^2W^3w^4N^5Q^6W^7V^8O^9L^{10}$)
1207.62	Phe^1-Pro^2	b_9 -NH_3	1207.62	$P^2W^3w^4N^5Q^6W^7V^8O^9L^{10}$
1111.56	Phe^1-Pro^2	b_8	1111.55	$P^2W^3w^4N^5Q^6W^7V^8O^9$
997.48	Phe^1-Pro^2	b_7	997.47	$P^2W^3w^4N^5Q^6W^7V^8$
881.39	Phe^1-Pro^2	b_6 -NH_3	881.39	$P^2W^3w^4N^5Q^6W^7$
712.33	Phe^1-Pro^2	b_5	712.32	$P^2W^3w^4N^5Q^6$
584.27	Phe^1-Pro^2	b_4	584.26	$P^2W^3w^4N^5$
470.22	Phe^1-Pro^2	b_3	470.22	$P^2W^3w^4$
429.20	any	internal fragment	429.19	$N^5Q^6W^7$
284.15	Phe^1-Pro^2	b_2	284.14	P^2W^3
256.15	Phe^1-Pro^2	a_2	256.13	P^2W^3
243.10	any	internal fragment	243.11	N^5Q^6

Table S10 Summary of fragment assignment of the product ions generated by CID of *m/z*=627.8 molecular ion of phenycidine A

m/z observed	Proposed ring opening	Proposed fragment type	*m/z* calculated	Sequence
627.80	-	$[M+2H]^{2+}$	627.83	cyclo($f^1P^2F^3f^4N^5Q^6F^7V^8O^9L^{10}$)
1155.60	Val^8-Orn^9	b_9	1155.60	O^9L^{10} $f^1P^2F^3f^4N^5Q^6F^7$
1008.53	Val^8-Orn^9	b_8	1008.53	O^9L^{10} $f^1P^2F^3f^4N^5Q^6$
994.52	Phe^1-Pro^2	b_8	994.52	$P^2F^3f^4N^5Q^6f^7V^8O^9$
880.46	Phe^1-Pro^2	b_7	880.44	$P^2F^3f^4N^5Q^6f^7V^8$
781.37	Phe^1-Pro^2	b_6	781.37	$P^2F^3f^4N^5Q^6f^7$
766.40	Val^8-Orn^9	b_6	766.43	O^9L^{10} $f^1P^2F^3f^4$
634.30	Phe^1-Pro^2	b_5	634.30	$P^2F^3f^4N^5Q^6$
619.34	Val^8-Orn^9	b_5	619.36	O^9L^{10} $f^1P^2F^3$
506.18	Phe^1-Pro^2	b_4	506.24	$P^2F^3f^4N^5$
472.28	Val^8-Orn^9	b_4	472.28	$O^9L^{10}f^1P^2$
392.20	Phe^1-Pro^2 any	b_3 internal fragment	392.20	$P^2F^3f^4$ $f^1P^2F^3$
245.12	Phe^1-Pro^2 any	b_2 internal fragment	245.13	P^2F^3 f^1P^2

SUPPLEMENTARY MATERIAL REFERENCES

Biemann K. (1988). Contributions of mass spectrometry to peptide and protein structure. *Biol Mass Spectrom* **16**, 99-111.

Bidlingmeyer B. A., Cohen S. A., Tarvin T. L. (1984). Rapid analysis of amino acids using pre-column derivatization. *J. Chromatogr—Biomed. Appl* **336**, 93-104
Cohen S. A., Meys M., Tarvin T. L. The Pico-Tag® Method: A manual of advanced techniques for amino acid analysis, distributed by Waters®, Millipore

Ellinger G.M. & Boyne E. B. (1965). Amino acid composition of some fish products and casein. *Br. J Nutr* **19,** 587-592

Gordon W. G., Semmett W. F., Cable R. S. & Morris M. (1949). Amino acid composition of α-casein and β-Casein2. *J Am Chem Soc* **71**, 3293-3297.

Roepstorff P. & Fohlman J. (1984). Proposal for a common nomenclature for sequence ions in mass spectra of peptides. *Biomed Mass Spectrom* **11**, 601.

Sundararajan T. & Sarma P. (1957). Preparation and amino acid composition of enzymically dephosphorylated casein. *Biochem J* **65**, 261-266.

Chapter 3

A model for incorporation of aromatic amino acids in the three variable residue positions for the different tyrocidines and analogues

3.1 Introduction

The tyrocidines are cyclic decapeptides produced by *Bacillus aneurinolyticus* in the late logarithmic growth phase [1-4]. These peptides are produced by a series of peptide synthetases that are encoded by the tyrocidine biosynthesis operon [5]. The peptide synthetases are a series of multi-domain enzymes that bind specific amino acids at their adenylation domains and systematically grow a polypeptide chain through the orderly addition of these amino acid residues. Ultimately, in the case of the tyrocidines, this process culminates in the cyclisation of the linear polypeptide chain by a terminal thioesterase [5-7].

Vosloo *et al*. [8] have previously established that the production of different tyrocidine analogues may be accomplished through supplementation of the growth medium of *B. aneurinolyticus* with certain amino acids. Promiscuity of certain of the peptide synthetases gives rise to the variability in the structure of the tyrocidines. Of particular interest in this study are the amino acids which are incorporated at the position 3 and 4 which may be either Phe or Trp, known as the variable dipeptide unit. Variability at the variable dipeptide unit accounts for the production of the A (Phe^3, Phe^4), B (Trp^3, Phe^4) and C (Trp^3, Trp^4) analogues. Variation at position 7 of either Tyr, Phe or Trp results in the production of the tyrocidines, phenycidines or tryptocidines respectively [8,9] (Fig. 3.1).

As such, it was observed that of the range of amino acids evaluated (Phe, Trp, Tyr, Cys, Lys and Arg); only supplementation with Phe and Trp significantly altered the tyrothricin production profile. Supplementation with Phe caused the predominant production of the A analogues. Supplementation with Trp resulted in the predominant production of the C analogues. The B analogues, however, where produced at intermediate ratios of Phe/Trp supplementation [8].

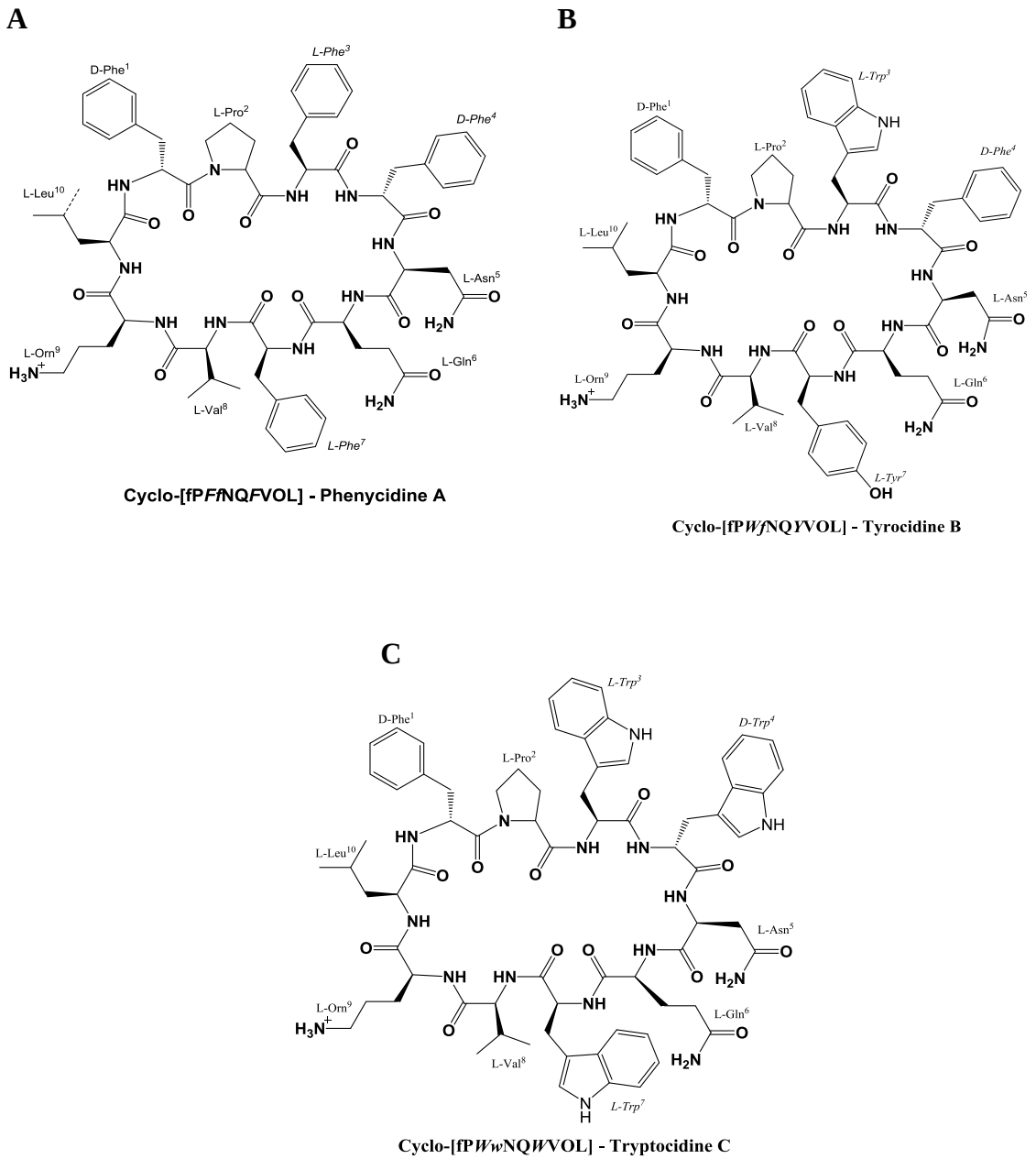

Figure 3.1 **S**tructure of the tyrocidine analogues depicting variable residues at positions 3, 4 and 7 in italics and D residues in lower case. (**A**) Phenycidine A with Phe at variable positions 3, 4 and 7. (**B**) Tyrocidine B with Trp, Phe and Tyr at variable positions 3, 4 and 7 respectively. (**C**) Tryptocidine C with Trp at variable positions 3, 4 and 7.

Vosloo *et al*. [8] established the shift in peptide production profile produced between the different A (Phe^3, Phe^4), B (Trp^3, Phe^4) and C (Trp^3, Trp^4) analogues, but the identities of these peptides, particularly concerning the identity of the residue in position 7, was not analysed. A more in depth view, where the exact identities of the different peptide analogues produced by *B. aneurinolyticus* under the different Phe and Trp supplemented growth conditions, is now

considered. From these data a competitive binding computational model was constructed which can be used to predict the occupancy at the three variable aromatic amino acid positions in the structure of the tyrocidines and their analogues. To our knowledge, this is the first study of its kind. The tyrothricin producer strain were initially referred to as the Dubos strain of *Bacillus brevis* [10], this strain was subsequently renamed *Bacillus aneurinolyticus* by Shida *et al*. [11] these authors subsequently suggested further reclassification of the strain to *Brevibacillus parabrevis* [12]. However, this organism will be referred to as *Bacillus aneurinolyticus* in keeping with the bacterial specie name used in the preceding published study [8] on which this work was based.

3.2 Materials

Bacillus aneurinolyticus ATCC 10068 was obtained from the American Type Culture Collection (Manassas, VA, USA). Deep 96-well plates, tryptone, yeast extract, peptone, glucose, agar, hydrochloric acid (HCl) and the L-amino acids lysine and arginine were from Merck (Darmstadt, Germany). The L-amino acids cysteine, phenylalanine, tyrosine and tryptophan were obtained from Sigma-Aldrich (Steinheim, Germany). Media was sterilized by means of filtration using either 0.22 µm pore size sterile bottle top filtration system from Whatman Klari-Flex (Piscataway, USA) or sterile syringes and 0.20 -25 µm syringe filters from Lasec (Cape Town, South Africa). Acetonitrile (HPLC-grade, far UV cut-off) was from Romil Ltd (Cambridge, UK). An Acquity UPLC® BEH C_{18} (1.7 µm particle size, 2.1 mm x 100 mm) ultra-performance liquid chromatography (UPLC) column was from Waters-Millipore (Milford, USA). Analytical grade water was prepared by filtering water from a reverse osmosis plant through a Millipore-Q® water purification system (Milford, USA).

3.3 Methods

3.3.1 Pre-culturing of the tyrothricin producer strain

As was previously described [8] using standard, sterile, microbiological culturing techniques, single colonies of *B. aneurinolyticus* were obtained from pre-culture plates (5.0 g peptone, 2.5 g yeast extract, 1.0 g glucose and 1.0 g skimmed milk powder, 15 g agar in 1.0 L water) that were seeded from freezer stocks. From these, single colonies were selected and incubated in Falcon® tubes containing 5 mL aliquots of TGS (tryptone, glucose and inorganic salts) culture media [13] while shaking at 220 rpm for 24 hours at 37 °C. Using the Pico-Tag® method [14], the final amino acid composition of the tryptone in TGS medium was previously

determined by high performance liquid chromatography (HPLC) and reported to contain 5.3±0.1, 1.2±0.1 and 3.1±0.4 mM of Phe, Trp and Tyr respectively [8].

3.3.2 Medium throughput deep well production of tyrothricin

Culturing of the tyrothricin producer strain *B. aneurinolyticus*, in deep 96-well plates was performed as previously described [8]. In essence; a pre-culture of *B. aneurinolyticus* was diluted four times using TGS culture medium, of which 10 µL was added to quadruplicate repeats of 500 µL TGS medium per well of the sterile deep 96-well plates containing either TGS medium alone or spiked with amino acids. The TGS medium was spiked with amino acids (Phe and/or Trp) ranging in concentration from 2.75 to 27.5 mM over seven steps of each amino acid prepared in TGS medium.

These plates were covered and incubated at 37 °C for 96 hours, following which they were acidified to pH 4.7 using HCl and allowed to stand at room temperature for 24 hours. The cell pellet in each well was subsequently obtained by centrifugation of the plates at 2200 × *g* for 60 minutes. The pellet was subsequently suspended in 200 µL of 100% acetonitrile, sonicated for 15 minutes, a further 200 µL of analytical grade water added followed by further sonication for 15 minutes. The supernatant was then obtained by centrifugation for 30 minutes at 2200 × *g*, pooled in analytically weighed vials. These were subsequently freeze dried and analysed via UPLC linked to ESMS (UPLC-MS).

3.3.3 ESMS and UPLC-MS analysis of tyrothricin extracts

Electrospray mass spectrometry (ESMS) was performed using a Waters Quadrupole Time-of-Flight Synapt G2 mass spectrometer, as previously described [8]. Particulate matter was removed by centrifugation at 8600 × g for 10 minutes. The extracts were diluted to a final concentration of 1.00 mg/mL and dissolved in 5% (*v/v*) acetonitrile in water. The extracts were separated *via* a Waters Acquity UPLC™ and introduced into the mass spectrometer using a Z-spray electrospray ionisation source in positive mode. Subsequently, the identities of the respective peptides were confirmed by means of high resolution mass spectrometry and sequenced via collision induced dissociation [8].

Using a 0.1% trifluoroacetic acid (A) to acetonitrile (B) gradient (100% A from 0 to 0.5 minutes for loading, a linear gradient was run from 0 to 58% B over 0.5 to 12 minutes followed by a linear gradient from 58 to 90% B over 12 to 13 minutes) 3 µL per sample was separated on an

Acquity UPLC® BEH C_{18} column at a flow rate of 0.450 mL/min. Analytes were subjected to a capillary voltage of 3.0 kV and cone voltage of 15 V at a temperature of 120 ºC at the source. Data acquisition was performed by scanning the second analyser (MS_2) through the mass over charge ratio (*m/z*) range of 400 to 2000. Data were then analysed using TargetLynx™ 4.1 (MassLynx Mass Spectrometry software, Waters, Milford, USA) [8].

3.3.4 Mathematical model analysis of the shift in the tyrocidine production profile

The shift in the tyrocidine production profile was influenced by variability at either: the variable dipeptide unit at positions 3 and 4, or at position 7. Having established that we were able to shift the tyrocidine production profile through the titration of the growth medium with Phe and Trp, a number of mathematical equations were derived to describe the amino acid occupation at these variable positions.

The concentration of an amino acid *x*, at a specific site *a* in a peptide, could be calculated by integrating its production rate Vx_a over the period of production. Therefore, the concentration observed at time *t*, $x_a\ (t)$ is equal to:

$$x_a(t) = \int_0^t Vx_a\, d(t) + x_a(0) \tag{1}$$

To analyse the relative concentrations of amino acids (*x*; *y*) at a specific site these integrals must be compared. At the beginning of the experiment no peptide was produced hence $x_a(0) = y_a(0) = 0$.

$$\frac{x_a(t)}{y_a(t)} = \frac{\int_0^t Vx_a d(t)}{\int_0^t Vy_a d(t)}, \text{ and if assumed } \frac{Vx_a}{Vy_a} = r \tag{2}$$

$$\frac{x_a(t)}{y_a(t)} = \frac{\int_0^t r \cdot Vy_a d(t)}{\int_0^t Vy_a d(t)} = r \tag{3}$$

If the ratio of the incorporation rates of *x* and *y* is constant then the concentration ratio of the amino acids is equal to the production ratio. As amino acids *x* and *y* are in competition with one another for inclusion in the peptide; a simple competitive binding mechanism was used to describe the rate of inclusion with a Michaelis Menten type equation:

$$Vx_a = \frac{Vx_a \cdot \frac{x}{Kxa}}{1 + \frac{x}{Kxa} + \frac{y}{Kya}} \text{ and } Vy_a = \frac{Vy_a \cdot \frac{y}{Kya}}{1 + \frac{x}{Kxa} + \frac{y}{Kya}} \text{ with ratios,} \tag{4}$$

$$\frac{Vx_a}{Vy_a} = \frac{Vx_a \cdot \frac{x}{Kxa}}{Vy_a \cdot \frac{y}{Kya}} = c \cdot \frac{x}{y} \tag{5}$$

Combining eq. 3 with 5 lead to the simple expression:

$$\frac{x_a(t)}{y_a(t)} = c \cdot \frac{x}{y} \tag{6}$$

Thus, the expected ratio of amino acids included at a specific site of the peptide is linear with the concentration ratio of the free amino acids. As a first approximation one could consider that the cytosolic ratio of concentrations of amino acids reflects the concentration ratio in the medium.

It is often more convenient to work with fractions or percentage occupation of a given amino acid per site than with ratios. As such, Eq. 6 is rearranged to a fractional relation, and allowing for a potential cooperative effect(s) this leads to:

$$\frac{x_a(t)}{x_a(t)+y_a(t)} = \frac{c_1 \cdot (\frac{x}{y})^n}{1+c_1 \cdot (\frac{x}{y})^n} \tag{7}$$

with $c_1 = \frac{Vx_a \cdot (K_{ya})^n}{Vy_a (K_{xa})^n}$ (8)

The analysis became slightly more complicated when three amino acids compete at a site, but with similar assumption as before we derived:

$$\frac{x_a(t)}{x_a(t)+y_a(t)+z_a(t)} = \frac{Vx_a}{Vx_a+Vy+Vz_a} = \frac{Vx_a \cdot (\frac{x}{K_{xa}})^n}{Vx_a \cdot (\frac{x}{K_{xa}})^n + Vy_a \cdot (\frac{y}{K_{ya}})^n + Vz_a \cdot (\frac{xz}{K_{za}})^n}$$

$$\frac{x_a(t)}{x_a(t)+y_a(t)+z_a(t)} = \frac{c_1 \cdot (\frac{x}{y+c_2 \cdot z})^n}{1+c_1 \cdot (\frac{x}{y+c_2 \cdot z})^n} \tag{9}$$

with C_1 as in Eq. 7 and $c_2 = \frac{Vz_a \cdot (K_{ya})^n}{Vy_a (K_{za})^n}$ (10)

Eq. 9 reduces to Eq. 7 when z is zero, otherwise the competitive effect of z was weighed according to C_2.

The previously derived mathematical equations describe the occupancy of position 3 and 4 by either Phe or Trp (Eq. 7); as well as occupancy of position 7 by the three aromatic amino acids Phe, Trp or Tyr (Eq. 9). As such, using the observed experimental data a competitive binding computational model was constructed.

3.4 Results

The data of four independent culture batches were subsequently used to not only determine the exact identity of the peptides produced utilising UPLC-MS, but also construct a competitive binding model which could be used to predict the identity and proportions of the peptides produced at given concentrations of the variable aromatic amino acids. Refer to Fig. 3.2 for representative examples of UPLC-MS analyses of the Trp and Phe supplemented culture extracts.

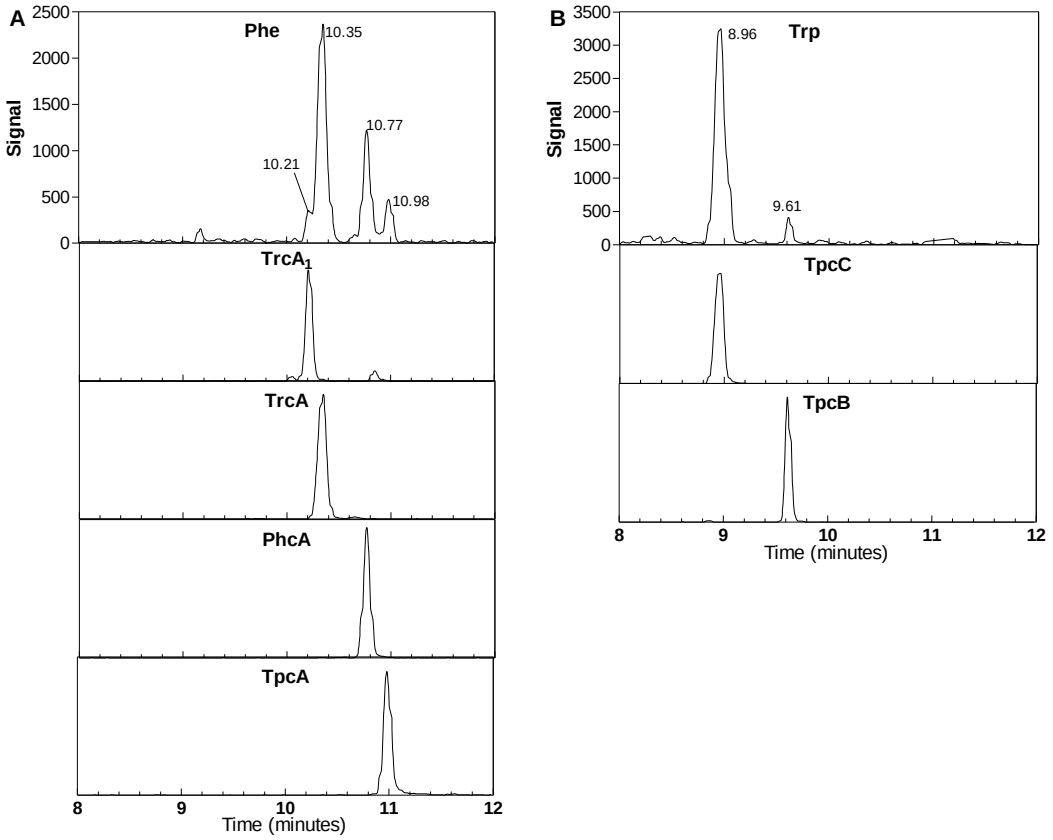

Figure 3.2 UPLC-MS chromatograms depicting the shift in the peptide production profile when the growth media was supplemented to contain a total of: (**A**) 32.8 mM Phe and 1.2mM Trp to produce a range of tyrocidine A analogues (Phe^3, Phe^4) or (**B**) 28.7 mM Trp and 5.3 mM Phe to produce the tryptocidine analogues (Trp^7).

3.3.1 Phe supplementation

Supplementation of the culture media with Phe resulted in the predominant production of a range of the A analogues (Phe at both positions of the variable dipeptide positions) and correlated well to the previous study by Vosloo *et al.* [8] (Fig. 3.3 A). Production of tyrocidine A> tryptocidine A> phenycidine A predominated; all of which contain Phe^3, Phe^4; but Tyr^7, Trp^7 or Phe^7 respectively at the variable aromatic site. Moreover, as the concentration

of Phe supplementation increased, a concomitant increase in the prevalence of the phenycidine A analogue was observed (Fig. 3.3 A).

3.4.2 Trp supplementation

A significant shift in the peptide production profile of *B. aneurinolyticus* toward the production of the tryptocidine analogues containing Trp^7 was observed, when Trp was supplemented to the growth medium (Fig. 3.3 B). Initially an increase in production of the tryptocidine B analogue was observed. However, above the supplemented Trp concentration of 4 mM (5.3 mM Phe and 5.2 mM Trp total in medium) the contribution of tryptocidine B analogue decreased and that of the tryptocidine C analogue increased (Fig. 3.3 B).

3.4.3 Supplementation with a combination of Phe and Trp

Having shifted the peptide production profile between two extremes in terms of the A and C analogues through supplementation of either Phe or Trp, the influence of the co-supplementation of Phe and Trp was assessed. Production of the tryptocidine analogues containing Trp^7 predominated in conditions when Trp was supplemented to the growth medium at fixed concentrations of 5.5, 11 or 16.5 mM (6.7, 12.2 or 17.7 mM Trp total in medium), irrespective of the co-supplemented Phe concentration. Supplementation of varied concentrations of Phe between 2.75 to 27.5 mM merely served to shift the peptide production profile between the different tryptocidine analogues (Fig. 3.3 C).

Substitution of Trp by Phe with increasing concentrations of the Phe only occurred at the variable aromatic dipeptide unit, but not at the variable aromatic residue 7 which was occupied by Trp^7 at all the Trp and Phe co-supplementation concentrations. Supplementation of the growth medium with 5.5 mM Trp (6.7 mM Trp total in medium) initially shifted the peptide production profile toward the predominant production of the tryptocidine C analogue. As the supplemented Phe concentration was increased above 3.4 mM (8.7 mM Phe and 6.7 mM Trp total in medium) the production of the tryptocidine B analogue predominated. Concomitantly the proportion of the peptide production profile contributed by the tryptocidine C analogue decreased.

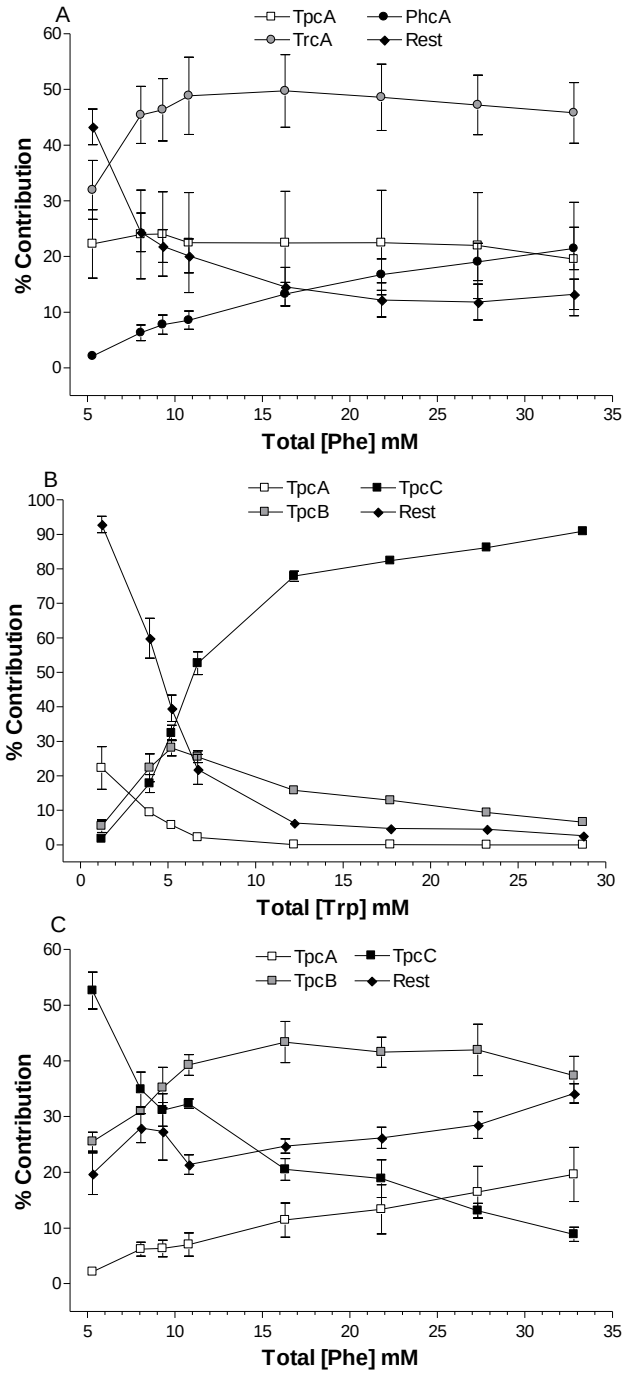

Figure 3.3 Peptide production profiles of extracts obtained from *B. aneurinolyticus* depicting the major peptide isoforms produced when the TGS base medium containing 5.3 and 2.1 mM Phe or Trp respectively was supplemented with: (**A**) Phe, varying the total Phe concentration between 5.3 and 32.8 mM; (**B**) Trp, varying the total Trp concentration between 1.2 and 28.7 mM; or (**C**) at a fixed total Trp concentration of 6.7 mM and varying the total Phe concentration between 5.3 and 32.8 mM. The percentage contribution of each of the respective analogues to the total peptide profile of the tyrocidines and their analogues is presented. Rest represents the sum of those analogues not specifically indicated on the graph. Each data point is the mean obtained from four independent cultures.

When the supplemented concentration of Phe exceeded 21 mM (26.3 mM Phe and 6.7 mM Trp total in medium) the production of tryptocidine A exceeded that of tryptocidine C analogue (Fig. 3.2 C). Similarly, the peptide production profile was shifted between the different tryptocidine analogues when higher concentrations of Trp were supplemented, albeit at higher Phe concentrations (data not shown). As such, the peptide production profile was shifted from tyrocidine production (peptides containing Tyr^7) in the non-supplemented state (5.3 mM Phe and 1.2 mM Trp in medium) to tryptocidine (peptides containing Trp^7) production in the presence of supplemented Trp.

3.4.4 Computational modelling of variability in residues in positions 3 and 4

Assuming a simple competitive mechanism for the incorporation of Phe and Trp at position 3 and 4, Eq. 7 was derived (refer to mathematical model analysis) for the relation between the fraction of an amino acid incorporated at the two respective positions and the concentration ratio in the medium of that amino acid and a competing amino acid. Thus, the percentage occupancy of Trp relative to Phe in the peptide was described using Eq. 7 and the fitted parameter values in Table 3.1 for position 3 (Fig. 3.4 A) and 4 (Fig. 3.4 B) respectively. Irrespective of the absolute concentrations of Trp and Phe in the medium, the occupancy of positions 3 and 4 by Trp in the peptide was described by a simple sigmoidal relationship for the Trp/Phe ratio at a fit of 96% and 37 degrees of freedom. At Trp/Phe ratios of 0.23 and 0.79 Trp had a 50% occupancy of positions 3 and 4 respectively (Fig. 3.4 A and B).

3.4.5 Computational modelling of variability in residues in position 7

Again, by assuming a relatively simple competitive mechanism, a functional relationship between the percentage occupation of a specific amino acid and the ratio of that amino acid and the weighed sum of the three competing amino acids was used to derive Eq. 9 (refer to mathematical model analysis). To analyse the incorporation of the three amino acids at position 7, Eq. 9 was used, and for each analysis a different amino acid is attributed to the variables x, y, and z in the equation.

As there are three amino acids competing for occupancy at position 7, it was necessary to transpose the data to include the weighing factor C_2 and the extent of cooperativity n. After this conversion, the data could be plotted as percentage occupancy of amino acid x, versus $\frac{x^n}{y^n+c_2z^n}$.

Using independently fitted values for Eq. 9 (Table 3.1), the occupancy of Tyr (Fig. 3.5 A) and Trp (Fig. 3.5B) at position 7 were well described by a simple hyperbolic relation. For the analysis of Phe incorporation at position 7, the C_1 and C_2 values obtained from the independent fits of Trp and Tyr incorporation were utilized. Using a value for n of 1.28 obtained from Tyr incorporation, the resulting fit of Phe incorporation emulated the trend followed by the experimental data (Fig. 3.5 C).

From these data it is apparent that Trp is preferentially incorporated at position 7, followed by Tyr. Incorporation of Phe at position 7 only occurred at increased Phe concentrations, then only reaching a maximum just exceeding 20% of the total contribution at the highest Phe supplementation at a ratio of 0.04 Trp/Phe in the medium (32.8 mM Phe and 1.2 mM Trp in medium).

Table 3.1 Fitted parameter values for Trp and Tyr incorporation in positions 3, 4 and 7

Position	Amino Acid	C_1	C_2	n
3	Trp	$\frac{V_{W3\cdot(K_{F3})^n}}{V_{F3\cdot(K_{W3})^n}} = 49.75$	0	2.62
4	Trp	$\frac{V_{W4\cdot(K_{F4})^n}}{V_{F4\cdot(K_{W4})^n}} = 1.47$	0	1.47
7	Trp	$\frac{V_{W7\cdot(K_{F7})^n}}{V_{F7\cdot(K_{W7})^n}} = 62.70$	$\frac{V_{Y7\cdot(K_{F7})^n}}{V_{F7\cdot(K_{Y7})^n}} = 49.88.$	1.36
7	Tyr	$\frac{V_{Y7(K_{W7})^n}}{V_{W7\cdot(K_{Y7})^n}} = 0.80$	$\frac{V_{F7\cdot(K_{W7})^n}}{V_{W7\cdot(K_{F7})^n}} = 0.02$	1.28

For each of the analyses the interpretation of C_1 and C_2 is different, they are not independent, see Table 3.1. For instance C_1 in the Trp analysis is equal to $\frac{1}{c_2}$ in the Tyr analysis at position 7. The numerical values that were obtained via the independent fits to the data set are internally

consistent. It was apparent, however, that the occupancy at position 7 was considerably more sensitive to minor variations that occurred between one production culture and the next, particularly concerning the occupancy of Phe and Tyr.

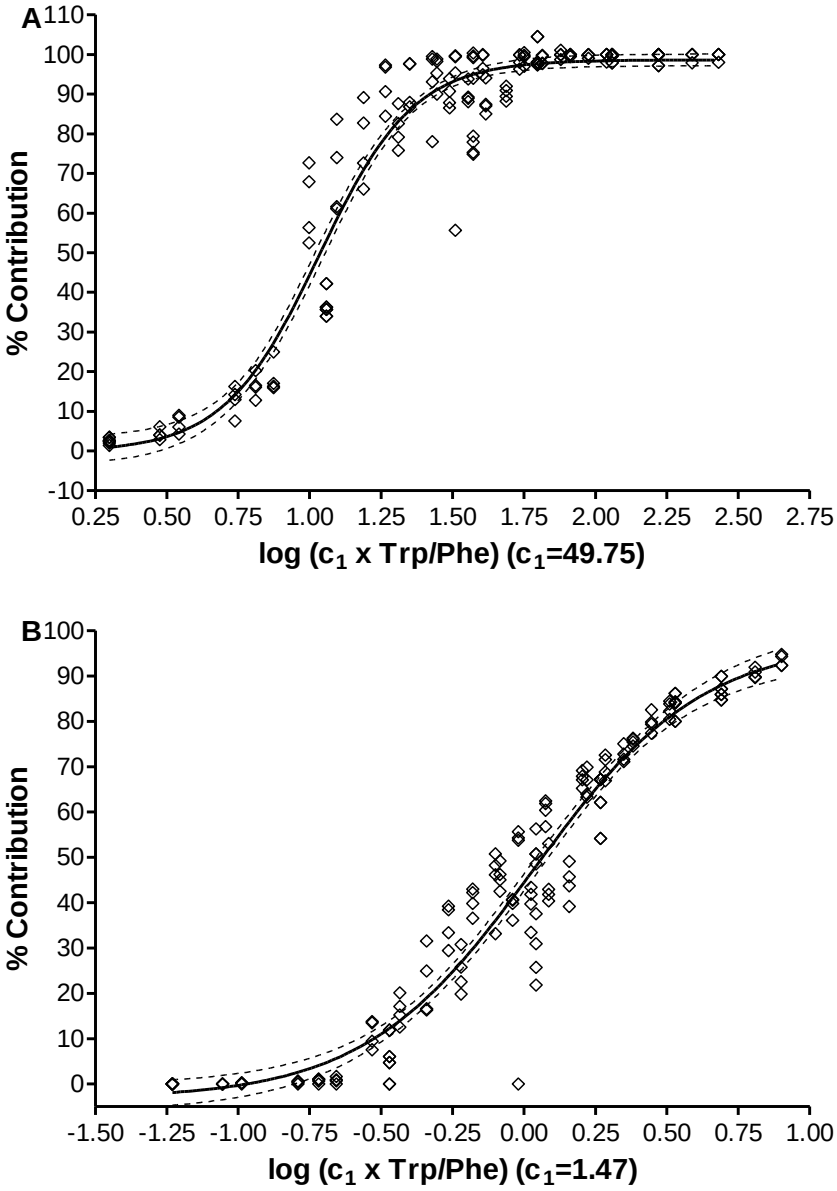

Figure 3.4 Percentage contribution of the sum tyrocidine analogues containing Trp at the positions (**A**) 3 and (**B**) 4 respectively relative to the total peptide profile of the tyrocidines and their analogues. The occupancy of Trp at variable positons (**A**) 3 and (**B**) 4, is described by a simple sigmoidal relationship (Fit of 96% and 37 degrees of freedom) relative to the ratio of total Trp/Phe within the culture media. Using Eq. 7 the c values were gained from the resultant fit of the data of four independent cultures used to construct the computational model. The solid lines represent the sigmoidal curve fits and the dotted lines the 95% confidence interval of the resultant curve fit in which all the individual data points were considered.

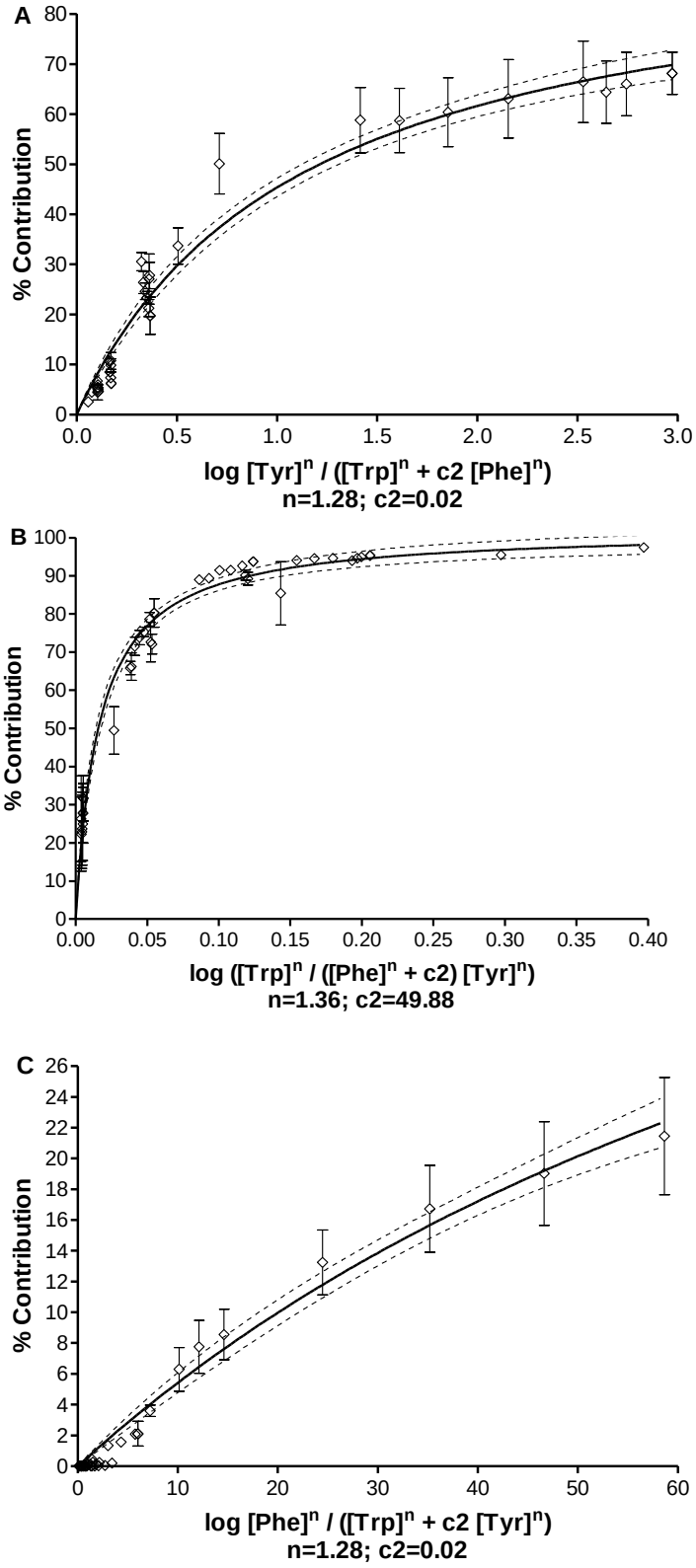

Figure 3.5 Percentage contribution of the analogues at position 7 containing Tyr (**A**), Trp (**B**), or Phe (**C**). The occupancy of a given amino acid is expressed relative to the total peptide profile of the tyrocidines and their analogues. Using Eq. 9 the *n* and *c* values for Tyr (**A**) and Trp (**B**) were fitted independently and used to predict the occupancy of Phe (**C**). The solid line represents the hyperbolic curve fit and the dotted lines the 95% confidence interval of the resultant curve fit in which all the individual data points were considered.

3.4.6 Direct comparison of variability in residues in position 3, 4 and 7

A comparison of Phe (Fig. 3.6 A) and Trp (Fig. 3.6 B) incorporation at the three variable positions revealed a variable rate of incorporation of Phe (Fig. 3.6 A) with position 4>3>>7 being occupied by Phe, containing a smaller side chain relative to Trp. In contrast, position 3 and 7 have a near equally strong preference for Trp relative to position 4. Position 3 and 7 are occupied by 50% Trp at Trp/Phe concentration ratio in the medium of 0.23 and 0.05 respectively, while at a concentration ratio of 1 the Trp occupancy is > 95% at both positions, indicating the preference for a larger aromatic amino acid such as Trp. In contrast, position 4 is occupied by 50% Trp at Trp/Phe concentration ratio in the medium of 0.79, indicating an increased preference for the smaller Phe residue at this position.

3.5 Discussion

The tyrothricin production profile has previously been found to be altered through supplementation of the growth medium with two amino acids namely Trp and Phe [8,15,16]. We have previously reported not only the effect of the mentioned amino acids on the growth of the producer strain, but also on total tyrothricin production. While this study also included variation in linear gramicidin production, it focused primarily on variation observed at the variable dipeptide unit (position 3 and 4) causing a shift in the production of the A, B and C cyclodecapeptide groups [8].

In this study the exact identities of the cyclodecapeptides produced with different Phe and Trp supplementation was elucidated and used, together with derived mathematical equations, to describe the variation at positons 3, 4 and 7. For the purposes of this study, a first approximation that the cytosolic ratio of concentrations of amino acids reflects the concentration ratio in the medium was made. As such, using the observed experimental data a competitive binding computational model was constructed which not only emulates these trends, but can also be used to determine the occupancy at the various sites and thereby the identity of the peptide/s formed at a given medium concentration of Phe and Trp.

The differences observed for cyclodecapeptide analogues produced under the respective amino acid supplemented conditions, may largely be attributed to a few key factors. The bioavailability or concentration of the variable amino acids is closely associated with the affinity (K_M) of the adenylation domains of the peptide synthetases for these residues. However, under saturated conditions the incorporation of these variable residues into the

growing polypeptide chain by the various peptide synthetases is influenced largely by production rate (Vx_a) and extent of cooperativity (n), as is evident from Eq. 9.

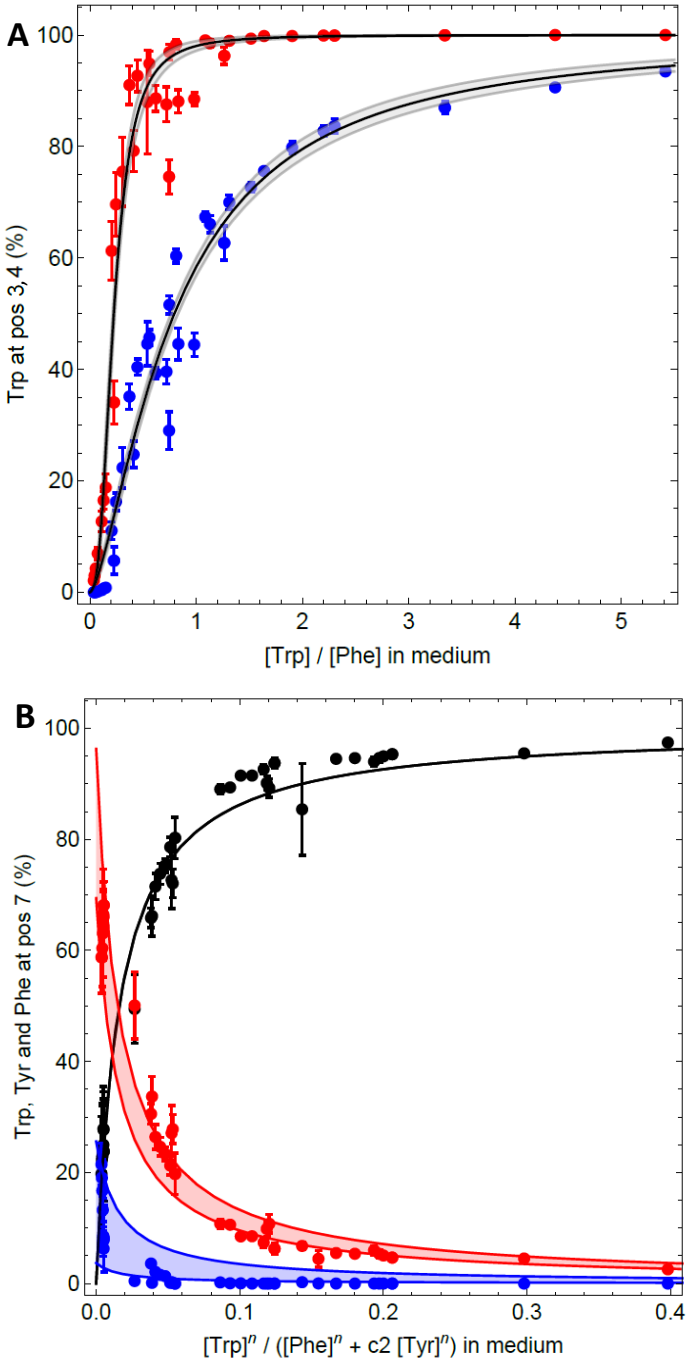

Figure 3.6 Comparison of the contribution of Phe and Trp at variable positions 3 and 4 (**A**), and 7 (**B**). The occupancy of a given amino acid is expressed relative to the total peptide profile of the tyrocidines and their analogues. The red symbols in **A** is for peptide with Trp in position 3 and blue for Trp in position 4 with grey shaded area indicating the confidence interval. The red symbols in **B** indicate peptides with Tyr^7, blue Phe^7 and black Trp^7. The shaded area in B indicates the boundary values of the model prediction under the experimental conditions used in its construction.

Once amino acids are in the cytosol of the cell they are available to the peptide synthetases to be bound and incorporated in the synthesis of the tyrocidines and their analogues. Consequently the affinity of the peptide synthetases for the variable amino acids influences the variation in the production of the different analogues. In the case of Phe and Trp supplementation; this is at the variable dipeptide unit, position 3 and 4, as well as the variable aromatic unit, position 7. The affinity of the adenylation domains responsible for the incorporation of the variable amino acids at positions 4 and 7 has been reported by Mootz and Marahiel [5]. The affinity of these domains is much higher for Trp than any of the other aromatic amino acids that may be incorporated. As such, the adenylation domain at position 4 has a K_M of 0.08 mM for L-Trp and 0.45 mM for L-Phe. The adenylation domain at position 7 has a K_M of 0.1 mM for L-Trp and 0.3 mM for L-Tyr. No K_M value is reported for Phe for the adenylation domain at position 7, or for any amino acids at the adenylation domain at position 3; these are reported to principally activate and thereby incorporate Trp, despite their ability to also incorporate Phe [5].

With the knowledge in hand of the affinity of the peptide synthetases for the different supplemented amino acids as well as the production rates observed, some light maybe shed on the different analogues produced under the respective growth conditions. It is apparent that the high affinity of the peptide synthetases for Trp results in its incorporation, particularly at position 7, consequentially the tryptocidine analogues are produced under Trp supplemented conditions (Fig. 3.3 B and C). However, substitution of Trp by Phe at the variable dipeptide unit at positions 3 and 4 is observed under Phe supplemented conditions (Fig. 3.3 A), despite the reported K_M values for positions 4 and 7 being similar, and positon 3 reported to principally active Trp [5].

When Phe was co-supplemented together with a fixed concentration of 5.5 mM Trp (6.7 mM Trp total in medium), the initial production of the tryptocidine C analogue is exceeded by tryptocidine B production once the concentration of Phe exceeded 3.4 mM (8.7 mM Phe total in medium) (Fig. 3.3 C). Similarly, tryptocidine B production increased at lower supplemented concentrations of up to 4.0 mM Trp (5.3 mM Phe and 5.2 mM Trp total in medium), where after production of tryptocidine C predominated when Trp alone was supplemented (Fig. 3.3 B). This attests to the ability of Phe to substitute Trp at position 4 at lower concentration ratios of Trp/Phe (Fig. 3.4 B), in relation to Trp substitution at position 3 (Fig. 3.4 A). The substitution of Trp by Phe at position 3 and the consequent production of

tryptocidine A, however, only occurred at increasing concentrations of Phe (Fig. 3.4 C), in keeping with the reported affinity [5].

Therefore, while the affinity of the peptide synthetases for a specific variable residue plays a large role in determining the incorporation of a specific residue at the variable positions, it is only part of the picture. In our production model, incorporation of the variable amino acids at a specific site takes not only the affinity of the peptide synthetases into consideration, but also production rate (Vx_a) and extent of cooperativity (n), as is evident from Eq. 9. These additional factors, acting together with the affinity (K_M), lead us to conclude that a higher production rate and affinity for Trp at position 7 leads to its preferential incorporation (Fig. 3.4 B), as is evident from the higher fitted C_1 value for Trp at position 7 (Table 3.1).

This hypothesis is corroborated by the production of a range of tyrocidine A analogues (Phe^3, Phe^4) when only Phe was supplemented to the growth medium, indicating a high production rate at positions 3 and 4 for Phe despite the affinity of both adenylation domains of the variable dipeptide positions being lower for Phe. At position 7, however, the production of tyrocidine A (Tyr^7) predominates (Fig. 3.5 A), indicating a high production rate for Tyr^7, as supported by the large C_2 value for Trp at position 7 (Table 3.1). Due to the lower affinity and production rate, incorporation of Phe^7 only increased marginally (Fig. 3.5 C), where production of phenycidine A comprised just 25% of the total production profile at the highest total Phe concentration of 32.8 mM (Fig. 3.3 A). Using the independently fitted parameters for Trp^7 and Tyr^7, our production model emulated the observed experimental data for Phe^7 (Fig. 3.4 C), thereby supporting the fitted parameter values used.

The incorporation of Phe at the three variable positions (Fig. 3.5 A) indicated a varied affinity and production rate at all the variable positions with position 4> 3>>7. The incorporation of Trp at the three variable positions (Fig. 3.6 B) indicated the preferential Trp^7 incorporation, which was marginally higher than Trp^3, both of which showed a higher preference for Trp relative to Trp^4. Ultimately, the specific ratio of competing amino acids, irrespective of their absolute concentrations, determined the incorporation of a residue at each of the variable positions relative to the unique kinetic properties of each of the peptide synthetases.

As the incorporation of at a specific variable positon is dependent on the ratio of the competing amino acids, production of tryptocidine B predominated at the lowest concentration which Trp was fixed. Lowering of the concentration of the co-supplemented Trp would most likely result

in an earlier increase in tryptocidine A production, while marginally increasing tyrocidine A and B analogues in the current production medium. Particularly when considering the high affinity and production rate at position 7 for Trp. Therefore, the presence of Trp in the medium shifts the peptide production profile away from tyrocidine production toward the production of a new subset of peptides, the tryptocidines.

3.6 Conclusions

While our results concur with kinetic data of Mootz and Marahiel [5], it clearly indicated a preferential substitution of Trp by Phe first at position 4 and only at increased Phe concentrations was Trp substituted by Phe at position 3. Position 7, however, was predominantly occupied by Trp in all of the cases where Trp was supplemented to the medium. Therefore the adenylation domains at position 3 and position 7 in particular, are found to be preferentially Trp activating domains [5]. The higher rate of incorporation of Trp^7 was likely to be due to the higher production rate at this position. Phe occupation of the variable aromatic positions only occurred at increased Phe concentrations and low basal Trp concentrations, and even more so at the variable aromatic position which only occurred at the highest Phe concentrations and in the absence of Trp supplementation.

Using the constructed competitive binding model we are able to predict the cyclodecapeptides production profile of the producer organism under given aromatic amino acid concentrations within the growth media. This allows for the increased production of selected analogues.

3.7 References

1. Dubos, R. J. and Hotchkiss, R. D. (1941) The production of bactericidal substances by aerobic sporulating bacilli. J. Exp. Med. **73**, 629-640
2. Dubos, R. J. (1939) Studies on a bactericidal agent extracted from a soil *Bacillus*: I. Preparation of the agent. Its activity *in vitro*. J. Exp. Med. **70**, 1-10
3. Hotchkiss, R. D. and Dubos, R. J. (1941) The isolation of bactericidal substances from cultures of *Bacillus brevis*. J. Biol. Chem. **141**, 155-162
4. Dubos, R. J. and Cattaneo, C. (1939) Studies on a bactericidal agent extracted from a soil *Bacillus*: III. Preparation and activity of a protein-free fraction. J. Exp. Med. **70**, 249-256
5. Mootz, H. D. and Marahiel, M. A. (1997) The tyrocidine biosynthesis operon of *Bacillus brevis*: Complete nucleotide sequence and biochemical characterization of functional internal adenylation domains. J. Bacteriol. **179**, 6843
6. Kopp, F. and Marahiel, M. A. (2007) Macrocyclization strategies in polyketide and nonribosomal peptide biosynthesis. Nat. Prod. Rep. **24**, 735-749

7. Marahiel, M. A. and Essen, L. O. (2009) Nonribosomal peptide synthetases: Mechanistic and structural aspects of essential domains. Meth. Enzymol. **458**, 337-351

8. Vosloo, J. A., Stander, M. A., Leussa, A. N., Spathelf, B. M. and Rautenbach, M. (2013) Manipulation of the tyrothricin production profile of *Bacillus aneurinolyticus*. Microbiology **159**, 2200-2211

9. Spathelf, B. M. (2010) Qualitative structure-activity relationships of the major tyrocidines, cyclic decapeptides from *Bacillus aneurinolyticus*. Stellenbosch University, Department of Biochemistry, Stellenbosch, South Africa. **PhD. Thesis**, http://hdl.handle.net/10019.1/4001

10. Okuda, K., Edwards, G. C. and Winnick, T. (1963) Biosynthesis of gramicidin and tyrocidine in the dubos strain of *Bacillus brevis* I: Experiments with growing cultures. J. Bacteriol. **85**, 329-338

11. Shida, O., Takagi, H., Kadowaki, K., Yano, H., Abe, M., Udaka, S. and Komagata, K. (1994) *Bacillus aneurinolyticus* sp. nov., nom. rev. Int. J. Syst. Bacteriol. **44**, 143-150

12. Shida, O., Takagi, H., Kadowaki, K. and Komagata, K. (1996) Proposal for two new genera, *Brevibacillus* gen. nov. and *aneurinibacillus* gen. nov. Int. J. Syst. Bacteriol. **46**, 939-946

13. Lewis, J., Dimick, K. P. and Feustel, I. (1945) Production of tyrothricin in cultures of *Bacillus brevis*. Ind. Eng. Chem. Res. **37**, 996-1004

14. Bidlingmeyer, B. A., Cohen, S. A. and Tarvin, T. L. (1984) Rapid analysis of amino acids using pre-column derivatization. J. Chromatogr. B Biomed. Sci. Appl. **336**, 93-104

15. Mach, B. and Tatum, E. (1964) Environmental control of amino acid substitutions in the biosynthesis of the antibiotic polypeptide tyrocidine. Proc. Natl. Acad. Sci. U. S. A. **52**, 876-884

16. Ruttenberg, M. A. and Mach, B. (1966) Studies on amino acid substitution in the biosynthesis of the antibiotic polypeptide tyrocidine. Biochemistry **5**, 2864-2869

Chapter 4
Production and purification of the tyrocidines and analogues

4.1 Introduction

The tyrocidines have shown great promise targeting pathogens which cause substantial damage in both the agricultural and food industries. These include the food spoilage Gram positive bacteria *Listeria monocytogenes* [1,2], as well as a multitude of pre- and post-harvest fungi [3]. The damage caused by these pathogens through food spoilage and reduced agricultural production results in not only severe economic hardship, but they also directly or indirectly lead to extensive morbidity and mortality, particularly in developing countries.

With existing chemical agents losing potency and increased resistance to their use; there is clearly a need for the development of novel, so called green-biocides [4]. These ideally need to have an alternate mode(s) of action to that of most conventional chemical control agents, as well as multiple cellular targets, thereby limiting the potential for resistance development. On the other hand these agents must be biodegradable, yet resistant enough to degradation that they may persist for long enough in the environment to offer protection against slow growing fungal pathogens or opportunistic bacteria, both in agricultural applications as well as in food packaging and storage.

The tyrocidines, produced by the soil bacterium *Bacillus aneurinolyticus*, generally fit the criteria of a green-biocide. These cyclodecapeptides are produced together with the linear 15-mer gramicidins after the logarithmic growth phase and are extracted as a complex known as tyrothricin (Table 4.1) [5,6]. They are safe for both topical applications [7-9] and oral consumption [10-14] and have been extensively utilised as the active ingredient in throat lozenges containing 1 mg tyrothricin under the trade name of Tyrozets® [15]. The cyclic structure of the tyrocidines increases their resistance to degradation by proteases, however, they remain biodegradable. They have multiple possible cellular targets ranging from the membrane and cell wall [16-18] to intracellular targets such as enzymes of the electron transport chain [19], while also including the ability to bind DNA and RNA [20-22].

The ability to shift the tyrothricin peptide production profile of the producer organism to increase the production of selected analogues with enhanced activity toward specific pathogens has previously been demonstrated [24]. The tyrocidines maintain their

antimicrobial activity in a range of different environments; demonstrating resilience to a number of salts [1]. In light of their promising antimicrobial activity toward the mentioned food and agricultural pathogens, including their other defining characteristics, the tyrocidines show potential to serve as novel green-biocides.

Table 4.1 Summary of the possible different peptides in the tyrothricin extract from *Bacillus aneurinolyticus*

Peptide	Abbr.	Sequence [a]	M_r Theoretical [b]	*m/z* Singly charged	*m/z* Doubly charged
Tyrocidine A analogues (Ff)					
Phenycidine A[c]	PhcA	Cyclo-(fPFfNQFVOL)	1253.6597	1254.6675	627.8377
Phenycidine A_1[c]	$PhcA_1$	Cyclo-(fPFfNQFVKL)	1267.6753	1268.6832	634.8455
Tyrocidine A	TrcA	Cyclo-(fPFfNQYVOL)	1269.6546	1270.6624	635.8351
Tyrocidine Av[c]	TrcAv	Cyclo-(fPFfNQYVOV)	1255.6390	1256.6468	628.8273
Tyrocidine A_1	$TrcA_1$	Cyclo-(fPFfNQYVKL)	1283.6703	1284.6781	642.8430
Tryptocidine A	TpcA	Cyclo-(fPFfNQWVOL)	1292.6706	1293.6784	647.3431
Tryptocidine A_1	$TpcA_1$	Cyclo-(fPFfNQWVKL)	1306.6862	1307.6941	654.3509
Tyrocidine B analogues (Wf)					
Phenycidine B[d] /B'[d]	PhcB	Cyclo-(fPWf/Fw)NQFVOL)	1292.6706	1293.6784	647.3431
Tyrocidine B/B'	TrcB	Cyclo-(fP(Wf/Fw)NQYVOL)	1308.6655	1309.6733	655.3406
Tyrocidine B_1/B_1'	$TrcB_1$	Cyclo-(fP(Wf/Fw)NQYVKL)	1322.6812	1323.6890	662.3484
Tryptocidine B/B'[d]	TpcB	Cyclo-(fP(Wf/Fw)NQWVOL)	1331.6815	1332.6893	666.8486
Tryptocidine B_1[c]/B_1'[d]	$TpcB_1$	Cyclo-(fP(Wf/Fw)NQWVKL)	1345.6971	1346.7050	673.8564
Tyrocidine C analogues (Ww)					
Phenycidine C[d]	PhcC	Cyclo-(fPWwNQFVOL)	1331.6815	1332.6893	666.8486
Tyrocidine C	TrcC	Cyclo-(fPWwNQYVOL)	1347.6764	1348.6842	674.8460
Tyrocidine C_1	$TrcC_1$	Cyclo-(fPWwNQYVKL)	1361.6921	1362.6999	681.8539
Tryptocidine C	TpcC	Cyclo-(fPWwNQWVOL)	1370.6924	1371.7002	686.3540
Tryptocidine C_1[c]	Tpc C	Cyclo-(fPWwNQWVKL)	1384.7080	1385.7159	693.3618
Linear gramicidins					
Val-Gramicidin A	VGA	VGAlAvVvW-lWlWlW	1881.078	1882.0862	941.5470
Val-Gramicidin B	VGB	VGAlAvVvW-lFlWlW	1842.067	1843.0753	922.0415
Val-Gramicidin C[c]	VGC	VGAlAvVvW-lYlWlW	1858.062	1859.0702	930.0390
Ile-Gramicidin A	IGA	IGAlAvVvW-lWlWlW	1895.094	1896.1018	948.5548
Ile-Gramicidin B[c]	IGB	IGAlAvVvW-lFlWlW	1856.083	1857.0909	929.0494
Ile-Gramicidin C[c]	IGC	IGAlAvVvW-lYlWlW	1872.078	1873.0858	937.0468

[a] Conventional one letter abbreviations used for amino acid sequences as obtained from Tang *et al.* [23] with O representing ornithine and lower case representing D-amino acids
[b] Sum of the monoisotopic residual molecular masses of constituent amino acids within the peptide
[c] Low to very low levels in tyrothricin
[d] Has not been detected or identified up to date

The use of the tyrocidines and their analogues as green-biocides, however, is dependent on their production and purification being both economically viable, as well as up-scalable to large scale production. Available literature on the production and purification of tyrothricin is

limited to the work of a few investigators world-wide. After the initial report on its discovery in 1939 [25], Dubos and a number of co-investigators described its production in stationary cultures in addition to subsequent purification and characterization [5,6,25,26]. Lewis *et al.* [27] reported in some depth the successful formation of tyrothricin in stationary cultures using both a tryptone based media as well as vegetable waste obtained from asparagus juice with yields in excess of 2000 mg/L.

Tyrothricin production in submerged, aerated cultures using defined media and simple nitrogen sources was first reported by Stokes and Woodward [28]. Appleby *et al.* [29,30] continued with the topic and succeeded in producing yields as high as 890 mg/L. The production of tyrothricin in submerged (fermentor) cultures, however, remained well below that achieved in stationary cultures using complex nitrogen sources. Increased tyrothricin production by submerged culturing is limited to a single patent using the effluent from corn starch production reporting a yield of 1600 mg/L [31]. Production levels of 1400 mg/L in submerged cultures are briefly mentioned by Lewis *et al.* [27] with the same tryptone-based media used successfully in stationary cultures.

Using the available literature as a basis, a study was performed where the yield of naturally produced tyrothricin by *Bacillus aneurinolyticus* was increased through the elucidation of the optimal production medium, as well as growth conditions. Furthermore, two purification methodologies were developed/optimised to purify the tyrocidines and their analogues from the culture broth of *B. aneurinolyticus* to an acceptable level of purity.

4.2 Materials

Bacillus aneurinolyticus ATCC 10068 was used as the tyrothricin producer strain while *Aspergillus fumigatus* ATCC 204305 served as the representative fungal target organism, both of which were from the American Type Culture Collection (Manassas, VA, USA). Gram positive bacteria target organisms *Micrococcus luteus* NCTC 8340 and *Bacillus subtilis* 168 were obtained from the National Collection of Type Cultures (Porton Down, Salisbury, England) and Bacillus Genetic Stock Centre (Ohio State University, OH, USA) respectively. A selection of culture broths, yeast extract, glucose, agar, diethyl ether, acetone, ethanol (EtOH), sodium chloride (NaCl), and hydrochloric acid (HCl) were from Merck (Darmstadt, Germany). The L-amino acids: phenylalanine and tryptophan were from Sigma-Aldrich (Steinheim, Germany). Ultra-pure urea was from ICN Biomedicals Inc (Aurora, USA).

Tween 20 and potato dextrose broth (PDB) were from Fluka (Buchs, Switzerland). Skimmed milk powder was from Clover (Roodepoort, South Africa). Activated carbon was from Lurgi (Frankfurt, Germany). Trifluoroacetic acid (TFA; >98%), tertiary butanol (>99%), a commercially available tyrothricin extract, gramicidin S (GS), and XAD-16 resin were from Sigma-Aldrich (St. Louis, USA). Standard, sterile 96-well flat bottom microtiter plates and petri dishes were from Corning Incorporated (USA) and Lasec (Cape Town, South Africa) respectively. Acetonitrile (ACN; HPLC-grade, far UV cut-off) was from Romill Ltd (Cambridge, UK). Falcon® tubes were from Becton Dickson Labware (Lincoln Park, USA). An AKTA® chromatographic system was from Amersham Pharmacia Biotech (Uppsala, Sweden). Electrospray mass spectrometry (ESMS) was performed using a Waters Synapt G2 mass spectrometer, NovaPak HR C_{18} HPLC semi-preparative column (6 µm particle size, 300 mm x 7.8 mm) and an Acquity UPLC® BEH C_{18} (1.7 µm particle size, 2.1 mm x 100 mm) ultra-performance liquid chromatography (UPLC) column were from Waters-Millipore (Milford, USA). Analytical grade water was prepared by filtering water from a reverse osmosis plant through a Millipore-Q® water purification system (Milford, USA). All media was sterilized by autoclaving for 15 minutes at 121 °C.

4.3 Methods

4.3.1 Culturing of organisms

Pre-culturing of the producer strain: Single colonies of the *Bacillus aneurinolyticus* producer strain were obtained from freezer stocks. Using conventional sterile techniques, culturing was done for 48 hours on pre-culture agar plates, containing 0.5% *(m/v)* peptone, 0.25% *(m/v)* yeast extract, 0.1% *(m/v)* glucose and 0.1% *(m/v)* skimmed milk powder, 1.5% *(m/v)* agar in analytical grade water; pH 7.0. Single colonies were selected and incubated while shaking at 220 rpm for 24 hours at 37 °C in Falcon® tubes containing 5 mL pre-culture medium (0.5% *(m/v)* peptone, 0.25% *(m/v)* yeast extract, 0.1% *(m/v)* glucose and 0.1% *(m/v)* skimmed milk powder; pH 7.0).

Pre-culturing of the indicator organism: Gram-positive bacteria *M. luteus* NCTC 8340 was cultured on Luria Bertani agar plates (LBA; 1% *(m/v)* tryptone, 0.5% *(m/v)* yeast extract, 1% *(m/v)* NaCl, 1.5% *(m/v)* agar, in analytical grade water), while *B. subtilis* OKB 168 was cultured on tryptone soy agar plates (TSA; 3% *(m/v)* TSB, 1.5% *(m/v)* agar in analytical grade water) for 48 hours at 37 °C. Using normal sterile techniques selected colonies were incubated while shaking at 150 rpm for 16 hours at 37 °C in LB broth (1% *(m/v)* tryptone,

0.5% *(m/v)* yeast extract, 1% *(m/v)* NaCl in analytical grade water) medium to an optical density (OD) of approximately 0.8 at 595 nm. These cultures were subsequently sub-cultured in tryptone-soy broth (3% *(m/v)* TSB in analytical grade water) and grown to an OD of 0.6 at 595 nm.

Pre-culturing of fungi: Spores of the fungi *A. fumigatus* ATCC 204305 were obtained from freezer stocks and cultured using conventional sterile techniques on potato dextrose agar plates (PDA; 2.4% (*m/v*) PDB, 1.5% *(m/v)* agar, in analytical grade water) for three weeks. Subsequently 7 mL of Tween water (20 µL of Tween in 200 mL analytical grade water and autoclaved) was added to the plates, the spores lightly loosened using a hockey stick and hydrated over night at 4 °C. These were subsequently counted using a standard counting chamber and diluted with sterile water to a concentration of 50 spores/µL.

4.3.2 Selection of high tyrothricin producers

A radial diffusion assay was performed using methods adapted from those described by Du Toit and Rautenbach [32] and Lehrer *et al.* [33]. A gel solution (1% *(m/v)* powdered TSB medium, 1% *(m/v)* agar powder and 0.02% *(v/v)* Tween 20) was prepared with analytical grade water and autoclaved. One millilitre of *M. luteus* at an OD of 0.6 at 595 nm was added to 9 mL of the gel at 45°C and homogenized by inversion. The gel was then poured into sterilized culture dishes on a level surface and allowed to set for 30 minutes. Single colonies of *B. aneurinolyticus* were then spotted onto the gel 1.25 cm apart. The plates were incubated for 16 hours at 37 °C and the inhibition zones observed. From these, high tyrothricin producers were selected and cultured on pre-culture plates for 48 hours at 37 °C. These were suspended in 10% *(m/v)* skimmed milk powder and lyophilised. Subsequently, a spatula tip of these dried cultures was suspended in 0.5 mL of culture medium and allowed to hydrate for 4 hours and streaked out on pre-culture plates prior to culturing in liquid pre-culture medium.

4.3.3 Tyrothricin production and extraction

For production the medium base (salts, sugars), N-source(s), metal ions, oxygenation and culture time was adapted to optimise production (medias A-D, refer to table 4.2). Due to future commercial applications of this part of the project very little detail of the production and purification methodologies can be revealed. The parameters and best media for the optimised productions in fermentation vessels have been determined by the BIOPEP® Peptide Group and are protected under non-disclosure agreements (NDAs) with all members working

on these fermentations to insure the future commercialisation potential of the peptide products.

Flask/Stationary cultures: A 1% (*v/v*) of pre-cultured *B. aneurinolyticus* was added to the selected medium containing protein as N-source and a carbohydrate carbon source at culture volumes from 20 mL to up to 2.5 L. These cultures were incubated at 37 °C over a time period of 8 to 28 days. Growth was evaluated in terms of gram dry cell mass to determine biomass production. Tyrothricin production was equated to the crude extract mass obtained.

Growth rate and tyrothricin production within the cultures was evaluated in 2 L Erlenmeyer flasks in quadruplicate (*n=4*). A 5 mL sample was taken every 24 hours until 240 hours, after which samples were taken every 48 hours until 384 hours.

Fermenter/Submerged cultures: Further efforts to increase tyrothricin production and shorten the production time required were performed in 1L bioreactors using Media C (refer to table 4.2). While the temperature was maintained constantly at 37 °C; the cultures were aerated with compressed air at one volume per volume per minute (VVM) and agitated at 60 rpm, unless otherwise stated. Samples of 5 mL were drawn off aseptically every two hours for the first 24 hours, and thereafter this was decreased to twice every 24 hours. The culturing period was extended up to a maximum of 240 hours. These cultures were run in parallel to stationary, shallow layer cultures to allow for direct comparison of the tyrothricin yields.

The pH was measured and growth determined spectrophotometrically by measuring the optical dispersion at 595nm (OD_{595}) from the samples taken of the respective cultures. A crude tyrothricin extract mass was obtained by extraction with 70% (*v/v*) ACN containing 0.3% (*v/v*) TFA in water. These samples were analysed by ESMS at a concentration of 1.0 mg/mL and the percentage of the detected tyrothricin peptide signal determined relative to the total signal. The mass of the extracts was subsequently adjusted relative to the earlier extracts where no peptide was detected.

4.3.4 Amino acid manipulated productions

The production of selected tyrocidine analogues was achieved through the supplementation of the growth medium with selected concentrations of phenylalanine (Phe) or tryptophan (Trp) established in Chapter 2 and 3. Production media was supplemented with either Phe or Trp alone or in combination at 5.5 and 16 mM. Pre-cultured *B. aneurinolyticus* were

inoculated at a volume of 1% (*v/v*) relative to the final volume production media and cultured in shallow stationary cultures as previously described.

4.3.5 Tyrothricin purification

The produced peptide was extracted according to an optimised method based on the original extraction methods [5,26]. The first optimised purification method (PM_1) of crude peptide can only be briefly described since it is currently protected under a NDA as it has been classified as trade-secret (BIOPEP®, University of Stellenbosch). The biomass was extracted using an extreme pH step, organic solvent extractions, precipitation steps and/or activated carbon treatments, followed by chromatographic purification. This yielded crude extracts of about 40% peptide and purified peptide fractions with >75 tyrothricin. The purified fractions were chemically characterised using UPLC-MS as described below and by Vosloo *et al.* [24].

The second purification methodology (PM_2) involved purification of the tyrothricin extract by means of adsorption chromatography. A XAD-16 resin was packed into a 0.8 cm radius glass column to a bed height of 12.75 cm and a column volume (CV) of 25.6 cm^3. The crude tyrothricin extracts were suspended in 50% (*v/v*) EtOH in water, centrifuged for five minutes at 3000 × g to remove any particulate and injected onto the column connected to an AKTA chromatographic system. Using 0.1% (*v/v*) TFA in water (A) and EtOH (B) as solvents, the column was conditioned at a flow rate of 1.5 mL/minute for 1×CV at 20% B. At 20% B and flow rate of 0.2 mL/minute, 1.0 mL of sample was loaded onto the column followed by a further 0.2×CV at the same flow rate to allow for increased interaction time of the sample with the resin. The elution flow speed was subsequently increased to 1 mL/minute and the sample eluted using a step wise gradient. The fractions were eluted from the column with 2×CV at 20% B, 3×CV at 50% B, 5×CV at 90% B, and 2×CV at 100% B. The column was then reconditioned using a linear gradient from 100% B to 20% B over 1×CV and then 20% B for 5×CV at a flow rate of 1.5 mL/minute.

4.3.6 Antimicrobial activity assays

Antibacterial activity assays: A variation of the microtiter broth dilution method described by Du Toit and Rautenbach [32] and Lehrer *et al.* [33] was used to test the antimicrobial activity of the peptides. A pre-culture of the *B. subtilis* was diluted with TSB to an OD of 0.2 at 595 nm (±10^8 CFU/mL). A volume of 90 µL of diluted *B. subtilis* was added to all of the wells of the 96-well microtiter plate except for the top four wells in first column which

received 90 µL of TSB. The wells of the first column received 10 µL of 15% (*v/v*) EtOH, thus served as sterility and growth controls respectively. Assays with the tyrocidine mixture obtained from commercial tyrothricin were repeated in triplicate (*n=3*) while those with GS were done in duplicate (*n=2*) in all the microtiter plates and served as positive controls. All the rest of the wells received 10 µL of one of the respective peptide extracts from the various purification steps repeated in triplicate (*n=3*). All peptides were suspended in 15% (*v/v*) EtOH, hence a final EtOH concentration of 1.5% (*v/v*) and peptide concentration ranging from 100 to 0.4 µg/mL. The microtiter plates were then covered and incubated for a period of 16 hours at 37 °C, following which the light dispersion was measured spectrophotometrically at 595 nm using a Bio Rad™ microtiter plate reader.

These data were analysed using GraphPad Prism® 4.03 (GraphPad Software, San Diego, USA) to plot the percentage growth inhibition of the respective peptide extract relative to the mean of the growth control, as previously described by Rautenbach *et al.* [34], using the following equation:

$$\% \text{ growth inhibition} = 100 - \frac{100 \times (A_{595} \text{ of well} - \text{Mean } A_{595} \text{ of background})}{(\text{Mean } A_{595} \text{ of growth control} - \text{Mean } A_{595} \text{ of background})}$$

Antifungal activity assays: A variation of the previously described microtiter broth dilution method optimised for antifungal assays was used to test the activity of the mentioned peptides toward *A. fumigatus* [35]. A volume of 50 µL of PDB was added to all the wells of a sterilized microtiter plate. The top four wells in the first column received 40 µL of sterilized water, while all the rest of the wells received 40 µL of the mentioned spore suspension. The rest of the assays setup was as described above for the bacterial assays. The microtiter plates were then covered and incubated for a period of 48 hours at 25 °C, following which the light dispersion was measured spectrophotometrically at 595 nm using a BioRad™ microtiter plate reader and the percentage growth inhibition determined as previously described.

4.3.7 Semi-preparative HPLC of extracts to purify single peptides

Selected extracts obtained were purified by reverse phase HPLC using methodology adapted from that previously described by Rautenbach *et al.* [1] and Eyéghé-Bickong [36]. Extracts were dissolved in 50% (*v/v*) ACN in water, centrifuged at 8600 × *g* for 10 minutes to remove any debris before being injected onto the column at a concentration of 10 mg/mL for crude samples and 4 mg/mL for partially purified samples. The chromatographic purification of the

tyrocidines and analogues was done according the method for the tyrocidines as described by Eyéghé-Bickong [36] and by Rautenbach *et al.* [1]. Briefly, a non-linear gradient (Waters gradient 6) at 3.0 mL/minute of 50% solvent A (0.1% (*v/v*) TFA in analytical grade water) to 80% solvent B (10% (*v/v*) solvent A in 90% (*v/v*) ACN) over a period of 23 minutes (Method A) was used to purify the major tyrocidines on a semi-preparative C_{18} HPLC column. Alternatively, an adapted method, as described by Eyéghé-Bickong [36], for the purification of gramicidins was used to purify the more hydrophobic analogues of interest. This method (Method B) comprised of a 25.5 minute non-linear gradient (Waters gradient 6) at 3.0 mL/minute of 60 to 100 % solvent B. Chromatography was monitored using a Waters Model 440 UV-detector at a wave length of 254 nm at a column temperature of 35 ºC, as described by Rautenbach *et al.* [1]. The respective fractions were then analysed by UPLC-MS to determine the purity of the isolated tyrocidines and analogues.

4.3.8 ESMS and UPLC-MS analysis of tyrothricin extracts and purified peptides

Samples were dissolved in 50% (*v/v*) ACN in analytical grade water to concentrations of 10 mg/mL or 2.5 mg/mL regarding the culture extracts or peptides purified by HPLC respectively. These were then centrifuged at 8600 × *g* for 10 minutes to remove any debris prior to being diluted ten-fold using analytical grade water. Sample solutions (2 µL for direct analysis or 3 µL for separation by UPLC) were introduced by a Waters Acquity UPLC™ into a Waters Quadrupole Time-of-Flight Synapt G2 mass spectrometer with a Z-spray electrospray ionisation source in positive mode. Peptide extracts were subjected to a capillary voltage of 3.0 kV and cone voltages of 15 V or 25 V at a temperature of 120 ºC at the source, desolvation gas of 650 L/h and desolvation temperature of 275 ºC. Data acquisition was performed by scanning over a mass over charge ratio (*m/z*) range of 300 to 2000 in continuum mode at a rate of 0.2 scans per second.

Separation of samples on an Acquity UPLC® BEH C_{18} column *via* the mentioned Waters Acquity UPLC™ chromatographic system was achieved at a column temperature of 60 ºC and flow rate of 0.300 mL/min; using a 1% (*v/v*) formic acid in analytical grade water (A) to ACN (B) gradient: 100% A from 0 to 0.5 minutes for loading, from 0 to 30% B over 0.5 to 1 minute, then 30 to 60% B from 1 to 10 minutes, 60 to 80% B from 10 to 15 minutes. Reconditioning of the column was done from 80 to 0% B from 15 to 15.1 minutes and then 100% A from 15.1 to 18 minutes.

4.4 Results and Discussion

4.4.1 Optimisation of tyrothricin production in different media compositions

In the present study a change in total tyrothricin production and colony morphology was observed with successive culturing on agar media. Variable tyrothricin production levels not only among different strains of the tyrothricin producers [26], but also between colonies of the same strain has been observed [27,29,30]. The maintenance of high producing colonies was instrumental for maximal tyrothricin production to occur. Selection of high producing colonies by spotting single colonies onto petri dishes seeded with *M. luteus* and production of freezer stocks prevented the systematic reduction of peptide production (data not shown).

Variations in media composition as well as the culturing conditions were performed in an effort to elucidate the optimal environment in which *B. aneurinolyticus* maximally produced tyrothricin. Four different media compositions were used and the tyrothricin yield and peptide profile was assessed (Table 4.2). Initial tyrothricin production was achieved in a mixed animal and digested protein extract containing together with urea (media A). This production medium was of similar composition to that used by the pioneers of tyrothricin research [26], with the addition of urea as a simple nitrogen source, which is proposed to increase tyrothricin yields [37]. Our yields of crude extract were similar to those obtained by Dubos and Hotchkiss [26] for tyrocidine production in this medium, with TrcA (M_r = 1269.7) and TrcB (M_r = 1308.7) being the most abundant peptides. However, similar to these investigators [26], some variability was observed in the yields obtained between different cultures. However, the relative peak area obtained by UPLC-MS analysis determined these extracts were only composed of 19% (*m/m*) tyrothricin peptides and only 80 mg/L tyrothricin (Table 4.2).

Increased tyrothricin production within stationary cultures is proposed to be dependent on the utilization of complex N sources [30]. Media B was as described by Appleby *et al.* [30] with a high percentage of complex nitrogen source instead of the additional simple nitrogen in the form of urea in Media A. Our yields were well below the 800 mg/L that they obtained, while UPLC-MS analysis determined the crude extract masses to contain only 15% (*m/m*) tyrothricin peptides with TrcA (M_r = 1269.7) being the most abundant peptide. In contrast, using Media C and D the crude extract masses obtained were greater than those of Lewis *et al.* [27] and contained 40% (*m/m*) tyrocidine peptides with TrcA (M_r = 1269.7) and TrcB (M_r = 1308.7) being the most abundant peptides in for Media C and TrcB (M_r = 1308.7)

and TrcC (M_r = 1347.7) for media D. The latter two media contained a high carbohydrate concentration, together with high concentrations of complex nitrogen. High tyrothricin production observed in Media C and D (Table 4.2) is supported by the Lewis *et al.* [27] who reported increased tyrothricin production in excess of 2000 mg/L to be dependent on the concentration of tryptone as a complex nitrogen source and glucose as carbohydrate source, which could be substituted with either glycerol or mannitol. The differences observed in the production levels found in this study relative to those of other investigators within the same or similar production media [26,28,30] could be because of differences in producer strains used by different investigators, as well as differences in culturing procedures. These results also corroborate our previous findings described in Chapter 2 and 3 on the sensitivity of the production profile towards the aromatic amino acid ratio, which probably differ substantially between the different media.

Table 4.2 Summary of the mean tyrothricin yield extracted from cultures of *B. aneurinolyticus* grown in the respective media compositions

Culture Medium (Fermentation Time)	**Media character**	**Crude extract mass ± SEM (g/L)**	**% Tyrocidine in extract***	**Calculated amount of tyrothricin (g/L)****
Medium A (10 days)	Mixed animal protein and digested protein + urea	0.32±0.03 (*n=20*)	19	0.08
Medium B (10 days)	High digested animal protein content	0.35±0.05 (*n=7*)	15	0.07
Medium C (10 days)	Glucose + digested milk protein	2.80±0.17 (*n=45*)	40	1.49
Medium D (10 days)	Glucose + digested milk and plant protein	2.40±0.20 (*n=7*)	40	1.28

SEM, standard error of the mean; * determined via UPLC-MS, calculated relative to commercial tyrocidine mixture; ** Calculated from the expected 20:20:60 ratio of contaminants: gramicidins: tyrocidines in the crude [5,26].

Analysis of the peptide production profiles in the four different production media by ESMS revealed an increase in the contribution of the linear gramicidin component to the tyrothricin extract in Media C and more so in Media D (data not shown). The lack of detection of the linear gramicidins in Media A and B (data not shown) is most likely due to the low tyrothricin peptide content of these extracts combined with the reduced ionisation of the linear gramicidins hampering their detection. As production of the tyrocidines and analogues

was the main focus of this research, Media C was used in further efforts at evaluation of the optimal production conditions.

4.4.2 Evaluation of the growth and tyrothricin production in Media C

The yields of tyrothricin obtained were found to be dependent on the growth state of the producer strain, as well as the ratio of starter culture to production medium. Moreover, the selection of large, darker colonies grown for 48 hours on pre-culture plates was instrumental to high tyrothricin production. These were suspended into pre-culture media, having reached an OD_{595} of 06-1.0 in 24 hours. These cultures were inoculated into the production media at a ratio 1% of the final culture volume. If too high a ratio of starter culture was used high growth was observed, but tyrothricin production was suppressed (data not shown). The influence of culture depth on the growth and tyrothricin production has been extensively researched by Lewis *et al.*[27]. The growth and tyrothricin production within these flask cultures was investigated over a period of 384 hours (16 days) (Fig. 4.1).

Production of the tyrocidines and related peptides in the tyrothricin complex is reported to commence toward the end of the logarithmic growth phase [25,25,26,38], as is evident in Fig. 4.1 after 48 hours. The end of the logarithmic growth phase was only reached after 72 hours, however, the producer strain then entered a second growth phase where maximal tyrocidine production occurred, as apparent from the diauxic growth curve. Peptide production increased steadily throughout the second growth phase until reaching a maximum after 336 hours (14 days) when production suddenly declined, despite maintaining a high OD_{595}. The pH of all the cultures increased systematically until 144 hours where after it started to decline steadily. Despite the variability of the pH it remained alkaline in all of the cultures, which is probably due to the high content of basic peptides that were produced.

In an effort to increase tyrothricin production while also decreasing the time required for production, submerged cultures were performed in one litre bioreactors. The initiation of bacterial growth in these cultures was erratic; while in control cultures run in parallel growth was consistently observed within six hours, cultures in the bioreactors frequently failed to start growing. Efforts to initiate growth were performed by briefly increasing the aeration to 2×VVM and/or agitation to 200 rpm. Once culture growth was initiated, the aeration and agitation were returned to their previous rates as maintenance at these increased rates resulted in high foam production which blocked the aeration source filters resulting in spillage and

subsequent termination of the cultures. After a lag of up to seven hours, the initiated cultures grew rapidly depleting the available dissolved oxygen concentration (dO_2) and reached the end of the logarithmic growth phase near 24 hours (Fig. 4.2).

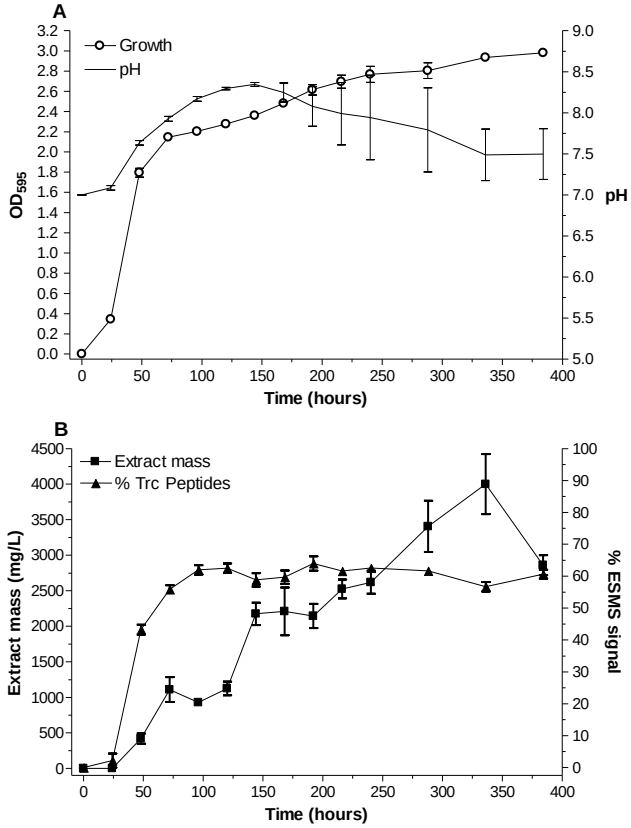

Figure 4.1 Growth and tyrothricin production of *B. aneurinolyticus* in flasks using Media C over a culturing period of 384 hours (16 days). **A** Growth of *B. aneurinolyticus* measured spectrophotometrically at OD_{595} and pH fluctuation over the growth period. **B** Extract mass obtained over the culturing period together with the percentage total tyrocidine peptide (Trc Peptides) relative to the total signal obtained in each ESMS analysis of the respective culture extracts.

The pH from one culture to the next very rarely gave identical curves, however, they did follow specific trends either in the stationary (Fig. 4.1) or submerged cultures (Fig. 4.2), as has been reported in literature [27,29]. In the submerged cultures reported in literature [28,29] as well as those of our own (Fig. 4.2), the pH dropped after an initial small spike. This initial drop in pH has been associated with a phase of rapid anaerobic glucose utilisation [29], which coincided with a spike in dO_2, after which the pH then rose again. Without doing any external pH adjustments in the fermenter, we observed after the logarithmic phase the pH oscillated between pH 5.9 and up to pH 7.4 throughout the rest of the culturing period. The fluctuation in pH varied greatly between one culture and the next going as low as 4.8 and as high as 10.3 in other cultures (data not shown). Appleby *et al.* [29] has suggested that the increase in pH

after glucose depletion is due to initial anaerobic carbohydrate metabolism leading to acidic metabolites followed by protein breakdown and the release of ammonia. However, the production of tyrocidines with a pI>9 can also lead to increase in pH. Further investigation of this phenomenon was, however, beyond the scope of this study.

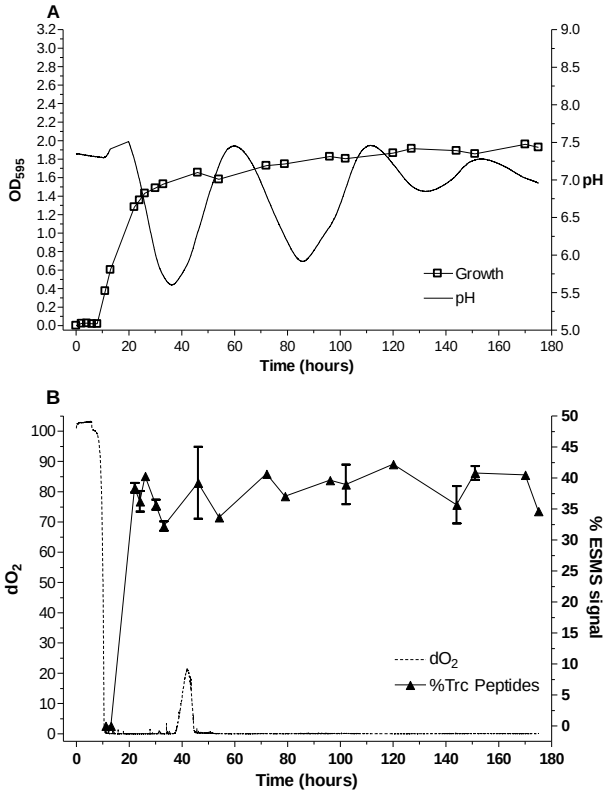

Figure 4.2 Growth and tyrothricin production of *B. aneurinolyticus* in Media C over a period of 175 hours cultured in a 1L bioreactor. **A** Growth of *B. aneurinolyticus* measured spectrophotometrically at OD_{595} and pH fluctuation over the growth period. **B** Variation of the dissolved oxygen concentration (dO_2) over the culturing period together with the percentage total tyrothricin peptide relative to the total signal obtained in each ESMS analysis of the respective culture extracts taken at the respective time points.

In contrast to what was observed in submerged cultures, glucose is reported to be utilised gradually throughout the culturing period in stationary cultures with tryptone as complex nitrogen sources and only depleted after 18 days of culturing [27]. The pH of these cultures also follows a different trend, where it steadily increases before beginning to decrease after an extended culturing period (Fig. 4.1). This would point toward altered metabolism of the cultures in the submerged relative to the stationary cultures and is supported by the observations described in literature [27-30].

The end of the logarithmic growth phase coincided with the first detection of the tyrothricin peptides in the culture extracts of the bioreactor cultures (Fig. 4.2) at 24 hours maintaining a

relative contribution of near 40% of the total ESMS signal. The flask cultures (Fig. 4.1) only reached the end of the logarithmic growth phase after 72 hours. The tyrothricin peptides were first detected in the culture extracts toward the latter end of the logarithmic growth phase at 48 hours. In the shallow stationary cultures the percentage contribution of the tyrothricin peptides relative to the total ESMS signal increased from near 50% to 60% when the cultures had entered the second growth phase. At the end of the logarithmic growth phase at 24 hours the submerged cultures had reached an OD_{595} of 1.36 at a growth rate (D ln OD_{595}/D time) of 0.202, while the stationary cultures took 72 hours to reach higher an OD_{595} of 2.15 which equated to a slower growth rate of 0.039. After the initial rapid growth rate the stationary cultures continued to increase in biomass at a second slower growth rate of 0.001. Concomitantly the extract masses obtained from the stationary culture samples increased steadily throughout the culturing period.

The ESMS spectra of the extracts obtained from the submerged cultures had a large amount of background noise due to much lower tyrocidine peptide peak intensity relative to those from the stationary cultures (data not shown). As a consequence of the low tyrothricin yield, co-extracted contaminants from the media and culture had a greater influence on the extract mass and ESMS spectrum. Therefore, the extracts obtained from the submerged cultures were highly variable with no discernible trend in tyrothricin production of the samples taken throughout the culturing period. Only the final extract mass of the total biomass extracted at the end of the culturing period was considered (Table 4.3).

Maximal tyrothricin production occurred when the stationary cultures reached the secondary growth phase was of sufficient biomass, yet had not depleted all of the available nutrients. As glucose is proposed to still be available [27], oxygen limitation after the initial biomass production is the most probable trigger in the initiation of the transcription of the genes responsible for tyrothricin production to occur in these cultures (Fig. 4.1). This hypothesis is supported by the observed detection of the tyrocidines in the stationary cultures after 48 hours. The cultures were then approaching the end of the logarithmic growth phase, however, there was still sufficient nutrients available for the cultures to continue increasing in biomass, albeit at a slower growth rate (Fig. 4.1).

Detection of tyrocidine peptides in the submerged cultures here too occurred within 24 hours at the end of the logarithmic growth phase. Despite the fact dO_2 already approached zero at 10.5 hours, approximately three hours after the cultures started actively growing (Fig. 4.2).

The stress trigger that initiated tyrocidine production in the submerged cultures was most likely nutrient depletion. As such, these aerated cultures depleted the available nutrients producing initial biomass. When the tyrocidine production was initiated only the biomass present at that time produced any peptide, in contrast to the stationary cultures where a large increase in biomass was observed well after the end of the logarithmic growth phase and initiation of tyrocidine production, particularly after 192 hours (8 days) (Fig. 4.1, Table 4.3).

Table 4.3 Summary of growth and tyrothricin production by *B. aneurinolyticus* in Media C under the respective culturing conditions and time periods. The final biomass obtained after 8 to 10 days culturing in four submerged cultures was used to represent the mean levels observed within the submerged cultures relative to those obtained from the stationary cultures over a period of between 8 and 18 days.

Culture	pH ± SEM	Dry cell mass ± SEM (g/L)	Extract mass ± SEM (g/L)	% Purity [a]
Submerged culture (*n=4*) [b]	7.29±0.76	2.6±0.6	0.74±0.19	ND
Stationary culture 8 days (*n=2*)	7.68±0.09	3.5±0.1	1.77±0.07	39
Stationary culture 10 days (*n=5*)	7.31±0.28	4.5±0.4	2.78±0.23	41
Stationary culture 12 days (*n=7*)	7.31±0.04	5.4±0.2	2.42±0.49	42
Stationary culture 14 days (*n=2*)	7.23±0.14	3.3±0.6	2.49±0.42	41
Stationary culture 16 days (*n=4*)	7.50±0.31	6.0±0.5	3.32±0.50	40
Stationary culture 18 days (*n=2*)	7.89±0.43	5.0±0.2	2.54±0.09	39

[a] The total peak area detected for the tyrocidine peptides in the UPLC-MS chromatogram is expressed as % relative to that of the commercial tyrocidine mixture at the same concentration of 1.00 mg/mL.
[b] Mean values obtained from the final biomass after 8 to 10 days culturing

Understanding the processes in control of the natural production of the tyrocidines is of particular relevance to the maintenance of high production. The initiation of tyrocidine production is under the control of the SpoA-AbrB regulatory pathway [39,40]; which is also associated with the activation of other genes responsible for the production of other secondary metabolites as well as sporulation [41]. The triggers for the initiation of these pathways are related to metabolic stress of the producer organism and include a range of factors ranging from oxygen limitation to nutrient starvation [42]. As the tyrocidines are extracted from the biomass, high tyrocidine production is dependent on increased biomass

production which has been sufficiently primed to produce peptide, yet not stressed to the extent that sporulation is initiated.

Production of tyrothricin in the stationary cultures reached increased levels after 10 days of culturing, despite marginally lower yield of biomass. Increasing the culturing period beyond this did not significantly increase the total tyrothricin production. Increased production observed in the 16 day cultures may possibly be attributed to the daily disturbance of the cultures that occurred when samples were taken (Fig. 4.1) as these increases were not observed in succeeding cultures.

Our results concur with those of Lewis *et al.* [27] who found that the tyrothricin yield within stationary cultures reached increased levels of production after 10 days of culturing. These investigators also report decreased growth and tyrothricin yields in cultures which had been disturbed and the pellicle layer of cells growing on top of the cultures disrupted. This was in contrast to what we observed after 16 days culturing. Extension of the culturing period for up to 28 days saw a considerable drop in the biomass and consequent peptide extracted relative to the initial culture volume (data not shown), attesting to the ability of the producer organism to sporulate once the nutrients had been depleted, similar as to what was observed in submerged cultures after nutrient depletion [28].

In an effort to emulate the production conditions observed in the stationary cultures, further submerged cultures were aerated through the head space of the bioreactor once the end of the logarithmic growth phase had been reached. This, however, did not increase the final biomass or tyrothricin production obtained from these cultures. The final biomass and tyrothricin production in the submerged cultures remained well below that of the stationary cultures (Table 4.3), despite the stationary cultures having a slower initial growth rate.

The suppression of tyrothricin production in submerged cultures in media containing complex nitrogen sources, such as the tryptone or a complex mixture of amino acids, is corroborated in literature [28,29]. These investigators were, however, able to produce tyrothricin in submerged cultures using defined minimal media which utilized glutamic acid, asparagine [28], ammonium succinate or urea as the sole nitrogen source [29]. In all of the later cases total tyrothricin production varied between 100 to 500 mg/L. This value could be increased to 890 mg/L with the addition of biotin to the ammonium succinate media [29]. Growth of the producer strain in stationary cultures using these defined media containing

simple nitrogen sources was, however, sparse and subsequent tyrothricin production was limited [30].

All of the evidence indicates toward the previously mentioned control of the balance between growth of the producer strain, tyrothricin production and sporulation. Tyrothricin production in submerged cultures using defined media occurred at slower growth rates, similar to what was observed in the stationary cultures cultured using complex nitrogen sources (Fig. 4.2). Therefore the low nutrient content of these media is the trigger for tyrothricin production and not oxygen limitation in these submerged cultures, in contrast to stationary cultures with complex nitrogen sources. Moreover, sporulation of the producer organism was observed after culturing in the defined media for over 40 hours when nutrients were being depleted [28]. This would then account for the extreme pleomorphism reported between stationary relative to aerated submerged cultures [30].

Tyrothricin production in submerged cultures has not been reported to exceed 890 mg/L using a chemically defined media of ammonium succinate with the addition of biotin [29]. Successful submerged production with complex nitrogen sources is limited to a patent using "corn steep water" [31] where a yield of 1600 mg/L was obtained after 12 days of culturing. While Lewis *et al* [27] reported a yield of 1400 mg/L after 48 hours of submerged culturing in Media C, they reported discrepancies between submerged versus stationary cultures. One aspect, however, is unclear from these older studies, namely the purity of the tyrothricin produced, as no detailed analysis is given. Quantification of tyrothricin production by these investigators was achieved means of antimicrobial activity [28-30] or haemolysis [5,26,27] assays. Our experience of tyrothricin production by submerged culturing using Media C was less satisfactory, with erratic initiation of culture growth. Peptide as well as biomass production in the submerged cultures was consistently well below that observed in the stationary cultures that were performed in parallel (Table 4.3). Consequently, our efforts to produce increased tyrothricin yield focused on stationary cultures.

4.4.3 Purification of the crude tyrothricin extract

Having increased tyrothricin production, a need existed to purify the tyrothricin extracts obtained from the different cultures. Certain cultures were found to produce a dark pigment which was co-extracted together with tyrothricin. Manipulation of the organic extraction step by limiting any heating, as well as starter colony selection reduced this contamination.

However, co-extraction of other unwanted pigments and other compounds remained a problem. To this end two purification methodologies were developed and optimised to purify the mixtures of tyrocidines and analogues to an acceptable level of purity (>75% in terms of peptide mass) for use in agricultural field trials by our group and the bee toxicity study reported in Chapter 7.

In the first purification methodology developed, PM_1, the solubility of the solution was manipulated to remove contaminants, including precipitation steps [5,6]. The rate at which the precipitate is formed has been suggested to increase with heating at 50 °C [27], however, due to our experience of increased pigment contamination observed with heating, the opposite was performed and precipitation was achieved at 4 °C within four hours. This step served to remove co-extracted hydrophilic contaminants from the extracts. In this purification step the purity was increased from 40% to about 60%, however, this varied between culture extracts. Interaction with activated carbon was used to remove a large part of the co-extracted yellow/brown pigment leading to >75% pure tyrothricin extract (Te). The production of pigment(s) could also be reduced by addition of glucose as a 20× stock to the rest of the growth medium only after separate sterilization by autoclaving at 120 °C for 15 minutes and removal from the autoclave within 25 minutes once the pressure had reduced sufficiently.

The removal of contaminating co-extracted culture pigments using activated carbon [43] was reportedly increased by heating at 60 °C, but we were unable to reproduce this result. Using the above purification methodology, PM_1, the antimicrobial activity and detected peptide, according to UPLC-MS, increased relative to the crude extract systematically through the progression of the sequential purification steps attributing to contaminant removal. Ultimately, a final mass yield of approximately 33% of that of the initial crude extract mass was obtained with near double the antibacterial activity and purity of the crude extract (data not shown).

Manipulation of the solubility of the initial crude extract (Fig. 4.3 A) resulted in the precipitation of the tyrothricin peptides from solution and the removal of hydrophilic contaminates (Fig. 4.3 B). Due to the lower solubility of the linear gramicidins, this may have resulted in a reduction in their concentration as deduced by their decreased signal intensity. This step, however, also removed some contaminants which aided the solubility of a group of hydrophobic contaminants which were insoluble in 90% ACN (Fig. 4.3 C). The presence of such hydrophobic contaminants has also been reported by others in literature [5,26]. After

treatment with activated carbon a large part of the co-extracted culture pigments could be removed. However, the presence of a contaminant observed at *m/z* value of 802.53 persisted throughout the various purification steps, indicating hydrophobicity similar to that of the tyrothricin peptides (Fig. 4.3). The Te obtained after the activated carbon step was composed primarily the tyrocidines with TrcA (Mr = 1269.7) and TrcB (Mr = 1308.7) being the most abundant peptides with a minor contribution of some of the linear gramicidins (Fig. 4.3 D).

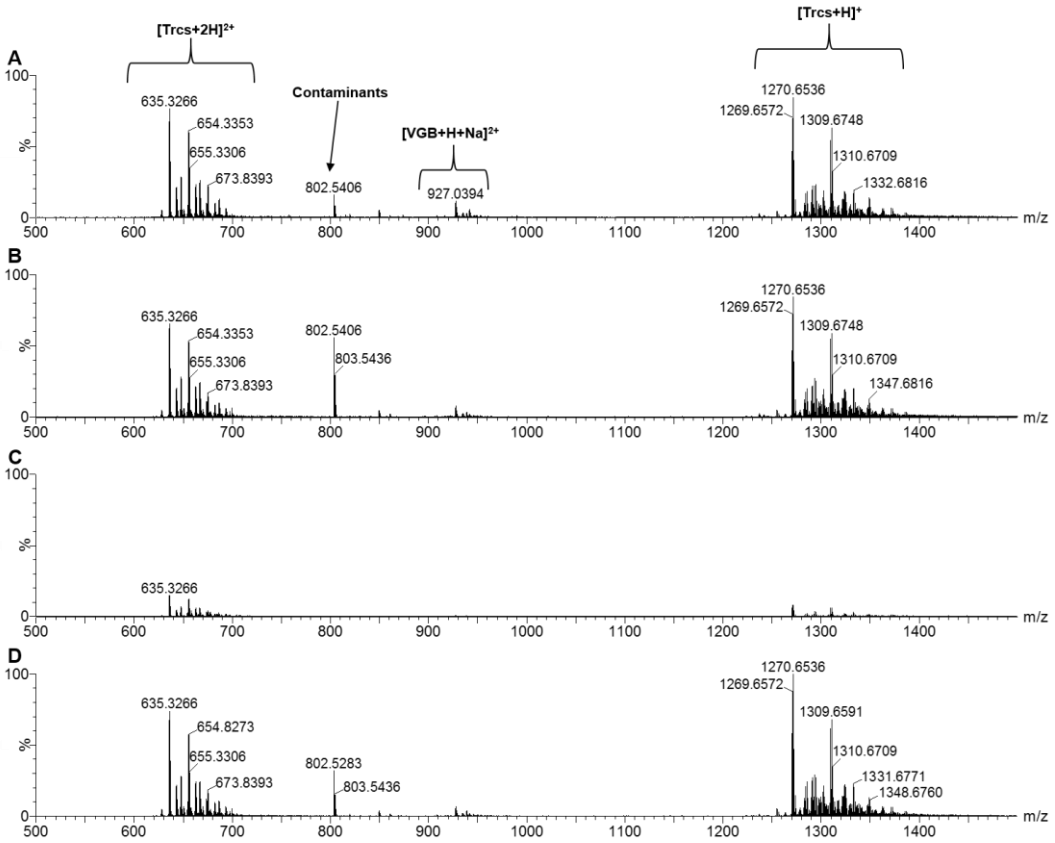

Figure 4.3 ESMS spectra depicting the various tyrothricin peptide fractions containing the tyrocidines (Trcs) and linear gramicidins (Grms, VGB) together with contamination observed at *m/z* value of 802.53 obtained through the progressive steps of PM_1 purification. **A** Crude culture extract: **B** Crude extract after precipitation: **C** Precipitate insoluble in 90% ACN after precipitation and **D** Crude extract to produce Te after treatment with activated carbon. The Y-axes of the spectra are linked in order to directly compare the intensity of the detected molecular ions of the different spectra.

The gramicidin fraction could largely be removed by treatment of the activated carbon fraction three times with a 1:1 ratio of ether: acetone washes with the more hydrophobic gramicidins soluble in the solvent mixture. As the tyrothricin complex is composed of between 10% to 20% gramicidins and 40% to 60% contributed by the tyrocidines and their analogues [5], it was suspected both the gramicidins and some the more hydrophobic tyrocidines may have been removed during ether: acetone in the wash steps. Analysis of these

two fractions by UPLC-MS confirmed the ether: acetone fraction also contained tyrocidines and analogues together with the gramicidins (Fig. 4.4 A), leaving a relatively pure extract of the tyrocidines and analogues (Fig. 4.4 B).

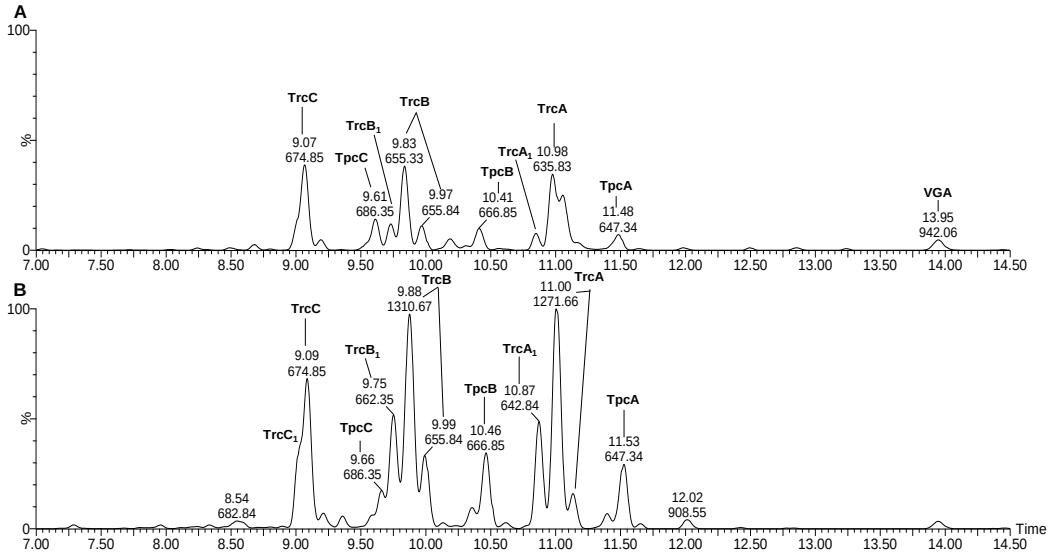

Figure 4.4 UPLC-MS chromatograms of tyrothricin extract after washing with 1:1 ratio of ether: acetone resulted in the fractionation of the tyrothricin peptides into two separate fractions: **A** Supernatant containing the linear gramicidins together with tyrocidines and **B** the final Te (acetone-ether precipitate) that remained containing relatively pure Trcs. The Y-axes of the chromatograms are linked in order to directly compare the resolved/detected peaks.

The principals used in PM_1 to purify the tyrothricin peptides are of such a nature that it may be adapted and up-scaled for purification of larger volumes. The tyrothricin peptides precipitated out of large volumes could be recovered using continuous flow centrifugation. Activated carbon would be utilised as a column chromatographic step. The large volumes of EtOH and ACN would be reduced by rotary evaporation or spray drying. However, one of the major limitations of PM_1 is the number of handling steps required in drying the peptide and changing solvents.

In the second purification methodology developed (PM_2), the tyrocidines and their analogues were purified by exploiting their amphipathic nature using adsorption chromatography on an Amberlite XAD-16 resin. This resin is reported to have a high hydrophobic character and large surface area of >800m^2/g, with resin beads composed of a skeleton of interlinked styrene-divinylbenzene copolymers [44]. After the initial organic extraction from the biomass, this purification entailed dissolving the dried crude extract in the minimal volume of 50% EtOH, centrifugation to remove particulate and loading of the sample on to a column packed with XAD-16 adsorption resin and drying of selected, pooled fractions. Purification

was achieved using step-wise gradient of EtOH and 0.1% (*v/v*) TFA in analytical grade water (PM_2; Fig. 4.5). Fractions were pooled from each of the respective step wise elution steps and their cyclodecapeptide composition and yield was determined using UPLC-MS, as well as the antimicrobial activity of fractions containing the most peptide.

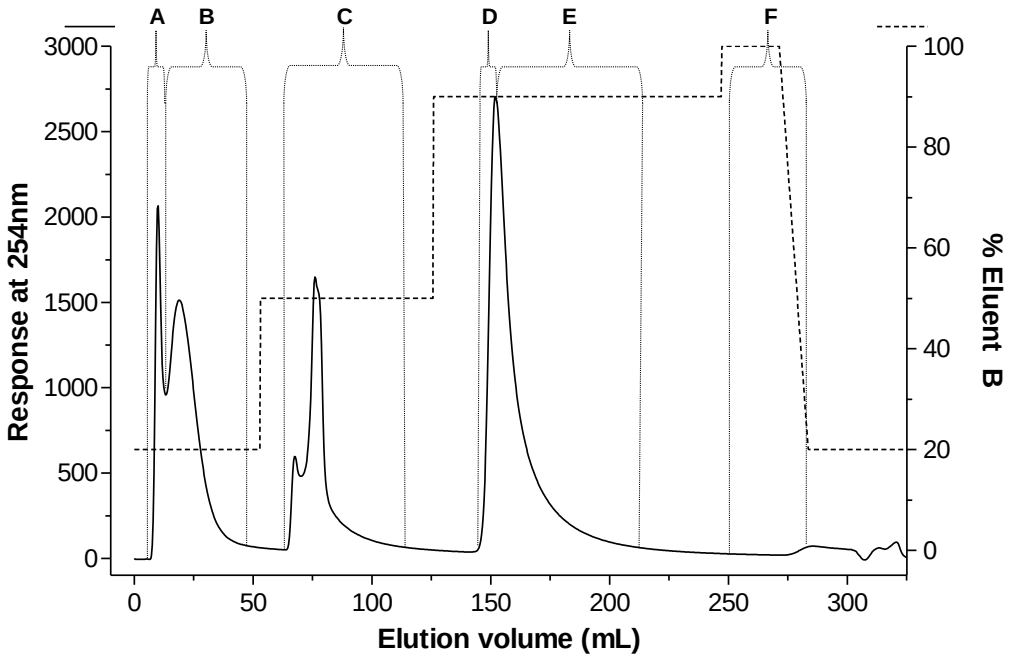

Figure 4.5 Elution profile obtained when loading 30 mg of crude tyrothricin extract on a column packed with XAD-16 resin and elution using a step wise gradient of 0.1% (*v/v*) TFA in analytical grade water and eluent B composed of 100% ethanol. Fractions were obtained at elution volumes of: **A** 6-12.5 mL using 20% B; **B** 12.5-50 mL using 20% B; **C** 64-120 mL using 50% B; **D** 142-152 mL using 90% B; **E** 152-210 mL using 90% B and **F** 250-285 mL using 100% B.

A large fraction of hydrophilic contaminants were removed at the 20% B (Fig. 4.6 A and B) and 50% B (Fig. 4.6 C) elution steps of PM_2. The first fraction collected at the 20% B elution step contained a minor amount of the tyrothricin peptides relative to the total amount of contaminants removed (Fig. 4.6 A). The vast majority of the tyrothricin peptides were eluted in the 90% B fraction (Fig. 4.6 D and E). The initial front part of the 90% B elution step (Fig. 4.6 D) contained predominantly tyrocidine peptides, while the tailing observed in the 90% B elution step contained tyrocidine peptides together with an increased proportion of the linear gramicidins (Fig. 4.7 E). A small fraction of hydrophobic contaminants eluted in the 100% B elution step (Fig. 4.7 F). The linear gramicidins, however, where observed to elute throughout the elution steps of PM_2 (Fig. 4.7), in contrast to what was observed with the tyrocidine peptides being primarily concentrated in a single elution step.

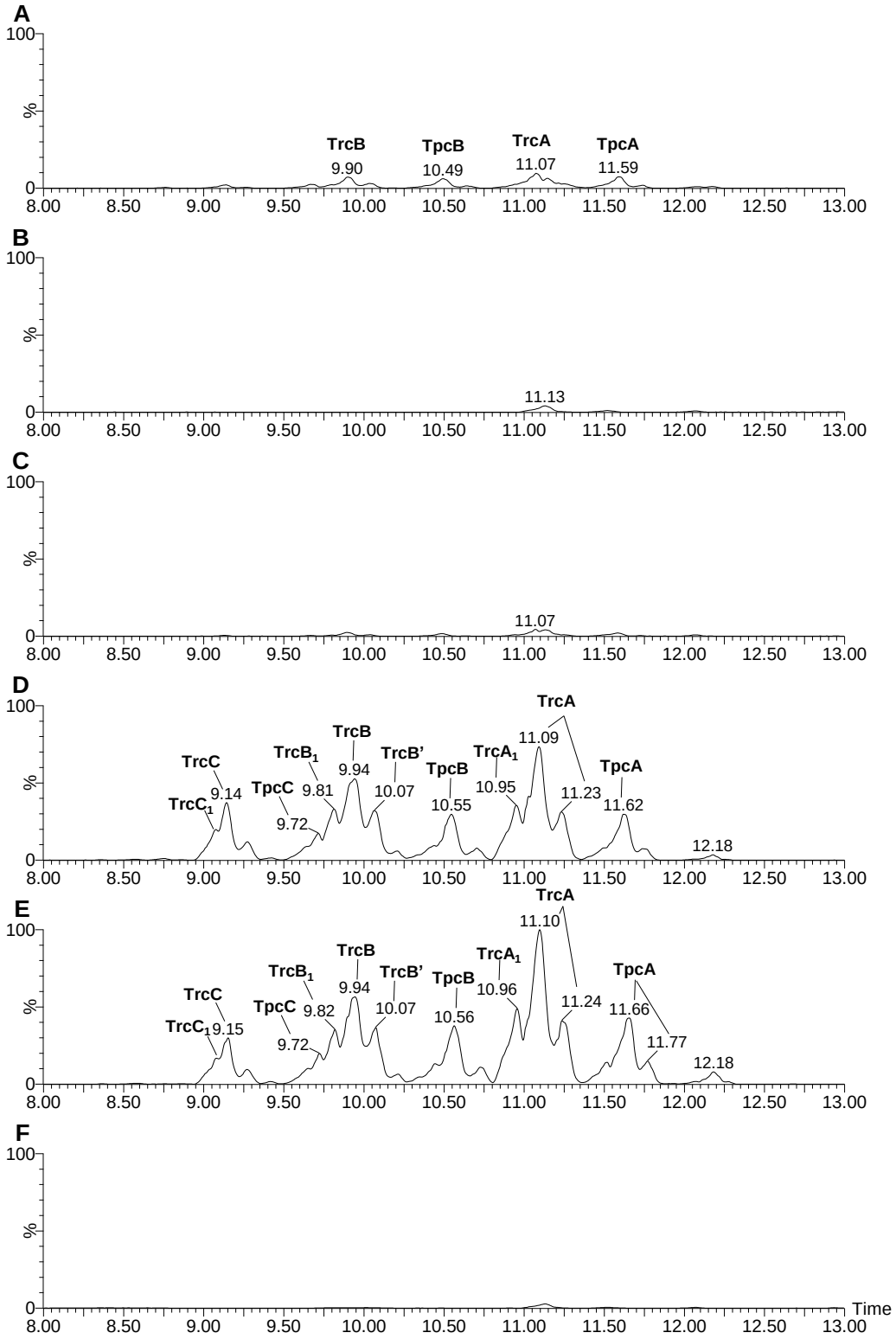

Figure 4.6 UPLC-MS chromatograms depicting the elution of the tyrocidines and their analogues (Trcs) obtained when loading 30 mg of crude tyrothricin extract on a column packed with XAD-16 resin and elution using a step wise gradient of 0.1% (*v/v*) TFA in analytical grade water and eluent B composed of 100% ethanol. Fractions were obtained at elution volumes of: **A** 6-12.5 mL using 20% B; **B** 12.5-50 mL using 20% B; **C** 64-120 mL using 50% B; **D** 142-152 mL using 90% B; **E** 152-210 mL using 90% B and **F** 250-285 mL using 100% B.

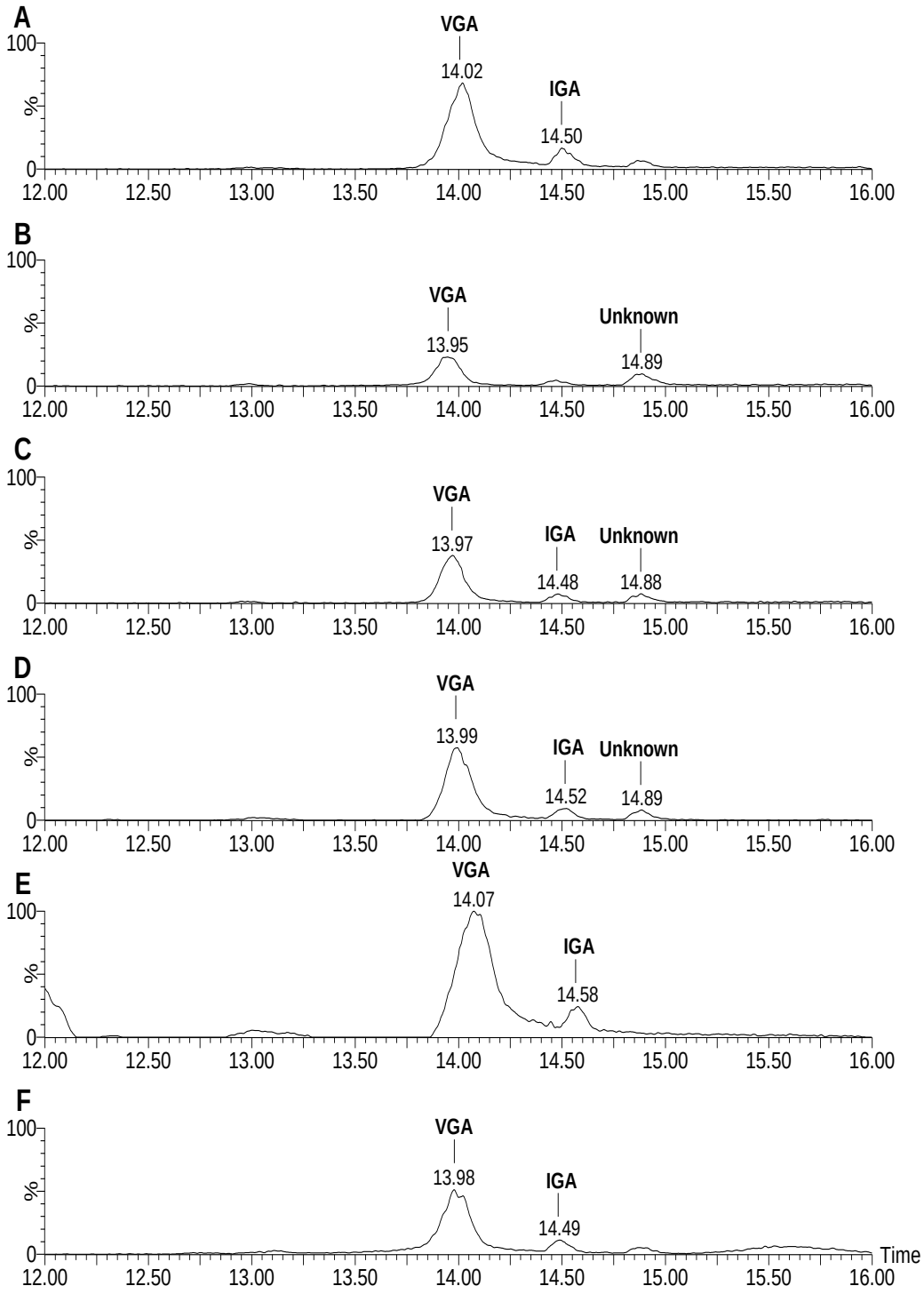

Figure 4.7 UPLC-MS chromatograms of the fractions obtained when loading 100 mg of crude tyrothricin extract on a column packed with XAD-16 resin and elution using a step wise gradient of eluent B composed of 100% ethanol illustrating the elution of the linear gramicidins. Fractions were obtained at elution volumes of: **A** 6-12.5 mL using 20% B; **B** 12.5-50 mL using 20% B; **C** 64-120 mL using 50% B; **D** 142-152 mL using 90% B; **E** 152-210 mL using 90% B and **F** 250-285 mL using 100% B.

Despite the minor losses of tyrothricin peptide observed, the 90% B elution step of PM_2 purification methodology yielded a peptide fraction of with approximately 1.5 times the peptide content in relation to the initial crude extract mass. After the initial four organic extraction steps, used in both purification methodologies, the number of handling steps were reduced from ten in PM_1 down to four in the PM_2 while still obtaining approximately the same purity (>75%) the remaining peptide yield was increased from in the vicinity of 33% to 50% in terms of the initial crude extract mass. Future work required to optimise this purification methodology for utilisation in up-scaled purifications would entail including a methodology more amenable to reducing the large volumes of solvents that would be generated. The use of traditional rotary evaporation to reduce these volumes would be unfeasible. Thus the use of other techniques compatible with the drying of these large volumes of EtOH, typically used in the industrial recovery of pharmaceutical and biotechnology products would need to be optimised, one of which is spray drying [45].

4.4.5 Characterization of Te for use in plant and bee studies

The antimicrobial activity of Te which had been purified by means of PM_1 was determined toward the representative fungi *A. fumigatus* as well as the Gram-positive bacteria *B. subtilis* and compered to that of the highly purified commercial tyrocidine (Tc) (Table 4.4).

Table 4.4 Activity of the tyrocidine extract (Te) relative to commercial tyrothricin (Tc) toward representative fungi *A. fumigatus* and Gram-positive bacteria *B. subtilis*.

Target organism	**Peptide formulation**	**IC_{50} (µg/mL) ±SEM**	**% relative activity ±SEM [a]**
Aspergillus fumigatus	Tc (*n=7*)	4.12±0.32	100±14.1
	Te (*n=37*)	6.21±0.26	66.3±2.8
Bacillus subtilis	Tc (*n=13*)	7.51±0.87	100±11.6
	Te (*n=50*)	8.58±0.141	87.5±1.4

[a] Activity relative to that observed for Tc

From these data it was apparent that the antimicrobial activity of Te was lower than that of Tc when the actual masses of the two peptide formulations were considered. Te was analysed further by means of fractionation into a hydrophilic, intermediate and hydrophobic fractions using semi-preparative HPLC (Fig. 4.8).

After pooling the fractions collected from consecutive runs 70% of the total collected mass was obtained in fraction 2 which corresponded with the known elution times of the tyrocidines and their analogues, while 16% and 14% of the total mass was obtained in the

first and third fractions respectively (Fig. 4.8). UPLC-MS analysis of three Te factions (Fig. 4.9) was performed to determine their purity relative to Tc (Table 4.5). These analysis revealed Te to be composed of 75% (*m/m*) tyrocidine peptides, shedding further light on the reduced antimicrobial activity relative to Tc.

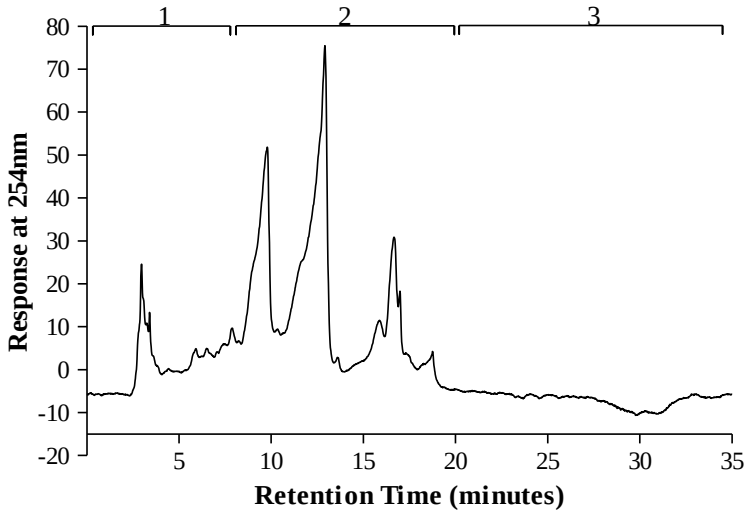

Figure 4.8 Chromatogram of the fractionation of the tyrothricin extract (Te) by semi-preparative HPLC on a reverse phase C18 column. Of the total 5.675mg collected, 16% (0.932 mg) was in fraction one at a retention time (Rt) 0-8.0 minutes, 70% (3.942 mg) was within fraction two at Rt 8.0-19.3 minutes and 14% (0.801 mg) in fraction three at Rt 19.3-35 minutes.

Table 4.5 Summary of the fractionation of Te by semi-preparative HPLC.

Fraction	Rt (min) [a]	% Yield [b]	% Purity [c]
Fraction 1	0-8.0	16	0
Fraction 2	8.0-19.3	70	99
Fraction 3	19.3-35	14	21
Total Te		100	75

Rt, retention time

[a] The retention time at which the fraction was collected by semi-preparative HPLC

[b] The percentage of the total mass of the fractions collected by semi-preparative HPLC

[c] The total peak area detected for the tyrocidine peptides in the UPLC-MS chromatogram is expressed as % relative to that of the commercial tyrocidine mixture at the same concentration of 1.00 mg/mL.

Considering the purity of Te, the antimicrobial activity is virtually identical to that of Tc, and even slightly higher towards *B. subtilis* (Table 4.4). Analysis of the three semi-preparative HPLC fractions of Te by UPLC-MS confirmed the majority of the tyrocidine peptides to be within fraction 2 together with a very small amount of VGA (Fig. 4.9 C) and had a purity of approximately 99% (Table 4.5).

Residual background contamination was observed in all of the different fractions as well as the blank and is most likely due to plasticiser contamination (Fig. 4.9). While no tyrocidines were detected in fraction 1, a small amount of the hydrophobic analogue TpcA was detected in fraction 3 together with IGB and VGA (Fig. 4.9 D).

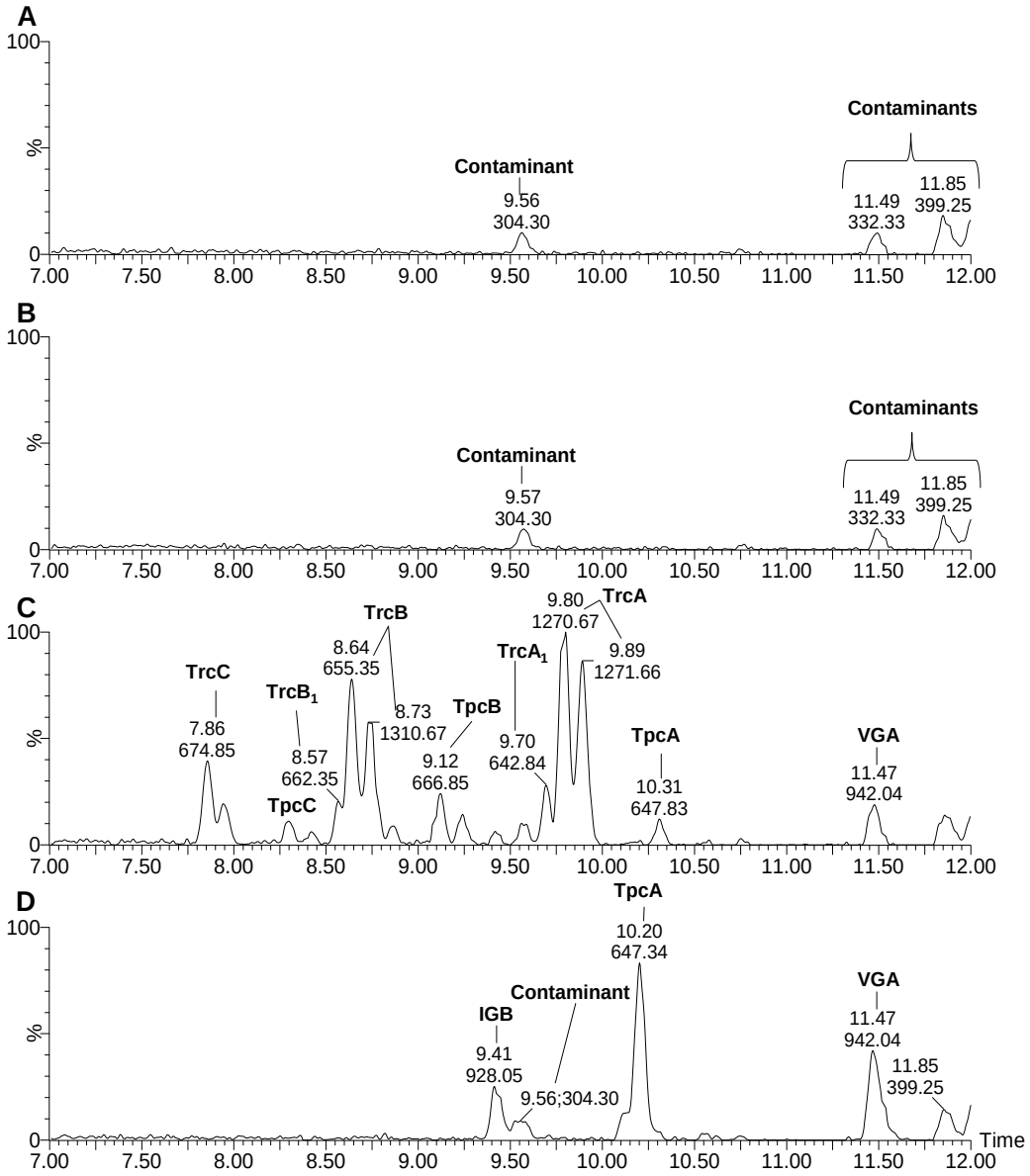

Figure 4.9 UPLC-MS chromatograms of the fractions obtained of a tyrothricin extract fractionated into three fractions by semi-preparative HPLC. **A** Blank containing plasticiser contaminants which contaminated all the fractions; **B** Fraction 1; **C** Fraction 2 containing the majority of the tyrocidine analogues (Trcs) and linear gramicidin A (VGA); **D** Fraction 3 containing a single hydrophobic TpcA analogue of the Trcs together with linear gramicidins VGA and IGB.

The composition of Te was elucidated from the UPLC-MS analysis of the total Te as well as that of the semi-preparative HPLC fractions. The Te composition was divided into three primary fractions composed of: hydrophilic pigment/contaminants contributing 16% (*m/m*), the tyrocidines and analogues contributing 75% (*m/m*), with TrcA>TrcB/B'>TrcC being the most abundant peptides, while the rest of the mass contributed by a hydrophobic fraction of 8% (*m/m*) composed of mainly VGA with the rest contributed by other linear gramicidins (Table 4.6).

Table 4.6 Summary of the composition of Te.

Component	**%** [a]
Pigment/hydrophilic contam.[b]	16.4
Tyrocidines and analogues [c]	
Tyrocidine A	21.1
Tyrocidine A_1	4.4
Tryptocidine A	6.3
Tryptocidine A_1	0.4
Tyrocidine B	9.4
Tyrocidine B'	8.5
Tyrocidine B_1	3.5
Tryptocidine B	6.2
Tryptocidine B_1	0.5
Tyrocidine C	10.7
Tyrocidine C_1	1.6
Tryptocidine C	2.5
Tryptocidine C_1	0.3
Linear gramicidins [c]	
Val-Gramicidin A	6.1
Val-Gramicidin B	0.6
Val-Gramicidin C	0.9
Ile-Gramicidin A	0.6

Contam, contamination
[a] The percentage mass contribution of each of the respective components relative to the total
[b] The percentage of the total mass of the fraction collected by semi-preparative HPLC
[c] The percentage contribution of each of the different analogues is expressed in relation to the purity determined relative to the commercial tyrocidine mixture obtained from the respective UPLC-MS peak areas of the total Te and fraction collected by semi-preparative HPLC.

4.4.6 Amino acid manipulated productions

Two amino acids, namely phenylalanine (Phe) and tryptophan (Trp), were found to have the largest effect when shifting the tyrocidine production profile (refer to Chapter 2 and 3). The influence of these two amino acids on the growth rate and tyrothricin production by

B. aneurinolyticus was investigated in detail as reported in Chapter 2. Supplementation with Phe increased the growth of the producer strain as well as tyrothricin production (Fig. 4.10 A). In contrast, the growth of the Trp supplemented cultures was similar or less than that observed in the control, while tyrothricin production was similar or greater than that of the control (Fig. 4.10 A). When considering tyrothricin production relative to cell mass attained, Phe stimulated growth rather than tyrothricin production in the culture. In contrast, Trp stimulated increased production of tyrothricin, particularly at increased Trp concentrations (Fig. 4.10 B).

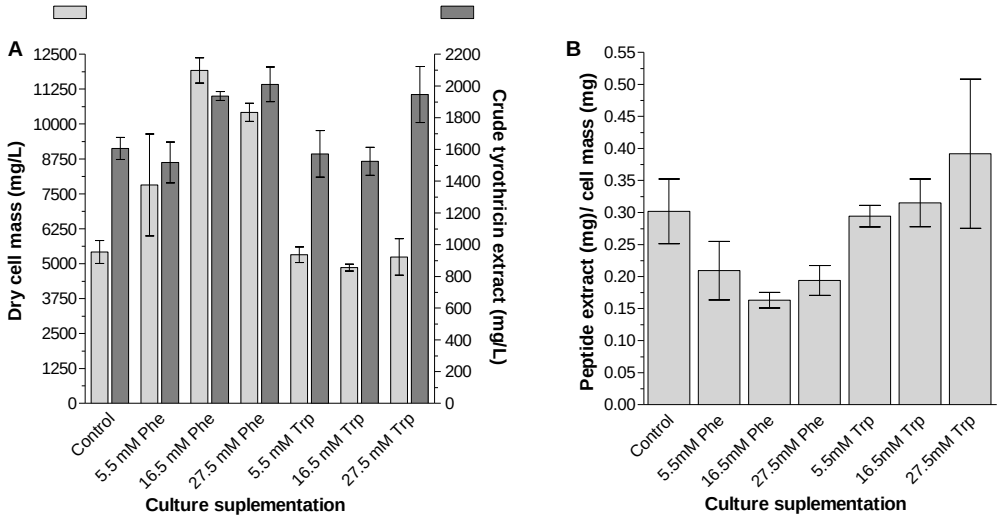

Figure 4.10 Effect of supplementation of the growth medium of *B. aneurinolyticus* with either phenylalanine (Phe) or tryptophan (Trp) compared to the non-supplemented growth control. **A** Dry cell mass as well as tyrothricin yield of the supplemented cultures relative to non-supplemented control. **B** The relative tyrothricin yield per mg of cells obtained under the different supplemented conditions.

The growth media of cultures were supplemented with specific ratios of Trp/Phe to increase the production of selected analogues relative to the non-supplemented control. These culture extracts were purified using PM_1 and PM_2 and their purity determined relative to Tc by means of UPLC-MS, as has been previously described (Fig. 4.11). Supplementation of the growth medium with Phe shifted the tyrocidine production profile toward the increased production of the more hydrophobic A analogues (Phe^3, Phe^4) (refer to table 4.1) which were the purified to ±70% purity in terms of tyrocidines and their analogues (Fig. 4.11 B).

Trp supplementation shifted the peptide production profile toward the production of another subset of cyclodecapeptides, the tryptocidines (Trp^7), predominantly tryptocidine C analogues (Trp^3, Trp^4), which were in turn purified to ±75% purity in terms of tyrocidines and their analogues (Fig. 4.11 C).

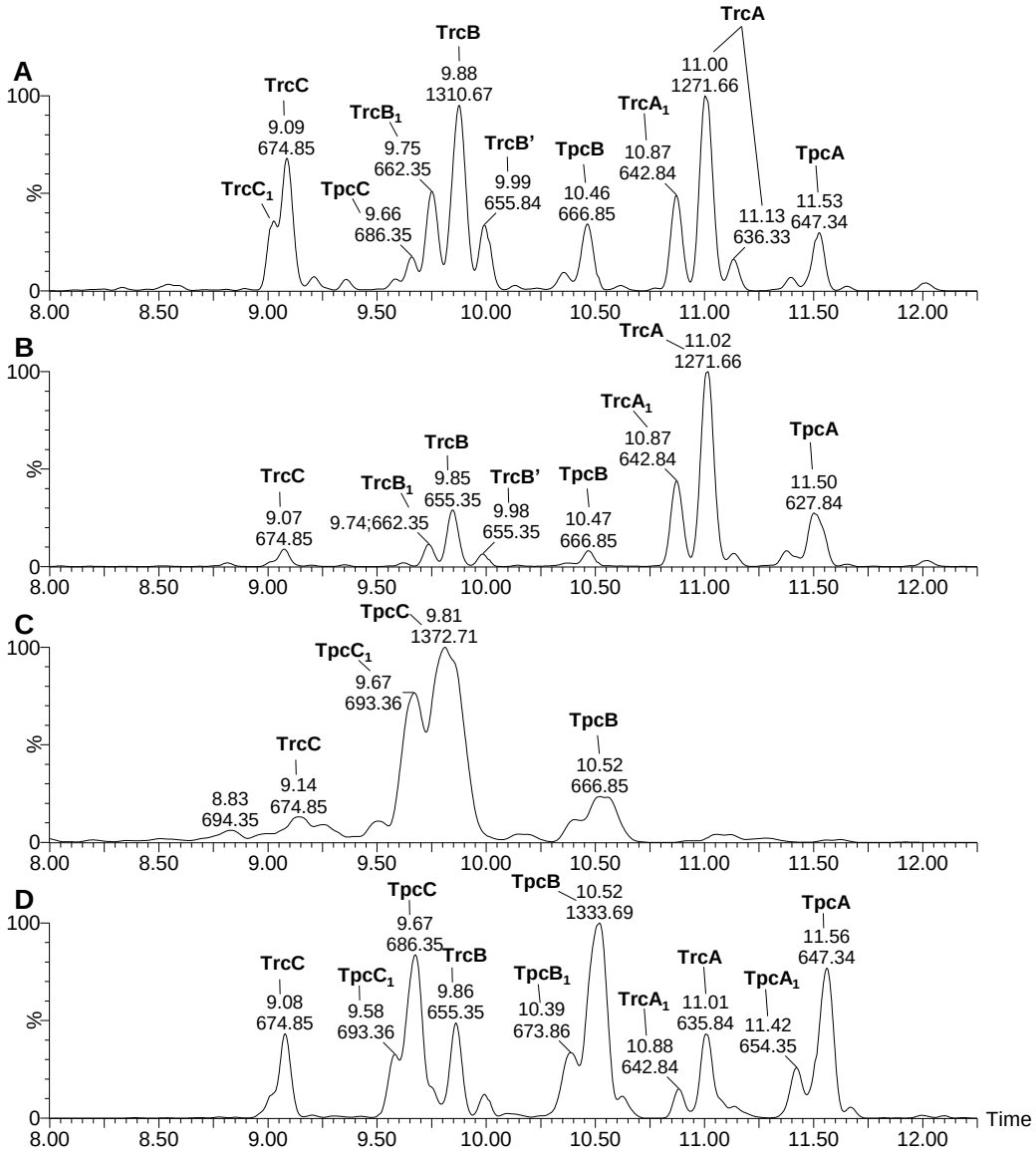

Figure 4.11 UPLC-MS chromatograms of culture extracts of *B. aneurinolyticus* which have been purified by PM_1 or PM_2. **A** Non-supplemented medium producing a wide range of tyrocidine analogues; relative to cultures supplemented with: **B** 27.5 mM Phe to produce predominantly the more hydrophobic A analogues (Phe^3, Phe^4), **C** 16.5 mM Trp resulting in increased tryptocidine C/C_1 (Trp^3, Trp^4) production and **D** a combination of 5.5 mM Trp and 16.5 mM Phe to yield increased tryptocidine (peptides with Trp^7) production.

Using defined ratios of these two amino acids the peptide production profile could be nudged to increase the production of selected intermediate analogues (refer to Chapter 2 and 3 for more detailed analysis). Supplementation with 5.5 mM Trp together with 16.5 mM Phe increased the proportional contribution of the tryptocidine A (Phe^3, Phe^4) and B (Trp^3, Phe^4) analogues in addition to the C analogue, after purification yielded a ±78% pure extract (Fig. 4.11 D).

4.4.7 Purification and analyses of single peptides

The different tyrocidine analogues may vary by as little as a single CH_2 group, this poses a significant challenge to the purification of selected analogues from the broad range of different analogues that are produced. Production and purification of the tyrocidines and their analogues was optimised according to the analogues of interest which were being purified.

The increased production of selected tyrocidine or analogues was increased by supplementing the growth medium of the producer organism with defined ratios of Trp/Phe (Fig. 4.11). Once the culture extracts were purified to an acceptable level of purity using PM_1 or PM_2 and the linear gramicidins had been removed by ether/acetone precipitation, the tyrocidines and analogues were purified from the culture extracts by semi-preparative HPLC. When the more hydrophilic tyrocidines and their analogues were purified, purification Method A was utilised for optimal purification. While when the purification was focused on the more hydrophobic phenylalanine rich tyrocidine analogues, Method B was utilised for purification. Using these adaptations to the production and purification methodologies greatly increased the ease of the purification of the different tyrocidine analogues.

The identity of the different tyrocidine analogues was confirmed by UPLC-ESMS/MS analysis (refer to Chapter 2, supplementary data). After a single round of semi-preparative HPLC purification the majority of the peptides were found to be of high purity as determined by UPLC-MS. In relation to a previous study using only the commercial tyrocidine extract as the source of peptide [46], considerably higher yields of purified peptides where attained, while also increasing the efficiency of purifying rare analogues which were absent or only present in very low quantities in the commercial tyrocidine extract (Table 4.7).

The selection of the peptide productions which had a compliment of peptides which were amenable to easy purification was found to be instrumental to the purification of selected analogues of >90% purity. Cultures extracts found to contain large amounts of co-produce TrcB and TpcC or, TrcA and TpcB posed a significant challenge for purification. These peptides were found to elute at similar times off the column and hence created a challenge to obtaining peptides of high purity. This was particularly evident in the purification of TpcB which could be produced at higher quantities in cultures co-supplemented with increased Phe and lower Trp concentrations (Fig. 4.11 D). Increased production of TpcA in the former co-

supplemented cultures allowed for its purification. This peptide has not been purified previous studies [1,18,46,47] due to a combination of its low yield and co-elution with TrcA.

In the present study the ease of the purification of selected analogues was greatly increased. In previous studies the purification of TrcA from $TrcA_1$ posed a significant challenge that required the use of their purification at very low concentrations using analytical HPLC methodology [1,18,46,47]. Through the high production protocol and supplementation of the growth medium with high concentrations of Phe the production of TrcA was increased, while its purification by semi-preparative HPLC was considerably improved using Method B (Table 4.7). Using the same purification method, TpcA and PhcA were purified. However, due to a combination of the similarity in their structures and a tendency of the tyrocidines and their analogues to aggregate some analogues required additional purification by semi-preparative HPLC.

Table 4.7 Summary of antimicrobial peptides purified from amino acid supplemented culture extracts.

Peptide	**mg yield from 10 L culture extract**	**mg yield 200 mg from commercial extract** [a]
Tyrocidine A	288.1	5.8
Tyrocidine B	51.5 [b]	9.4
Tyrocidine C	31	13.6
Tryptocidine A	67.6 [b]	-
Tryptocidine B	74.3 [b]	-
Tryptocidine C	47.3	-
Phenycidine A/A_1	28.5	-

[a] Purification yields obtained from Spathelf [46] and Eyéghé-Bickong [36]
[b] Purity <90% calculated from UPLC-MS and required additional purification by semi-preparative HPLC

As the aim in this study was the upscaling of the production and purification of the tyrocidines and their analogues for application in food and agricultural environments, it was decided to focus purification on the major tyrocidine analogues which were produced under the different culturing conditions. A substantial amount of purified peptides were needed to elucidate the aggregation phenomena of the different peptides under different solvent conditions (Chapter 5). Moreover, substantial quantities of purified peptide were required to investigate the synergistic interaction of different tyrocidine analogues (Chapter 6). These investigations were performed in order to facilitate the optimal formulation of peptides,

allowing for the selection of which culture extracts or combination of extracts should be tailored for different applications.

Several selected culture extracts were purified further in order to obtain the major tyrocidines and analogues for utilisation in for more detailed bio-activity and biophysical studies. More than 330 mg of peptide with purity >90% was obtained (refer to Table 4.7), while 220 mg peptide that was >80% enriched in one peptide was utilised in further purifications (Table 4.8).

These high mass yields compared to those of previous studies [36,46] illustrated the success of the purification approach. Supplementation with tyrosine marginally increased TrcB production (data not shown), the intermediate hydrophobicity of TrcB (Trp^3, Phe^4) posed a challenge to its purification where co-production of $TrcB_1$ and background levels of TpcC contaminated the elution peak captured via the initial semi-preparative HPLC run and required additional purification or purification from the commercial tyrocidine extract. Similarly, TpcA was contaminated by aggregation with TrcA, however, >90% purity, as determined with high sensitivity and resolution UPLC-MS, could be attained with additional purification.

In contrast, only 80% purity was obtained for PhcA with 12% of the contamination contributed by $PhcA_1$. TpcB could not be fully purified to more than 53% purity from culture extracts that had been co-supplemented with 5.5 mM Trp and 16.5 mM Phe, despite being produced in larger quantities in these cultures as these cultures also produced TrcA, which co-eluted together with TpcB (Fig. 4.11 D). Despite much lower levels of production, subsequent purifications performed by members of our group have demonstrated TpcB could be purified from cultures only supplemented with Trp where the production of TpcC predominated together with lower levels of TpcB (Fig. 4.11 C) (personal communication W. Laubscher). This illustrated the importance of culture selection in the purification of different analogues. A summary of the purity of the tyrocidine and analogues that was obtained through the combine approach of manipulated culturing and the utilisation of different HPLC methods is presented (Table 4.8).

High resolution ESMS confirmed the chemical integrity and purity and none of the purified cyclodecapeptide preparations contained any traces of gramicidins and contamination was primarily with traces of the co-produced tyrocidines and analogues (Fig.4.12).

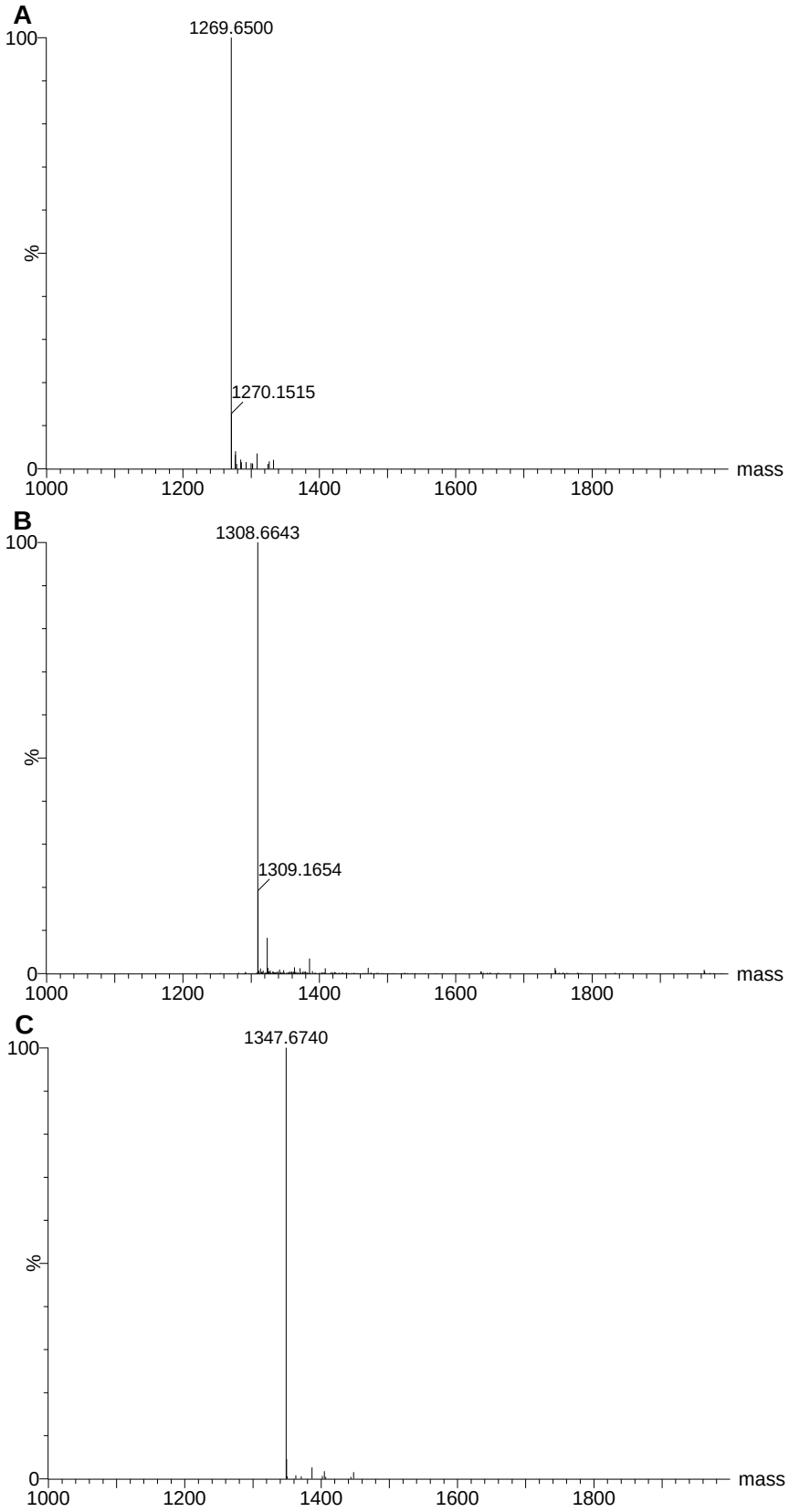

Figure 4.12 ESMS mass spectra generated with the MaxEnt algorithm of the purified peptides with experimental M_r (theoretical M_r). **A** tyrocidine A 1269.6500 (1269.6546), **B** tyrocidine B 1308.6643 (1308.6655), **C** tyrocidine C 1347.6740 (1347.6764).

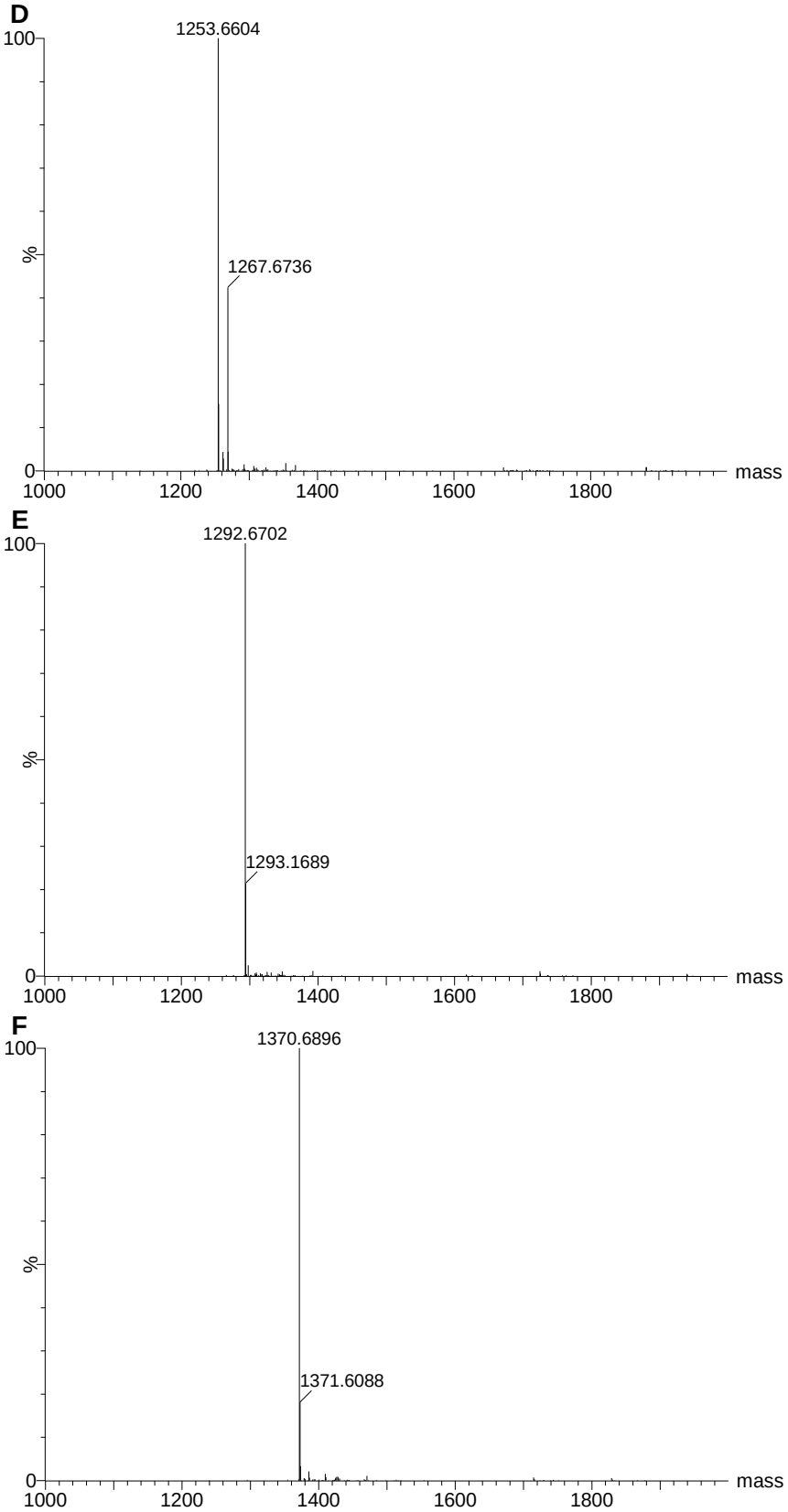

Figure 4.12 (continued) ESMS mass spectra generated with the MaxEnt algorithm of the purified peptides with experimental M_r (theoretical M_r). **D** phenycidine A/A_1 1253.6604 (1253.6597)/ 1267.6736 (1267.6753), **E** tryptocidine A 1292.6702 (1292.6706), **F** tryptocidine C 1370.6896 (1370.6924).

Table 4.8 Summary of ESMS and LC-MS analysis data of the peptides purified in this study and used in subsequent studies reported in Chapter 5 and 6.

Identity	**Culture source**	**Exp M_r (Theor M_r)**	**UPLC-MS chromatogram**	**UPLC R_t**	**% Purity**
Tyrocidine A	16.5 mM Phe	1269.6500 (1269.6546)	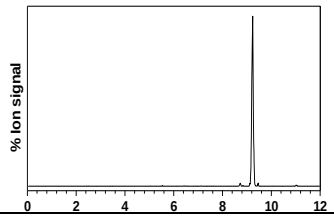	9.68	94
Tyrocidine B	Non-supplemented/ commercial extract	1308.6643 (1308.6655)	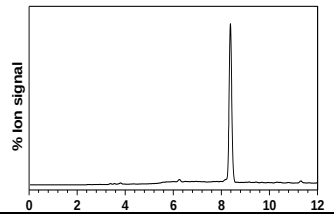	8.38	90
Tyrocidine C	Non-supplemented/ 16.5 mM Phe + 5.5mM Trp	1347.6740 (1347.6764)	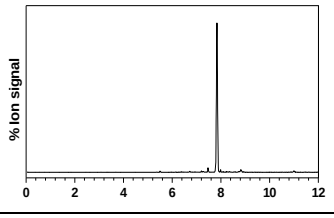	8.08	91
Phenycidine A/A_1	16.5 mM Phe	1253.6604/ 1267.6736 (1253.6597)/ (1267.6753)	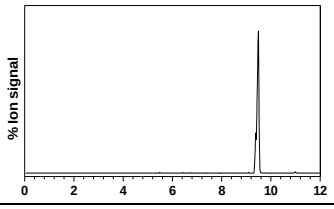	9.49	92 (80/12)
Tryptocidine A	16.5 mM Phe + 5.5mM Trp	1292.6702 (1292.6706)	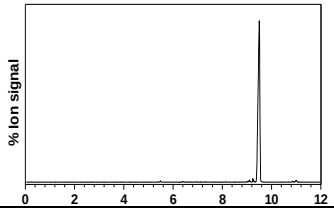	9.50	94
Tryptocidine B + Tyrocidine A	16.5 mM Phe + 5.5mM Trp	1331.6815/ 1269.6534? (1331.6710)/ (1269.6546)	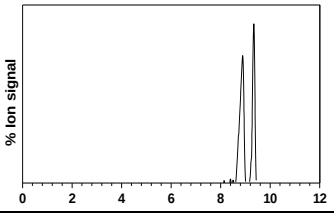	8.89	87 (53/34)
Tryptocidine C	16.5 mM Trp	1370.6877 (1370.6924)	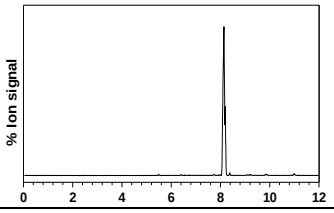	8.13	91

4.5 Conclusions

To allow for the successful utilisation of the tyrocidines as green-biocides; high production yields need to be maintained and activity of the final product needs to remain consistent. The naturally obtained tyrothricin yields have been greatly increased. In this study it has been shown that consistent tyrothricin production can be obtained by careful selection of bacterial cultures in a medium with both protein nitrogen and carbohydrate as nutrients (Table 4.2). The production of the tyrothricin peptides occurs after the logarithmic growth phase [25,25,26,38] upon initiation by metabolic stress signals [42]. Oxygen limitation within the early culturing stages around 48 hours was the most likely trigger of tyrothricin production within the flask cultures, sufficient nutrients were still available to support biomass production and resultant increased tyrothricin production while not stressed to the extent of sporulation [41] (Fig. 4.1).

In contrast, in aerated submerged cultures performed in bioreactors the producer organism had an alternate metabolism [30] as apparent in the difference in pH profile between the two culturing environments (Fig. 4.1 and 4.2). The trigger for tyrothricin production within the submerged cultures is most likely nutrient depletion. Tyrothricin production was thus suppressed in these submerged cultures having depleted the available nutrients before peptide production commenced. Successful tyrothricin production within submerged cultures using defined minimal media containing simple nitrogen sources [28-30] is well below that observed in stationary cultures. It is thus questionable whether tyrothricin production by submerged culturing would yield sufficient product at a cost which would make it feasible for agricultural or industrial applications.

Having increased total tyrothricin production to well above initial yields (Table 4.2), two purification methodologies were developed and/or optimised that are of such a nature as to allow for future cost effective, high volume through-put purification of the tyrocidines and their analogues. The first methodology used to purify the tyrothricin peptides (PM_1) involved manipulation of the solubility of the tyrothricin peptides to purify them from a large contingent of the contaminants increasing the tyrocidines and analogues to approximately 75% (*m/m*) the extract content. The main limitation was the number of handling steps. Utilising a chromatographic separation (PM_2) the crude extract could be purified from the co-extracted contaminants with four handling steps after the initial extraction. Approximately 50% of the initial mass was recovered with peptide purity similar to PM_1 which entailed ten

handling steps after the initial extraction and recovery of 33% of the initial mass. Antimicrobial activity of these purified fractions was increased to an acceptable level for agricultural and industrial applications (Table 4.4).

Using the knowledge garnered to shift the antimicrobial peptide production profile, together with judiciously considered semi-preparative HPLC methodology greatly eased the purification of selected tyrocidine analogues. Large quantities of single peptides were obtained using a minimal number of semi-preparative HPLC purifications.

Progress has been made toward making it feasible to use the tyrocidines in agricultural and industrial applications. We have demonstrated the ability to produce high, economically viable yields of tyrothricin that were used in an *in vivo* trail to assess bee toxicity (Chapter 7). The characterisation and interaction of the major cyclodecapeptide analogues produced in these cultures were investigated and reported in Chapter 5 and 6. More knowledge regarding the behaviour of the peptides in the tyrothricin mixture would allow for informed decisions to be made on which cultures extracts or blends thereof, as well as formulations, should be used in different applications to target fungi and/or bacteria.

4.6 References

1. Leussa, N. A. (2014) Characterisation of small cyclic peptides with antilisterial and antimalarial activity. Stellenbosch University, Department of Biochemistry, Stellenbosch, South Africa. **PhD. Thesis**, http://hdl.handle.net/10019.1/86161
2. Spathelf, B. M. and Rautenbach, M. (2009) Anti-listerial activity and structure-activity relationships of the six major tyrocidines, cyclic decapeptides from *Bacillus aneurinolyticus*. Bioorg. Med. Chem. **17**, 5541-5548
3. Troskie, A. M., de Beer, A., Vosloo, J. A., Jacobs, K. and Rautenbach, M. (2014) Inhibition of agronomically relevant fungal phytopathogens by tyrocidines, cyclic antimicrobial peptides isolated from *Bacillus aneurinolyticus*. Microbiology **160**, 2089-20101
4. Montesinos, E. (2007) Antimicrobial peptides and plant disease control. FEMS Microbiol. Lett. **270**, 1-11
5. Hotchkiss, R. D. and Dubos, R. J. (1941) The isolation of bactericidal substances from cultures of *Bacillus brevis*. J. Biol. Chem. **141**, 155-162
6. Dubos, R. J. and Hotchkiss, R. (1942) Origin, nature and properties of gramicidin and tyrocidine. Trans.Coll.Physicians Phila. **10**, 11-19
7. Henderson, J. (1946) The status of tyrothricin as an antibiotic agent for topical application. J. Am. Pharm. Assoc. **35**, 141-147

8. Goldman, L., Feldman, M. D. and Altemeier, W. A. (1948) Contact dermatitis from topical tyrothricin and associated with polyvalent hypersensitivity to various Antibiotics. J. Invest. Dermatol. **11**, 243-244

9. Wigger-Alberti, W., Stauss-Grabo, M., Grigo, K., Atiye, S., Williams, R. and Korting, H. C. (2013) Efficacy of a tyrothricin-containing wound gel in an abrasive wound model for superficial wounds. Skin Pharmacol. Physiol. **26**, 52-56

10. Weinstein, L. and Rammelkamp, C. H. (1941) A study of the effect of gramicidin administered by the oral route. Exp. Biol. Med. **48**, 147-149

11. Dubos, R. J. and Cattaneo, C. (1939) Studies on a bactericidal agent extracted from a soil *Bacillus*: III. Preparation and activity of a protein-free fraction. J. Exp. Med. **70**, 249-256

12. Kolmer, J. A. and Rule, A. M. (1946) Toxicity and therapeutic activity of tyrothricin by oral administration. Proc. Soc. Exp. Biol. Med. **63**, 315-317

13. Rammelkamp, C. H. and Weinstein, L. (1942) Toxic effects of tyrothricin, gramicidin and tyrocidine. J. Infect. Dis. **71**, 166-173

14. Robinson, H. J. and Molitor, H. (1942) Some toxicological and pharmacological properties of gramicidin, tyrocidine and tyrothricin. J. Pharmacol. Exp. Ther. **74**, 75-82

15. Kagan, G., Huddlestone, L. and Wolstencroft, P. (1982) Two lozenges containing benzocaine assessed in the relief of sore throat. J. Int. Med. Res. **10**, 443-446

16. Munyuki, G., Jackson, G. E., Venter, G. A., Kövér, K. E., Szilágyi, L., Rautenbach, M., Spathelf, B. M., Bhattacharya, B. and van der Spoel, D. (2013) β-Sheet structures and dimer models of the two major tyrocidines, antimicrobial peptides from *Bacillus aneurinolyticus*. Biochemistry. **52**, 7798-7806

17. Loll, P. J., Upton, E. C., Nahoum, V., Economou, N. J. and Cocklin, S. (2014) The high resolution structure of tyrocidine A reveals an amphipathic dimer. BBA-Biomembranes. **1838**, 1199-1207

18. Troskie, A. M. (2014) Tyrocidines, cyclic decapeptides produced by soil bacilli, as potent inhibitors of fungal pathogens. Stellenbosch University, Department of Biochemistry, Stellenbosch, South Africa. **PhD. Thesis**, http://hdl.handle.net/10019.1/86162

19. Seddon, B. and Fynn, G. (1973) Energetics of growth in a tyrothricin-producing strain of *Bacillus brevis*. Microbiology **74**, 305-314

20. Schazschneider, B., Ristow, H. and Kleinkauf, H. (1974) Interaction between the antibiotic tyrocidine and DNA *in vitro*. Nature **249**, 757-759

21. Bohg, A. and Ristow, H. (1987) Tyrocidine-induced modulation of the DNA conformation in *Bacillus brevis*. Eur. J. Biochem. **170**, 253-258

22. Bohg, A. and Ristow, H. (1986) DNA- supercoiling is affected *in vitro* by the peptide antibiotics tyrocidine and gramicidin. Eur. J. Biochem. **160**, 587-591

23. Tang. X.J., Thibault. P., Boyd. R.K. (1992) Characterization of the tyrocidine and gramicidin fractions of the tyrothricin complex from *Bacillus brevis* using liquid chromatography and mass spectrometry. Int. J. Mass Spectrom. Ion Processes. **122**, 153-179

24. Vosloo, J. A., Stander, M. A., Leussa, N. A., Spathelf, B. M. and Rautenbach, M. (2013) Manipulation of the tyrothricin production profile of *Bacillus aneurinolyticus*. Microbiology **159**, 2200-2211

25. Dubos, R. J. (1939) Studies on a bactericidal agent extracted from a soil *Bacillus*: I. Preparation of the agent, its activity *in vitro*. J. Exp. Med. **70**, 1-10

26. Dubos, R. J. and Hotchkiss, R. D. (1941) The production of bactericidal substances by aerobic sporulating bacilli. J. Exp. Med. **73**, 629-640

27. Lewis, J., Dimick, K. P. and Feustel, I. (1945) Production of tyrothricin in cultures of *Bacillus brevis*. Ind. Eng. Chem. Res. **37**, 996-1004

28. Stokes, J. L. and Woodward, C. R. (1943) Formation of tyrothricin in submerged cultures of *Bacillus brevis*. J. Bacteriol. **46**, 83-88

29. Appleby, J., Knowles, E., Mcallister, R., Pearson, J. and White, T. (1947) The production of tyrothricin by submerged culture of *Bacillus brevis* in synthetic media. J. Gen. Microbiol. **1**, 145-157

30. Appleby, J., Knowles, E., Pearson, J. and White, T. (1947) A preliminary study of the formation, assay and stability of tyrothricin. J. Gen. Microbiol. **1**, 137-144

31. Mitchell, W. R. (1952) Method for producing tyrothricin. USA patent office. **2602043**

32. Du Toit, E. and Rautenbach, M. (2000) A sensitive standardised micro-gel well diffusion assay for the determination of antimicrobial activity. J. Microbiol. Methods. **42**, 159-165

33. Lehrer, R. I., Rosenman, M., Harwig, S. S. S. L., Jackson, R. and Eisenhauer, P. (1991) Ultrasensitive assays for endogenous antimicrobial polypeptides. J. Immunol. Methods. **137**, 167-173

34. Rautenbach, M., Gerstner, G. D., Vlok, N. M., Kulenkampff, J. and Westerhoff, H. V. (2006) Analyses of dose-response curves to compare the antimicrobial activity of model cationic α-helical peptides highlights the necessity for a minimum of two activity parameters. Anal. Biochem. **350**, 81-90

35. Troskie, A. M., Vlok, N. M. and Rautenbach, M. (2012) A novel 96-well gel-based assay for determining antifungal activity against filamentous fungi. J. Microbiol. Methods. **91**, 551-558

36. Eyéghé-Bickong, H. (2011) Role of surfactin from *Bacillus subtilis* in protection against antimicrobial peptides produced by *Bacillus* species. Stellenbosch University. **PhD. Thesis**, http://hdl.handle.net/10019.1/6773

37. Baron, A. L. (1949) Preparation of tyrothricin. USA patent office. **2482832**

38. Lee, S. G., Littau, V. and Lipmann, F. (1975) The relation between sporulation and the induction of antibiotic synthesis and of amino acid uptake in *Bacillus brevis*. J. Cell Biol. **66**, 233-242

39. Fürbass, R., Gocht, M., Zuber, P. and Marahiel, M. A. (1991) Interaction of AbrB, a transcriptional regulator from *Bacillus subtilis* with the promoters of the transition state-activated genes tycA and spoVG. Mol. Gen. Genet. **225**, 347-354

40. Fürbaβ, R. and Marahiel, M. A. (1991) Mutant analysis of interaction of the *Bacillus subtilis* transcription regulator AbrB with the antibiotic biosynthesis gene tycA. FEBS Lett. **287**, 153-156

41. Robertson, J. B., Gocht, M., Marahiel, M. A. and Zuber, P. (1989) AbrB, a regulator of gene expression in *Bacillus*, interacts with the transcription initiation regions of a sporulation gene and an antibiotic biosynthesis gene. Proc. Natl. Acad. Sci. U. S. A. **86**, 8457-8461

42. Marahiel, M. A., Nakano, M. M. and Zuber, P. (1993) Regulation of peptide antibiotic production in *Bacillus*. Mol. Microbiol. **7**, 631-636

43. Kumar, C. G. P. (2003) Activated charcoal: A versatile decolorization agent for the recovery and purification of alkaline protease. World J. Microb. Biot. **19**, 243-246

44. Saxena, R. and Meena, P. L. (2014) Flow injection online solid phase extraction system using amberlite XAD-16 functionalized with 8-hydroxyquinoline for copper and zinc determination by flame atomic absorption spectrometry. RSC Advances. **4**, 20216-20225

45. Mujumdar, A. S. (2014) Handbook of industrial drying. CRC Press

46. Spathelf, B. M. (2010) Qualitative structure-activity relationships of the major tyrocidines, cyclic decapeptides from *Bacillus aneurinolyticus.* Stellenbosch University, Department of Biochemistry, Stellenbosch, South Africa. **PhD. Thesis**, http://hdl.handle.net/10019.1/4001

47. Rautenbach, M., Vlok, N. M., Stander, M. and Hoppe, H. C. (2007) Inhibition of malaria parasite blood stages by tyrocidines, membrane-active cyclic peptide antibiotics from *Bacillus brevis*. Biochim. Biophys. Acta. **1768**, 1488-1497

Chapter 5
Structure and oligomerisation relationships of the six major cyclodecapeptides purified from *Bacillus aneurinolyticus* cultures

5.1 Introduction

The antimicrobial activity of the tyrocidines and their analogues (Trcs) is proposed to primarily be as a result of their interaction with the cell membrane [1], causing its permeabilization [2] and ultimately cell lysis [3]. Interaction with the cell membrane and permeabilization, however, is proposed to be dependent on the oligomerisation of the peptides into dimers which are proposed to be the active structures required for antibacterial activity [4,5]. Excessive aggregation, forming oligomers greater than dimeric structures, however, causes deceased antimicrobial activity [6-10]. To assess the influence of solvent environment in Trc formulations, used for *in vivo* studies, and carbohydrates, used in activity assays it was necessary to gain an understanding of the structure, self-assembly/aggregation and activity relationships of these peptides.

The aggregation of cyclic peptides in general is determined by the influence of both their own characteristics, derived from their primary structure, as well as that of the environment; both of which act in union to determine the forces which act on the molecule [6,7,11-14]. The primary structure will largely dictate the conformation of the Trcs in relation to the distribution of different amino acid side chains (containing groups of different charge, size and polarity) determines the amphipathicity and charge distribution of the monomeric peptide will in turn dictate the propensity to aggregate into higher order structures [6,7,9,15,16].

The Trcs contain a fairly conserved cyclic decapeptide structure (Fig. 5.1). Tang *et al.* [17] have identified 28 different analogues with minor variations of the primary peptide sequence composed of both D and L amino acid residues. The Trcs in this study contain a primary structure composed of cyclo(D-Phe^1-L-Pro^2-L-X^3-D-X^4-L-Asn^5-L-Gln^6-L-X^7-L-Val^8-L-Orn^9-L-Leu^{10}) [17], with three letter amino acid abbreviations indicating the respective residues and ornithine (Orn), while the three variable positions are depicted by X. Analogues of the Trcs containing L-Phe^3, D-Phe^4 or L-Trp^3, D-Phe^4 or L-Trp^3, D-Trp^4 at the variable dipeptide unit L-X^3-D-X^4 are referred to as the A, B or C analogues respectively. While analogues in which the

variable aromatic amino acid position L-X^7 is occupied by L-Tyr^7, L-Trp^7 or L-Phe^7 are referred to as the tyrocidines, tryptocidines or phenycidines respectively [18] (Fig 5.1). These peptides share 50% sequence homology with the cyclic peptide gramicidin S (GS) composed of two repeating subunits of the conserved region of the Trcs (L-Val^8-L-Orn^9-L-Leu^{10}-D-Phe^1-L-Pro^2). Consequently, many studies regarding the conformation of the Trcs have been done using GS as a reference point [11,12,14,19].

Supplementation of the growth medium of the producer organism, *Bacillus aneurinolyticus* with various ratios of Trp and Phe caused the increased production of selected Trcs [18]. Seven different cyclodecapeptides were produced in larger quantities under the latter conditions; of which three contained the L-Phe^3-D-Phe^4 dipeptide moiety: tyrocidine A (TrcA), phenycidine A (PhcA) and tryptocidine A (TpcA) (Fig. 5.1 A, C and E), one peptide with L-Trp^3-D-Phe^4 tyrocidine B (TrcB) and two peptides with L-Trp^3-D-Trp^4 namely tyrocidine C (TrcC), and tryptocidine C (TpcC) (Fig. 5.1 B, D and F) were purified from the culture extracts of the producer organism (refer to Chapter 4).

Previous investigators have noted a structure-activity relationship of the various Trc analogues toward a range of target organisms including: the Gram-positive bacteria *Listeria monocytogenes* [20,21], the fungi *Fusarium solani* and *Botrytis cinerea* [22], as well as the malaria parasite *Plasmodium falciparum* [23,24]. Among the range of different analogues produced, maximal activity toward a specific target organism has been observed to be determined by characteristics of both the target organism, as well as those of the different Trcs that result due to variation in their primary structure [20-23].

The cyclic conformation of the TrcA and TrcC monomers have an amphipathic type I β-turn and type II β-turn in antiparallel β-pleated sheet conformation stabilised by four intramolecular hydrogen-bonds, as determined from X-ray crystallography and nuclear magnetic resonance studies [4,5,25-28]. Oligomerisation in an aqueous environment by TrcA [4,5] and TrcC [4] into amphipathic dimers are proposed to be the active units of the peptides which interact with the cell membrane [4,5].

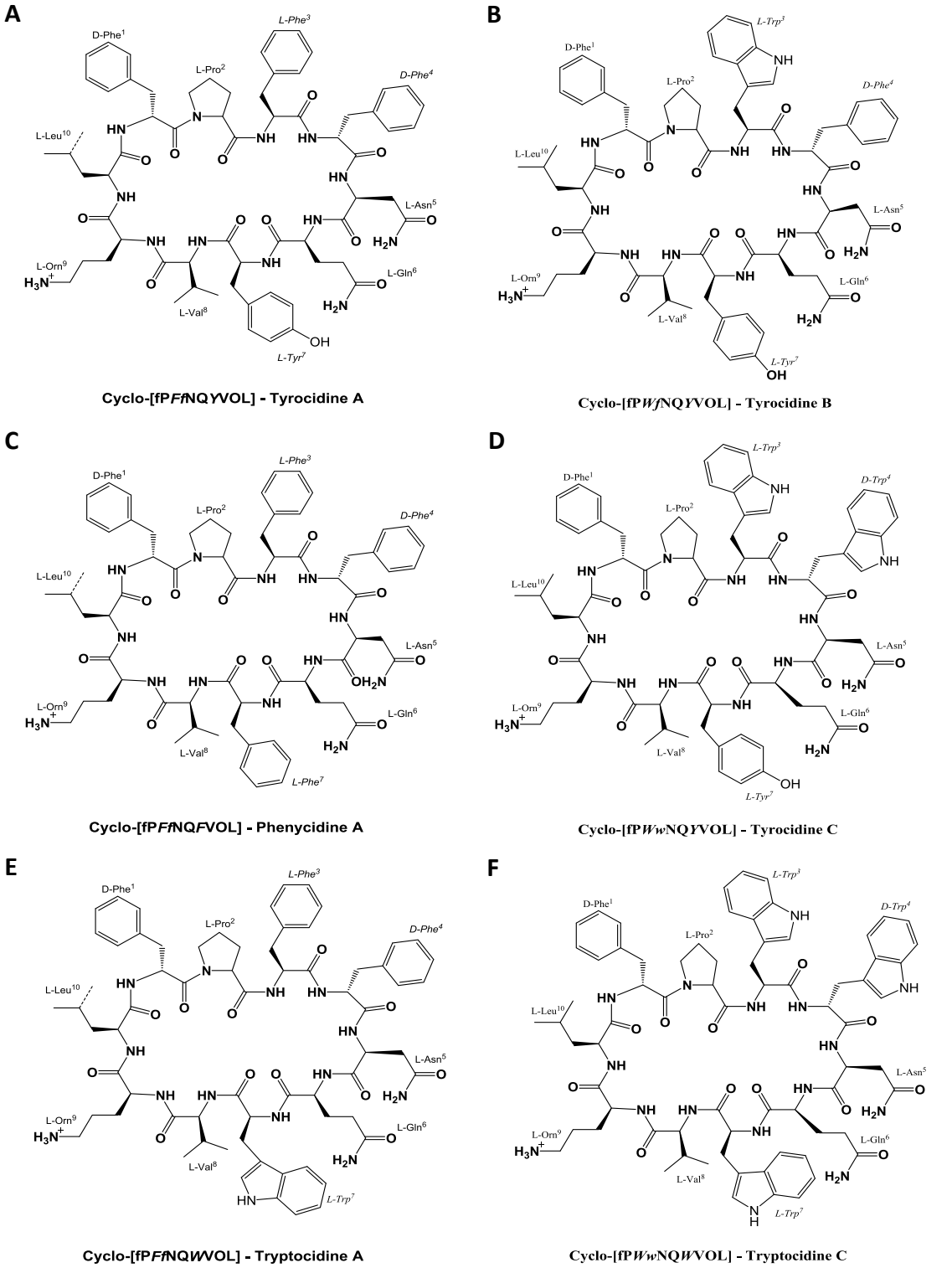

Figure 5.1 Primary structures of the six cyclodecapeptides used in this study. Structures of the three cyclodecapeptides containing L-Phe^3-D-Phe^4 dipeptide moiety: **A** tyrocidine A (TrcA), **C** phenycidine A (PhcA) and **E** tryptocidine A (TpcA); and L-Trp^3-D-Phe^4 containing dipeptide moiety **B** tyrocidine B (TrcB) and two peptides with L-Trp^3-D-Trp^4, namely **D** tyrocidine C (TrcC) and **F** tryptocidine C (TpcC). Residues are referred to using standard three or one letter amino acid abbreviations with Orn/O representing ornithine. Residues are numbered according to their order of incorporation during biological synthesis, with variable amino acids represented in italics.

Upon membrane interaction β-sheet peptides, such as the Trcs, have been observed to form ion conducting pore/channel like structures in model membranes [unpublished results, personal communication E Zaitseva, University of Freiburg] which are possibly related to their lytic activity [29]. Oligomerisation of these small peptides would be necessary to form transmembrane pores. Oligomerisation into large aggregate structures in aqueous environments, however, has been attributed to a reduction of the antimicrobial activity of these peptides [6-10]. Therefore, a fine balance is proposed to exist between the extent of oligomerisation aggregation by these peptides and antimicrobial activity. The aggregation of cyclic peptides in general is determined by the influence of both their own characteristics derived from their primary structure, as well as that of the environment; both of which act in union to determine the forces which act on the molecule [6,7,11-14].

The structural predictors of the Trcs to oligomerize into higher ordered structures was investigated further by means of electrospray mass spectrometry (ESMS), circular dichroism (CD) and fluorescence spectroscopy (FS), which are techniques which are well established in the field of studying the interactions of biomolecules [30-37]. Each of the three techniques could make a valuable contribution to understanding some of the characteristics associated with the oligomerisation of the Trcs. ESMS has proven to be a valuable methodology to study the non-covalent interactions of different biomolecules [34,35,38-41]. As such, ESMS has been used as a means to illustrate the oligomerisation of the Trcs [4]. However, interaction of biomolecules detected by ESMS are devoid of hydrophobic non-covalent interactions [38,39,41]. ESMS is complemented by optical spectrometry such as CD and FS which study the structures of biomolecules in both aqueous and membrane mimicking environments.

Using the sensitivity of the chiral properties related to the peptide bond to changes in solvent environment, CD is a well-established technique used to study the structural features of proteins and peptides [31,32], including the Trcs [4,14,16]. FS utilises the fluorescent properties associated with the four aromatic amino acids in the Trcs and their sensitivity to local environment changes. Differences in their fluorescent yields can be used to indicate structural changes due to differences in the local environment of these residues, especially Trp. The three aromatic amino acids Phe, Tyr and Trp show maximal absorbance at wavelengths of 256 nm, 276 nm and 282 nm and emission maximum at wavelengths of 282 nm, 303 nm and 357 nm respectively [30,42-46]. As Trp has the largest extension coefficient and absorbs at the highest wavelength, this causes its emission spectra to overshadow that of the other two

aromatic amino acids. Moreover, in many instances the energy absorbed by Tyr and Phe is often transferred to the Trp residue by resonance energy transfer [47]. Only in the absence of Trp does the fluorescence of Tyr make a significant contribution to the fluorescent signal observed [30,37]. The fluorescence due to Phe is not observed due to a combination of its lower quantum yield and excitation at 280 nm or 295 nm, above its maximum absorption wavelength.

5.2 Materials and Methods

5.2.1 Materials and Reagents

The peptides: TrcA, TrcB, TrcC, TpcA, TpcC and PhcA where purified from culture extracts of *Bacillus aneurinolyticus* ATCC 10068 using modified organic extraction methodology [48] as well as from commercial tyrocidine mixture obtained from Sigma-Aldrich (Steinheim, Germany). Peptides were purified using semi-preparative reverse phase high performance liquid chromatography (RP-HPLC). Purity of TrcA, TpcA, TrcC and TpcC was confirmed >90% by ultra-performance liquid chromatography linked to mass spectrometry (UPLC-MS) as described in Chapter 4. The enriched PhcA preparation contained 12 % $PhcA_1$ (92% combined purity) and was referred to as PhcA in this study. Acetonitrile (HPLC-grade, far UV cut-off) was from Romil Ltd (Cambridge, UK) and 2,2,2-trifluoreoethanol (TFE) was from Sigma (St. Louis, USA). Glucose (Glc), ethanol (EtOH), and N,N-Dimethylformamide (DMF) were obtained from Merck (Darmstadt, Germany). Analytical grade water was prepared by filtering water from a reverse osmosis plant through a Millipore-Q® water purification system (Milford, USA).

5.2.2 Detection of oligomerisation with ESMS

Dried analytical aliquots of the purified tyrocidine peptides were dissolved in 50% (*v/v*) of DMF and diluted to a concentration of 0.200 mM at a solvent concentration of 5% (*v/v*) in water. These samples were allowed to stand at room temperature overnight prior to being diluted to a final concentration of 0.100 mM and final solvent concentration of 2.5% (*v/v*).

The type of predominant aggregates/oligomers formed within the above formulations was determined by means of high resolution ESMS using a Waters Q-TOF Synapt G2 mass spectrometer with a Z-spray electrospray ionisation source. Injections of 2 µL of sample were introduced directly into the mass analyser in positive mode at a flow rate of 0.3 mL/minute and a carrier solvent concentration of 60% (*v/v*) acetonitrile (ACN) containing 1% (*v/v*) formic acid in water. Peptides were subjected to a capillary voltage of 2.5 kV and cone voltages of 15 V at

a source temperature of 120 ºC, desolvation gas of 650 L/h and desolvation temperature of 275 ºC. Data acquisition was performed by scanning over a mass over charge ratio (*m/z*) range of 300 to 2000 in continuum mode at a rate of 0.2 scans per second. Data analysis was performed using MassLynx V4.1 (Waters, Miliford, USA).

The ESMS spectral data was analysed using MassLynx V4.1 (Waters, Miliford, USA) to determine the proportion of the different types of oligomers formed. Set to auto-peak width determination the MaxEnt 3 algorithm was used to determine the oligomeric species between a range of 300 to 10 000 amu with a maximum of 10 charges and 50 iterations. From these data the percentage of the different oligomers formed by each of the respective peptides was determined using the ion signal of each oligomer in relation to the total ion signal intensity of all the different oligomers detected in each of the respective spectra.

5.2.3 Optical spectrometric analysis of the influence of different solvent environments on peptide structure

Due to the high background absorbance of DMF, dried aliquots of the purified peptides were dissolved in 50% (*v/v*) ACN in water and diluted to a concentration of 200 µM at a solvent concentration of 5% (*v/v*). These samples were incubated overnight prior to dilution to a concentration of 100 µM in water with or without the addition of 5% (*m/v*) of either Glc or 50% (*v/v*) TFE. Samples were analysed at 37 ºC on a Chirascan Plus circular dichroism (CD) spectrometer (Applied Photophysics, UK). CD scans were performed between 185 to 295 nm at a band width of 0.5 nm using a quartz cuvette with a path length of 0.05 cm simultaneously collecting CD as well as the ultra violet (UV) absorption spectra.

FS was performed on the same instrument using a quartz cuvette with a path length of 1 cm using samples at a concentration of 33 µM. Scans were performed detecting emission spectra at a band width of 1 nm between 300 to 400 nm at 90 ºangle to the excitation source at 280 or 295 nm. Each of the CD and FS spectra is the representation of three scans from which the blank had been subtracted and normalised.

5.2.4 Curve fitting and data analysis

All curve fits and statistical analysis were done using GraphPad Prism® 4.03 (GraphPad Software, San Diego, USA). Curves were fitted to the data using first or second order polynomial correlations (linear or quadratic equations) which best described the trend of

structure-oligomerisation relationships observed. Single data points that did not allow a fit with R^2>0.7 where excluded as indicated on the respective graphs.

5.3 Results and Discussion

As the interaction of the Trcs with one another [4,5] and their membrane targets [1] relies heavily on the contribution of hydrophobic interactions [5], it is vitally important that the contribution of the higher order structures formed by the respective peptides be considered to obtain a more in depth understanding of the true nature of the active structures.

The Trcs in this study differ at the variable dipeptide positions 3 and 4, occupied by either Trp or Phe; or at position 7 which may be occupied by any one of the three aromatic amino acids Phe, Trp or Tyr [17]. The three amino acid residues variable hydropathy of 2.8, -0.9 and -1.3 for Phe, Trp and Tyr respectively [49] alters the hydrophobicity, amphipathicity, ionizability, side chain surface area and ability of the different analogues to form hydrogen bonds. As a result of the variation in peptide sequence, the latter may influence the aggregation/oligomerisation of the different analogues into higher order structures [4-7,11] as well as the strength of their interactions with the target cell membrane [12,19,23] which are proposed to influence the antimicrobial activity of the Trcs.

5.3.1 Analysis of the cyclodecapeptides oligomerisation in aqueous and hydrophobic environments

5.3.1.1 ESMS detection of different homo-oligomers

The use of ESMS to detect the extent of the oligomerisation of the Trcs has previously been reported [4]. Analysis of the type of oligomeric structures formed by the different analogues of the Trcs in DMF by ESMS revealed a general trend of an increased proportion of dimeric oligomers relative to monomeric peptides, particularly by the more hydrophobic analogues (Figs. 5.2 and 5.3). For example, under the set ESMS conditions we observed oligomers up to pentamers for TrcA and only trimers for TrcC (Fig. 5.2).

Using the UPLC retention times (R_t; refer to Chapter 4) as an indication of hydrophobicity of the different Trcs, it was evident that increased dimerization was more prevalent in the more hydrophobic A analogues (Phe^3, Phe^4), than in the more polar C analogues (Trp^3, Trp^4) (Fig. 5.4). This phenomenon may possibly be related to an altered conformation adopted by the

different analogues that arises due to variation of the aromatic amino acid identity in their primary structures, leading to different propensities to form dimers and larger oligomers.

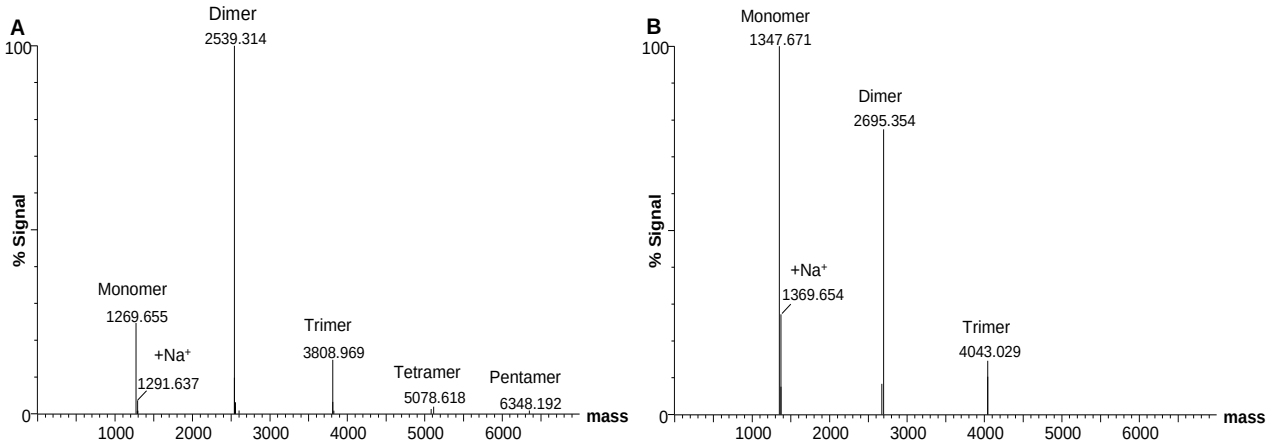

Figure 5.2 ESMS mass spectra generated with the maxEnt algorithm depicting the difference in oligomerisation between **A** the more hydrophobic A analogue (Phe^3, Phe^4) TrcA where oligomers as large as pentamers detected and **B** the more polar C analogue TrcC, where the monomeric peptide species was the predominant isoform that was detected.

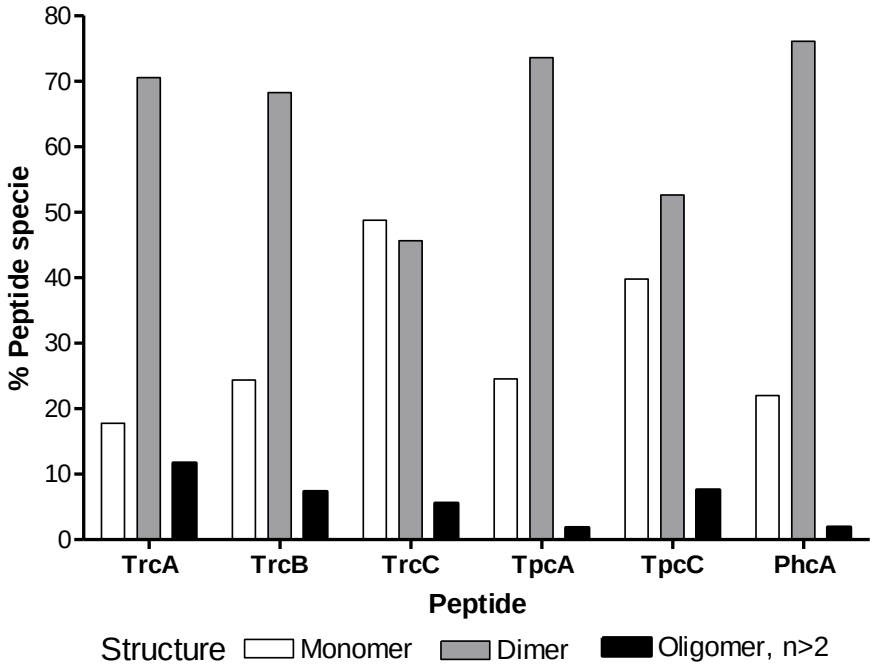

Figure 5.3 Comparison of the proportion of different oligomeric structures formed by the respective Trc analogues, as determined with ESMS. Peptides where dissolved in a final solvent concentration of 2.5% (*v/v*) DMF. The proportion contribution of the detected monomer, dimer or oligomers (n>2) is expressed as a percentage relative to the total ion signal for all the detected peptide species.

A decrease in the proportion of oligomers larger than dimers was noted for the two most hydrophobic peptides, according retention on the C_{18} matrix during UPLC, namely TpcA and PhcA (Fig 5.3 and 5.4). This, however, may be as a result of the precipitation of larger aggregates out of solution prior to analysis by ESMS or that formation of these aggregates relied primarily on hydrophobic forces, which are removed during ESMS desolvation [38,39,41].

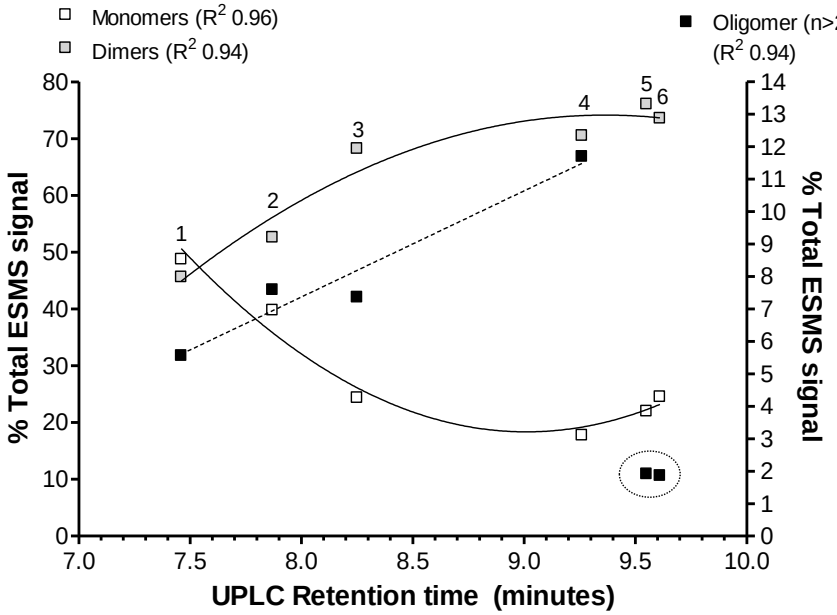

Figure 5.4 Comparison of the proportion of different oligomeric peptide species formed by the respective Trcs determined by ESMS analysis relative to their respective UPLC retention times (R_t) in minutes, Trc analogues numbered accordingly: 1 TrcC, R_t 7.46; 2 TpcC, R_t 7.87; 3 TrcB, R_t 8.25; 4 TrcA, R_t 9.26; 5 PhcA, R_t 9.55; 6 TpcA, R_t 9.61. The proportion contribution of the detected monomer, dimer or oligomers (n>2) is expressed as a percentage relative to the total ion signal detected for all the oligomeric species. Curves indicate trends for monomers and dimers fitted with a second order polynomial (quadratic equation). The circled Trc analogues did not fit the linear regression line fitted for the oligomers (n>2).

Apart from the higher order oligomers, a good relationship between retention on C_{18} and dimerization was found with a concomitant increase in dimer detection with the increase in retention (Fig. 5.4). The process of ionisation of a molecule ESMS removes water from the molecular or aggregate ion, thereby negating the hydrophobic non-covalent interactions [38,39,41]. Therefore, the oligomers and in particular the dimers detected by ESMS can be regarded as the result of mostly electrostatic interactions such as ionic interactions and hydrogen bonding between the peptide molecules. This finding correlates with the dimers modelled from X-ray crystallography and nuclear magnetic resonance studies performed in methanol or in a 50% ACN solution, respectively [4,5].

5.3.3.2 Analysis of the cyclodecapeptide structures by circular dichroism

Circular dichroism of the cyclodecapeptides in water and TFE can serve as a valuable means of elucidating the contribution of hydrophobic forces to the aggregation and self-assembly of peptides. This technique is well established in the study of structural changes of proteins and peptides by utilizing the sensitivity of the chiral properties related to peptide bond to different solvent environments [31,32].

The structure of the Trcs has previously been investigated by means of CD [14]. Due to the presence of D-amino acids the CD spectra of the Trcs is distorted to resemble that of an α–helix. However, in conformation with the determined X-ray crystal structure of the Trcs [5,25-28], their structure together with that of the analogous GS has been confirmed by CD to be composed of β-turns and β-sheets which correspond to two negative minima at 205-207 nm and 215-217 nm [14,50-53]. An increase in the intensity of these minima is associated with an increase in the proportion of ordered β-turn and β-sheet structures [4,11,12,54-56]. A change in the ratio of the two negative ellipticity minima ($\theta_{206\pm2\ nm}/\theta_{215\pm2\ nm}$) is associated with a change is the backbone conformation [11,50]. An increase in the hydrophobicity of the solution by suspending the peptides in TFE increases the stability of the higher ordered β-turn and β-sheet structures by placing the peptides in a model membrane environment [55,57-59]. Therefore, the latter can be used as a reference point to indicate increased ordered structures that are due to the backbone structure as would be delineated by increased negative minima.

These data could compliment the observations made by ESMS to shed some light on the relationship between the primary sequences of the peptides and oligomerisation. However, the shape and intensity of the CD spectra could be influenced by the aromatic amino acids (which contribute 40% of the amino acid content to the structure of the Trcs [17]), as well as the aggregation state [14,52]. Specifically the second minimum at 215 nm could be influenced by the contribution of aromatic amino acids, particularly Trp that influences the UV spectrum around 220 to 230 nm [16,42,43]. In future, more detailed studies must be performed, using for example fluorescence detected CD, to elucidate the influence of the aromatic residues on the CD spectra of these cyclodecapeptides. The varied aromatic amino acid identity between the different Trc analogues therefore poses a challenge to the direct comparison of the ellipticity of the different Trcs [52,60]. Consequently, as an indication of change in ordered structures of a particular analogue, the ellipticity changes were considered at the lower wavelength of

206 nm, which is due to the n to π* transition of 2p unpaired electrons of the carbonyl oxygen [54].

The cyclodecapeptide CD spectra in water and TFE correlated well with previous studies [4,14,16], showing minima at 206±2 nm and 215±2 nm (Fig. 5.5). TFE, a so-called membrane mimicking solvent [58], lead to a substantial increase in the negative ellipticity at 206±2 nm for all the peptides, indicating increased β-turn structures [4,11,12,54-56] (Fig 5.5; Table 5.1). Although similar minima were observed, the L-Trp^3 containing peptides (TrcB, TrcC and TpcC) presented visibly different spectra to the L-Phe^3 (TrcA, TpcA and PhcA) containing peptides (compare Fig. 5.5 A, C, E with B, D, F; Table 5.1).

Increased negative ellipticity of both the minima was observed for the L-Phe^3 containing peptides in TFE, while for the L-Trp^3 containing peptides the 215 nm minimum either remained the same (TrcC and TrcB) or decreased (TpcC) (Fig. 5.5). Consideration of the ellipticity ratio ($\theta_{206\pm2nm}/\theta_{215\pm2nm}$) [11,12,16] of the two peptide groups indicates a separation in the type of backbone structure adopted in TFE. The ellipticity ratio of the L-Phe^3 containing peptides was lower than that of the L-Trp^3 containing peptides, possibly indicating an increased proportion of β-sheet structures by L-Phe^3 containing peptides (Table 5.1).

These results could indicate that residue 3 influences the oligomeric structures and/or the backbone structure in TFE. These L-Trp^3 containing peptides also showed a similar increase in positive ellipticity up to the measured 185 nm in both water and TFE, with TpcC showing a maximum at 188 nm in water and the rest of the peptides at <185 nm (Fig. 5.5 B, D and F). This could be a blue shifted maximum of the π→π* transition of p-electrons from carbonyl groups (C=O) [54,61].

A red shifted maximum at 194±1 nm was observed for all the L-Phe^3 containing peptides in water and TFE, indicating participation of the carbonyl groups in hydrogen bonding [54,61] (Fig. 5.5 A, C and E). TFE increased the ellipticity for this maximum as well as both negative minima, which could also indicate the formation of more β-sheet type structures [14,54,61], possibly in oligomers (Fig. 5.5 A, C and E). The intensity of the maxima at 194±1 nm was greatest for TrcA>PhcA>>TpcA which may also be an indication of the degree of higher order structure formation through the oligomerisation. This indicates that residue 7 has an influence on the structure and possibly oligomerisation of these hydrophobic analogues.

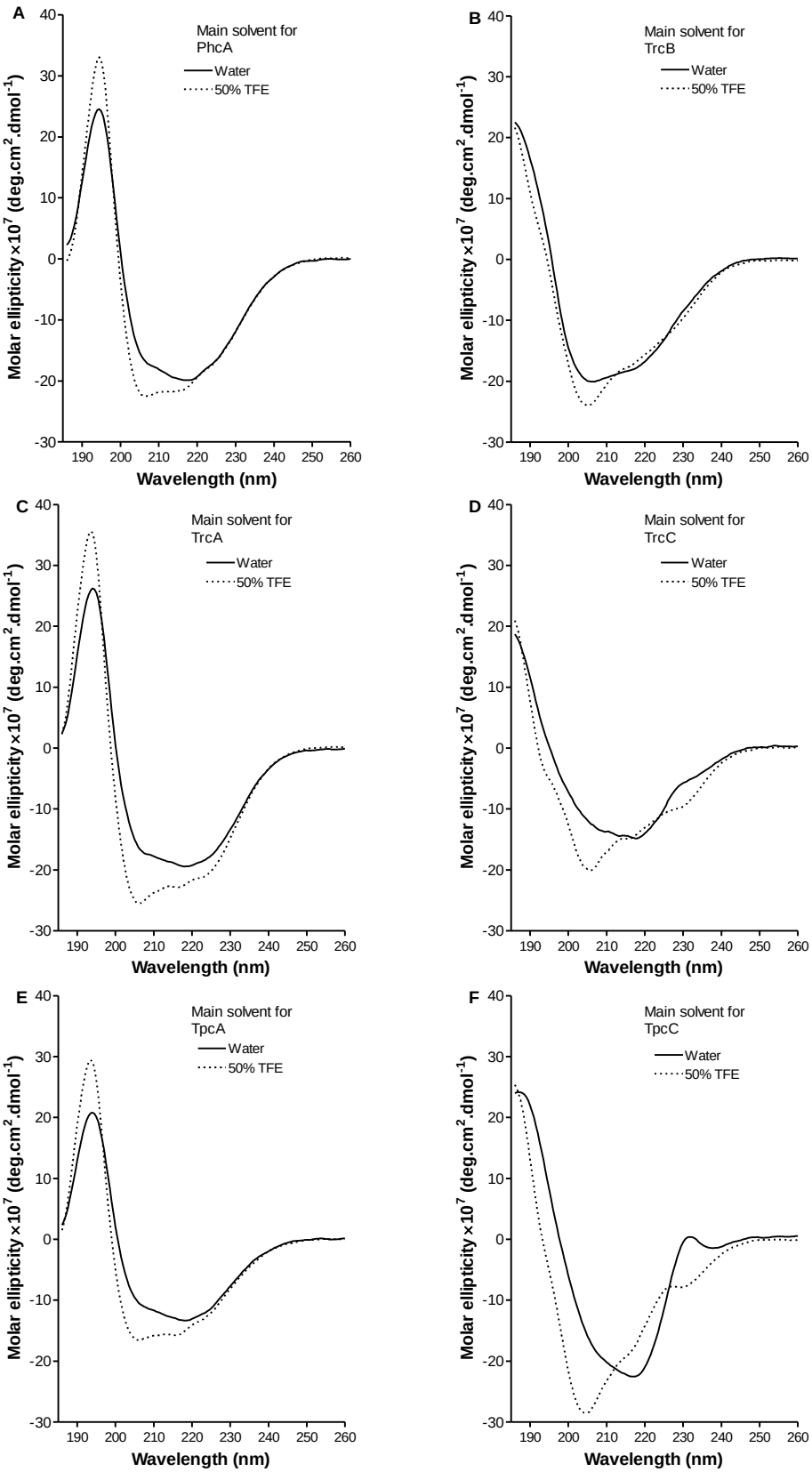

Figure 5.5 CD spectra of the different tyrocidine analogues at a concentration of 100 µM in an aqueous (water) and membrane mimicking environment (50% TFE). **A** PhcA, **C** TrcA, **E** TpcA, analogues with Phe^3, Phe^4 and Phe^7, Tyr^7 or Trp^7 respectively. **B** TrcB with Trp^3, Phe^4 and Tyr^7 and **D** TrcC, **F** TpcC, with Trp^3, Trp^4 and Tyr^7 or Trp^7 respectively.

Table 5.1 Variability in the CD spectra of the different tyrocidine analogues in an aqueous or membrane mimicking environment.

Peptide (*n=3*)	In water			In 50% TFE		
	$\theta_{206\pm2\ nm}$	$\theta_{215\pm2\ nm}$	$\theta_{206\pm2\ nm}/\theta_{215\pm2\ nm}$	$\theta_{206\pm2\ nm}$	$\theta_{215\pm2\ nm}$	$\theta_{206\pm2\ nm}/\theta_{215\pm2\ nm}$
TrcA	-15.8±0.12	-18.8±0.12	0.841±0.0011	-25.0±0.042	-22.8±0.043	1.10±0.0022
TrcB	-19.9±0.064	-18.4±0.085	1.08±0.0055	-23.5±0.011	-17.9±0.033	1.31±0.0029
TrcC	-12.4±0.11	-14.5±0.18	0.854±0.0033	-19.6±0.0073	-14.9±0.021	1.31±0.0023
TpcA	-10.2±0.089	-12.9±0.085	0.789±0.0024	-16.3±0.021	-15.7±0.041	1.04±0.0029
TpcC	-16.9±0.11	-22.1±0.11	0.765±0.0036	-27.6±0.24	-19.3±0.14	1.43±0.0023
PhcA	-16.0±0.074	-19.6±0.071	0.818±0.0025	-22.0±0.097	-21.6±0.074	1.02±0.0057

Molar ellipticities (θ) in 10^7 × deg.dmol^{-1}.cm^{-1}. Each minima or ratio thereof is expressed as the mean value obtained from three spectra ± SEM.

The D-Trp^4 containing peptides, TrcC and TpcC, also presented an additional shoulder at 230 nm, which presents as a negative minimum in TFE (Fig. 5.5 D and F). This could indicate a difference in the backbone structure or the influence of this aromatic amino acid on the CD spectrum [11,12,50,52,60].

Comparison of the ellipticity minima at 206 nm in water indicated a decreased proportion of ordered structures by the Trcs with the lowest and highest UPLC R_t, TrcC and TpcA respectively (Table 5.1; Fig. 5.6). The rest of the Trcs displayed an increased degree of ordered structure indicating oligomerisation, with ordered structure sequence as follows: TrcB>TpcC≥PhcA~TrcA>TrcC>TpcA.

The above relationship is put into perspective when comparing the ellipticity observed at 206 nm in an aqueous (water) and membrane mimicking (TFE) environments relative to: hydrophobicity (R_t) (Fig. 5.6 A and C), or proportion of dimers formed by the respective Trcs (Fig. 5.6 B and D). Good quadratic trends, separating the peptide in two distinct groupings, of increased intensity of the negative minima at 206 nm was observed with both R_t and dimerization. This indicated the formation of a higher proportion of ordered structures by the peptides of intermediate hydrophobicity (R_t~8.5) and of ~60% dimer population. As dimerization had already been established to be directly correlated with hydrophobicity a similar trend was to be expected. TrcB (Trp^3, Phe^4) as the intermediate between the A and C analogues it contains properties of both groups, thus it is observed to associate with both the A analogues (Ff) and C analogues (Ww) or not fit into the observed trend (Fig. 5.6).

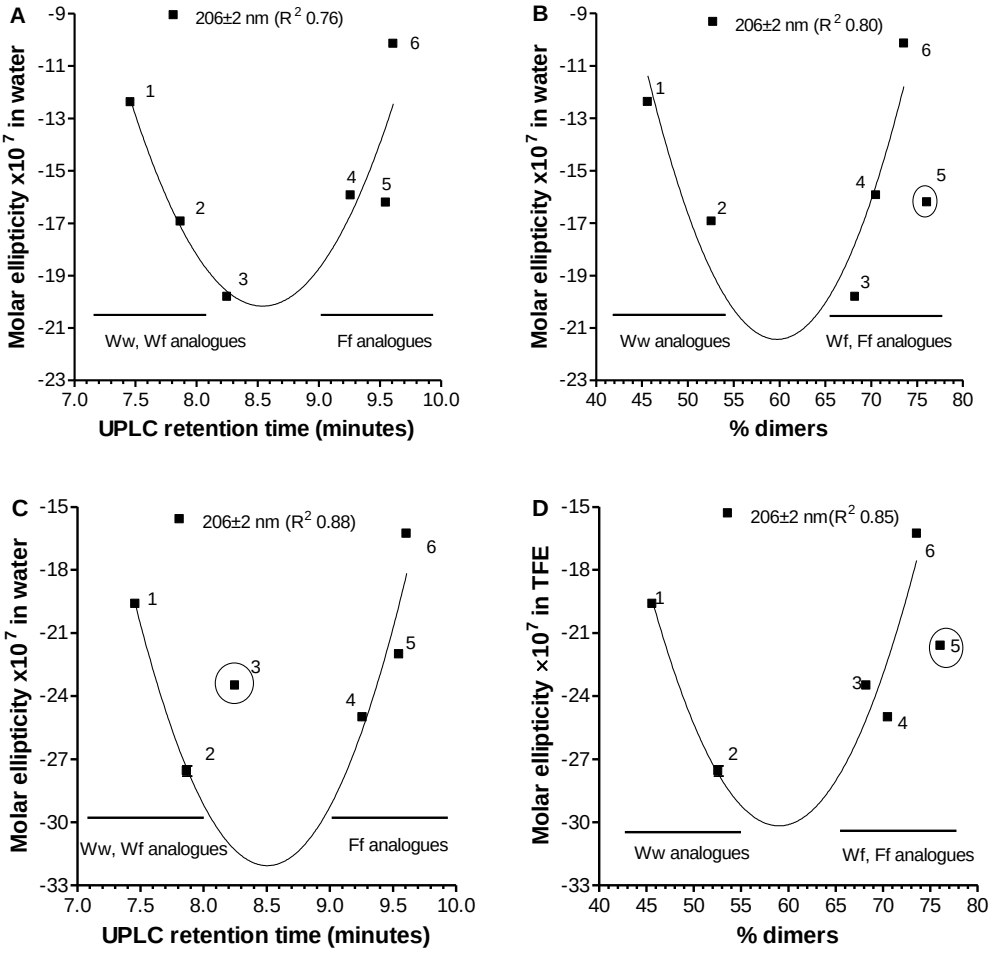

Figure 5.6 Comparison of the ellipticity minima of the different Trcs observed at 206±2 nm in an aqueous (water) or membrane mimicking (TFE) environment respectively relative to: the UPLC R_t as in indication of hydrophobicity (**A** and **C**) and the proportion of dimers detected by ESMS for the respective Trc (**B** and **D**),. Curves indicate trends fitted with a second order polynomial. The encircled data point in each graph indicate the peptide that was excluded to obtain a fit with R^2>0.5 Trc analogues numbered: 1 TrcC, R_t 7.46; 2 TpcC, R_t 7.87; 3 TrcB, R_t 8.25; 4 TrcA, R_t 9.26; 5 PhcA, R_t 9.55; 6 TpcA, R_t 9.61.

The difference in hydrophobicity of the Trcs is determined by the variation of aromatic amino acids in their primary structures which in turn governs the higher order conformation(s) of the different analogues. The potential steric hindering of the larger Trp residue could in turn determine how different monomers associate with one another to oligomerize into higher order structures. It is interesting to note that the most hydrophobic peptide PhcA did not fit well into the trends, which could indicate that either some peptide was lost due to precipitation during the analyses or that a residue with hydrogen bonding character in position 7 is important for increased intensity of the negative ellipticity. The fact that this preparation contains 12% of the Lys analogue $PhcA_1$ could also lead to skewing of the results.

Modelling of the monomeric structure of TrcA using information regarding conformation obtained from X-ray crystal structure resulted in an amphipathic two-stranded, antiparallel β-sheet monomeric structure with a defined curved structure with most of the amino acid side chains forming the hydrophobic convex side and only the side chain of positively charged ornithine on the polar concave side [5].

Dimerization of these monomers forms an amphipathic four-stranded sheet structure which is stabilised by both backbone-backbone hydrogen bonds and hydrophobic interactions. Further stabilisation of the dimer occurs through "edge to face" interaction of the ring structures of Phe^{1} and Tyr^{7} [5]. These active structures then interact with membrane targets, the hydrophobic Phe^{4} inserting deep into the membrane while the more hydrophilic Tyr^{7} is nearer to the surface [5].

Munyuki *et al.* [4] proposed a model for the dimerization of both TrcA and the TrcC analogue in an aqueous environment. Disagreement regarding the location of the Phe^{4} side chain resulted in these investigators proposing the monomeric peptide has low amphipathicity in contrast to the structure proposed by Loll *et al.* [5]. However, in agreement with Loll *et al.* [5], these investigators proposed dimerization by means of sideways association and stabilisation by predominantly backbone-backbone hydrogen bonding results in an amphipathic structure. Munyuki *et al.* [4] proposed dimerization may also occur by π-stacking interactions between the aromatic ring structures of the aromatic amino acids, resulting in stacking of residues on top of one another through association by hydrophobic interactions.

The oligomerisation of the Trcs may thus occur through both the interaction of different residues by means of hydrophobic interactions and hydrogen bonding. Comparison of the ellipticity of the different A analogues (Phe^{3}, Phe^{4}) provides evidence of the influence of the variability of the aromatic amino acid at position 7 on oligomerisation of the Trcs in relation to Phe occupying both positions of the variable dipeptide unit.

As has been previously proposed [5], the Tyr^{7} found in TrcA may optimally stabilise the active dimer structure formed by backbone-backbone hydrogen bonding, and result in increased membranolytic antimicrobial activity. Substitution of Tyr^{7} with Trp^{7} to form TpcA may disrupt the optimal interaction of Phe^{1} and residue 7 (Trp^{7}), the indole group of which now forms a bulkier protruding side chain in the dimerised structure creating a protruding surface where previously the smaller phenol group of Tyr^{7} was found. This conjugated ring structure can still

serve as an anchoring point for further hydrophobic interactions with other dimers or monomers, but is sub-optimal thereby disrupting the formation of ordered structures (Fig. 5.5 and 5.6). This may elude to why increased proportion of dimeric structures of TpcA where observed by ESMS (Fig. 5.3 and 5.4), but did not increase proportions of ordered structures detected by CD (Fig. 5.5 and 5.6) where the combined influence of hydrophobic interactions resulted in association of residues unable to assemble into higher order structures.

In contrast, a different scenario may be at play where Tyr^7 is substituted with Phe^7 in the PhcA analogue. The smaller size of Phe would allow it to act as an anchoring point for hydrophobic interactions. Therefore, the observed dimer population (Fig. 5.3 and 5.4), as well as ordered structures detected by CD (Fig. 5.5 and 5.6), are similar to that observed for TrcA. If the three peptides with an L-Trp^3 are compared we find that the ellipticity at 206 nm decrease as follows, TrcB>TpcC>>TrcC, which could indicate a more complicated role of Trp and other aromatic residues in oligomerisation (Table 5.1; Fig. 5.6).

In order to assess the overall influence of structure on the backbone structure of the peptides the ellipticity ratio between the two major minima ($\theta_{206\pm2nm}/\theta_{215\pm2nm}$) was considered [11,12,16,56,56]. Good quadratic trends of the ellipticity ratio with UPLC R_t and % dimers detected by ESMS were only found for the peptides in TFE, indicating that this parameter is not only dependent on dimerization, but also the hydrophobicity of the peptides (Fig. 5.7).

The ratio of the two minima was >1.0 for the TrcB analogue in an aqueous environment, in contrast to the rest of the Trcs (Fig. 5.7), suggesting TrcB has a backbone conformation containing a greater proportion of β-turn structures [11,12,50,54,56,61] in an aqueous environment which differed from that of the rest of the peptides in the study (Table 5.1; Fig. 5.7 A and B). TrcB (Wf) acts as an intermediate having characteristics of both the A and C analogues. Oligomerisation of TrcB followed a similar trend to that observed for TrcA to form an increased proportion of dimeric oligomers as determined by ESMS (Fig. 5.2 and 5.3). TrcB would seem to form an increased proportion of ordered structures when the added influence of hydrophobic effect was included, as deduced by the increased intensity of the minima observed at 206 nm by CD analysis (Table 5.1; Fig. 5.3 and 5.4). This is most likely due to the influence of Phe^3 to Trp^3 substitution between TrcA and TrcB resulting in an altered conformation which was influenced to a greater degree by hydrophobic effect in an aqueous environment. The negative minima of the TrcB analogue at 206 nm increased the least of all the peptides in the study between the aqueous and membrane mimicking environments

(Table 5.1). It is postulated that TrcB adopts a similar structure as proposed for TrcA by Loll *et al*. [5], but the steric bulk of Trp^3 indole group may force the hydrophobic Phe^4 benzyl side chain into a more solvent exposed environment, thereby allow it to act as anchoring point for further hydrophobic interactions and higher order structure formation.

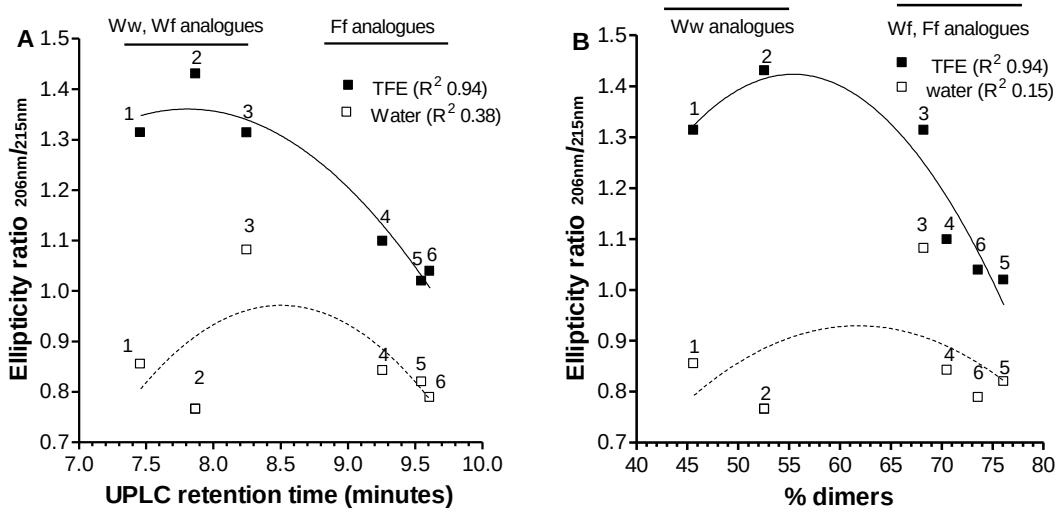

Figure 5.7 The ratio of the ellipticity minima 206 nm/215 nm in the two respective solvent environments versus **A** UPLC Rt and **B** versus % dimers detected via ESMS. Trc analogues numbered: 1 TrcC, Rt 7.46; 2 TpcC, Rt 7.87; 3 TrcB, Rt 8.25; 4 TrcA, Rt 9.26; 5 PhcA, Rt 9.55; 6 TpcA, Rt 9.61. Curves indicate trends fitted with a second order polynomial (quadratic function).

The ratio of the two minima were observed to be >1.0 only in the membrane mimicking environment for the rest Trcs indicating an altered backbone conformation between the two environments (Table 5.1). While the ellipticity ratio of TrcB still increased upon exposure to the membrane mimicking environment, this was to a lesser degree than was observed by TpcC and TrcC, where a sharp increase in the intensity of the minima was observed between water and TFE. This indicated TrcB was in a more ordered structure before exposure to the membrane mimicking environment (Fig. 5.7, refer to data points numbered 1, 2 and 3). Again a distinct separation is observed between the backbone conformation adopted by the C analogues (Ww) relative to the A analogues (Ff), with TrcB (Wf) as an intermediate has characteristics of both (Fig. 5.7). This indicated a difference in backbone structures as determined by the identity of the variable dipeptide position. Moreover, a much smaller increase in the ratio was found for the A analogues, indicating that these peptides already have a highly ordered backbone structure in water.

Substitution of Phe^3, D-Phe^4 with Trp^3, D-Trp^4 at the variable dipeptide unit which occurs between the A and C analogues could alter the backbone conformation adopted by the C

analogues. The greater steric bulk of Trp at the variable dipeptide unit may influence the structure of the dimers as well as their propensity to form; that is if TrcC and TpcC follow a similar structural conformation to the TrcA proposed by Loll *et al.* [5]. This hypothesis is supported by the decreased proportion of dimeric oligomers observed for the TrcC analogue (Fig. 5.2 and 5.3). This also concurred with the decreased proportion of ordered structures and lower ellipticity ratio in water, as detected for this analogue by CD (Table 5.1; Fig. 5.5, 5.6 and 5.7).

In contrast to TrcC, the TpcC analogue was observed to form just in excess of 52% dimeric oligomers (Fig. 5.2) as well as exhibit an increased negative ellipticity (Table 5.1; Fig. 5.5). The presence of Trp at all three of the variable aromatic amino acid positions may alter the conformation of the TpcC monomer which is possibly quite different to that proposed for TrcA by Loll *et al.* [5]. Dimerization may also occur by π-stacking interactions between the aromatic ring structures as proposed by Munyuki *et al.* [4]. The high prevalence of Trp increases the steric bulk attributed to the indole side chains. This results in an altered capacity to form hydrogen bonds, ring stacking and hydrophobic interactions with other monomers, thereby influencing the propensity to dimerize, as well as form higher order structures. The TpcC analogue displayed an increase in the intensity of the minima observed at 215 nm in water which results in lower ellipticity ratio, eluding to an altered back bone conformation.

An altered conformation adopted by the C analogues (Fig 5.3 D and F) is supported by an altered CD spectrum displaying a shoulder attributed to Trp^4 [4,14,16], observed at 230 nm in this study. An altered peptide backbone conformation may also be the cause of a red-shift in the ellipticity of the β-sheets resulting from altered hydrogen bonding [16].

Variability of the aromatic amino acid composition of the different Trcs influences the conformation which they adopt. This in turn has a downstream knock on effect regarding their propensity to oligomerize into higher order structures.

5.3.3.3 Assessment of the influence of aromatic amino acids by fluorescence spectroscopy

Further information regarding changes in the location/exposure of the aromatic side chain, particularly those of Trp, may be made using FS. The indole group of the Trp residue is highly sensitive to its local environment and polarity [33,37,43,62]. Exposure of Trp to a hydrophobic environment results in a blue shift in the emission maxima from the usual 348 nm observed in an aqueous environment [30,33,42,62]. Moreover, Trp fluorescence is a good indicator of

aggregation/oligomerisation state of the Trcs due to its high sensitivity to hydrophobic environments and solvent/polar environment quenching [30,33,42,62]. The latter occurs *via* numerous avenues including: complex formation in the ground state, collisional quenching by exposure of Trp to an aqueous environment, as well as excited-state reaction with surrounding polar groups [30,33,42,62]. These groups include amide groups located in the peptide backbone, as well as side chains of Asn and Gln, amino group of Orn and hydroxyl group of Tyr [30,62].

The fluorescence emission spectra of the four Trp containing Trc analogues were examined to elucidate the orientation and effect of aggregation on the Trp residues. In all of the Trcs a shift in the emission maxima was observed from the expected 357 nm [46] to 347 nm, indicating the Trp residues are located in a hydrophobic environment within an oligomeric structure (Fig. 5.8).

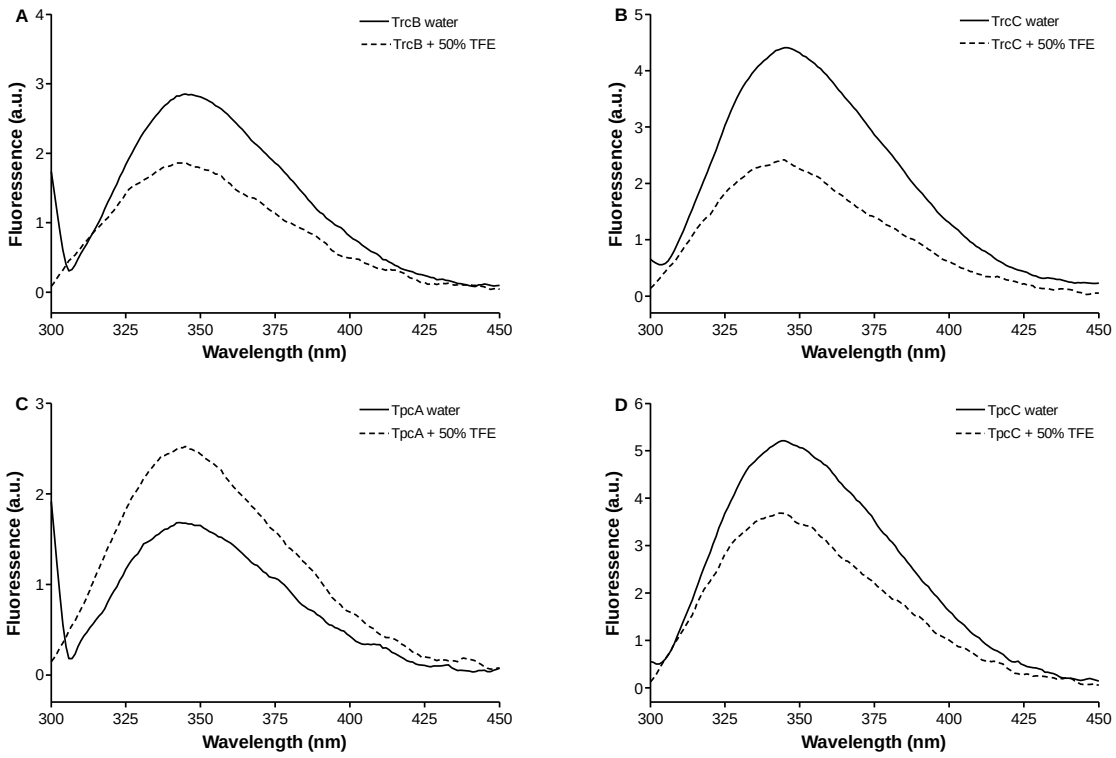

Figure 5.8 Fluorescence emission spectra of the Trp containing Trc analogues in an aqueous (water) or membrane mimicking (TFE) environment. Excitation at 295 nm to comparing the Trp emission of: **A** TrcB with Trp^4, **B** TrcC Trp^3, Trp^4, **C** TpcA with Trp^7 and **D** TpcC with Trp^3, Trp^4 and Trp^7. Fluorescence quantum yield indicated in arbitrary units (a.u).

For all the analogues containing L-Trp^3, namely TrcB, TrcC and TpcC, increased fluorescence intensity was observed in an aqueous environment relative to the TFE membrane mimicking

environment, while the fluorescence maximum was blue shifted to 342 nm (Fig. 5.8). The blue shifted λ_{max} implies that the indole group(s) is transferred into an even more hydrophobic environment [46].

If the fluorescence or quantum yields are compared between the four Trp containing peptides, we find no direct relationship in either of the two solvents (Fig. 5.9). This is particularly apparent when comparing the fluorescent yields obtained for TrcB with Trp^3 and TpcA with Trp^7 in the two solvent environments (Fig. 5.9). Both of these peptides contain a single Trp residue but are located at different positions in the backbone structure. This result indicates that the Trp residue(s) in the different peptides are possibly in different environments leading to differences in fluorescence.

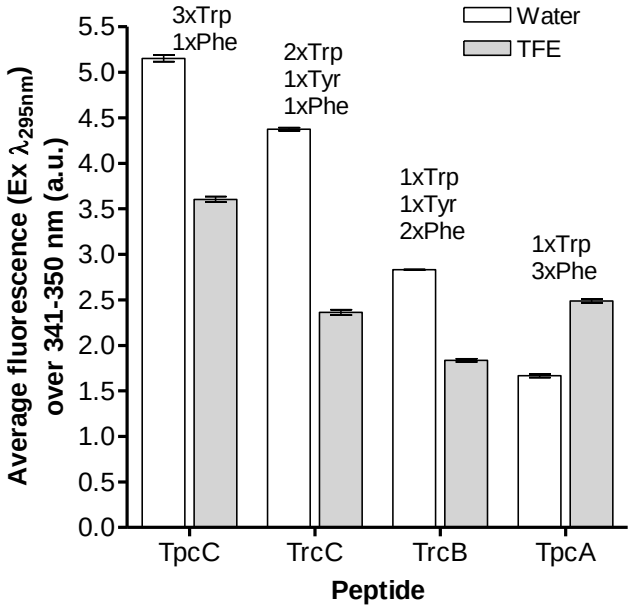

Figure 5.9 Comparison of the fluorescence quantum yield obtained from emission spectra of the Trp containing Trc analogues in an aqueous (water) or membrane mimicking (TFE) environment. Excitation at 295 nm to comparing the Trp emission of: TpcC with Trp^3, Trp^4 and Trp^7, TrcC with Trp^3, Trp^4, TrcB with Trp^3 and TpcA with Trp^7.

When TrcB, TrcC and TpcC are in a membrane mimicking environment an altered backbone conformation is adopted (as indicated by our CD results, Table 5.1) and quenching of their fluorescence yields was observed (Fig 5.8 A, B and D). The altered backbone conformation could lead to the formation of higher order structures that expose Trp^3 to the solvent environment resulting in collisional quenching, as would occur when forming β-sheet structures. Alternatively, substantial quenching could occur as a result of a resonance energy

transfer interaction between Trp^3 in the variable dipeptide unit and other chromophores, such as Phe and Tyr [47]. Higher order structure formation could also lead to quenching by excited-state reactions which resulted due to conformations bringing the Trp residues into close proximity of polar chains or amide and amine groups [33,37,46,62]. This hypothesis is supported by the large change in the ellipticity ratio observed for the C analogues within the two solvent environments by CD (Fig. 5.7 A and B), implying a large change in backbone structure and oligomerisation by these analogues between the two environments. Moreover, a similar blue shifted λ_{max} and quenching of TrcB fluorescence were observed by Leussa [24] in the presence of liposomes mimicking the membranes of Gram-positive bacteria.

In contrast to what was observed for the peptides with Trp^3, the opposite was observed with TpcA containing Trp^7. In an aqueous environment this residue displayed a decreased fluorescent intensity relative to that observed in a membrane mimicking environment. Indicating that the position of this residue allowed for its fluorescence to be quenched (Fig. 5.5 C). This supports our earlier hypothesis proposing that the steric properties of the indole group within this position may cause this residue to be more solvent exposed. This could result in collisional quenching due exposure to the hydrophilic environment. Alternately quenching of this residue may be due to ground-state interaction of the Trp^7 residue. The latter would also result in increased proximity of excited-state quenchers; such as those of the peptide backbone, other amides or amines, such as the Asn, Gln or Orn residues or resonance energy transfer to the Phe residues in the peptide. The increased fluorescent yields observed in a membrane mimicking environment implied location within a more hydrophobic environment, where hydrophobic exclusion which caused interaction with quenchers was removed.

5.3.2 Influence of glucose on the cyclodecapeptides

The importance of environmental factors such as the presence of calcium are shown to alter the antifungal [22] and antibacterial activity [16,24] of the Trcs changing the mode of action from primarily a lytic to a non-lytic which causes the disruption of intracellular processes. Differences in target cell properties, together with the environment, have been observed to influence a broad range of antimicrobial peptides [63-67], including the Trcs [20-24].

Glucose (Glc) is ubiquitously present, not only in the environments of the agricultural and food industries where the microbial pathogens which the Trcs target exist in, it also forms part of the target cell structures. The cell wall of fungi is compromised predominantly of glycoproteins

and polysaccharides of mainly glucan and chitin whose monomeric subunits are derived from Glc [68]. The importance of the fungal cell wall on the antifungal activity of the Trcs has previously been shown by Troskie [69]. Moreover, Glc is present at 0.25% (*m/v*) and 1.0% (*m/v*) in TSB or half strength PDB respectively; the growth media used to culture the two model target organisms in this study *B. subtilis* and *A. fumigatus*. Glc may thus have a profound influence on the activity of the Trcs. It was therefore decided to elucidate the influence of Glc on the oligomerisation of the Trcs into higher order structures

Analysis of the influence of Glc on the oligomerisation of the different tyrocidine analogues in this study revealed it to have the largest influence on TrcB>PhcA>>TrcA decreasing the intensity of the minima at 206 nm and 215 nm, but without causing a substantial change in the ellipticity ratio of the two minima (Table 5.2, Fig. 5.10). This would indicate that Glc possibly acts as chaotropic agent on these Trc analogues, decreasing the proportion of higher order structures formed in an aqueous environment as it has a minimal influence on the backbone conformation. The change in ellipticity observed in the vicinity of 195 nm in all the analogues is attributed to light scattering due to the presence of Glc [70].

The ellipticity minimum at 206 nm was again used to compare the influence of Glc on oligomerisation of the different Trcs (Fig. 5.11). We again found good quadratic trends similar to those in water, except that TrcB did not fall into the trend observed with UPLC R_t (Fig 5.11 A). Glc had a major influence on the ellipticity of TrcB (Fig. 5.11 B, data point 3) and Phc A (Fig. 5.11, data point 5), containing Phe^4 and Tyr^7 or Phe^7 residues respectively. The decreased intensity of the ellipticity minima in the presence of Glc indicated its interference with the higher order structures. The influence of Glc on the other four peptides was minimal. Glc but did not have a noteworthy effect on the backbone structure as indicated by the similar trends and intensities observed for the ratio of the two ellipticity minima (Fig. 5.11 C).

The interaction of Glc with the Trcs was investigated further by means of fluorescence to deduce if it causes a change in conformation which would influence the orientation and exposure of Trp residues (Fig. 5.12). Concurring with the observations made in CD, Glc did not change the conformation of the TpcC analogue hence the fluorescence yield remained fairly constant between the two environments (Fig. 5.12 D).

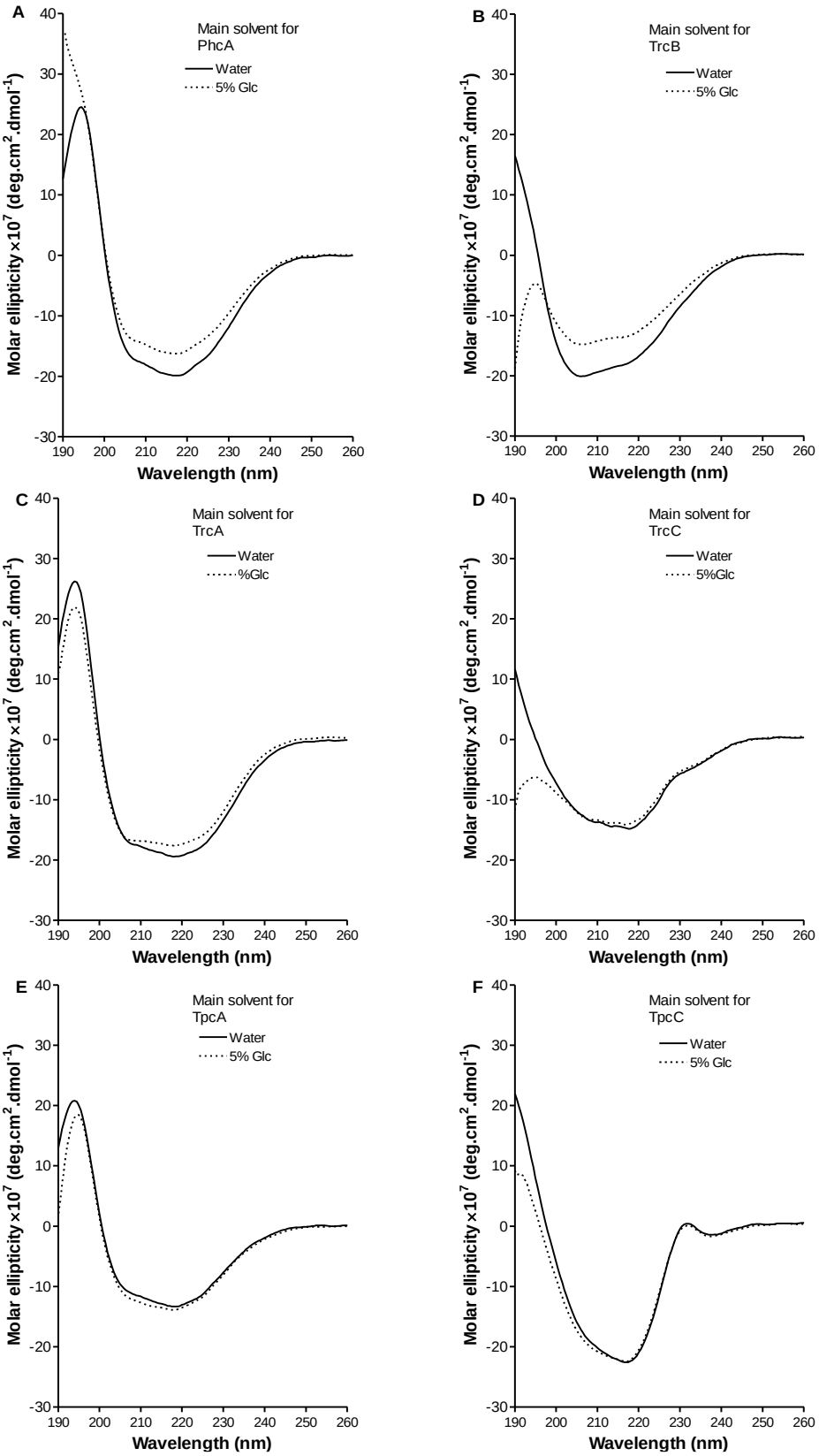

Figure 5.10 CD spectra of the different tyrocidine analogues at a concentration of 100 µM in an aqueous (water) or in water together with 5% (*m/v*) glucose (Glc). **A** PhcA, **C** TrcA, **E** TpcA, analogues with Phe[3], Phe[4] and Phe[7], Tyr[7] or Trp[7] respectively. **B** TrcB with Trp[3], Phe[4] and Tyr[7] and **D** TrcC, **F** TpcC, with Trp[3], Trp[4] and Tyr[7] or Trp[7] respectively.

Table 5.2 Variability in the CD spectra of the different tyrocidine analogues in an aqueous environment or together with 5% (*m/v*) glucose

Peptide (*n=3*)	In water			In 5% Glucose		
	$\theta_{206\pm2\ nm}$	$\theta_{215\pm2\ nm}$	$\theta_{206\pm2\ nm}/\theta_{215\pm2\ nm}$	$\theta_{206\pm2\ nm}$	$\theta_{215\pm2\ nm}$	$\theta_{206\pm2\ nm}/\theta_{215\pm2\ nm}$
TrcA	-15.8±0.12	-18.8±0.12	0.841±0.0011	-15.8±0.073	-17.3±0.165	0.912±0.0045
TrcB	-19.9±0.064	-18.4±0.085	1.08±0.0055	-14.7±0.11	-13.6±0.12	1.08±0.0029
TrcC	-12.4±0.11	-14.5±0.18	0.854±0.0033	-12.5±0.089	-13.9±0.157	0.897±0.0040
TpcA	-10.2±0.089	-12.9±0.085	0.789±0.0024	-11.0±0.157	-13.6±0.21	0.814±0.0017
TpcC	-16.9±0.11	-22.1±0.11	0.765±0.0036	-18.2±0.31	-22.1±0.46	0.821±0.0031
PhcA	-16.0±0.074	-19.6±0.071	0.818±0.0025	-13.2±0.067	-16.0±0.053	0.823±0.0019

Molar ellipticities (θ) in 10^7 × deg.dmol^{-1}.cm^{-1}. Each minima or ratio thereof is expressed as the mean value obtained from three spectra ± SEM.

In support of the minimal change in ordered structure formation, observed in CD of TrcC in the presence of Glc, only a marginal decrease in fluorescence yield was observed, indicating a slightly different conformation adopted by TrcC relative to that of TpcC. The substitution of Trp^7 with Tyr^7 may thus alter the conformation adopted by TrcC to cause Trp^3, Trp^4 to be exposed to a greater degree on the surface of the higher order structure thereby allow for interaction with water and Glc causing marginal quenching of the fluorescence yield to occur but without disrupting the higher order structures (Fig. 5.12 B).

The structure adopted by TpcA has been shown *via* ESMS to allow dimerization (Fig. 5.3), but not form increased proportions of higher order structures. The addition of Glc in an aqueous environment did not disrupt the aqueous structures that were observed *via* CD (Fig. 5.10 E), however, it did increase the fluorescence yield (Fig. 5.12 C), indicating that the Trp^7 residue moved into a more hydrophobic environment. Alternatively, this could indicate that Glc acted as a chaotropic agent disrupting the association of quenchers with Trp^7 allowing this residue to associate with hydrophobic groups, thereby be protected from collisional or dynamic quenching. The removal of water may also slightly ease the conformation adopted by the dimerised structure to allow Trp to move away from active groups which quenched the excited-state Trp^7.

The substitution of Trp^4 with Phe^4 between TrcC and TrcB caused an entirely different scenario to occur. The increased hydrophobicity of Phe is observed to increase the dimerization (Fig. 5.3). A conformation adopted when the peptide structure contained Phe^4 together with Tyr^7 or Phe^7 allowed interaction with Glc that resulted in decreased ordered structure formation, with the most pronounced effect observed in TrcB (Fig. 5.12 A).

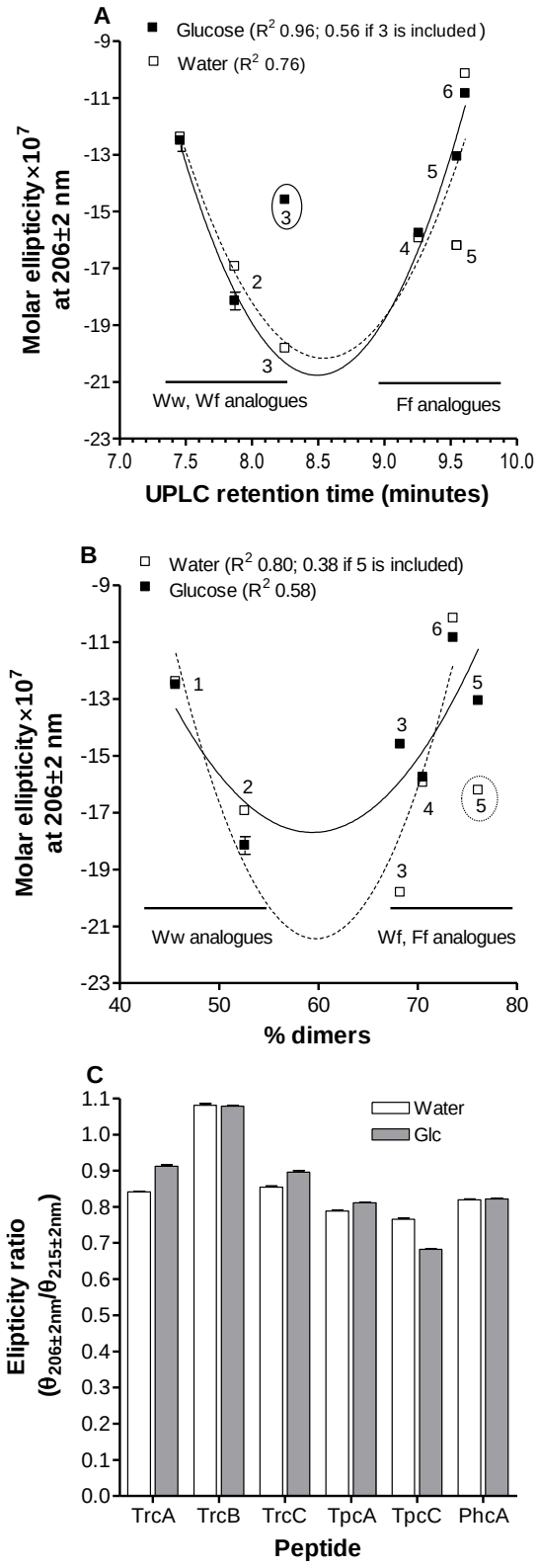

Figure 5.11 Comparison of the change in ellipticity minima of the different Trcs in an aqueous (water) environment only or together with glucose (Glc). Change in ellipticity minima observed at 206 nm relative to **A** the UPLC R_t as in indication of hydrophobicity and **B** the % dimers detected by ESMS. **C** The ellipticity ratio 206 nm/215 nm of the two minima for the different peptides. The respective Trc analogues are numbered as before. Circled analogues were not included in the second or third order polynomial trends fitted for the rest of the Trcs.

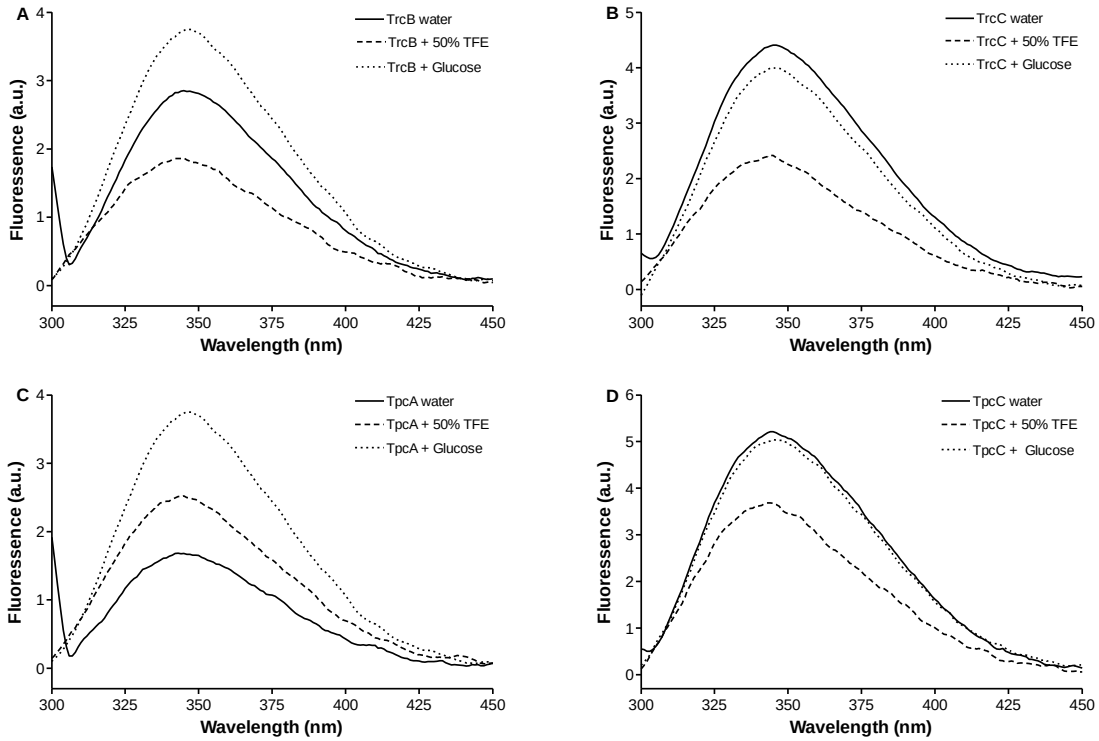

Figure 5.12 Fluorescence emission spectra of the Trp containing Trc analogues membrane mimicking (TFE) or in an aqueous (water) environment alone or together with glucose. Excitation at 295 nm to comparing the Trp emission of: **A** TrcB with Trp^4, **B** TrcC Trp^3, Trp^4, **C** TpcA with Trp^7 and **D** TpcC with Trp^3, Trp^4 and Trp^7.

The difference in fluorescence emission spectra observed between TrcB and TrcC may elude to a difference in the conformation adopted by the residues of the variable dipeptide unit (Fig. 5.12 A and B). The Trp^3, Phe^4 intermediate nature of the variable dipeptide unit causes a possible change in conformation, which suggests to greater exposure of the hydrophobic Phe^4 residue which resulted in increased higher order structure formation. This change allowed for increased interaction between dimerised peptides to form higher ordered structures (Fig. 5.4). The disruption of higher order structures by Glc is proposed to be related to the nature of the interaction caused by the hydrophobic Phe^4 residue in higher order structure formation. Disruption of higher order aggregates by Glc may alter the conformation of the peptides, in the case of TrcB result in the Trp^3 residue being placed in a more hydrophobic environment away from quenching groups, hence the increased fluorescence yield observed in the presence of Glc (Fig. 5.12 A).

It is thus proposed that the chaotropic effect observed by Glc on TrcA, TrcB and PhcA may form part of their mode of antimicrobial activity through a balance between the disruption of higher order structures formed in an aqueous environment by these more hydrophobic Trc analogues and interaction with the target cell. Glc may most likely influence hydrophobic

packing interactions between the aromatic ring structures in the side chain of Phe and Tyr. Furthermore, it also has the potential to disrupt hydrogen-bonding networks and other electrostatic interactions which stabilise the higher order structures. Glc, however, was found to have lesser of an influence on Trp^7. Eluding to a possible alternate conformation adopted by the active structures of these peptides which was less accessible to Glc.

5.3 Conclusions

Changes in the aromatic amino acid content of the Trcs and analogues results in variation in the conformation and character affecting their oligomerisation and higher order structure formation. Increased dimerization is observed by the more hydrophobic analogues (Fig. 5.3 and 5.4), although increased ordered structure formation, as observed *via* CD, was dependent on an intermediate hydrophobicity and dimerization (Fig. 5.6). A distinct separation was observed between the characteristics of the A and C analogues containing Phe^3, Phe^4 or Trp^3, Trp^4, respectively in the variable dipeptide unit. While TrcB with Trp^3, Phe^4, as an intermediary peptide, tended to have characteristics of both, or at times didn't associate with either of the two peptide trends (Fig. 5.7). Changes of the variable aromatic amino acid between Tyr^7, Phe^7 or Trp^7 altered the character of the different analogues as exemplified by the differences in the three different A analogues (TrcA, PhcA and TpcA). The C analogues (TrcC and TpcC) and TrcB containing Trp^3 showed variable higher ordered structure formation, demonstrating the influence of the three variable aromatic amino acids acting to alter the conformation and character.

The model structure and membrane interaction proposed by Loll *et al*. [5] for dimers of TrcA will need some amendments for the other cyclodecapeptides, as one model might not fit all. The model by Loll *et al*. [5] still only eludes to the initial membrane interaction by these peptides. Due to the curvature of the dimeric structure proposed by Loll *et al*. [5] they questioned the feasibility of linking the dimeric structures into extended sheets. The high stability oligomers observed for the cyclodecapeptides in this study and also reported in literature [6-8,10] point to a high tendency to form structures larger than dimers. Furthermore our group in collaboration with Dr E. Zaitseva (University of Freiburg) observed ion conducting pore/channels for all the peptides in this study in a variety of model membranes [unpublished results]. To form such pores, higher order structure formation is most likely due to a combination of hydrogen bonding and stacking interactions in addition to other non-

covalent interactions, which would correlate better with the models for TrcC and TrcA proposed by Munyuki *et al.* [4].

The variability of the structures of the different Trcs and analogues leads one to question whether the different conformations may dictate the specificity toward different pathogens. Moreover, as these cyclodecapeptides are co-produced, the question is whether combinations of different analogues with different conformations could complement each other's antimicrobial activity. This aspect of the activity and oligomerisation of selected peptide combinations will be addressed in Chapter 6.

5.4 References

1. Aranda, F. J. and de Kruijff, B. (1988) Interrelationships between tyrocidine and gramicidin A′ in their interaction with phospholipids in model membranes. Biochim. Biophys. Acta. 937, 195-203.
2. Goodall, M. C. (1970) Structural effects in the action of antibiotics on the ion permeability of lipid bilayers. I. Tyrocidine B. BBA-Biomembranes. **203**, 28-33.
3. Dubos, R. J. (1939) Studies on a bactericidal agent extracted from a soil *Bacillus*: I. Preparation of the agent. its activity *in vitro*. J. Exp. Med. **70**, 1-10
4. Munyuki, G., Jackson, G. E., Venter, G. A., Kövér, K. E., Szilágyi, L., Rautenbach, M., Spathelf, B. M., Bhattacharya, B. and van der Spoel, D. (2013) β-Sheet structures and dimer models of the two major tyrocidines, antimicrobial peptides from *Bacillus aneurinolyticus*. Biochemistry **52**, 7798-7806
5. Loll, P. J., Upton, E. C., Nahoum, V., Economou, N. J. and Cocklin, S. (2014) The high resolution structure of tyrocidine A reveals an amphipathic dimer. BBA-Biomembranes. **1838**, 1199-1207
6. Ruttenberg, M. A., King, T. P. and Craig, L. C. (1966) The chemistry of tyrocidine. VII. Studies on association behavior and implications regarding conformation. Biochemistry **5**, 2857-2864
7. Ruttenberg, M. A., King, T. P. and Craig, L. C. (1965) The use of the tyrocidines for the study of conformation and aggregation behaviour. J. Am. Chem. Soc. **87**, 4196-4198
8. Paradies, H. H. (1979) Aggregation of tyrocidine in aqueous solutions. Biochem. Biophys. Res. Commun. **88**, 810-817
9. Stern, A., Gibbons, W. A. and Craig, L. C. (1969) Effect of association on the nuclear magnetic resonance spectra of tyrocidine B. J. Am. Chem. Soc. **91**, 2794-2796
10. Williams Jr, R. C., Yphantis, D. A. and Craig, L. C. (1972) Noncovalent association of tyrocidine B. Biochemistry **11**, 70-77
11. Jelokhani-Niaraki, M., Prenner, E. J., Kay, C. M., McElhaney, R. N., Hodges, R. S. and Kondejewski, L. H. (2001) Conformation and other biophysical properties of cyclic antimicrobial peptides in aqueous solutions. J. Pept. Sci. **58**, 293-306

12. Jelokhani-Niaraki, M., Prenner, E. J., Kay, C. M., McElhaney, R. N. and Hodges, R. S. (2002) Conformation and interaction of the cyclic cationic antimicrobial peptides in lipid bilayers. J. Pept. Sci. **60**, 23-36

13. Laiken, S., Printz, M. and Craig, L. (1971) Studies on the mode of self-assembly of tyrocidine B. Biochem. Biophys. Res. Commun. **43**, 595-600

14. Laiken, S., Printz, M. and Craig, L. C. (1969) Circular dichroism of the tyrocidines and gramicidin S-A. J. Biol. Chem. **244**, 4454-4457

15. Eyeghe-Bickong, H. (2011) Role of surfactin from *Bacillus subtilis* in protection against antimicrobial peptides produced by *Bacillus* species. Stellenbosch University. **Phd. Thesis** http://hdl.handle.net/10019.1/6773

16. Spathelf, B. M. (2010) Qualatative structure-activity relationships of the major tyrocidines, cyclic decapeptides from *Bacillus aneurinolyticus.* Stellenbosch University, Department of Biochemistry, Stellenbosch, South Africa. **PhD. Thesis** http://hdl.handle.net/10019.1/4001

17. Tang. X.J., Thibault. P., Boyd. R.K. (1992) Characterization of the tyrocidine and gramicidin fractions of the tyrothricin complex from *Bacillus brevis* using liquid chromatography and mass spectrometry. Int. J. Mass Spectrom. Ion Processes. **122**, 153-179

18. Vosloo, J. A., Stander, M. A., Leussa, A. N., Spathelf, B. M. and Rautenbach, M. (2013) Manipulation of the tyrothricin production profile of *Bacillus aneurinolyticus*. Microbiology **159**, 2200-2211

19. Jelokhani-Niaraki, M. (2009) Effect of ring size on conformation and biological activity of cyclic cationic antimicrobial peptides. J. Med. Chem. **52**, 2090

20. Leussa, A. N. and Rautenbach, M. (2014) Detailed SAR and PCA of the tyrocidines and analogues towards leucocin A-Sensitive and leucocin A-Resistant *Listeria monocytogenes*. Chem. Biol. Drug Des. **84**, 543-557

21. Spathelf, B. M. and Rautenbach, M. (2009) Anti-listerial activity and structure-activity relationships of the six major tyrocidines, cyclic decapeptides from *Bacillus aneurinolyticus*. Bioorg. Med. Chem. **17**, 5541-5548

22. Troskie, A. M., de Beer, A., Vosloo, J. A., Jacobs, K. and Rautenbach, M. (2014) Inhibition of agronomically relevant fungal phytopathogens by tyrocidines, cyclic antimicrobial peptides isolated from *Bacillus aneurinolyticus*. Microbiology. **160**, 2089-20101

23. Rautenbach, M., Vlok, N. M., Stander, M. and Hoppe, H. C. (2007) Inhibition of malaria parasite blood stages by tyrocidines, membrane-active cyclic peptide antibiotics from *Bacillus brevis*. Biochim. Biophys. Acta. **1768**, 1488-1497

24. Leussa, N. A. (2014) Characterisation of small cyclic peptides with antilisterial and antimalarial activity. Stellenbosch University, Department of Biochemistry, Stellenbosch, South Africa. **PhD. Thesis** http://hdl.handle.net/10019.1/86161

25. Gibbons, W. A., Beyer, C. F., Dadok, J., Sprecher, R. F. and Wyssbrod, H. R. (1975) Studies of individual amino acid residues of the decapeptide tyrocidine A by proton double-resonance difference spectroscopy in the correlation mode. Biochemistry **14**, 420-429

26. Kuo, M. and Gibbons, W. A. (1979) Total assignments, including four aromatic residues, and sequence confirmation of the decapeptide tyrocidine A using difference double resonance. qualitative nuclear overhauser effect criteria for beta turn and antiparallel beta-pleated sheet conformations. J. Biol. Chem. **254**, 6278-6287

27. Kuo, M. and Gibbons, W. A. (1979) Determination of individual side-chain conformations, tertiary conformations, and molecular topography of tyrocidine A from scalar coupling constants and chemical shifts. Biochemistry. **18**, 5855-5867

28. Kuo, M. and Gibbons, W. (1980) Nuclear overhauser effect and cross-relaxation rate determinations of dihedral and transannular interproton distances in the decapeptide tyrocidine A. Biophys. J. **32**, 807-836

29. Yount, N. Y. and Yeaman, M. R. (2005) Immunocontinuum: Perspectives in antimicrobial peptide mechanisms of action and resistance. Protein Peptide Lett. **12**, 49-67

30. Lakey, J. H. and Raggett, E. M. (1998) Measuring protein—protein interactions. Curr. Opin. Struct. Biol. **8**, 119-123

31. Greenfield, N. J. (2006) Using circular dichroism spectra to estimate protein secondary structure. Nat. Protoc. **1**, 2876-2890

32. Kelly, S. M., Jess, T. J. and Price, N. C. (2005) How to study proteins by circular dichroism. BBA-Proteins and Proteomics. **1751**, 119-139

33. Lakowicz, J. R. (2013) Principles of fluorescence spectroscopy. Springer Science & Business Media

34. Hilton, G. R. and Benesch, J. L. (2012) Two decades of studying non-covalent biomolecular assemblies by means of electrospray ionization mass spectrometry. J. R. Soc. Interface. **9**, 801-816

35. Liu, J. and Konermann, L. (2011) Protein–protein binding affinities in solution determined by electrospray mass spectrometry. J. Am. Soc. Mass Spectrom. **22**, 408-417

36. Biemann, K. (1988) Contributions of mass spectrometry to peptide and protein structure. Biol. Mass Spectrom. **16**, 99-111

37. Chattopadhyay, A. and Raghuraman, H. (2004) Application of fluorescence spectroscopy to membrane protein structure and dynamics. Curr. Sci. **87**, 175-180

38. Bich, C., Baer, S., Jecklin, M. C. and Zenobi, R. (2010) Probing the hydrophobic effect of noncovalent complexes by mass spectrometry. J. Am. Soc. Mass Spectrom. **21**, 286-289

39. Daniel, J. M., Friess, S. D., Rajagopalan, S., Wendt, S. and Zenobi, R. (2002) Quantitative determination of noncovalent binding interactions using soft ionization mass spectrometry. Int. J. Mass Spectrom. **216**, 1-27

40. Mathur, S., Badertscher, M., Scott, M. and Zenobi, R. (2007) Critical evaluation of mass spectrometric measurement of dissociation constants: Accuracy and cross-validation against surface plasmon resonance and circular dichroism for the calmodulin–melittin system. Phys. Chem. Chem. Phys. **9**, 6187-6198

41. Robinson, C. V., Chung, E. W., Kragelund, B. B., Knudsen, J., Aplin, R. T., Poulsen, F. M. and Dobson, C. M. (1996) Probing the nature of noncovalent interactions by mass

spectrometry. A study of protein-CoA ligand binding and assembly. J. Am. Chem. Soc. **118**, 8646-8653

42. Bent, D. and Hayon, E. (1975) Excited state chemistry of aromatic amino acids and related peptides. III. Tryptophan. J. Am. Chem. Soc. **97**, 2612-2619

43. Teale, F. W. and Weber, G. (1957) Ultraviolet fluorescence of the aromatic amino acids. Biochem. J. **65**, 476-482

44. Bent, D. and Hayon, E. (1975) Excited state chemistry of aromatic amino acids and related peptides. I. tyrosine. J. Am. Chem. Soc. **97**, 2599-2606

45. Bent, D. and Hayon, E. (1975) Excited state chemistry of aromatic amino acids and related peptides. II. Phenylalanine. J. Am. Chem. Soc. **97**, 2606-2612

46. Creed, D. (1984) The photophysics and photochemistry of the near-uv absorbing amino acids–I. tryptophan and its simple derivatives. Photochem. Photobiol. **39**, 537-562

47. Andrews, D. L. (1989) A unified theory of radiative and radiationless molecular energy transfer. Chem. Phys. **135**, 195-201

48. Hotchkiss, R. D. and Dubos, R. J. (1941) The isolation of bactericidal substances from cultures of *Bacillus brevis*. J. Biol. Chem. **141**, 155-162

49. Kyte, J. and Doolittle, R. F. (1982) A simple method for displaying the hydropathic character of a protein. J. Mol. Biol. **157**, 105-132

50. Jelokhani-Niaraki, M., Hodges, R. S., Meissner, J. E., Hassenstein, U. E. and Wheaton, L. (2008) Interaction of gramicidin S and its aromatic amino acid analogue with phospholipid membranes. Biophys. J. **95**, 3306-3321

51. Lee, D., Powers, J., Pflegerl, K., Vasil, M., Hancock, R. and Hodges, R. (2004) Effects of single D-amino acid substitutions on disruption of β-sheet structure and hydrophobicity in cyclic 14-residue antimicrobial peptide analogues related to gramicidin S. J. Pept. Res. **63**, 69-84

52. Krittanai, C. and Johnson, W. C. (1997) Correcting the circular dichroism spectra of peptides for contributions of absorbing side chains. Anal. Biochem. **253**, 57-64

53. Kondejewski, L. H., Farmer, S. W., Wishart, D. S., Kay, C. M., Hancock, R. E. W. and Hodges, R. S. (1996) Modulation of structure and antibacterial and hemolytic activity by ring size in cyclic gramicidin S analogs. J. Biol. Chem. **271**, 25261

54. Woody, R. W. (1974) Studies of theoretical circular dichroism of polypeptides: Contributions of β-turns. In Peptides, Polypeptides and Proteins, Blout, E. R.; Bovey, F. A.; Goodman, M. and Lotan, N. John Wiley & Sons 338-350

55. Kondejewski, L. H., Jelokhani-Niaraki, M., Farmer, S. W., Lix, B., Kay, C. M., Sykes, B. D., Hancock, R. E. and Hodges, R. S. (1999) Dissociation of antimicrobial and hemolytic activities in cyclic peptide diastereomers by systematic alterations in amphipathicity. J. Biol. Chem. **274**, 13181-13192

56. Jelokhani-Niaraki, M., Kondejewski, L. H., Farmer, S., Hancock, R. E. W., Kay, C. M. and Hodges, R. S. (2000) Diastereoisomeric analogues of gramicidin S: Structure, biological activity and interaction with lipid bilayers. Biochem. J. **349**, 747-755

57. Chen, Y., Liu, B. and Barkley, M. D. (1995) Trifluoroethanol quenches indole fluorescence by excited-state proton transfer. J. Am. Chem. Soc. **117**, 5608-5609

58. Rajan, R. and Balaram, P. (1996) A model for the interaction of trifluoroethanol with peptides and proteins. Int. J. Pept. Protein Res. **48**, 328-336

59. Kondejewski, L. H., Lee, D. L., Jelokhani-Niaraki, M., Farmer, S. W., Hancock, R. E. and Hodges, R. S. (2002) Optimization of microbial specificity in cyclic peptides by modulation of hydrophobicity within a defined structural framework. J. Biol. Chem. **277**, 67-74

60. Sreerama, N., Manning, M. C., Powers, M. E., Zhang, J., Goldenberg, D. P. and Woody, R. W. (1999) Tyrosine, phenylalanine, and disulfide contributions to the circular dichroism of proteins: Circular dichroism spectra of wild-type and mutant bovine pancreatic trypsin inhibitor. Biochemistry **38**, 10814-10822

61. Manning, M. C., Illangasekare, M. and Woody, R. W. (1988) Circular dichroism studies of distorted α-helices, twisted β-sheets, and β-turns. Biophys. Chem. **31**, 77-86

62. Chen, Y. and Barkley, M. D. (1998) Toward understanding tryptophan fluorescence in proteins. Biochemistry. **37**, 9976-9982

63. Zasloff, M. (2002) Antimicrobial peptides of multicellular organisms. Nature **415**, 389-395

64. Andreu, D. and Rivas, L. (1998) Animal antimicrobial peptides: An overview. Biopolymers. **47**, 415-433.

65. Hancock, R. E. and Sahl, H. (2006) Antimicrobial and host-defense peptides as new anti-infective therapeutic strategies. Nat. Biotechnol. **24**, 1551-1557

66. van't Hof, W., Veerman, E. C., Helmerhorst, E. J. and Amerongen, A. V. (2001) Antimicrobial peptides: Properties and applicability. Biol. Chem. **382**, 597-619

67. Hwang, P. M. and Vogel, H. J. (1998) Structure-function relationships of antimicrobial peptides. Biochem. cell Biol. **76**, 235-246

68. Bowman, S. M. and Free, S. J. (2006) The structure and synthesis of the fungal cell wall. Bioessays. **28**, 799-808

69. Troskie, A. M. (2014) Tyrocidines, cyclic decapeptides produced by soil bacilli, as potent inhibitors of fungal pathogens. Stellenbosch University, Department of Biochemistry, Stellenbosch, South Africa. **PhD. Thesis** http://hdl.handle.net/10019.1/86162

70. Kohl, M., Essenpreis, M., Böcker, D. and Cope, M. (1994) Influence of glucose concentration on light scattering in tissue-simulating phantoms. Opt. Lett. **19**, 2170-2172

Chapter 6
Oligomerisation-activity relationships of the single and combinations of the six major cyclodecapeptides purified from *Bacillus aneurinolyticus* cultures

6.1 Introduction

Supplementation of the *Bacillus aneurinolyticus* producer organism's growth media with defined ratios of two aromatic amino acids, Trp and Phe, resulted in the increased production of defined subsets of different tyrocidines and their analogues (Trcs) as determined by variation of their aromatic amino acid content [1]. Changes in the aromatic amino acid content of the Trcs results in the variable character and activity profiles of the different analogues [2-6]. The antimicrobial activity of the Trcs is proposed to be primarily the result of their interaction with the cell membrane [7] causing its permeabilization [8] and ultimately cell lysis [9]. This mode of action is probably associated with higher order structure formation in the membrane to form pores.

The Trcs have been shown to readily associate by non-covalent interaction to form larger aggregates which are attributed to a reduction in their antimicrobial activity [10-15], while association into amphipathic homo-dimeric structures is proposed to be the active units responsible for membrane interaction [16,17]. Therefore an interplay may exist between the non-covalent self-association of the cyclodecapeptides and their antimicrobial activity against certain targets. Considering the variable degree of higher order structure formation observed by the different Trcs (Chapter 5), the influence of non-covalent association by different analogues and combinations of peptides on their antimicrobial activity was questioned.

In this chapter the ability of the different Trcs and analogues to oligomerize into dimers, as well as higher order structures (Chapter 5), is related to their antimicrobial activity. The six different cyclodecapeptides and five peptide combinations were tested against two representative target organisms namely, the Gram-positive bacteria *Bacillus subtilis* 168 (non-peptide producer) and the ubiquitous fungal pathogen *Aspergillus fumigatus* and related to the oligomerisation parameters of the single peptides and peptide pairs.

6.2 Materials and Methods

6.2.1 Materials and Reagents

Peptides and solvents were as describe in Chapter 5, ethanol (EtOH), tryptone soy broth (TSB), agar, and N,N-dimethylformamide (DMF) were obtained from Merck (Darmstadt, Germany). Gramicidin S (GS) was obtained from Sigma-Aldrich (Steinheim, Germany) and served as the positive control in all antimicrobial activity assays. Tween 20, potato dextrose agar (PDA) and potato dextrose broth (PDB) were from Fluka (Buchs, Switzerland). Sterile polystyrene 96-well flat bottom microtiter plates were from either Greiner bio-one (Frickenhausen, Germany) or Corning (Corning, NY, USA). Petri dishes were from Lasec (Cape Town, South Africa). Falcon® tubes were from Becton Dickson and Company (Franklin Lakes, NJ, USA). Analytical grade water was prepared by filtering water from a reverse osmosis plant through a Millipore-Q® water purification system (Milford, USA).

Aspergillus fumigatus ATCC 204305 was from the American Type Culture Collection (Manassas, VA, USA). *Bacillus subtilis* 168 obtained from the *Bacillus* Genetic Stock Centre (Ohio State University, OH, USA).

6.2.2 Detection of oligomerisation with ESMS

Dried analytical aliquots of purified tyrocidine peptides were dissolved in 50% (*v/v*) DMF in water to a concentration of 2.00 mM. Single peptides as well as five selected co-produced peptide pairs were prepared to a final concentration of 0.200 mM and final solvent concentration of 2.5% (*v/v*) high purity DMF. Peptide pairs consisted of 1:1 ratio of: TrcA and TrcB; TrcB and TrcC; TrcC and TpcC; TpcC and TpcA, as well as TrcA and PhcA. These samples were allowed to stand at room temperature overnight prior to the type of predominant hetero-oligomers formed within the above formulations being determined by means of high resolution electrospray mass spectrometry (ESMS) using a Waters Q-TOF Synapt G2 mass spectrometer with a Z-spray electrospray ionisation source as described in Chapter 5.

6.2.3 Preparation of peptides for antimicrobial activity assays

Analytically weighed aliquots of the dried peptides were dissolved in 50% (*v/v*) DMF in water. These were subsequently diluted to a concentration of 1.00 mM at a solvent concentration of 10% (*v/v*) DMF in sterilised water. While maintaining the solvent concentration, the respective peptides were prepared in a doubling dilution series over eight dilution steps. The concentration of the single Trc peptides was varied between 500 to 40 µM, while preparations of the five previously mentioned peptide pairs were prepared at 3:1 and 1:1 ratios of the former dilution series for both peptides. Preparation of the GS control peptide was done in 15% (*v/v*) EtOH in a doubling dilution series with concertation varied between 440 to 30 µM. These were subsequently diluted 10x to a final solvent concentration of 1% (*v/v*) DMF in the growth media used in the respective antimicrobial activity assays.

6.2.4 Antifungal activity assays

Using standard sterile practices, spores of the fungi *A. fumigatus* ATCC 204305 were obtained from freezer stocks and cultured using normal sterile techniques on PDA plates for three weeks. Subsequently 7 mL of 0.01% Tween (20 µL of Tween in 200 mL analytical grade water and autoclaved) was added to the plates, the spores lightly loosened using a glass rod and hydrated overnight at 4 °C. The spores were subsequently counted using a haemocytometer and diluted with sterile water to a concentration of 50 spores/µL.

A variation of a microtiter broth dilution method, as described by Troskie *et al.* [18], was used to test the antimicrobial activity of the respective peptides toward *A. fumigatus*. A volume of 50 µL of PDB was added to all the wells of a sterile microtiter plate. The top four wells of the first column received 40 µL of sterilized water, while all the rest of the wells received 40 µL of the mentioned spore suspension. The wells of the first column received 10 µL of 10% (*v/v*) DMF, thus the first column served as sterility and growth controls respectively. All the rest of the wells received 10 µL of one of the respective peptides prepared as previously described. The single Trc peptides and combinations of two peptides were applied in duplicate (*n=2*) in each dose response assay, while a single column was reserved for application of the GS control peptide.

The microtiter plates were then covered and incubated for a period of 48 hours at 25 °C, following which the light dispersion was measured spectrophotometrically at 595 nm using a

BioRad™ microtiter plate reader. Using these data the percentage growth inhibition was plotted and used to derive the related activity parameters.

6.2.5 Antibacterial activity assays

Single colonies of the Gram-positive bacteria *B. subtilis* 168 were obtained from freezer stocks by culturing using normal sterile techniques on tryptone soy agar (TSA) plates (3.0% (*w/v*) TSB and 1.5% (*w/v*) agar in analytical grade water). Single colonies were selected and incubated while shaking at 220 RPM for 16 hours at 37 °C in Falcon® tubes containing 20 mL TSB (3.0% (*w/v*) TSB in analytical grade water; pH 7.0) medium to an optical density (OD) of approximately 0.8 at 595 nm. These cells were subsequently sub-cultured in TSB and grown to an OD of 0.6 at 595 nm.

A variation of the previously described microtiter broth dilution method [19,20] as used to determine the activity of the mentioned peptides toward the Gram-positive bacteria. A pre-culture was diluted with TSB to an OD of 0.2 at 595 nm ($\pm 10^8$ CFU/mL). A volume of 90 µL of the diluted culture was added to all of the wells of the microtiter plate except for the top four wells first column which received 90 µL of TSB. The peptide and solvent controls were as previously described. These microtiter plates were then covered and incubated for a period of 16 hours at 37 °C, following which the light dispersion was measured spectrophotometrically at 595 nm using a Bio Rad™ microtiter plate reader. The percentage growth inhibition and related activity parameters were determined from these data.

6.2.6 Data analysis

The percentage growth inhibition of the respective peptides in all antimicrobial activity assays was determined relative to the mean of the growth control, as previously described by Rautenbach *et al.* [21], using the following equation:

$$\% \text{ growth inhibition} = 100 - \frac{100 \times (A_{595} \text{ of well} - \text{Mean } A_{595} \text{ of background})}{(\text{Mean } A_{595} \text{ of growth control} - \text{Mean } A_{595} \text{ of background})}$$

GraphPad Prism® 4.03 (GraphPad Software, San Diego, USA) was used to plot all graphs as well as perform all statistical analysis, except for those obtained by ESMS analysis. The dose response curves generated where fitted by non-linear regression to sigmoidal curves with a

slope set at <7 [21]. Antimicrobial activity parameters determined from these plots included: IC_{50} (concentration causing 50% growth inhibition) and IC_{max} (calculated concentration causing 100% growth inhibition). IC_{max} is directly related to the minimum inhibitory concentration (MIC, lowest concentration used where no growth is visually observed), but was calculated from the dose response curve as described by Du Toit and Rautenbach [20].

Using the determined IC_{50} activity parameters possible interaction by antagonism, synergism or sum of activities within the five peptide pairs was evaluated by calculation of fractional inhibition (FIC) and FIC index (FICI) in each assay performed using the following equations [22].

FIC (A) = IC_{max} (peptide [A] in A+B mixture)/ IC_{max} (peptide A alone)

FIC (B) = IC_{max} (peptide [B] in A+B mixture)/ IC_{max} (peptide B alone)

with FIC index = FIC (A) + FIC (B)

The FIC index a value of one indicated a sum of activities and no interaction between the peptide pair. FIC index >1 indicating antagonistic activity while FIC index <1 delineated synergistic interaction between peptides A and B [22].

The data obtained by means of ESMS was analysed using MassLynx V4.1 (Waters, Miliford, USA) to determine the proportion of the different types of oligomers formed. Set to auto-peak width determination the MaxEnt 3 algorithm was used to determine the oligomers between a range of 300 to 10 000 amu containing a maximum of 10 charges and 50 iterations. From these data the percentage of the different oligomers formed by each of the respective peptides was determined using the ion signal of each oligomer in relation to the total ion signal intensity of all the different oligomers detected in each of the respective spectra.

6.3 Results

6.3.1 Formation of homo- and hetero-oligomers by the cyclodecapeptides

The Trcs have been shown to readily oligomerize in dimeric structures [16,17] as well as larger oligomers [10-15]. Analysis of the types of oligomeric species formed by ESMS showed that the Trcs tended to dimerize. The more hydrophobic Trcs showed a tendency to

form larger oligomers, where up to pentamers where detected for TrcA (refer to Chapter 5). In the more polar analogues such as TrcC, decreased oligomerisation was observed together with an increase in the monomeric peptide species.

Analysis of the oligomerization of peptide mixtures, however, revealed a change in oligomerisation trend. Irrespective of the hydrophobicity of the two peptides in the mixture, dimeric oligomers were predominantly formed. The latter is exemplified by comparison of the oligomers formed by TrcA and PhcA relative to those of TpcC and TrcC; the most and least hydrophobic peptide pairs analysed respectively (Fig. 6.1 A, B). Comparison of the composition of oligomeric structures revealed an increased contribution of dimers while trimers where generally the largest oligomers detected in any appreciable amount. Moreover, comparison of the signal intensities reveals a lower amount of the monomers of the more hydrophilic analogue in the peptide pair. Concomitantly, a reduction in homodimers of the more hydrophilic peptide was observed, while the highest signal intensity was detected for the heterodimer (Fig. 6.1, 6.2 B, C).

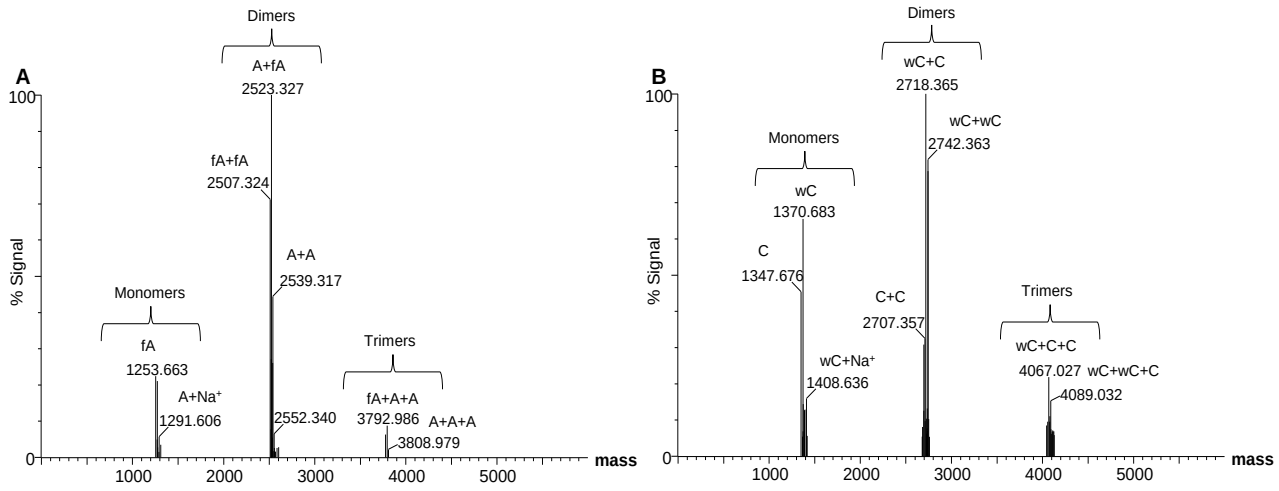

Figure 6.1 ESMS mass spectra generated with the maxEnt algorithm depicting the difference in oligomerisation between **A** the more hydrophobic peptide pair TrcA (A) and PhcA (fA) relative to **B** the more polar peptide pair TpcC (wC) and TrcC (C). Irrespective of the peptide combination, the dimers were the predominant peptide species detected while trimers where the largest oligomeric species detected in any appreciable amounts.

Comparison of the oligomeric structures formed by single peptides (Fig. 6.2 A) relative to those formed by the peptide pairs (Fig. 6.2 B) revealed the largest shift in the oligomerisation pattern by the hydrophilic C analogues (TrcC and TpcC) toward mixed heterodimer formation (Fig. 6.2 C). Similar dimerization of TrcA and PhcA was observed for the single peptides

(Fig. 6.2 A) as well as in their mixtures (Fig. 6.2 B), where heterodimers were the predominant isoform (Fig. 6.2 C). Peptide mixtures containing TrcB still predominantly formed dimeric oligomers, but the predominant isoform were homodimers of the more hydrophobic peptide in the peptide pair (Fig. 6.2 C). This may elude to a conformation adopted by TrcB which makes it less amenable to heterodimer formation.

6.3.2 Variability in antimicrobial activity of different cyclodecapeptides

The antimicrobial activity of these selected analogues was then determined toward two representative target organisms namely, the Gram-positive bacteria *B. subtilis* and the ubiquitous fungal pathogen *A. fumigatus* (Table 6.1). Although the activity parameters were within a narrow concentration range, the nature of our assays and number of repeats allowed statistical comparisons. Statistical analysis of the determined activity parameters showed that the activity of most of the peptides were indeed significantly different from each other to allow activity-structure correlations (Table 6.2). The activity parameters were therefore correlated with their observed oligomerisation (ESMS study), structure (circular dichroism study) and hydrophobicity (retention time during C_{18} UPLC analysis).

Toward the fungus *A. fumigatus* nearly equivalent antifungal activity was observed for TrcA and TrcB analogues followed by TpcC and PhcA, while the TrcC and TpcA analogues had the lowest activity (Table 6.1). When considering the antibacterial activity of the different cyclodecapeptide analogues, the TrcA analogue was again observed to display the most potent activity. In contrast to what was observed toward the representative fungal pathogen *A. fumigatus,* TpcC was now the second most active analogue, the TrcB analogue now had reduced activity and TpcA the lowest antibacterial activity (Table 6.1).

Variability was thus observed in antimicrobial activity of not only the different cyclodecapeptides, but also toward the different representative target organisms. These differences were put into context by relating the differences in antimicrobial activity to the various properties of the different peptides (Fig. 6.3). In Chapter 5 it was shown that the more hydrophobic A analogues containing Phe3, Phe4 exhibited increased dimerization and higher order oligomers, while the more hydrophilic C analogues were less inclined to dimerization and formation of higher order oligomers.

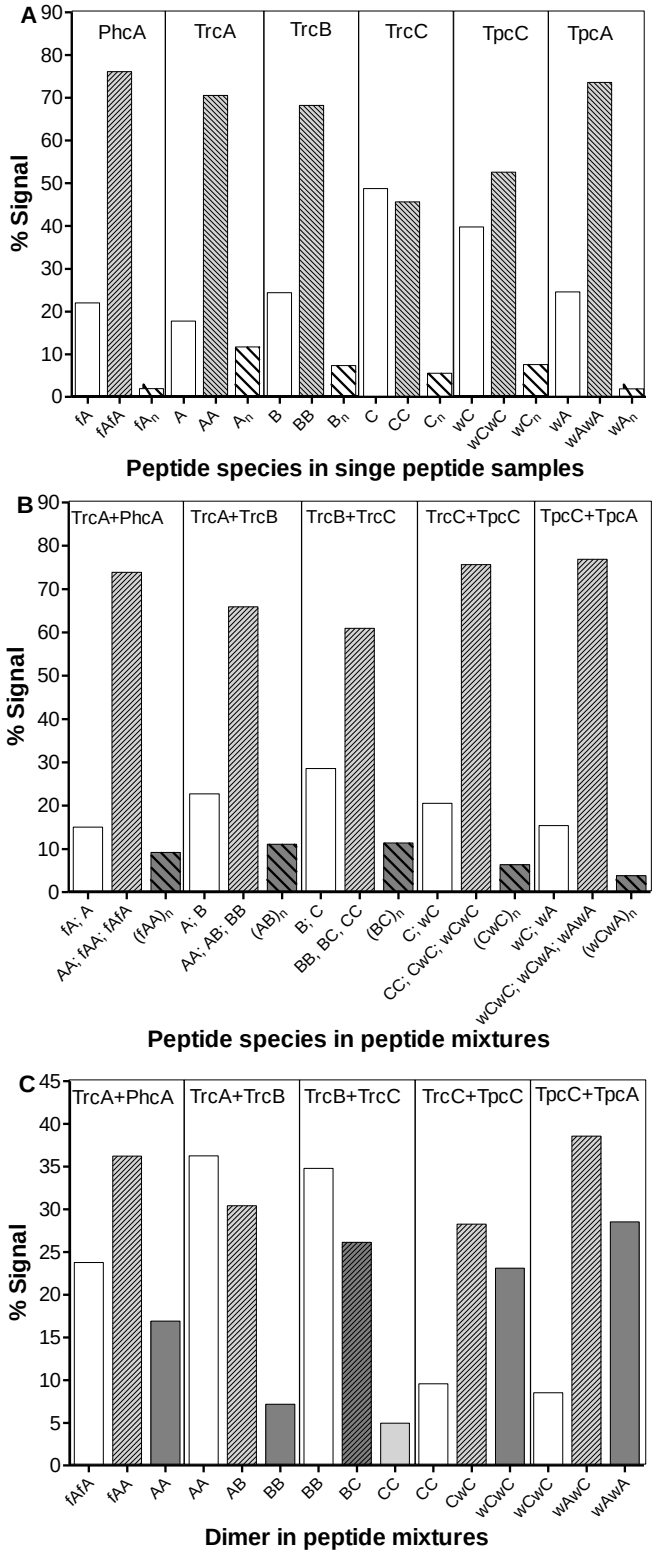

Figure 6.2 Comparison of the proportion of oligomeric structures formed by the respective cyclodecapeptides determined with ESMS of: **A** single peptides, **B** 1:1 peptide mixtures, and **C** composition of the dimeric species detected in the peptide mixtures in **B** depicting the proportions of homo- and heterodimers. The proportion contribution of the detected monomer (X), dimer (XX) or oligomers $(X)_n$ is expressed as a percentage relative to the total ion signal for all the detected peptide species. Abbreviations used: TrcA, A; TrcB, B; TrcC, C; TpcA, wA and TpcC, wC.

Table 6.1 Activity parameters of the purified peptides toward the representative fungi *A. fumigatus* and Gram-positive bacteria *B. subtilis*.

Peptide	IC_{50} ± SEM (µM)	IC_{max} ± SEM (µM)
Aspergillus fumigatus		
TrcA (*n=16*)	2.58±0.23	3.56±0.29
TrcB (*n=16*)	2.54±0.20	3.84±0.26
TrcC (*n=16*)	4.21±0.08	5.87±0.13
TpcA (*n=8*)	3.48±0.21	5.68±0.18
TpcC (*n=16*)	3.23±0.22	5.09±0.31
PhcA (*n=8*)	3.89±0.29	5.33±0.37
Bacillus subtilis		
TrcA (*n=16*)	4.47±0.28	8.13±0.75
TrcB (*n=16*)	9.54±0.46	13.84±0.69
TrcC (*n=16*)	8.04±0.46	12.13±0.72
TpcA (*n=8*)	10.26±0.64	28.06±1.58
TpcC (*n=16*)	5.67±0.31	10.85±0.64
PhcA (*n=8*)	8.50±1.2	13.79±0.76

SEM, standard error of the mean.

Table 6.2 Summary of the P-values from statistical analysis of the activity parameters in Table 6.1, using the Newman-Keuls multiple comparison test (One way Anova). In the table "ns" denotes a P-value > 0.05 and the top and bottom values to the maximum P-value for *A. fumigatus* and for *B. subtilis* as target organisms, respectively.

		Tpc A	**Trc A**	**Trc B**	**Trc C**	**TpcC**
Phc A	IC_{max}	ns 0.001	0.001 0.001	0.01 ns	ns ns	ns ns
	IC_{50}	ns ns	0.001 0.001	0.001 ns	ns ns	ns 0.01
Tpc A	IC_{max}		0.05 0.001	0.001 0.001	ns 0.001	ns 0.001
	IC_{50}		0.001 0.001	0.05 ns	ns 0.05	ns 0.001
Trc A	IC_{max}			ns 0.001	0.001 0.001	0.001 0.05
	IC_{50}			ns 0.001	0.001 0.001	0.05 ns
Trc B	IC_{max}				0.001 ns	0.001 0.05
	IC_{50}				0.001 ns	0.05 0.001
TrcC	IC_{max}					ns ns
	IC_{50}					0.01 0.001

A general trend of increased antifungal activity was observed with increased oligomerisation of the analogues containing Trp^3, Trp^4/Phe^4 (Wx) (Fig. 6.3 A).

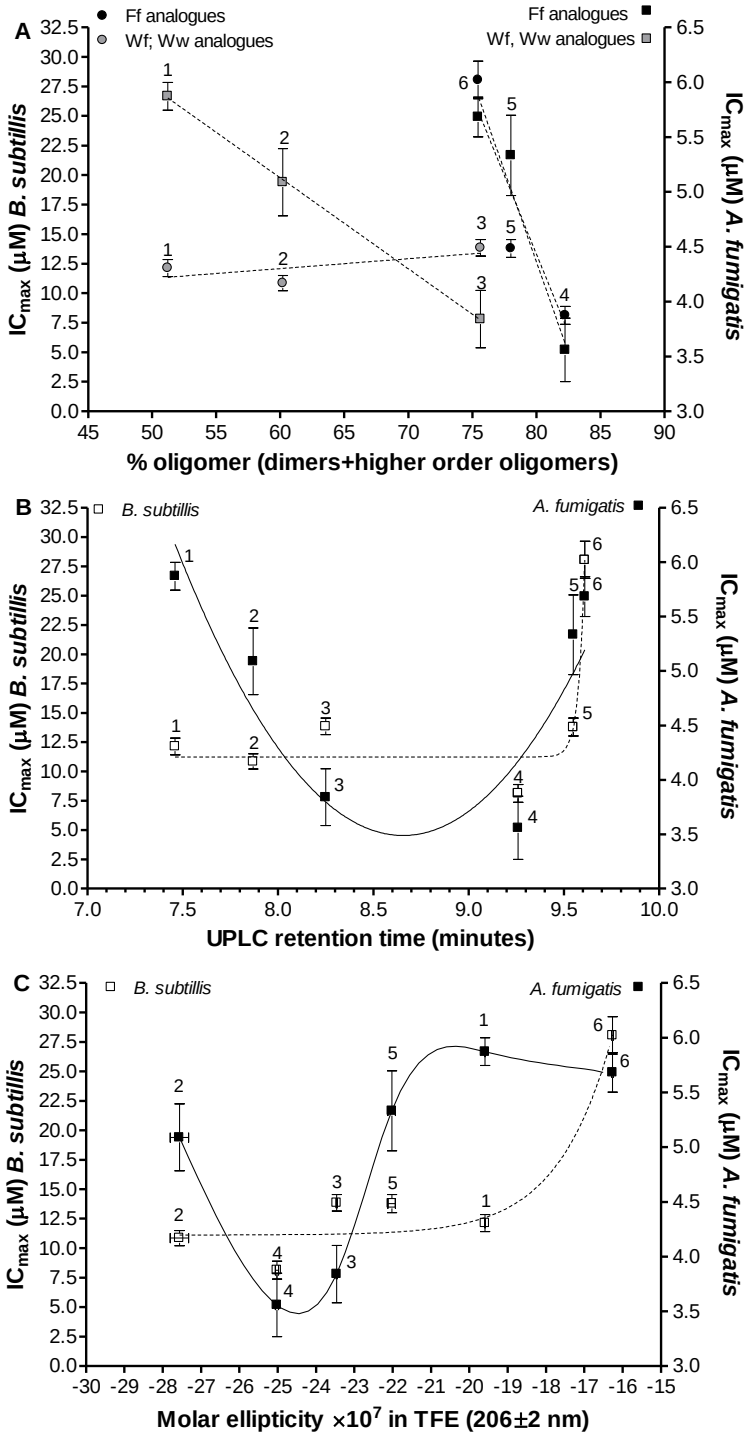

Figure 6.3 Relation of the antimicrobial activity of the different Trc analogues to variation in their character derived from changes in their aromatic amino acid content. Antimicrobial activity relative to: **A** the proportion of different oligomeric species formed in an aqueous environment, **B** UPLC retention time as an indication of hydrophobicity, **C** ellipticity at 206 nm in TFE emulating higher order structure formation in a membrane mimicking environment. Trc analogues numbered as follows on the here graphs: 1 TrcC, 2 TpcC; 3 TrcB; 4 TrcA; 5 PhcA; 6 TpcA. (Biophysical data were as reported in Chapter 5).

High antifungal activity was only observed for one of the A analogues (Ff), namely TrcA. Despite increased proportions of dimerized species, antifungal activity of the other two Ff analogues decreased to that observed for the more hydrophilic Wx analogues which contained decreased proportions of the dimeric species. This would indicate that dimerization alone is not the only determining factor for increased antifungal activity. The relation of the antifungal activity to hydrophobicity indicates increased activity by analogues of intermediate hydrophobicity, namely TrcA and TrcB (Fig. 6.3 B). Moreover, from the circular dichroism studies reported in Chapter 5 the increased ellipticity intensity at 206 nm of these two analogues in trifluoroethanol (TFE) indicate the probable formation of ordered structures within membrane-like environments (Fig. 6.3 C). However, these consistent trends must be tested with a larger library to clarify if the antifungal activity towards *A. fumigatus* is determined by both oligomerisation into higher ordered structures, as well as an intermediate hydrophobicity to allow for optimal membrane or target interaction.

No overt trend of antibacterial activity with increased oligomerisation was observed for the C group (including TrcB) (Fig. 6.3 C). Furthermore, the A analogues showed a high tendency to form dimers while their activity was significantly different, in particular TpcA's activity was the lowest while TrcA the highest (Fig. 6.3 A), hence again no clear conclusion could be drawn on the role of dimerization. Correlating the antibacterial activity with hydrophobicity and ordered structure formation (Fig. 6.3 B and C) it is observed that despite minor variation of increased TrcA and reduced TrcB activity, no overt trend was observed for the Trcs, with only the least active peptide TpcA indicating a loss of activity with increase in hydrophobicity. Near equivalent antimicrobial activity was found by the C analogues and TrcB containing Trp^3, Trp^4/Phe^4 (Wx), as well as the A analogues containing Phe^3, Phe^4 (Ff) which produced variable amounts of oligomeric species. However, extensive aggregation and lack of ordered structure formation may be attributed the lack of antimicrobial activity of the TpcA analogue. This correlated with previous studies by Leussa and Rautenbach [2].

6.3.3 Activity of peptide mixtures

The antimicrobial activity of the single peptides was now established toward the two representative target organisms; five pairs of cyclodecapeptides which were co-produced under the same culturing conditions (Fig. 6.4; refer to Chapter 2 and 3 for more detail) were selected to determine if these peptides displayed any interaction with one another which may

influence their antimicrobial activity. TrcA and TrcB are the predominant co-produced analogues under non-supplemented growth conditions. The latter two peptides showed an increased tendency to form higher order structures, particularly dimers (Chapter 5). TrcC and TrcB are co-produced at intermediate concentration of Trp and Phe in the growth media, while also being the predominant Trcs found in the commercial Trc extract (Fig. 6.4, refer to Chapter 2 and 3). The latter two peptides have been reported to display increased antibacterial activity [4]. The peptide pairs: TpcC:TrcC and TrcA:PhcA, are produced at high Trp and high Phe concentrations, with the TpcC and TrcA the major species, respectively (Fig. 6.4). TpcC and TpcA represent the odd combination that are co-produced under a low Trp/Phe ratio. While five peptide pairs were selected for analysis in this study; it should be noted that there are numerous further possible co-produced peptide pairs such as tryptocidine B (TpcB):TpcC, TrcA:TrcC and TpcA:TrcA (refer to Chapter 2 and 3). In this current exploratory study, we did not consider mixtures with more than two peptides.

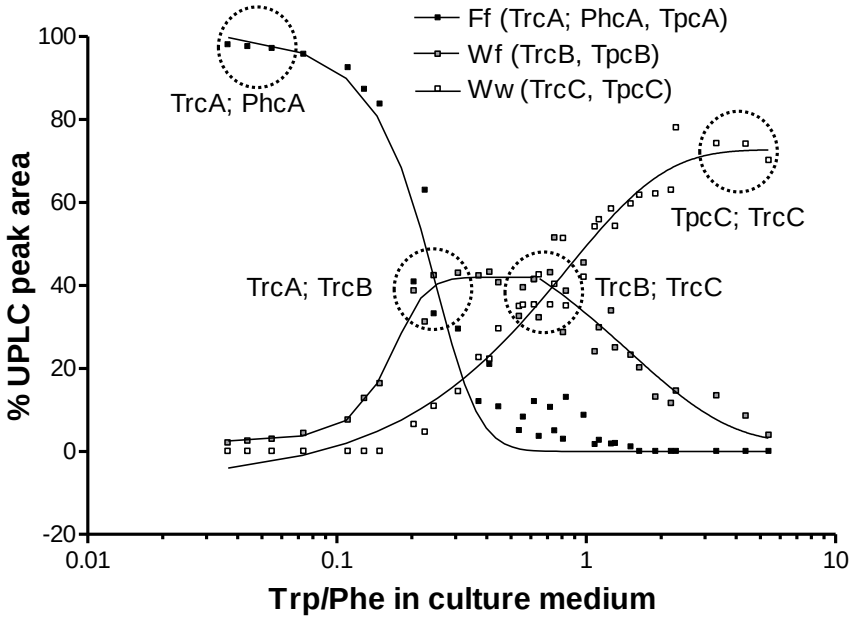

Figure 6.4 Depiction of the shift in the cyclodecapeptide production profile of *B. aneurinolyticus* at different concentration ratios of Phe and Trp. The contribution of each subset: Ff, Wf or Ww was calculated as a percentage of the sum of the total UPLC peak areas of the different peptides as determined by the identity of the variable aromatic amino acids dipeptide unit. The selected co-produced peptide pairs are indicated. (Cyclodecapeptide production data were as reported in Chapter 2, figure adapted from [1]).

Using the IC_{max} values obtained for the single peptides, as well as the respective peptide mixtures toward the two representative target organisms possible synergistic/antagonistic relationships were established between the peptide pairs using FIC-derived isobolograms. The

antimicrobial activity of the peptide pairs containing an A analogue (Phe^3, Phe^4) (Fig. 6.5) or C analogues (Trp^3, Trp^4) (Fig. 6.6) indicated difference in the sensitivity of two target organisms toward the different peptide pairs.

Peptide pairs containing TrcA displayed appreciable synergism toward *A. fumigatus*. The trend of synergistic activity in a peptide combination containing TrcA:TrcB was slightly weaker toward *A. fumigatus*, particularly at increased TrcB concentrations where an additive relationship was observed (Fig. 6.5 A). The synergistic response towards *A. fumigatus*, of PhcA and TrcA was improved, particularly at increased concentrations of PhcA, where an FIC index of 0.6 is observed (Fig. 6.5 C). The combination of TpcC with TpcA proved to weaken the activity towards this fungal target (Fig. 6.5 E). Toward *B. subtilis* as target an overt synergistic relationship of the TrcA:TrcB combination was observed with FIC index of 0.9 to 0.7 (Fig. 6.5 B), while a general additive relationship is observed by the other two A analogue peptide combinations toward *B. subtilis* (Fig. 6.5 D, F).

For the combinations with C analogues only a combination of TrcC and TrcB showed synergism toward *B. subtilis* with the FIC index of between 0.75 and 0.8 (Fig. 6.6 B), while this combination showed additive activity against *A. fumigates* (Fig. 6.6 A). Slight antagonistic activity is observed in peptide combinations containing TpcC toward both *A. fumigatus* and *B. subtilis* (Fig. 6.6 C, D, E).

Comparison of the FIC index calculated for the different peptide pair at 1:1 equimolar ratio showed that only the TrcC:TpcC pair to be slightly antagonistic towards both organisms while all the other pairs benefitted antibacterial activity (Fig. 6.7 A). Furthermore all the pairs containing a peptide with Trp^4 (C analogues) led to lower activity against the fungal target, while those with a Phe^4 (A analogues) in the peptide pair showed improved antibacterial and antifungal activity (Fig. 6.7 A). Correlation of the FIC index with the proportion of dimers formed by the different peptide pairs again displays a relationship of optimal antifungal activity by peptide pairs forming an intermediate proportion of ~65 to 75% dimers which corresponds with the peptide pairs of TrcA:TrcB and TrcA:PhcA (Fig. 6.7 B refer to data points 2 and 3). This result correlates with the proportion of dimers formed by the two single peptides TrcA and TrcB, which were most active against *A. fumigates*, as well as the proportion of dimeric species detected in the peptide combinations with these two analogues (refer to Fig. 6.3). The dimer populations of the TrcA:TrcB combination where

predominantly composed of homodimer species of TrcA and to a slightly lesser degree heterodimers of both the latter analogues. However, this trend will have to be tested with a larger library of mixed peptide pairs in future studies.

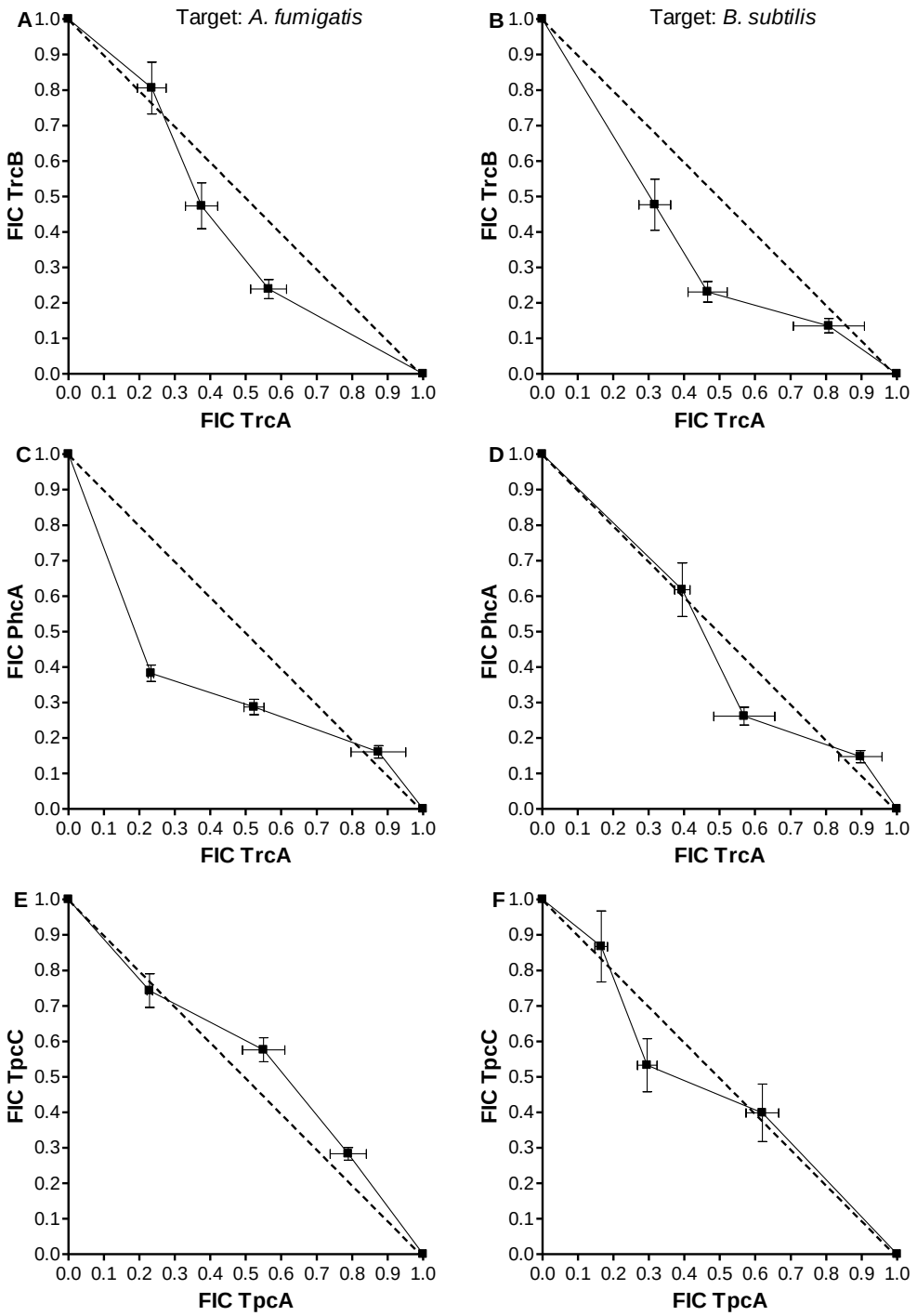

Figure 6.5 Isobolograms constructed using the FIC values of peptide pairs containing A analogues: TrcA and TrcB (**A** and **B**); TrcA and PhcA (**C** and **D**); TpcA and TpcC (**E** and **F**) toward *A. fumigatus* or *B. subtilis* respectively. Each data point depicts the mean of 8 replicates ± SEM. Note that the data points and solid line below the dotted line suggests synergism, on the dotted line additive activity and above the dotted line antagonistic activity.

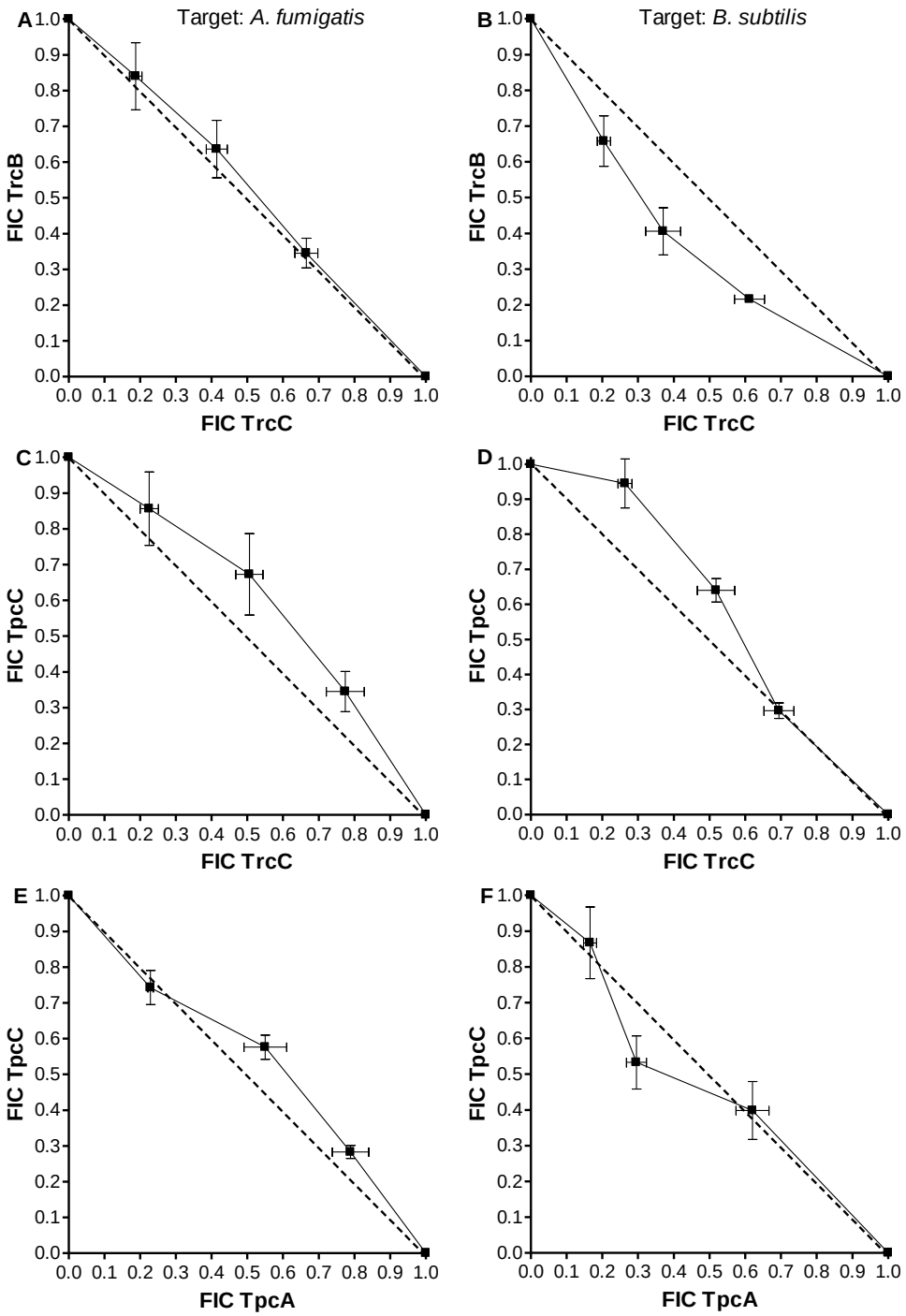

Figure 6.6 Isobolograms constructed using the FIC values of peptide pairs containing C analogues: TrcC and TrcB (**A** and **B**); TrcC and TpcC (**C** and **D**); TpcA and TpcC (**E** and **F**) toward *A. fumigatus* or *B. subtilis* respectively. Each data point depicts the mean of 8 replicates ± SEM. Note that the data points and solid line below the dotted line suggests synergism, on the dotted line additive activity and above the dotted line antagonistic activity.

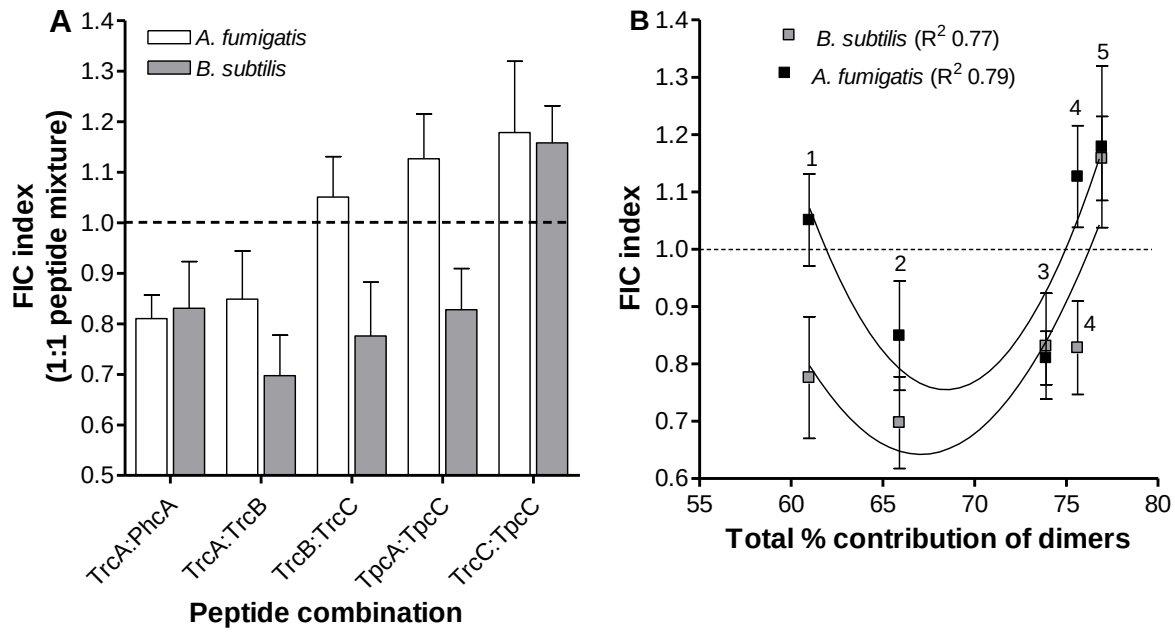

Figure 6.7 **A.** Comparison of the FIC index of the five peptide pairs at a 1:1 ratio toward the two representative target organisms. **B.** Correlation of the % dimer population formed by the respective peptide combinations with their observed antimicrobial activity toward *A. fumigatus* or *B. subtilis*. FIC index values of peptide pairs are indicated by increasing proportions of dimeric species: TrcC and TrcB (**1**); TrcA and TrcB (**2**); TrcA and PhcA (**3**); TpcA and TpcC (**4**); TrcC and TpcC (**5**).

It is possible that the antifungal activity was influenced to a larger degree by TrcA activity and would account for synergistic effect observed for this peptide combination. The proportion of heterodimer formed by PhcA together with TrcA was reduced relative the homodimers formed by PhcA, as a single peptide (refer to Fig. 6.2), possibly eluding to a slightly altered conformation adopted by PhcA together with TrcA in heterodimers which may have caused an increase in activity.

In contrast, all the peptide pairs and dimer populations displayed similar activity toward *B. subtilis*, barring the highest dimer population of the TrcC:TpcC pair (Fig. 6.7 B). The slightly antagonistic activity correlated with the formation of heterodimeric structures with TpcC, containing Trp^{7}, whose steric bulk could hinder optimal interaction and higher order structure formation.

A possible structure-activity relationship arising due to changes in the dipeptide unit may account for the differences observed in antimicrobial activity (Fig. 6.8). Synergistic activity toward *A. fumigatus* would seem to be dependent on peptide pairs containing Phe^{3} in one or both of the peptides (Fig. 6.8 A). This would include TrcA:PhcA and TrcA:TrcB

combination, while TpcA:TpcC is hindered by the reduction in activity of this odd combination containing Phe[3], Trp[4], and Trp[7].

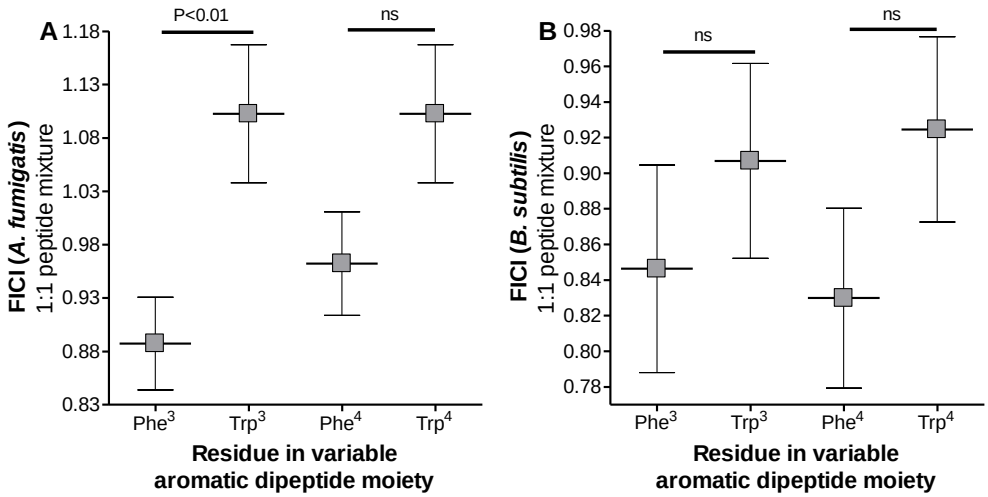

Figure 6.8 Correlation of the peptide structure at variable dipeptide unit and interaction. Occupancy of the variable dipeptide unit with FIC value obtained by the respective peptides at a 1:1 ratio toward **A** *A. fumigatus* or **B** *B. subtilis* respectively.

No statistical correlation of the FIC indexes was observed for activity toward *B. subtilis* indicating activity is independent of the aromatic residues in the dipeptide unit. (Fig. 6.8 B). Reduction of antibacterial activity probably occurs due to excessive aggregation, as observed for TpcA, which may be due to an altered conformation which enables greater oligomerisation into unordered structures (aggregates) (refer to Chapter 5). However, it has to be taken into account that the combined activity of peptide pairs was mostly additive. The data presented in Fig. 6.8A was therefore influenced by the overt synergism observed in combinations of TrcA:PhcA and TrcA:TrcB toward *A. fumigatus.*

6.4 Discussion

All the peptides in this study had a high tendency to dimerize, which was also found for peptide mixtures where high proportions of heterodimers were observed (Fig. 6.1, 6.2). However, the propensity to form heterodimers were highly dependent on the character of the aromatic dipeptide moiety (Fig. 6.2 C), indicating a role of this moiety in dimerization. The antibacterial activity of the Trcs is proposed to be reliant on their oligomerisation into active dimeric structures which allow for optimal interaction with membrane targets [16,17]. Variability in the antimicrobial activity of the Trcs has been reported by previous

investigators who found the more polar of the major tyrocidine analogues (Tyr^7) namely TrcB and TrcC to be most active toward the Gram-positive bacteria *L. monocytogenes* [4]. However, subsequent investigators have also reported increased activity of TrcA [2], as was observed in the present study. Variation in the antimicrobial activity of the Trcs has been reported by Leussa and Rautenbach [2] toward different bacterial strains and organisms. We observed that the antibacterial activity of the Trcs toward *B. subtilis* was largely independent of the variable characteristics of the different analogues (Table 6.1). Our results indicate that the variable aromatic dipeptide moiety and in general dimerization (Fig. 6.2) does not influence the activity against *B. subtilis* (Fig. 6.3). This implies that the antibacterial activity could be more dependent on the conserved gramicidin S pentapeptide (VOLfP) in these peptides.

Variation in antifungal activity has also been reported toward different fungal organisms [6]. Antifungal activity toward *A. fumigatus* depended on a fine interplay between the variable characteristics of the cyclodecapeptides where those of intermediate character, such as TrcA and TrcB, displayed the highest activity, while TrcC and TpcA showed the lowest activity (Table 6.1, Fig. 6.2, 6.3, refer to Chapter 5). Troskie *et al*. [6] reported near equivalent antifungal activity towards *Fusarium solani* and *Botrytis cinerea* in PDB growth medium for the analogues containing Tyr^7 which include TrcA, TrcB and TrcC, with the lowest antifungal activity for the TpcC analogue containing Trp^7. When the fungi were cultured in yeast supplemented tryptone soy broth (YTSB), Troskie *et al*. [6] reported a significant decrease in the antifungal activity of PhcA, while that of TpcC increased to within the range observed for the rest of the analogues with Tyr^7. As YTSB contains a higher salt content than PDB, this result indicates that aggregation could play a role in antifungal activity.

The higher antifungal activity of TrcA and TrcB may be also attributed to their optimal balance between hydrophobicity and target cell interaction which allowed for the increased formation of higher order pore like structures in the cell membrane after initial contact with the carbohydrate moieties in cell wall. Glucose caused little or no disruption of the ordered structures formed by TpcA the least active peptide, indicating that this interaction may be important for activity. The lower antimicrobial activity of TpcA may also be attributed to its hydrophobicity. Adopting a conformation similar to that proposed for TrcA by Loll *et al.* [17], the steric bulk of Trp^7 may hinder optimal higher order structure formation and would account for decreased higher oligomers despite increased dimerization being

observed. Alternatively, decreased antimicrobial activity may be attributed to tighter membrane binding of the indole group through hydrogen bonding to lipid carbonyl groups [27]. The peptide complex may be trapped in a conformation unable to optimally interact with other peptides to possibly form a pore/channel like structure and cause permeabilization of the cell membrane.

The different target cell properties influence the selectivity and mode of action of the Trcs, as has been observed for a broad range of antimicrobial peptides [28-32]. The Trcs are proposed to primarily execute their antimicrobial activity through their interaction with the cell membrane [7] and its subsequent permeabilization [8] and/or cell lysis [9]. However, Troskie [33] also illustrated the importance of the cell wall in the antifungal activity of the Trcs in addition to the cell membrane. The potent activity of the cyclodecapeptides activity toward *A. fumigatus* would indicate a strong relation to the target cell properties. It is highly likely that one of these properties is the hexose content of the fungal cell wall. The role of hexoses, such as glucose and it's analogues, in antimicrobial activity of the Trcs may involve balancing the disruption of higher order oligomers formed in aqueous environment and association with polysaccharides such as the β-glucan, chitin and peptidoglycans in the target cell wall structure [34]. These interactions may then serve as the seeding intermediates for further membrane penetration and disruption. The slight variations in conformation of the different Trcs could be the reason for variable interaction with different target cells which influences their antimicrobial activity and possibly eluding to an evolutionarily role of producing such a wide spectrum of peptides by the producer organism. Previous investigators have reported high antibacterial [2,4] and antifungal [6] for TrcB and TrcC analogues. The variability in antimicrobial activity observed in the current study may be attributed to differences in peptide character and different target cell properties. This is exemplified by the aberration in TrcB activity toward the two different target organisms. TrcB maintained high antifungal activity, its relative antibacterial activity was reduced, indicating an influence of the properties of the different targets.

With peptides that are co-produced in culture were combined, we observed that the activity of most of the peptide pairs were additive, while those containing tryptocidines were slightly antagonistic, which offers no benefit to the producer organism. Combinations of the peptides with Tyr^7 proved to be superior to those with Trp^7 and overt synergism was observed in combinations of TrcA:PhcA and TrcA:TrcB toward the fungal target, and TrcA:TrcB and

TrcB:TrcC toward the bacterial target. The observed synergism is possibly related to an intermediate hydrophobicity and dimerization allowing for active structures which optimally interact with the fungal target cell structure. These peptide combinations formed similar proportions of dimers to those seen for the most active analogues TrcA and TrcB (Fig. 6.2). Synergism observed in combinations of TrcA:PhcA toward *A. fumigatus* is possibly due to PhcA forming reduced dimers caused by an altered heterodimer structure relative to that formed by homodimers (Fig. 6.2, 6.5 and 6.7). The antagonism of pairs containing TpcC toward both the bacterial and fungal targets correlates with the increased formation of heterodimers, which indicates that TpcC related activity may be less dependent on dimerization (Fig. 6.2, 6.6 and 6.7).

6.5 Conclusion

The differences in antimicrobial activity observed in this study are most likely due to differences in target cell properties, as well as the character of the cyclodecapeptides, as has been noted by other investigators [2-4,6], However, when peptides are combined a more complicated scenario that is closer to the natural process is simulated. We found that combinations of peptides with TpcC may not be beneficial to the producer organism, which is probably why TpcC is almost exclusively produced in Trp-rich media. The fact that TrcA, TrcB and TrcC are naturally produced in the highest concentrations (>40%) and that their combinations are synergistic, does benefit the producer organism by providing and improved overall antimicrobial defence. This study therefore reveals the first evidence for the natural production of such a complex peptide cyclodecapeptide library. The identification of synergistic pairs also aids the formulation of peptide mixtures for specific applications. We therefore decided to use the natural tyrothricin extract with high TrcA and TrcB in an *in vivo* study using honey bees and their larvae as our model insect (Chapter 7).

6.5 References

1. Vosloo, J. A., Stander, M. A., Leussa, A. N., Spathelf, B. M. and Rautenbach, M. (2013) Manipulation of the tyrothricin production profile of *Bacillus aneurinolyticus*. Microbiology **159**, 2200-2211

2. Leussa, A. N. and Rautenbach, M. (2014) Detailed SAR and PCA of the tyrocidines and analogues towards leucocin A-Sensitive and leucocin A-Resistant *Listeria monocytogenes*. Chem. Biol. Drug Des. **84**, 543-557

3. Leussa, N. A. (2014) Characterisation of small cyclic peptides with antilisterial and antimalarial activity. Stellenbosch University, Department of Biochemistry, Stellenbosch, South Africa. **PhD. Thesis**, http://hdl.handle.net/10019.1/86161

4. Spathelf, B. M. and Rautenbach, M. (2009) Anti-listerial activity and structure-activity relationships of the six major tyrocidines, cyclic decapeptides from *Bacillus aneurinolyticus*. Bioorg. Med. Chem. **17**, 5541-5548

5. Rautenbach, M., Vlok, N. M., Stander, M. and Hoppe, H. C. (2007) Inhibition of malaria parasite blood stages by tyrocidines, membrane-active cyclic peptide antibiotics from *Bacillus brevis*. Biochim. Biophys. Acta. **1768**, 1488-1497

6. Troskie, A. M., de Beer, A., Vosloo, J. A., Jacobs, K. and Rautenbach, M. (2014) Inhibition of agronomically relevant fungal phytopathogens by tyrocidines, cyclic antimicrobial peptides isolated from *Bacillus aneurinolyticus*. Microbiology **160**, 2089-20101

7. Aranda, F. J. and de Kruijff, B. (1988) Interrelationships between tyrocidine and gramicidin A′ in their interaction with phospholipids in model membranes. Biochim. Biophys. Acta. **937**, 195-203

8. Goodall, M. C. (1970) Structural effects in the action of antibiotics on the ion permeability of lipid bilayers. I. Tyrocidine B. BBA-Biomembranes. **203**, 28-33

9. Dubos, R. J. (1939) Studies on a bactericidal agent extracted from a soil *Bacillus*: I. Preparation of the agent. Its activity in vitro. J. Exp. Med. **70**, 1-10

10. Ruttenberg, M. A. and Mach, B. (1966) Studies on amino acid substitution in the biosynthesis of the antibiotic polypeptide tyrocidine. Biochemistry **5**, 2864-2869

11. Ruttenberg, M. A., King, T. P. and Craig, L. C. (1966) The chemistry of tyrocidine. VII. Studies on association behaviour and implications regarding conformation. Biochemistry **5**, 2857-2864

12. Paradies, H. H. (1979) Aggregation of tyrocidine in aqueous solutions. Biochem. Biophys. Res. Commun. **88**, 810-817

13. Williams Jr, R. C., Yphantis, D. A. and Craig, L. C. (1972) Noncovalent association of tyrocidine B. Biochemistry **11**, 70-77

14. Stern, A., Gibbons, W. A. and Craig, L. C. (1969) Effect of association on the nuclear magnetic resonance spectra of tyrocidine B. J. Am. Chem. Soc. **91**, 2794-2796

15. Laiken, S., Printz, M. and Craig, L. (1971) Studies on the mode of self-assembly of tyrocidine B. Biochem. Biophys. Res. Commun. **43**, 595-600

16. Munyuki, G., Jackson, G. E., Venter, G. A., Kövér, K. E., Szilágyi, L., Rautenbach, M., Spathelf, B. M., Bhattacharya, B. and van der Spoel, D. (2013) β-Sheet structures and dimer models of the two major tyrocidines, antimicrobial peptides from *Bacillus aneurinolyticus*. Biochemistry **52**, 7798-7806

17. Loll, P. J., Upton, E. C., Nahoum, V., Economou, N. J. and Cocklin, S. (2014) The high resolution structure of tyrocidine A reveals an amphipathic dimer. BBA-Biomembranes. **1838**, 1199-1207

18. Troskie, A. M., Vlok, N. M. and Rautenbach, M. (2012) A novel 96-well gel-based assay for determining antifungal activity against filamentous fungi. J. Microbiol. Methods. **91**, 551-558

19. Lehrer, R. I., Rosenman, M., Harwig, S. S. S. L., Jackson, R. and Eisenhauer, P. (1991) Ultrasensitive assays for endogenous antimicrobial polypeptides. J. Immunol. Methods. **137**, 167-173

20. Du Toit, E. and Rautenbach, M. (2000) A sensitive standardised micro-gel well diffusion assay for the determination of antimicrobial activity. J. Microbiol. Methods. **42**, 159-165

21. Rautenbach, M., Gerstner, G. D., Vlok, N. M., Kulenkampff, J. and Westerhoff, H. V. (2006) Analyses of dose-response curves to compare the antimicrobial activity of model cationic α-helical peptides highlights the necessity for a minimum of two activity parameters. Anal. Biochem. **350**, 81-90

22. Hall, M. J., Middleton, R. F. and Westmacott, D. (1983) The fractional inhibitory concentration (FIC) index as a measure of synergy. J. Antimicrob. Chemother. **11**, 427-433

23. Jelokhani-Niaraki, M., Hodges, R. S., Meissner, J. E., Hassenstein, U. E. and Wheaton, L. (2008) Interaction of gramicidin S and its aromatic amino acid analogue with phospholipid membranes. Biophys. J. **95**, 3306-3321

24. Jelokhani-Niaraki, M. (2009) Effect of ring size on conformation and biological activity of cyclic cationic antimicrobial peptides. J. Med. Chem. **52**, 2090

25. Kondejewski, L. H., Jelokhani-Niaraki, M., Farmer, S. W., Lix, B., Kay, C. M., Sykes, B. D., Hancock, R. E. and Hodges, R. S. (1999) Dissociation of antimicrobial and haemolytic activities in cyclic peptide diastereomers by systematic alterations in amphipathicity. J. Biol. Chem. **274**, 13181-13192

26. Jelokhani-Niaraki, M., Kondejewski, L. H., Farmer, S., Hancock, R. E. W., Kay, C. M. and Hodges, R. S. (2000) Diastereoisomeric analogues of gramicidin S: Structure, biological activity and interaction with lipid bilayers. Biochem. J. **349**, 747-755

27. Norman, K. E. and Nymeyer, H. (2006) Indole localization in lipid membranes revealed by molecular simulation. Biophys. J. **91**, 2046-2054

28. Zasloff, M. (2002) Antimicrobial peptides of multicellular organisms. Nature **415**, 389-395

29. Andreu, D. and Rivas, L. (1998) Animal antimicrobial peptides: An overview. Biopolymers. **47**, 415-433

30. Hancock, R. E. and Sahl, H. (2006) Antimicrobial and host-defence peptides as new anti-infective therapeutic strategies. Nat. Biotechnol. **24**, 1551-1557

31. van't Hof, W., Veerman, E. C., Helmerhorst, E. J. and Amerongen, A. V. (2001) Antimicrobial peptides: Properties and applicability. Biol. Chem. **382**, 597-619

32. Hwang, P. M. and Vogel, H. J. (1998) Structure-function relationships of antimicrobial peptides. Biochem. Cell Biol. **76**, 235-246

33. Troskie, A. M. (2014) Tyrocidines, cyclic decapeptides produced by soil bacilli, as potent inhibitors of fungal pathogens. Stellenbosch University, Department of

Biochemistry, Stellenbosch, South Africa. **PhD. Thesis**, http://hdl.handle.net/10019.1/86162

34. Bowman, S. M. and Free, S. J. (2006) The structure and synthesis of the fungal cell wall. Bioessays. **28**, 799-808

Chapter 7
Formulation of tyrothricin extracts and *in vivo* toxicity testing toward honey bees

7.1 Introduction

The tyrocidines and analogues have been shown to display potent activity toward agronomically relevant fungal pathogens [1], including the ability to target these pathogens as well as Gram-positive bacteria in plants [2]. However, to allow for the use of these peptides in an agricultural environment their influence on non-target, beneficial organisms such as honey bees needs to be determined. Honey bees are central to the survival and maintenance of a healthy ecosystem through their role in the pollination of flowers [3]. Their role as pollinators is of the utmost importance to humans not only from the perspective of maintaining balanced ecosystems [4], they are pivotal to global food security [5] which goes hand-in-hand with their economic value [6]. The commercial use of honey bees as crop pollinators has exemplified the dangers of their exposure to chemical fungicides increasing susceptibility toward pathogens [7].

The combination of increased antimicrobial resistance toward many chemical antimicrobial agents, together with increased awareness of the negative impact of chemical control agents has driven the impetus for alternate so called green-biocides [8]. The tyrocidines (Trcs) are cyclic antimicrobial peptides produced by the soil bacterium *Bacillus aneurinolyticus* together with the linear gramicidins and are extracted together in what is known as the tyrothricin complex [9-12]. These antimicrobial peptides fit the criteria as green-biocides (refer to Chapter 4), however, for them to truly be considered green-biocides, they should not negatively affect non-target species.

Antimicrobial peptides are ubiquitously present throughout prokaryotic and eukaryotic kingdoms [13-15] as such are often considered the natural way of maintaining a balanced ecology [16]. Many antimicrobial peptides are produced naturally in healthy soil and water bodies by bacteria and are natural products that are biodegraded to nutrients, as are the peptides of focus in this research, the peptides in the tyrothricin complex. Plants have been shown to be protected from numerous fungal pathogens by soil bacteria which produce a variety of cyclic antimicrobial peptides including: iturin [17,18], iturin A and surfactin [19],

as well as gramicidin S [20-22], a peptide with 50% analogy to the tyrocidines and analogues. The peptides surfactin and fengycin are also shown to protect plant by inducing systemic resistance [23]. Additionally, antimicrobial peptide producing bacteria have been shown to promote plant growth [24]. Consequently, many of these antimicrobial peptide producing microorganisms have been used as bio-control agents in agricultural applications [17,19-21,25]. Their natural role in maintaining healthy, balanced ecosystems and use as bio-control agents has been recognised as early as the middle of the last century [16]. With the movement away from chemical control agents, there has been a resurgence of interest in these natural bio-control agents to control plant diseases [26-28].

In this study the focus was on the economical, natural production of the Trcs extracted from their producers and applications in agriculture and industry (refer to Chapter 4). As these antimicrobial peptides can be economically produced in large quantities, it enables the use of the extracts and purified peptides in a broader range of applications and control, circumventing the inherent unpredictability and limitations of utilising only the producer microorganism in agricultural conditions. As such, Rautenbach *et al.* [2] were the first to utilize the tyrothricin peptides within an agricultural environment to treat plants.

The tyrothricin peptides, as well as other amphipathic antimicrobial peptides, have been proposed to work *via* a rapid membranolytic mode of action [29], in addition to a number of other less overt antimicrobial targets [30]. In the case of the tyrothricin peptides, potential targets vary widely from the ubiquitous membrane [29,31], to also include the cell wall [32], enzymes of the electron transport chain [33] and also possibly including DNA and RNA [34-36]. With these multiple cellular targets there is thus a reduced likelihood of resistance development [37]. Part and parcel with the membranolytic activity, some toxicity of the tyrothricin peptides has been reported when applied intravenously [38,39]. There disruption of cell membranes is particularly evident in their haemolytic [10,39-43] as well as their leukocytic toxicity [38]. However, these peptides have been safely utilised when applied topically [44-47] or when taken orally in mammals [39,48-51].

To our knowledge, however, only a single report exists reporting the maximum tolerable dosage of a highly purified tyrocidine analogue to treat the nematode *Caenorhabditis elegans* in a medical infection model of the yeast *Candida albicans* [52]. This is the first extensive evaluation of the toxicity of the tyrothricin peptides toward insects, and more specifically

honey bees. Before the bee study could be executed the feeding formulation of the tyrothricin peptides in the solvent, as well as the influence of the main sugars in their feeding solutions was evaluated. After determining the oral toxicity of the tyrothricin peptides toward adult bees and their larvae; the potential of these peptides to protect honey bees from pathogens affecting them within their larval developmental stage was evaluated. Thereby establishing the relative safety of the tyrothricin containing culture extracts in environments where they would be utilised to target agronomically relevant pathogens.

7.2 Materials and Methods

7.2.1 Materials and Reagents

Sucrose (Suc), glucose (Glc), fructose, ethanol (EtOH), tryptone soy broth (TSB), agar, sodium bicarbonate and N,N-Dimethylformamide (DMF) were obtained from Merck (Darmstadt, Germany). Tyrothricin, and gramicidin S (GS), lactalbumin hydrolysate, gentamycin, penicillin, streptomycin, amphotericin B and dimethoate (DiM) were obtained from Sigma-Aldrich (Steinheim, Germany). Tween 20, potato dextrose agar (PDA) and potato dextrose broth (PDB) were from Fluka (Buchs, Switzerland). Sterile polystyrene 96-well flat bottom microtiter plates were from either Greiner bio-one (Frickenhausen, Germany) or Sarstedt (Nümbrecht, Germany). Petri dishes were from Lasec (Cape Town, South Africa). Grace's insect cell culture medium and pluronic F-68 were from Gibco Life Technologies (Waltham, MA, USA). Falcon® tubes, Columbia sheep blood agar plates, yeast extract and yeastolate were from Becton Dickson and Company (Franklin Lakes, NJ, USA). Promega (Madison, USA) supplied the Cell Titer-Blue™ Cell Viability Assay kit. Polycarbonate Erlenmeyer flasks were from Corning Incorporated (Corning, NY, USA). Foetal bovine serum was from Biochrom GmbH (Berlin, Germany). Brain, heart infusion (BHI), glycerol, glucose, fructose, potassium sulfate (K_2SO_4) used in assays toward bee larvae were from Roth (Karlsruhe, Germany). Royal jelly was from Imkereitechnik Möller (Borsum, Germany). Grafting cells where supplied by Nicotplast (Maisod, France). Dental roll and 48-well culture dishes were from Celluron (Wiener Neudorf, Austria) and Greiner bio-one (Frickenhausen, Germany) respectively. Analytical grade water was prepared by filtering water from a reverse osmosis plant through a Millipore-Q® water purification system (Milford, USA). Tyrothricin (Te) was obtained from culture extracts of *Bacillus aneurinolyticus* ATCC 10068 using an

organic extraction methodology [12] modified as previously described (Chapter 4). Temperature and humidity were recorded using Thermochron DS1922L i-Buttons from Maxim Integrated Products (San Jose, USA).

Aspergillus fumigatus ATCC 204305 was from the American Type Culture Collection (Manassas, VA, USA). *Bacillus subtilis* 168 was obtained from the Bacillus Genetic Stock Centre (Ohio State University, OH, USA). *Spodoptera frugiperda* (Sf9) cells were obtained from Allele Biotechnology and Pharmaceuticals/Orbigen (San Diego, CA, USA). *Paenibacillus larvae* reference strains DSM 7030 (ERIC I), DSM 25430 (ERIC II) and LMG 16252 (ERIC III), LMG 16247 (ERIC IV) were obtained from the German Collection of Microorganisms and Cell Cultures, Leibniz Institute DSMZ (Braunschweig, Germany) and Belgian Co-ordinated Collection of Microorganisms, Ghent University (Ghent, Belgium) respectively. Isolates of *P. larvae* were obtained from American Foulbrood positive honey/food or scale/glue-like liquid collected at the Lower Saxony State Office for Consumer Protection and Food Safety, Institute for Apiculture (Celle, Germany). The strain identity of the isolates was confirmed by 16S rRNA-PCR [53], and the genotype (ERIC) was confirmed by rep-PCR (Genersch et al. 2006) using ERIC-primers obtained from Eurofins Genomics (Ebersberg, Germany). *Melissococcus plutonius* LMG 20360, *Comamonas denitrificans* LMG 21602, *Bacillus pumilus* LMG 3455, *Delftia acidovorans* LMG 1226, *Ralstonia Picketti* LMG 5342, *Saccharibacter floricola* LMG 23170, *Janthinobacterium lividum* LMG 2892, *Pedobacter africanus* LMG 10345, *Bacillus megaterium* LMG 7127 and *Bacillus subtilis* LMG 2099 were obtained from the Belgian Co-ordinated Collection of Microorganisms, Ghent University (Ghent, Belgium). *Paenibacillus alvei* DSM 29, *Enterococcus faecalis* DSM 20376, *Pseudomonas fluorescens* DSM 6147, *Brevibacillus borstelensis* DSM 6347, *Planococcus maritimus* DSM 17275, *Salmonella enterica* subsp. *enterica* DSM 11320, *Staphylococcus pasteuri* DSM 30868, *Gluconobacter oxydans* DSM 2003, *Streptomyces griseus* DSM 1471 and *Planomicrobium okeanokoites* DSM 15489 were from the German Collection of Microorganisms and Cell Cultures, Leibniz Institute DSMZ (Braunschweig, Germany).

Oral toxicity studies were performed using adult African honey bees, *Apis mellifera scutellata*, at the Agricultural Research Council Plant Protection Research Institute, Vredenburg Research Centre (Stellenbosch, South Africa). Carniolan honey bee, *Apis mellifera carnica*, larvae were obtained from hives at the Technische Universität

Braunschweig (Braunschweig, Germany) using queen bees that were bred at the Lower Saxony State Office for Consumer Protection and Food Safety, Institute for Apiculture (Celle, Germany).

7.2.2 Preparation of peptide formulations for antimicrobial activity assays

Analytically weighed aliquots of the dried peptide formulations, tyrocidine extract from commercial tyrothricin complex (Tc) and tyrothricin extract (Te) from *B. aneurinolyticus* (refer to Chapter 4) were dissolved in either 50% (*v/v*) DMF in water or 75% EtOH (*v/v*) in water. These were subsequently diluted using either sterilised water or one of the respective sugars to a concentration of 1.00 mg/mL at a solvent concentration of either 10% (*v/v*) DMF or 15% EtOH (*v/v*) in either water or 50% (*m/v*) of one of the respective sugars. While maintaining the solvent and sugar concentration, the respective peptide formulations were prepared in a doubling dilution series. These were subsequently diluted 10-fold in the antimicrobial assays to a final solvent concentration of either 1% (*v/v*) DMF or 1.5% (*v/v*) EtOH in either water and/or 5% (*m/v*) of one of the respective sugars.

7.2.3 Antifungal activity assays toward Aspergillus fumigatus

Spores of the fungi *A. fumigatus* ATCC 204305 were obtained from freezer stocks and cultured using normal sterile techniques on PDA plates for three weeks. Subsequently 7 mL of Tween water (20 µL of Tween in 200 mL analytical grade water and autoclaved) was added to the plates, the spores lightly loosened using a hockey stick and hydrated over night at 4 °C. These were subsequently counted using a haemocytometer and diluted with sterile water to a concentration of 50 spores/µL.

A variation of a microtiter broth dilution method, as described by Troskie *et al.* [54], was used to test the antimicrobial activity of the tyrothricin extracts toward *A. fumigatus*. A volume of 50 µL of PDB was added to all the wells of a sterile microtiter plate. The top four wells of the first column received 40 µL of sterilized water, while all the rest of the wells received 40 µL of the mentioned spore suspension. The wells of the first column received 10 µL of solvent or sugar formulation at a concentration equivalent to that the peptide formulations were dissolved in, thus the first column served as sterility and growth controls respectively. All the rest of the wells received 10 µL of one of the respective peptides

dissolved in the respective solvents or sugar formulations. Application of Tc and Te were repeated in triplicate (*n=3*) at a final concentration ranging from 100.0 to 0.80 µg/mL; while those of GS were in duplicate (*n=2*) at a final concentration ranging from 50.0 to 0.40 µg/mL.

The microtiter plates were then covered and incubated for a period of 48 hours at 25 °C, following which the light dispersion was measured spectrophotometrically at 595 nm using a BioRad™ microtiter plate reader. From which the percentage growth inhibition was determined.

7.2.4 Antibacterial activity assays toward Bacillus subtilis

Single colonies of the Gram-positive bacteria *B. subtilis* 168 were obtained from freezer stocks by culturing using normal sterile techniques on tryptone soy agar (TSA) plates (3.0% (*w/v*) TSB and 1.5% (*w/v*) agar in water). Single colonies were selected and incubated while shaking at 220 rpm for 16 hours at 37 ºC in Falcon® tubes containing 20 mL TSB (3.0% (*w/v*) TSB in water; pH 7.0) medium to an optical density (OD) of approximately 0.8 at 595 nm. These cells were subsequently sub-cultured in TSB and grown to an OD of 0.6 at 595 nm.

A variation of the microtiter broth dilution method as described by Du Toit and Rautenbach [55] and Lehrer *et al.* [56] was used to determine the activity of the mentioned peptide formulations toward the Gram-positive bacteria *B. subtilis* 168. A pre-culture was diluted with TSB to an OD of 0.2 at 595 nm (±10^8 CFU/mL). A volume of 90 µL of the diluted culture was added to all of the wells of the microtiter plate except for the top four wells first column which received 90 µL of TSB. The peptide and solvent controls were as previously described. These microtiter plates were then covered and incubated for a period of 16 hours at 37 ºC, following which the light dispersion was measured spectrophotometrically at 595 nm using a Bio Rad™ microtiter plate reader. The percentage growth inhibition was then determined [55,57].

7.2.5 Influence of different solvents and sugars on aggregation

Dried peptide aliquots of the Tc and Te were dissolved in 50% (*v/v*) of either DMF or EtOH and diluted to a concentration of 260.0 µg/mL with 5% (*v/v*) solvent in analytical grade water. These samples were allowed to stand at room temperature overnight prior to being diluted to

a final concentration of 130.0 µg/mL with 2.5% (*v/v*) solvent in analytical grade water with or without the addition of 5% (*m/v*) of either Suc or Glc.

The type of predominant aggregates/oligomers formed within the above formulations was determined by means of high resolution electrospray mass spectrometry (ESMS) using a Waters Q-TOF Synapt G2 mass spectrometer with a Z-spray electrospray ionisation source. Injections of 2 µL of sample were introduced directly into the mass analyser in positive mode at a flow rate of 0.3 mL/minute using 60% (*v/v*) acetonitrile. Peptide extracts were subjected to a capillary voltage of 2.5 kV and cone voltages of 15 V at a temperature of 120 ºC at the source, desolvation gas of 650 L/h and desolvation temperature of 275 ºC. Data acquisition was performed by scanning mass over charge ratio (*m/z*) range of 300 to 2000 in continuum mode at a rate of 0.2 scans per second.

Particle size of the aggregates formed within these formulations was then determined by means of dynamic light scattering (DLS) using a Malvern ZetaSizer 1000HSa instrument equipped with a He-Ne laser. Samples were placed in a 1.0 cm diameter quartz cuvette and allowed to equilibrate at 37 ºC within the instrument. Operating at 633 nm wavelength, scattered light was detected at a 90º angle. The mean of three measurements, each composed of 10 sub-runs, was used to determine the particle size and distribution from particle size was calculated using CONTIN analysis and expressed as the diameter of the particles in nanometres (nm).

7.2.7 Toxicity toward insect cell lines

Insect cells toxicity assays were done at Stellenbosch University (Stellenbosch, South Africa) in collaboration with Timo Tait. *Spodoptera frugiperda* (Sf_9) cells were initially grown as monolayers in a non-humidified, ambient air-regulated incubator set to 27 ºC in complete TNM-FH medium (Grace's insect cell culture medium supplemented with: 3.33 g/L yeastolate, 3.33 g/L lactalbumin hydrolysate, 0.35 g/L sodium bicarbonate, 10% (*v/v*) foetal bovine serum, 100 U penicillin, 100 mg/L streptomycin, 10 mg/L gentamycin and 2.5 g/L amphotericin B in analytical grade water). Cells were habitually counted by means of a haemocytometer to assess cell density while cell viability was assessed by the resorufin-resazurin (also known CellTiter-Blue™ or Trypan Blue) assay. Passages of monolayers were performed at 90–95% confluence; cells were subsequently plated at seeding densities of

5 x 10^4 viable cells/cm^2. Sf9 cells were transferred to suspension culture once regular exponential growth was obtained at a sustained cell viability of greater than 90%. Cells were suspended in 100 ml complete TNM-FH in sterile 250 mL polycarbonate Erlenmeyer flasks at constant agitation of 100 rpm at 27 °C. Pluronic F-68 was added at a final concentration of 0.1 % (*v/v*) to reduce cell shearing. Cells were routinely passaged to a cell density of 2 x 10^5 viable cells per millilitre when the culture reached a density of > 2 x 10^6 viable cells/mL.

Prior to the assays being performed cells were collected by centrifugation at 500 ×*g* for 5 minutes. The pelleted cells were then washed with 10 mL sterile phosphate buffered saline and suspended at a concentration of 2 x 10^5 viable cells/mL in complete TNM-FH barring the addition of antibiotics (penicillin, streptomycin, gentamycin and amphotericin B). The toxicity of Te was performed through a variation of the previously described microtiter broth dilution method [55,57]. Briefly, the adjusted TNM-FH media alone or including Sf9 cells at a cell density of 2 x 10^5 viable cells/mL served as the sterility and growth controls respectively, as such they were only treated with solvent at an equivalent concentration used to apply the peptides. The peptides exposure ranged in concentration between 100.0 to 0.40 µg/mL in 1% (*v/v*) DMF. These treated cells were subsequently incubated for 24 hours at 27 ºC. The metabolic activity of the cells was then determined by adding 10 µL of CellTiter-Blue™ reagent to every well and incubated for an additional two hours upon which the fluorescence (excitation $\lambda_{530\ nm}$, emission $\lambda_{590\ nm}$) was measured on a Thermo Verioskan™ spectrophotometer.

7.2.8 Acute oral toxicity testing of tyrothricin toward adult honeybees

The oral toxicity study of tyrothricin to honeybees was done at the Agricultural Research Council Plant Protection Research Institute, Vredenburg Research Centre (Stellenbosch, South Africa) in collaboration with Dr. Mike Allsopp. The oral toxicity of tyrothricin to honeybees was evaluated using methodology described in OECD/OCDE Test Guideline (TG) 213 [58]. A brood frame was removed from a queen-right colony and maintained at 25±2ºC and 50% relative humidity. Emerged worker bees were subsequently marked every 24 hours using coloured markers and returned to the hive. Subsequently after a period of ten days these marked bees were re-captured and ten bees placed in each wooden cage (10 × 8.5 × 5.5cm; mesh covered two sides and Perspex the front). These were then fed a feeding solution 50% (*m/v*) sucrose in water from a reverse osmosis plant and sterilized by means of

autoclave) in a glass tube (50 mm long, 8 mm wide tapering to 2.5 mm), while being maintained at 27±2ºC and 52±5% relative humidity to allow the bees to acclimatise to the experimental conditions for 24 hours. After which the feeders were removed for a period of two hours. Bees were maintained in the dark throughout all of the experimental phases barring periods of observation.

At least four cages were randomly assigned to each of the experimental groups. Three control groups received; only feeding solution or feeding solution together with 1% (*v/v*) DMF (dosing vehicle) and a positive control group received 17.5 µg/mL DiM in feeding solution and dosing vehicle. Te stock solutions were prepared in 50% DMF (*v/v*) in analytical grade water. These were diluted to concentrations of between 2500 and 30 µg/mL Te ranging over eight concentrations dissolved in feeding solution and 1% (*v/v*) DMF. Feeders containing 200 µL of each of the respective dosages where then replaced and the feed consumed, as well as mortality recorded after four and six hours. After which any unconsumed feed was removed and the volume recorded. A fresh feeder was then replaced containing only 50% (*m/v*) Suc. Bees which displayed any sub-lethal effects, including lack of mobility, were recorded together with mortality and removed every 24 hours until a maximum of 96 hours. Bees were subsequently fed a diet of only the mentioned concentration range of Te, together with the respective controls, for up to 72 hours. As previously described, feed volume consumed, sub-lethal effects and mortality were recorded and bees which had succumbed were removed. Mortalities were adjusted relative to those observed in the uninfected controls using Abbots correction [59].

7.2.9 Delayed toxicity testing and survival in hives after tyrothricin exposure

Freshly emerged worker honey bees from three different hives were marked and placed in the previously described cages, with no more than 300 bees per cage. By means of three 20 mL glass feeders per cage, bees from each of the different hives were fed a diet composed of 50% Suc and 1% DMF (control), or 50% Suc and 1.5 µg/mL Te dissolved in 1% DMF for 48 hours. Mortality, sub-lethal effects and volume consumed were recorded for the first six hours and every 24 hours thereafter until 48 hours. Bees of the control and experimental groups were then lightly sprayed with a water/honey/alcohol solution and returned to the hive from which the respective brood frames originated. Bees were then counted after three days and weekly thereafter until 28 days. A sample of 10 bees from each experimental group was

collected at each counting until 28 days when all the remaining marked bees where collected. These bees were stored in an air tight container at -20 C for dissection and analysis.

7.2.10 Antibacterial activity assays toward foulbrood associated pathogens

The antibacterial activity assays toward foulbrood associated pathogens were done at the Technische Universität Braunschweig (Braunschweig, Germany) in collaboration with Hannes Beims. Antimicrobial activity assays were performed against: all four known genotypes of *P. larvae* (ERIC I, DSM 7030; ERIC II, DSM 25430; ERIC III, LMG 16252; ERIC IV, LMG 16247) [60], the causative agent of American foulbrood; *M. plutonius*, the causative agent of European foulbrood, as well as the associated secondary invaders *P. alvei* and *E. faecalis* [61].

Single colonies were obtained from freezer stocks and grown on Columbia sheep blood agar for 16 hours at 37 °C. A loop of bacteria was used inoculated into 5 mL of BHI (3.7% (*m/v*) BHI, 0.3% (*m/v*) yeast extract), this pre-culture was cultured at 37 °C while shaking at 200 rpm for approximately six hours. The pre-culture was then diluted to a final OD of 0.2 at 600 nm in the described BHI broth.

Activity assays were performed in triplicate for each strain containing three technical repeats of Te. Sterility, growth controls and peptide formulations were prepared at a final EtOH concentration of 1.5% (*v/v*) as previously described. The plates were incubated at 37 °C for 16 hours on a thermo shaker (Grant-bio, PHMP-4) while shaking at 600 rpm. Only *M. plutonius* was cultivated without shaking at 37 °C and under anaerobic conditions. The OD_{595} was measured in a multiplate reader (Thermo Fischer, VARIOSKAN FLASH) and percentage growth inhibition determined [55,57].

7.2.11 Toxicity of tyrothricin peptides toward bee larvae

The toxicity studies against bee larvae were done at the Technische Universität Braunschweig (Braunschweig, Germany) in collaboration with Hannes Beims. The *in vivo* toxicity of tyrothricin formulations toward *A. mellifera* larvae was tested according to the OECD/OCDE TG 237 [62]. An apparatus, consisting of a Plexiglas desiccator (NALGENE, 5317-0120), containing a dish filled with K_2SO_4 sutured solution, was placed in an incubator (WiseCube, WIS-30R) at 35 °C. Larvae were collected from three different, unrelated colonies of

A. mellifera carnica. These were reared in polystyrene grafting cells, which were placed in a 48-well plate containing pieces of dental roll wetted with 500 µL 15% (*v/v*) glycerol. Larval food (frozen royal jelly, yeast extract, glucose and fructose) was prepared and adjusted relative to the various developmental stages of the larvae [62]. Aliquoted dry masses of Te were dissolved in 15 µL 99.9% (*v/v*) DMF and 165 µL of deionised water. An aliquot of 1.5 mL Diet C (50% (*m/v*) royal jelly, 2% (*m/v*) yeast extract, 9% (*m/v*) glucose, 9% (*m/v*) fructose) [62] was added to 150 µL of the prepared peptide solution. Larvae were fed 33 µL of the prepared Diet C on day 4 containing concentrations of 6.17 µg/mL, 18.5 µg/mL, 55.6 µg/mL, 167 µg/mL or 500 µg/mL of Te. This equated to a single exposure of 0.204, 0.611, 1.83, 5.5 or 16.5 µg/larva. Controls were performed for: the natural mortality (diets without ingredients), for 0.76% (*v/v*) DMF solvent (as derived above) and for the reference chemical insecticide DiM at a concentration of 267 µg/mL, thus 8.8 µg/larva. Three replicates containing a minimum of 12 larvae were repeated for each colony for each of the respective test conditions. The development of the larvae was assessed and any sub lethal effects were recoded as well as the mortality up to day 7, after which the tests were terminated [62]. Mortalities were adjusted relative to those observed in the uninfected controls using Abbots correction [59].

7.2.12 Curing assays of Paenibacillus larvae infected bee larvae

The curing assays of invested bee larvae were done at the Technische Universität Braunschweig (Braunschweig, Germany) in collaboration with Hannes Beims. Rearing of bee larvae were performed as previously described [63,64]. At day 1, 1500 spores of *P. larvae* ERIC I (DSM 7030) or ERIC II (DSM 25430) were added to Diet A [62] to infect the larvae [65]; barring those which served as uninfected controls. Peptide formulations of Te prepared as previously described were fed to cure the infected larvae on day 4 in Diet C [62]. A concentration of 55.6 µg/mL (1.83 µg/larva) of Te was used as this concentration was judged to not show significant differences in larval survival relative to the respective control. Infected control larvae were fed diet C without any additives. Three different, unrelated colonies were used in replicates of 36 larvae each. Larvae were inspected for 14 days post-infection and the mortality recorded every day. Dead individuals were homogenized and plated out on blood agar in order to confirm killing by *P. larvae* using a *P. larvae*-specific 16S rRNA-PCR detection [53]. Mortalities were adjusted relative to those observed in the

uninfected controls using Abbots correction [59]. The percentage relative mortality was plotted against time and compared to describe mortalities of infected larvae [65].

7.2.13 Antibacterial activity toward gut microbiota of honey bee larvae

To exclude any ecological damage after application of the respective peptide formulations on bee larvae, their antimicrobial activity was determined toward several members of the gut microbiota of *A. mellifera* [66]. The growth media and cultivation conditions used were as described elsewhere (https://www.dsmz.de/). A single indicative activity assay was performed toward each strain. Application of Te was as described toward the causative agents of foulbrood.

7.2.14 Data analysis

The effect of natural mortality observed in bees and their larvae was removed by adjusting the mortalities relative to those observed in the uninfected controls using Abbots correction [59] by means of the following equation:

$$\text{\% Mortality (Abbots correction)} = \frac{\text{(Mean \% mortality due to treatment – Mean \% control mortality)}}{\text{(100 – Mean \% control mortality)}}$$

The percentage growth inhibition of the peptide extract in all antimicrobial activity assays was determined relative to the mean of the growth control, as previously described by Rautenbach *et al.* [57], using the following equation:

$$\text{\% growth inhibition} = 100 - \frac{100 \times (A_{595} \text{ of well} - \text{Mean } A_{595} \text{ of background})}{(\text{Mean } A_{595} \text{ of growth control} - \text{Mean } A_{595} \text{ of background})}$$

GraphPad Prism® 4.00 (GraphPad Software, San Diego, USA) was used to plot all graphs as well as perform all statistical analysis, except for those obtained by ESMS analysis. Antimicrobial activity parameters were determined from these plots included: IC_{50} (concentration causing 50% growth inhibition) and IC_{max} (concentration causing 100% growth inhibition). IC_{max} is directly related to the minimum inhibitory concentration (MIC, lowest concentration used where no growth is visually observed), but was calculated from the dose response as described by Du Toit and Rautenbach [55].

The data obtained by means of ESMS was analysed using MassLynx V4.1 (Waters, Miliford, USA) to determine the proportion of the different types of oligomers formed.

7.3 Results and Discussion

The tyrocidines have shown great promise targeting pathogens in the food and agricultural industries [1,2,67,68]. For these peptides to be considered safe to use within these industries, particularly in agriculture, their influence on non-target, beneficial honey bees needed to be evaluated.

For this to be achieved the formulation of our tyrothricin extract (Te) for application in a honey bee studies was evaluated relative to the purified commercial Trcs mixture (Tc) (refer to Chapter 2 for detailed analysis). As EtOH cannot be used as solvent in the toxicity testing towards bees, we investigated the use of an alternative solvent, DMF. The influence of 1.0% DMF on the antimicrobial activity and aggregation of the tyrothricin peptides was compared relative to the established 1.5% EtOH solvent used in prior antimicrobial activity assays. The influence of two sugars Suc and Glc, present in the feeding solutions used to administer the tyrothricin peptides to adult bees and their larvae, was also investigated prior to *in vivo* toxicity studies being performed toward bees and larvae.

7.3.1 Influence of peptide formulation on aggregation

Aggregation of the tyrothricin peptides and assembly/oligomerization into higher order structures is central to their antimicrobial activity [1,29,31,69,70], however, premature aggregation before coming into contact with the membrane targets has a negative influence on their antimicrobial activity [71-73]. Te has been shown to contain a natural pigment together with linear gramicidins which were co-extracted from the culture extracts (Chapter 4). The influence of these co-extracted factors on the aggregation of the tyrothricin peptides was evaluated by comparing the aggregation of Te in different environments relative to that of the highly cleaned Tc, shown to contain only the tyrocidines and their analogues (Trcs) (Chapter 2, [1]).

The influence of dissolving the tyrothricin peptides in the different solvents, EtOH or DMF, on their aggregation into higher order structures was investigated by means of ESMS (Fig. 7.1). Analysis of the respective peptide formulations dissolved in the two solvents

revealed a difference in the aggregation characteristics of the tyrothricin peptides. In both of the peptide formulations the monomeric species of Trcs was the predominant species detected when dissolved in EtOH, (Fig. 7.1 A and C). In contrast, when dissolved in DMF the dimeric form of Trcs was predominantly detected. Variability in the detected masses of the oligomeric structures was observed between Te and Tc reflecting the difference in composition where Tc only contains Trcs, Te also contained a small amount of linear gramicidins together with the culture pigment (Fig. 7.1, Chapter 4).

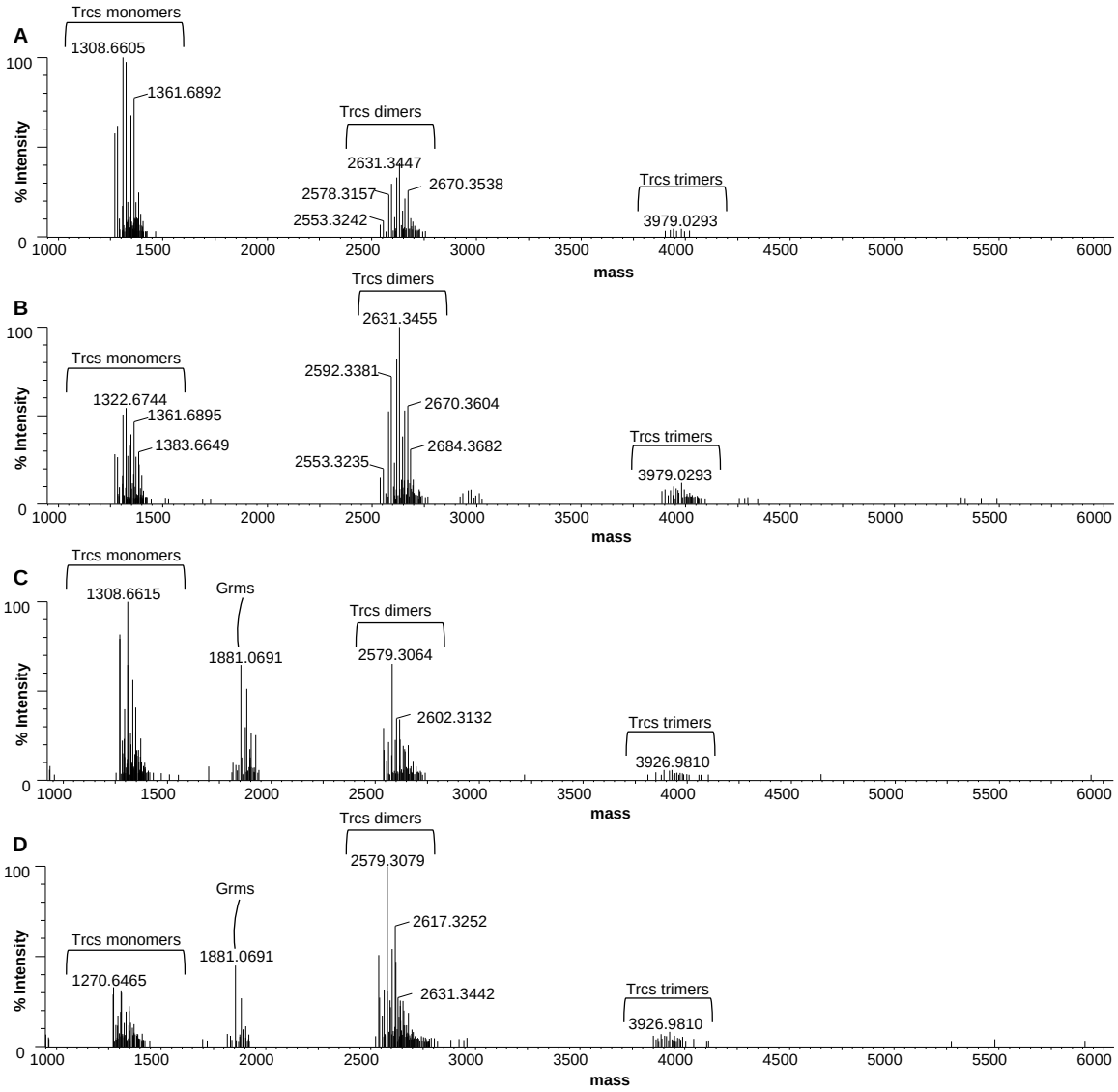

Figure 7.1 ESMS spectra of the tyrothricin formulations depicting the aggregation of the tyrocidines and their analogues (Trcs) forming monomer, dimers or trimers. Tc dissolved in water with 2.5% **A** EtOH or **B** DMF or Te dissolved in **C** EtOH or **D** DMF. Te contains linear gramicidins (Grms) in addition to the tyrocidines and their analogues

Attempts to characterise the oligomerization of the Trcs in the presence of sugars by ESMS where hindered by the suppression of the peptide ion signal by the sugars (data not shown). Therefore the influence of the sugars Suc and Glc on the size of the aggregates of the tyrothricin peptides dissolved in either EtOH or DMF was investigated further by means of DLS (Fig. 7.2).

Variability was observed in the particle size of Tc and Te in the both of the solvent compositions. Tc tended to produced larger aggregates at a greater intensity indicating an increased proportion of these aggregates to the total aggregate profile. However, when considering the two formulations individually within the two solvents, only minor variability is observed in the size of the aggregates (Fig. 7.2 A and B).

The sugars had a chaotropic effect, causing a disruption of the aggregation of Tc in EtOH and decreased the proportion of the aggregates with a diameter of around 220 nm (Fig. 7.2 C). The variation in aggregation was more pronounced in the presence of Suc as is evident from the decreased intensity signal of the aggregates at 220 nm, concomitantly the diameter of the aggregates varied greatly from as low as 33 nm to as large as 825 nm, with the larger aggregates as observed in EtOH alone (Fig. 7.2 C). The disruption of the aggregation of Tc in the presence of both Glc and Suc also resulted in the presence of a small proportion of smaller aggregates with 0.7 to 1 nm diameter (Fig 7.2 C).

When Tc was dissolved in 2.5% DMF as solvent a more pronounced effect of the sugars reducing aggregation was observed producing aggregates within a narrow size window and increased intensity (Fig. 7.2 E). In water with 2.5% DMF the majority of the aggregates had a mean maximum diameter of approximately 260 nm together with a smaller fraction of 42 nm; these aggregates where dispersed over two size windows ranging between 20 nm to 116 nm for the smaller aggregates and 116 nm to 540 nm for the larger aggregates. In the presence of Suc and Glc, the smaller fraction with an average diameter of 42 nm had a much narrower size window ranging between 28 nm and 48 nm, together with even smaller aggregates ranging between 3 nm and 12 nm in diameter, indicating a chaotropic effect of the sugars in the presence of DMF. In both instances the signal intensity of the larger aggregated obtained in the presence of Glc exceeded that of Suc, indicating a large chaotropic effect of Suc on the peptide aggregation.

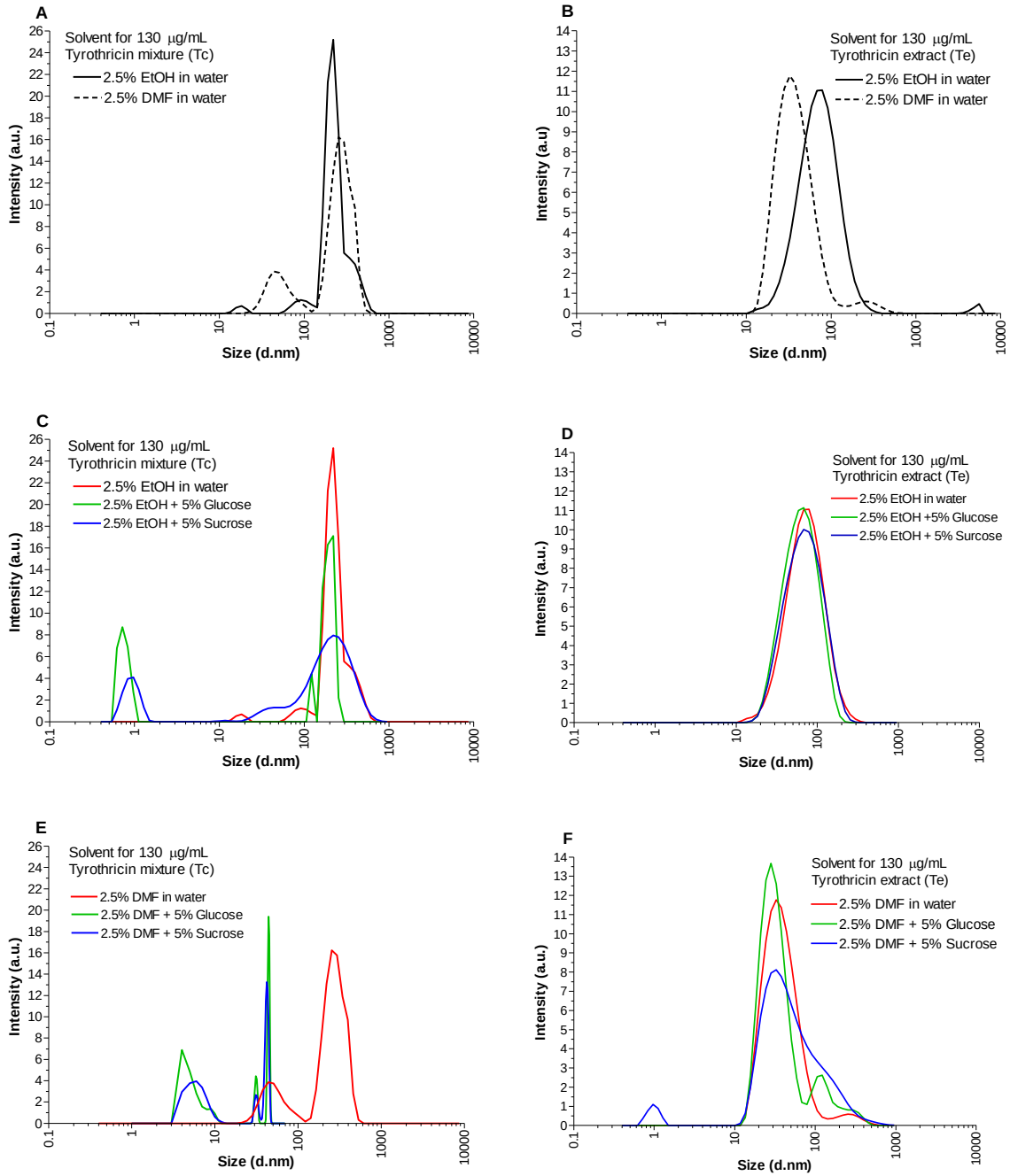

Figure 7.2 Comparison of the size of aggregates of Tc (A, C, E) and Te (B, D, F) formed in different environments. Size of aggregates formed in water with 2.5% of EtOH or DMF solvent and water of **A** Tc or **B** Te. In combination with 5% of either sucrose or glucose and 2.5% of either EtOH or DMF of Tc in **C** and **D** or Te in **E** and **F** respectively.

The smaller aggregate size of Te remained fairly consistent in the presence of Suc and Glc when dissolved in EtOH with an average aggregate diameter of approximately 70 nm (Fig. 7.2 D). As opposed to what was observed in EtOH, the aggregation profile of Te was disrupted in the presence of DMF together with Suc and Glc. In the presence of Glc a slight

increase in the intensity of aggregates of 32 nm average diameter was observed, while in the presence of Suc the intensity of aggregates of the latter diameter decreased concomitantly increasing the proportional contribution of larger aggregates between 100 nm and 400 nm as well as smaller aggregates of 1 nm average diameter (Fig. 7.2 F).

The sugars thus had a chaotropic effect on the aggregation of Te when it was dissolved in DMF (Fig. 7.2 F) which was not observed when dissolved in EtOH (Fig. 7.2 D). This concurs with the altered oligomerization of the peptides in DMF (Fig. 7.1 C and D), attesting to a possible conformational change which made the aggregates more accessible to the sugars. The aggregate size of Te was consistently smaller than that of Tc when dissolved in only the solvent. Only in DMF together with the respective sugars did the aggregate size of Tc approach that of Te (Fig. 7.2 E and F). This alludes to the possibility of the culture pigment within Te having a chaotropic effect on aggregation similar to what was observed by the sugars in Tc.

7.3.2 Toxicity toward insect cell lines

Having determined the influence of the respective sugars on the aggregation of the Te and Tc formulations, their toxicity alone, as well as in the sugar formulations was determined toward Sf9 insect cells. The toxicity of Te, containing linear gramicidin as well as culture pigment, was compared to that of Tc, composed of only the Trcs (refer to Fig. 7.1). Only the DMF solvent was considered in combination with Suc and Glc as this was the relevant solvent used in the *in vivo* studies performed toward adult honey bees as well as their larvae (Table 7.1).

Table 7.1 Toxicity of Te and Tc in 1% DMF in different solvent compositions toward *Spodoptera frugiperda* (Sf9) insect cells.

Peptide formulation	**LC_{max} (µg/mL)±SEM**
Tc (*n=6*)	11.3±0.25
Tc + 5% Suc (*n=3*)	13.2±3.53
Tc + 5% Glc (*n=3*)	7.32±0.54$^{\$}$
Te (*n=6*)	18.3±0.98$^{\$}$
Te + 5% Suc (*n=3*)	16.7±1.19$^{\$}$
Te + 5% Glc (*n=3*)	15.1±3.88

SEM, standard error of the mean. Statistical analysis performed by unpaired Student t-test with $ P<0.001 relative to Tc, Activity of Te relative to addition of sugars was not statistically significant P>0.05

From these data it was evident Te was less toxic than Tc toward Sf9 cells, despite containing linear gramicidins. The difference in toxicity of Te in the presence of sugars was not statistically significant, however, Glc showed a tendency of augmented toxicity of Tc toward the insect cells.

The culture pigment may also have a modulatory effect on the toxicity of Te. The presence of the linear gramicidins has been shown to increase the toxicity of tyrothricin relative to tyrocidines alone [41,74] which are found in Tc. However, the opposite was observed in the case of Te which displayed less toxicity than Tc toward insect cells (Table 7.1). Taking into consideration the fact that Te only contained approximately 75% the peptide content of Tc (determined by UPLC-MS analysis, refer to Chapter 4), the toxicity of Te in the presence or absence of Suc and Glc was approximately 50% less than that of Tc toward insect cell lines despite compensation for the difference in peptide content. Overall the reduction in toxicity of Te is attributed to the influence of the culture pigment, which may be acting as a chaotropic agent to decrease the formation of toxic oligomers.

7.3.3 Antimicrobial activity of peptide formulations

Having observed a change in the aggregation of Te in the different solvents (Fig. 7.1 C and D, Fig. 7.2 B), as well as in the presence of sugars when dissolved in DMF (Fig. 7.2F), it was investigated whether these changes may have influenced its antimicrobial activity.

The antimicrobial activity of the Te in either 1.0% DMF or 1.5% EtOH was compared to that of the Tc toward A. fumigatus and B. subtilis which served as representative fungi and Gram-positive bacteria respectively (Table 7.2).

In both of the solvents the activity of Te was less than that of Tc toward both of the respective target organisms. A slight reduction in antimicrobial activity of Te relative to Tc in the two respective solvents (Table 7.2) may be attributed to the antagonistic effect of the co-extracted linear gramicidins [80]. However, in consideration of the tyrocidine peptide content of Te was approximately 75% that of Tc (Chapter 4), this reduction in activity was only truly relevant toward *A. fumigatus* when Te was dissolved in EtOH displaying 66% the activity relative to Tc. Te displayed near equivalent activity to that of Tc (if purity is considered) in DMF toward *A. fumigatus*. The antibacterial activity toward *B. subtilis* in EtOH or DMF increased to 85% and 91% respectively relative to Tc, which could indicate higher potency than that of Tc if the

75% purity of Te is taken into consideration. However, additional factors such as the influence of the culture pigment may have a positive influence on the antimicrobial activity which would account for the increased antibacterial activity relative to the peptide content.

Table 7.2 Activity of the tyrocidine extract (Te) relative to commercial tyrothricin (Tc) in different solvent compositions toward representative fungi *Aspergillus fumigatus* and Gram-positive bacteria *Bacillus subtilis*

Microbial target **Peptide complex**	**1.5% Ethanol IC_{max} (µg/mL) ±SEM**	**1% DMF IC_{max} (µg/mL) ±SEM**
Aspergillus fumigatus		
Tc	8.93±1. 3 $^{\#\,c}$ (*n=7*)	6.77±0.52 $^{\#\,c}$ (*n=12*)
Te	12.2±0.48 $^{\#\,c}$ (*n=37*)	10.3±1.30 $^{\#\,c}$ (*n=20*)
Bacillus subtilis		
Tc	12.1±1.6 ^{a} (*n=15*)	11.0±0.37 ^{c} (*n=6*)
Te	13.3±0.42 ^{*a} (*n=50*)	12.9±0.59 $^{*\,c}$ (*n=6*)

Statistical analysis performed by means of an unpaired Student t test comparing ethanol vs DMF with # P<0.001; * P<0.05 or Tc vs Te a P<0.001; c P<0.05

With the influence of the two solvents on the antimicrobial activity of Te relative to the purified Tc now firmly established, the influence of Suc and Glc on the antimicrobial activity of Te in the two the different solvent compositions was evaluated toward the two model fungal and bacterial target organisms. The investigation of the influence of these sugars on the antimicrobial activity of the tyrothricin peptides is of particular relevance due to their ubiquitous presence in not only microbial growth media, but also in environments where target pathogens of these peptides reside. The variation of Te activity was compared in the different solvent environments relative to that in EtOH alone using the respective IC_{max} values to highlight the influence of the different sugars on antimicrobial activity in the different solvent compositions (Fig. 7.3).

In the two solvents alone, an increase in activity was observed toward the representative fungi *A. fumigatus* when the mentioned peptide formulation was dissolved in DMF, together with a marginal decreased in antibacterial activity relative to EtOH (Fig. 7.3). When Te was dissolved in EtOH together with the additional 5% (*m/v*) sugars, the antimicrobial activity was greatly decreased (Fig. 7.3). The decrease of antifungal activity was alleviated when the peptides were dissolved in DMF where Te regained 97% and 83% activity in the presence of Suc and Glc respectively, relative to approximately 25% relative activity observed in EtOH

together with both sugars (Fig. 7.3 A). The antibacterial activity of Te in the presence of Suc increased to 53% activity when dissolved in DMF in relation to 20% observed when dissolved in EtOH. Moreover, the activity of Te increased to 103% when dissolved in DMF in the presence of Glc in relation to 27% when dissolved in EtOH (Fig. 7.3 B). Fructose was also observed to suppress the antimicrobial activity when Te was dissolved in EtOH and was greatly relieved when dissolved in DMF (data not shown).

Analysis of the aggregation of the tyrothricin peptides into higher order structures in DMF or EtOH by ESMS indicated an increase in the prevalence of the dimeric form in DMF relative to the monomeric form detected in EtOH (Fig. 7.1). The dimeric form of the tyrocidines is proposed be the active amphipathic structure of these cyclodecapeptides that is important in their membranolytic mode of action when targeting bacteria [29,31]. Pre-incubation of Te together with the various sugars severely suppressed the antimicrobial activity of Te when dissolved in EtOH, this was largely relieved when dissolved in DMF. Both Glc and Suc reduced the size of the aggregates formed when the peptides where dissolved in DMF, indicating an increased chaotropic effect and optimally dimerised antimicrobial formulation as shown in Chapters 5 and 6 (Fig. 7.2).

Increased antimicrobial activity when dissolved in DMF was attributed to the sugars having a further chaotropic effect on the aggregates formed in the pre-incubated peptide formulations by disrupting the hydrogen bonding networks (refer to Chapter 5) and consequently increasing the formation of the more favourable dimeric oligomeric structures [29,31]. The chaotropic effect of the sugars is acutely apparent in the Tc peptide formulation. The large aggregates formed in EtOH (Fig. 7.2 C) and DMF (Fig. 7.2 E) where disrupted in the presence of the sugars as apparent in the decreased signal intensity, increasing the proportion of smaller aggregates. However in Te, the sugars only disrupted the aggregation when dissolved in DMF (Fig. 7.2 F). The smaller aggregates and increased proportion of dimers as indicated by ESMS (Fig. 7.1) correlated with the increased antimicrobial activity observed when the peptides where dissolved in DMF together with the sugars relative to its suppression of antimicrobial activity by the latter observed when dissolved in EtOH (Fig. 7.3). This was particularly evident in the increased antibacterial activity observed in the presence of Glc exceeding that observed in either solvent alone (Fig. 7.3 B).

The influence of the respective solvents and sugars on the identity of the higher order aggregates formed is particularly relevant to the mode of action targeting different pathogens. The bacterial membrane is proposed to be targeted by the dimeric oligomers [29,31] formed in DMF (Fig. 7.1), which are increased in the presence of Suc and particularly Glc, as deduced from the change in aggregation (Fig. 7.2) and antibacterial activity (Fig. 7.3 B). However, antifungal activity of the Trcs is probably also dependent on cell wall binding [32]. Considering the difference in recovery of antifungal activity in the presence of the two sugars (Fig. 7.3 A), it may be due to the fungal target depending on an alternate conformation induced by the different sugars to achieve maximal activity. Alternately, this may elude to a balance between interaction with the sugars in solution and the fungal cell wall as target cell structure [1].

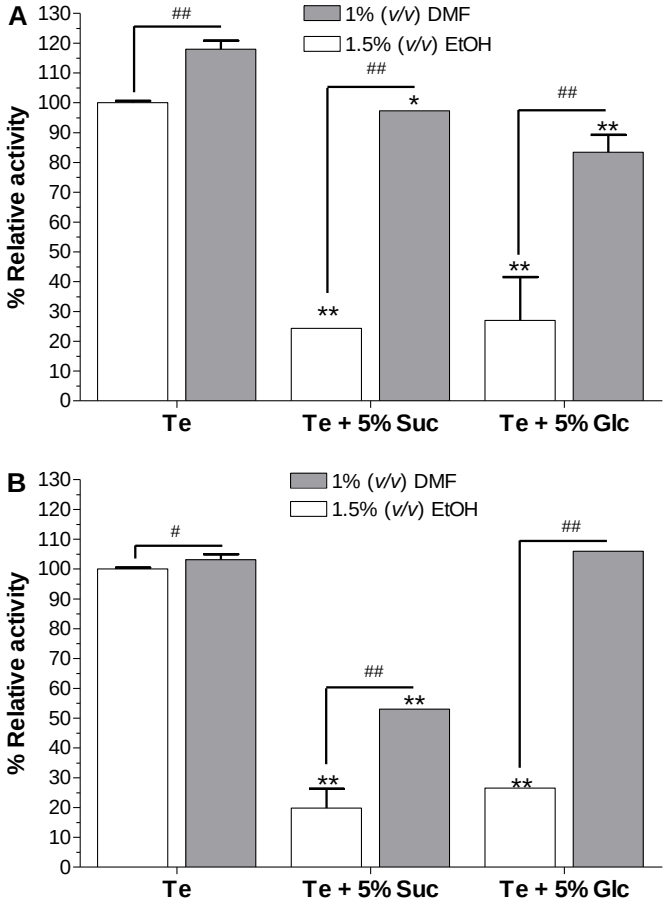

Figure 7.3 Comparison of the relative activity of Te toward **A** the representative fungi *A. fumigatus*, and **B** Gram-positive bacteria *B. subtilis*. Te was dissolved in either 1.5% EtOH or 1.0% DMF together with 5% (*m/v*) of either sucrose (Suc), glucose (Glc). IC_{max} values determined in EtOH were set as 100%. Statistical analysis was done using Bonferroni's Multiple comparison test (One Way ANOVA) with ## $P<0.001$; # $P<0.05$ when comparing formulations (with and without sugars) in the two solvents and ** $P<0.001$; * $P<0.05$ when comparing the sugar formulations relative to the respective solvents alone.

7.3.4 In vivo toxicity of the tyrothricin extract toward adult honey bees

The influence of the formulation of Te in the DMF solvent as well as the influence of different sugars on the activity and aggregation was now firmly established. The acute oral toxicity of the Te formulation, which was to be utilized within agricultural applications, was evaluated toward adult bees using methodology described in OECD guidelines [58]. Due to limitations in solubility, fresh preparations of Te were prepared from freeze dried stocks prior to feeding experiments commencing at a maximum concentration of 2500 µg/mL. Despite using concentrations of approximately 200 times the IC_{max} observed toward the representative target organisms, toxicity was not observed at any of the concentrations of Te when bees were exposed to the test compound for a period of up to six hours having consumed 44.70±1.98 µg of Te at the highest concentration (data not shown). Due to the low solubility of these peptides in water, it was not possible to increase the mass of peptide consumed within the given time frame. In an effort to increase the amount of Te consumed, bees were fed a diet of 50% (*m/v)* Suc and various Te concentrations for up to 72 hours (Fig. 7.4). The procedure for application of the DiM control, however, remained as described in OECD guidelines [58] with bees consuming 50% (*m/v)* Suc spiked with DiM at a concentration of 35 µg/mL for six hours where after the diet was replaced with 50% (*m/v)* Suc only. In conformation of the sensitivity of our experimental conditions, after the six hours of exposure bees consumed 0.48±0.04 µg of DiM (data not shown); consequently near 100% mortality was observed in the DiM control within 24 hours (Fig. 7.4 C).

A maximum concentration of Te at 1500 µg/mL was considered to prevent the influence of Te precipitation out of the feeding solution over the extended feeding period. Consumption of such high amounts of Te would be highly unlikely in a field application in light of the solubility of Te, this was purely performed as an exercise to determine at what concentration the peptide became toxic to adult honey bees. A reduction in feed volume consumed was observed in all the Te treatments barring the lowest concentration of 50 µg/mL (Fig. 7.4 A). Further emphasising how unlikely it would be for bees to consume such extremely high tyrothricin concentrations used in our attempt to determine the level of oral toxicity toward honey bees. After 48 hours of consuming a diet of only Suc and peptide, with 76 µg consumed per bee at 1500 µg/mL Te (Fig. 7.4 B), the percentage mortality was still within the levels observed in the control (Fig. 7.4 C). Considering an average mass obtained from 68

bees of 66 mg, bees consumed 1200 mg per kg body mass at 48 hours before any significant toxicity was observed at 72 hours.

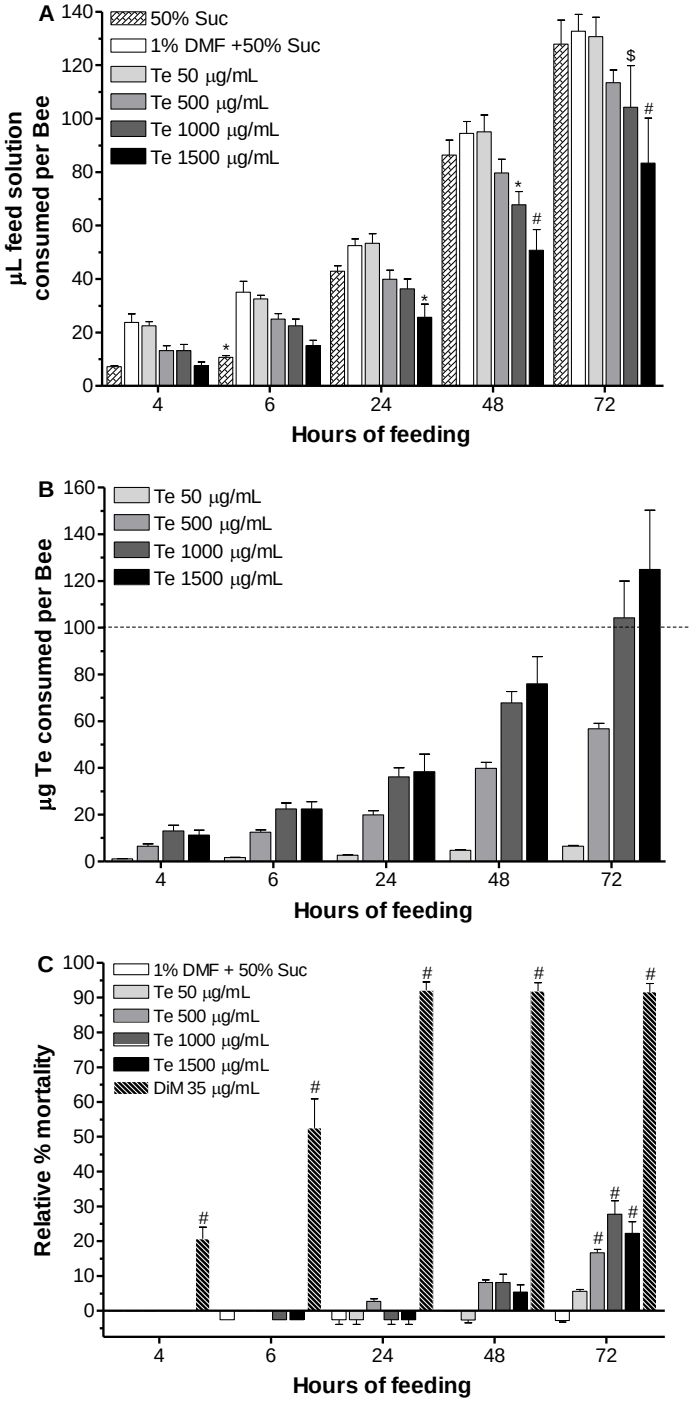

Figure 7.4 Consumption of Te by adult African honey bees relative to the 50% Suc, 1% DMF and DiM controls. **A** Volume consumed per bee in the different feeding solutions. **B** Amount of Te in µg consumed per bee in each of the respective Te containing feeding solutions. **C** The relative percentage mortality of bees observed in each of the different feeding solutions over the 72 hour feeding period corrected relative to the natural mortality in 50% Suc using Abbots correction. Statistical analysis were done using Bonferroni's Multiple comparison test (Two Way ANOVA) with # P<0.001; $ P<0.01; * P<0.05 relative to 1% DMF.

These data concur with those of numerous others in literature reporting the relative safety of the oral consumption of tyrothricin in mammals [38,39,48,75,76]. Oral dosages as high as 1000 mg per kg body mass were not toxic to mice and rats [39]. While a maximum tolerated tyrothricin dosage of 0.8 mg per mouse was found after being successively fed three times a day for 10 days [75].

At 72 hours an increase in mortality in all the conditions tested was observed, barring the 1% DMF control. At the 1000 µg/mL and 1500 µg/mL Te concentrations of in excess of 100 µg was consumed per bee and a mortality of approximately 25% was reached (Fig. 7.4 B and C). The observed toxicity only occurred when the amount of Te consumed was in the excess of 100 µg/bee (Fig. 7.4 C), the limit amount for a product to be considered safe [58]. It was postulated that the increase in mortality may have arisen due the inability of the bees to defecate, either as a result of confinement or due to damage to their digestive tract.

7.3.5 Survival in hives after tyrothricin exposure

Having observed an increase in mortality after 48 hours in honey bees fed soley a diet spiked with Te, this observed toxicity was analysed further in a semi-field trial application. A Te concentration of 1500 µg/mL was used, being the highest concentration of Te which could be maintained in the feeding solution over the extended feeding exposure to Te. After 48 hours (2 days) of caged feeding no difference in survival was observed between the bees fed 1.500 µg/mL Te relative to the 1% DMF dosing vehicle control where a survival >90% was observed (Fig 7.5).

After returning the bees to their hives of origin, retrieval of the Te fed bees was 25-75% greater than the control (Fig. 7.5). However, this difference was only statistically significant for day 20 (Fig. 7.5 A), although there were major differences between hives with some hives showing >200% retrieval of bees compared to the untreated controls (Fig. 7.5 B).

Weighing and dissection of bees after caged feeding for 48 hours, as well as those recovered from the hives showed no discernible difference between the Te fed bees relative to those of the control (data not shown). Thus, even at such extremely high concentrations, consumption of tyrothricin by adult bees was safe and may even have been to an advantage to them.

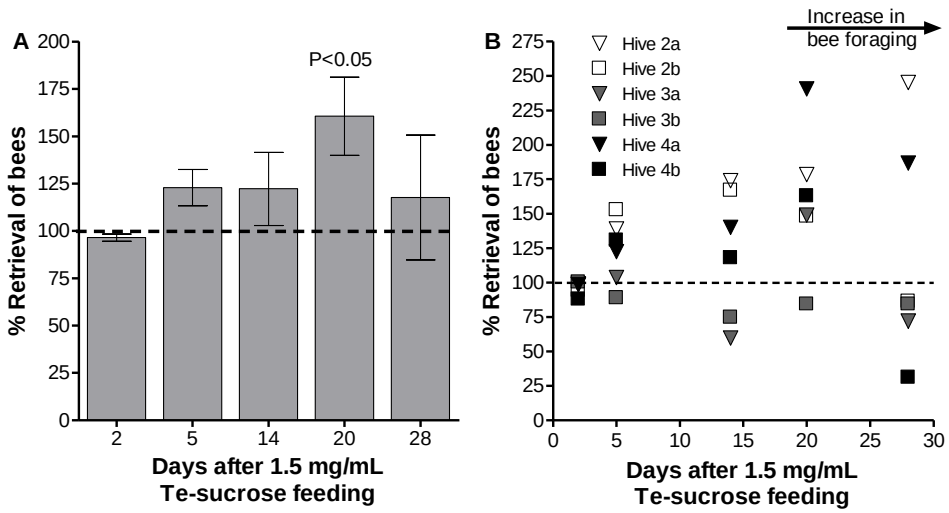

Figure 7.5 Comparison of the retrieval of African honey bees fed 1500 µg/mL Te dissolved in 50% sucrose feeding solution relative to the 1% DMF control for 2 days then returned to their hives of origin. With **A** showing the average % retrieval compared to the control and **B** the retrieval in the respective hives compared to the untreated controls. Statistical analysis was done using student t test.

7.3.6 Toxicity testing of tyrothricin extract toward bee larvae

Honey bees progress through four different developmental stages between eggs being laid by queen bee and incubation (day 1 to 3), they then develop into larvae (day 4 to 9), progress into pre-pupa (day 9 to 12), pupa (day 13 to 20) before finally emerging as adult bees (day 21) [77]. As larvae are fed by the adult bees that may have ingested Te, the toxicity of Te needed to be determined toward honey bee larvae.

To remove the influence of natural mortality, the percentage mortality was adjusted relative to that observed in the control fed the feeding solution only using Abbots correction [59] (Fig. 7.6). A concentration of 55.6 µg/mL (1.8 µg/larva) of Te was found to be the highest concentration the bee larvae could tolerate with without any toxicity, as determined relative to the percentage mortality observed in the two negative controls (Fig. 7.6). Only a single other report of the toxicity of the tyrothricin peptides toward insects exists where a concentration of 6 µM (7.62 µg/mL) of the purified tyrocidine A analogue was found to be the maximum tolerable concentration used in the successful treatment of *Candida albicans* infections in the nematode *Caenorhabditis elegans* [52]. Our results would seem to suggest that bee larvae were considerably more resilient to Te than the nematodes were to the purified single peptide.

7.3.7 Activity of peptide formulations toward honey bee pathogens causing foulbrood

In light of the low toxicity of Te toward adult bees, trend of increased survival of bees released into hives after being treated with Te and tolerance of the bee larvae to Te at a concentration of up to 55.6 µg/mL. It was questioned whether these peptides would have any potential to combat pathogens affecting honey bee larvae, as it is at these earliest, brood developmental stages while still in the hive where honey bees are most sensitive to pathogens [78]. The tyrothricin peptides had already displayed potent activity toward the opportunistic fungi *A. fumigatus* (Table 7.2, Fig. 7.3 A), one of the causative agents of stonebrood disease or aspergillosis in honey bee larvae [79]. As the next step in this direction the *in vitro* activity of Te was evaluated toward a range of bee pathogens associated with foulbrood (Table 7.3).

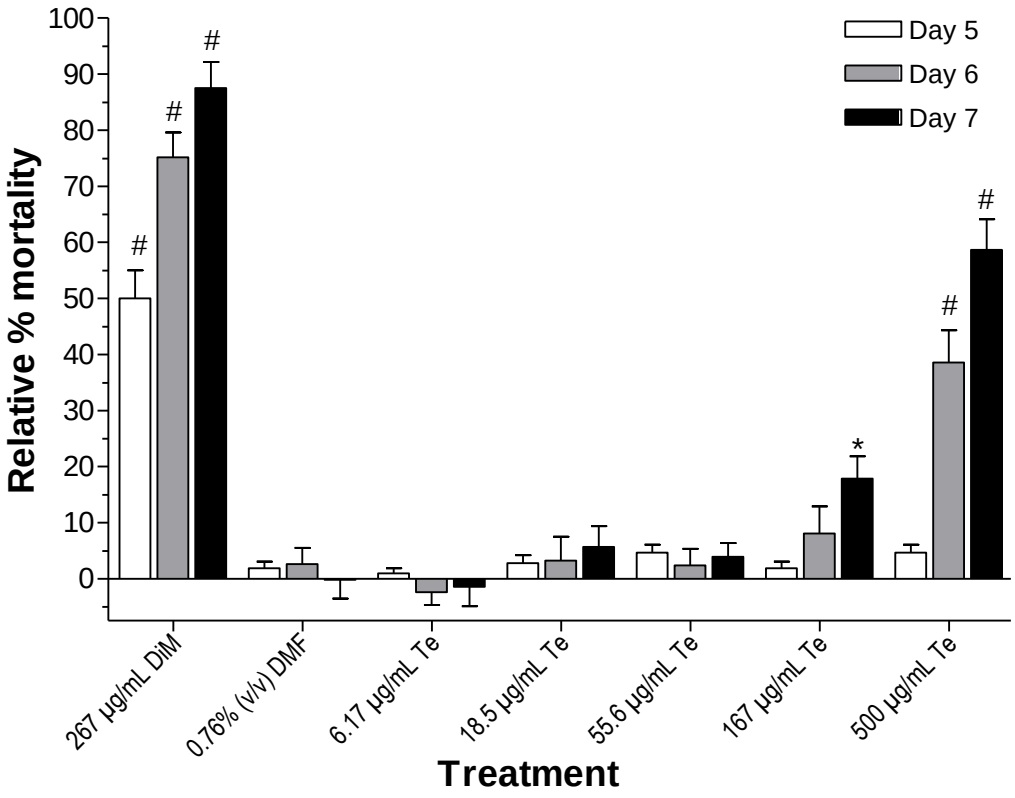

Figure 7.6 Bar graph of the relative percentage mortality of *Apis mellifera carnica* honey bee larvae after a single exposure to varied concentrations of Te together with the insecticide DiM at day 4. The percentage mortality was adjusted relative to the natural mortality observed in feeding solution only using Abbots correction [59]. Statistical analysis done using Bonferroni's Multiple comparison test (One Way ANOVA) the relative mortality after exposure to 0.76% DMF feeding vehicle was compared to each of the respective treatments at days 5, 6 and 7 # $P<0.001$; * $P<0.05$.

These included a range of different strains of *P. larvae*, the causative agents of American foulbrood [60]; *M. plutonius*, the causative agent of European foulbrood in honey bees, as well as associated secondary invaders *P. alvei* and *E. faecalis* [61]. All of the different strains of *P. larvae* where sensitive to Te, ERIC I isolate 25 and 145, as well as ERIC II isolate 1 where less sensitive. *M. plutonius*, the secondary invaders *P. alvei* and *E. faecalis*, also showed high sensitivity toward the peptide formulation. Considering the promising antimicrobial activity of Te toward these pathogens *in vitro*, it begged to question whether Te would be able to target these pathogens *in vivo*.

Table 7.3 Activity of tyrothricin extract (Te) dissolved in 1.5% ethanol toward honey bee pathogens causing foulbrood and associated secondary invaders.

Bacterial species	**Strain**	**IC_{max} (µg/mL) ±SEM**
Paenibacillus larvae	ERIC I, DSM 7030 (*n=2*)	6.25±0
	ERIC II, DSM 25430 (*n=3*)	2.73±1.8
	ERIC III, LMG 16252 (*n=3*)	2.08±0.52
	ERIC IV, LMG 16247 (*n=3*)	7.29±2.8
	ERIC I, Isolate 11 (*n=3*)	1.23±0.17
	ERIC I, Isolate 15 (*n=3*)	<<0.781
	ERIC I, Isolate 24 (*n=2*)	<<0.781
	ERIC I, Isolate 25 (*n=3*)	29.2±11
	ERIC I, Isolate 138 (*n=3*)	<<0.781
	ERIC I, Isolate 145 (*n=3*)	21.6±1.7
	ERIC II, Isolate 1 (*n=3*)	25±0
	ERIC II, Isolate 3 (*n=2*)	3.13±0
	ERIC II, Isolate 6 (*n=3*)	1.27±0.41
	ERIC II, Isolate 7 (*n=3*)	3.13±0
	ERIC II, Isolate 17 (*n=3*)	<<0.781
Melissococcus plutonius	LMG 20360 (*n=3*)	12.5±0
Paenibacillus alvei	DSM 29 (*n=2*)	1.56±0
Enterococcus faecalis	DSM 20376 (*n=3*)	8.33±2.1

7.3.8 Assessment of the potential of tyrothricin to treat infected bee larvae

Having established toxicity parameters for Te toward honey bee larvae, a concentration of 55.6 µg/mL (1.83 µg/larva) was used to establish if the promising *in vitro* activity toward *P. larvae* could be emulated *in vivo*. Larvae were infected with spores of either *P. larvae*

reference strains ERIC I (DSM 7030) or ERIC II (DSM 25430) at day 1 and treated with Te at the previously mentioned concentration on day 4 (Fig. 7.7).

It was apparent that the *in vivo* antimicrobial activity of Te toward *P. larvae* was not as high as had been observed *in vitro*. Te slowed down the rate at which the infection progressed of both strains, but was more effective at slowing down infection of ERIC II (DSM 25430) (Fig. 7.7). This was particularly evident at day 5 when there was near 60% mortality in the untreated group with Eric II infection and only 13% in the Te treated group (Fig. 7.7 B). However, Te on its own had no long term therapeutic or curative effect and a final mortality similar to that observed in the infection control was obtained toward both *P. larvae* reference strains.

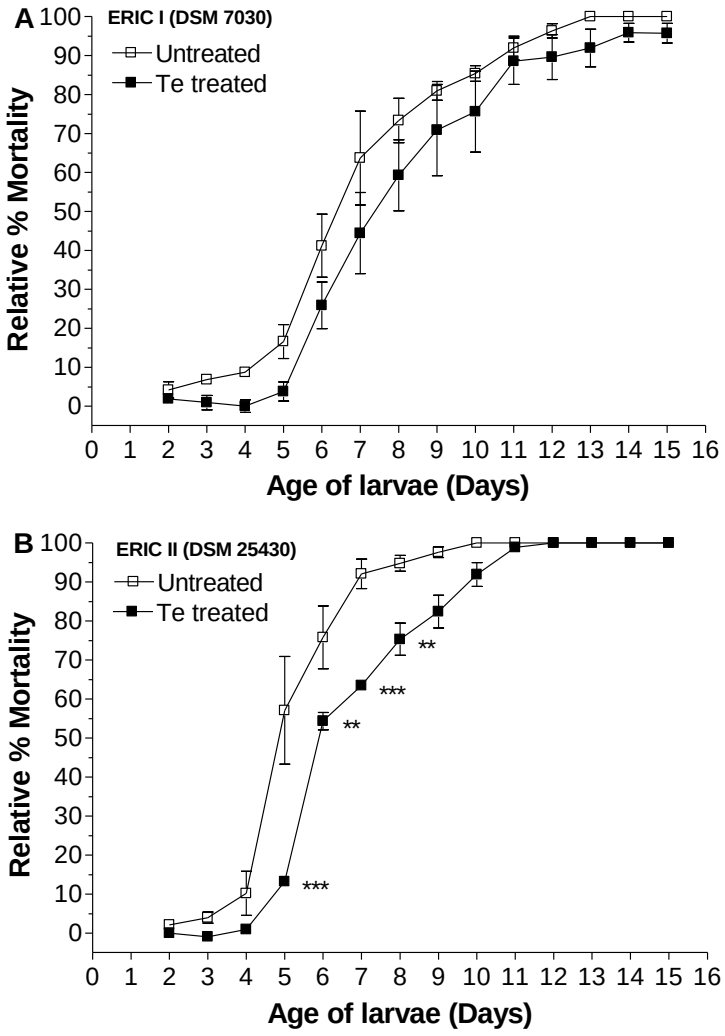

Figure 7.7 Curing assays of *Apis mellifera carnica* honey bee larvae after a single exposure of tyrocidine extract (Te) at 55.6 µg/mL (1.83 µg/larva) on day 4 after being pre exposed to *Paenibacillus larvae* spores on day 1 of either **A** ERIC I (DSM 7030) or **B** ERIC II (DSM 25430) strain. Statistical analysis was done using a Two way ANOVA and Bonferroni's post-test with *** P<0.001 and ** P<0.01.

Surviving larvae were also observed to reside for longer within the larval stage resisting transition to the pre-pupa stages of development. Moreover, those larvae which succumbed while still within the pre-pupa stage of development failed to defecate, correlating with the observation in the caged bees (data not shown). Barring a single other report of the maximum tolerable concentration the purified tyrocidine A analogue used in the successful treatment of *C. albicans* infections in the nematode *C. elegance* [52], all the rest of the reports of treatment of infections using the tyrothricin peptides are limited to mammalian systems, primarily using mouse models. Some authors have reported being able to successfully treat some strains of *Pneumococcus* and *Streptococcus* infections in mice by the oral administration of tyrothricin [75,76]. However, toward other strains of *Pneumococcus* and *Streptococcus* it slowed down the rate of infection [75].

No therapeutic effect was reported in the latter [75] or toward *Lactobacillus acidophilus* [48], despite tyrothricin displaying high antimicrobial activity *in vitro* [38,48]. The latter is similar to what was observed within our own results. While the tyrothricin peptides, Te in particular, showed potent *in vitro* activity against a broad range of bee-pathogens it was ineffective at treating pathogens in bee larvae. Therefore, despite any positive effects observed toward adult bees, it is not be recommended to use the tyrothricin peptides to treat honey bee pathogens as an additive in feeders to treat infected hives.

7.3.9 Activity of tyrothricin extracts toward beneficial gut microbiota of honey bees and larvae

To negate the any influence Te may have had on the beneficial gut microbiota of honey bees [66], exploratory *in vitro* activity assays were performed toward a range of representative bee gut microorganisms (Table 7.4).

It was apparent from these data that Te does display antimicrobial activity toward the majority of the Gram-positive and even some Gram-negative bacteria found in the gut of honey bees and larvae. Mice orally treated with tyrothricin, however, were observed to shown no change in their intestinal microbiota [38,48]. It is thus questionable whether the observed *in vitro* activity toward the gut microbiota significantly contributes toward the aberration in the observed development of the honey bee larvae, particularly when considering the lack of *in vivo* activity observed toward *P. larvae*. The inability to defecate observed in the larvae, as

well as in the adult bees after extended feeding of extremely high concentrations of Te may elude to a possible disruption in the mid to hind gut. It was postulated that this may be associated with cyclic structure of the peptides in combination their protein-like nature making them more resistant to degradation, thus resulting in an immobility of the gut and/or constipation.

Table 7.4 Antimicrobial activity of Te toward a representative sample of the gut microbiota of the honey bee

Bacterial species	IC_{max}
Gram-positive	
Bacillus megaterium LMG 7127	18.5
B. pumilus LMG 3455	15.3
B. subtilis LMG 2099	21.1
Brevibacillus borstelensis DSM 6347	>100
Planococcus maritimus DSM 17275	15.9
Staphylococcus pasteuri DSM 30868	10.3
Streptomyces griseus DSM 1471	10.8
Gram-negative	
Comamonas denitrificans LMG 21602	47.9
Delftia acidovorans LMG 1226	>100
Gluconobacter oxydans DSM 2003	>100
Janthinobacterium lividum LMG 2892	>100
Pedobacter africanus LMG 10345	76.6
Planomicrobium okeanokoites DSM 15489	>100
Pseudomonas fluorescens DSM 6147	>100
Ralstonia Picketti LMG 5342	.>100
Saccharibacter floricola LMG 23170	19. 3
Salmonella enterica DSM 11320	>100

7.4 Conclusions

In light of the promising antimicrobial activity of the tyrocidines to treat pathogens in the agricultural and food industries, the safety of utilising these peptides within an agricultural environment was assessed by determining their toxicity toward honey bees, which served as a corner stone, representative non-target beneficial organism. The culture extracts of tyrothricin, Te, which were to be used in the proposed agricultural applications, aggregation and antimicrobial activity were investigated in the DMF solvent as well as various sugars used to test their toxicity toward honey bees. The parameters obtained from the latter formulation were compared to those in EtOH, the solvent used in the application of these

peptides. Due to the complex nature of Te it is necessary to study the influence of different additives in purified Tc formulation allowing some deductions to be made regarding the influence of the culture pigment, as well as the linear gramicidins in Te.

The formulation of the tyrothricin peptides for application toward honey bees has brought the potential of different solvents such as DMF to light. Future work would entail exploring the formulation of the tyrothricin peptides in different solvent environments to optimise their activity in different applications. In DMF an increase in the prevalence of the dimeric form was observed relative to the monomeric form detected in EtOH (Fig 7.1). The dimeric form of the tyrocidines is shown be the active form of the peptides in their membranolytic mode of action when targeting bacteria [29,31]. Increased antimicrobial activity when dissolved in DMF was attributed to the sugars having a further chaotropic effect on the aggregates formed in the pre-incubated peptide formulations by disrupting the hydrogen bonding networks (refer to Chapter 5) and consequently increasing the formation of the more favourable dimeric oligomeric structures [29,31]. Over all, the slight reduction in antimicrobial activity of Te relative to Tc in the two respective solvents (Table 7.2) may be attributed to the antagonistic effect of the co-extracted linear gramicidins [80] and lower purity of the samples. It was however postulated that the culture pigments have a chaotropic effect on aggregation and thereby influence the antimicrobial activity and toxicity of Te. Similarly, the culture pigment was postulated to also have a modulatory effect on the toxicity of Te, however, this needs to be investigated further before definitive conclusions can be made.

The reduced toxicity of Te toward insect cells supports the very low toxicity of Te observed toward adult honey bees. Using concentrations of approximately 200 times the IC_{max} observed toward the representative target organisms, no influence of the peptide was observed toward the bees fed for the conventional six hours proposed in the usual toxicity testing [58]. Due to the low solubility of these peptides in water, mortality in adult bees only occurred when they were exclusively fed Te for extended time periods. These mortalities occurred at extremely high concentrations of tyrothricin which would be unattainable by bees foraging within a natural environment. Even if bees were to be drenched with the peptide solution during application, their low solubility in water would limit the exposure to minute amounts. Moreover, due to their hydrophobic nature, these peptides adhere very strongly to surfaces [81] and would therefore further limit any exposure that may occur to larvae after application. It is therefore concluded that the tyrothricin peptides have a very low toxicity toward honey

bees and would be extremely unlikely to cause an adverse effect toward them when applied within agricultural applications.

This study showed the safety of the application of Te in agricultural settings as it was found to generally be non-toxic to adult bees, while their larvae were resilient to high levels of the Te formulation (Fig. 7.6). The potent *in vitro* antimicrobial activity observed toward *P. larvae* unfortunately did not result in curing of *P. larvae* infected bee larvae in *in vivo* assays (Fig. 7.7). Treatment with Te only slowed down the progression of the infection and had little or no long term therapeutic effect on its own. Therefore, despite any positive effects observed toward adult bees, the use of the tyrothricin peptides as an additive in feeders is not recommended to treat hives infected with honey bee pathogens, particularly those affecting their larval developmental stages.

7.5 References

1. Troskie, A. M., de Beer, A., Vosloo, J. A., Jacobs, K. and Rautenbach, M. (2014) Inhibition of agronomically relevant fungal phytopathogens by tyrocidines, cyclic antimicrobial peptides isolated from *Bacillus aneurinolyticus*. Microbiology **160**, 2089-20101
2. Rautenbach, M., Troskie, A. M., De Beer, A. and Vosloo, J. A. (2013) Antimicrobial peptide formulations for plants. WO/2013/150394 A1, P2366CN00 China (TBA, 21/10/2014); P2366EP00 Europe (13717558.4, 22/09/2014); P2366IN00 India (1963/KOLNP/2014; 16/09/2014); P2366US00 United States (14380518, 22/08/2014); P2366ZA01South Africa (2014/06499; 04/09/2014)
3. Buchmann, S. L. and Nabhan, G. P. (1997) The forgotten pollinators. Island Press
4. Costanza, R., d'Arge, R., De Groot, R., Farber, S., Grasso, M., Hannon, B., Limburg, K., Naeem, S., O'neill, R. V. and Paruelo, J. (1998) The value of the world's ecosystem services and natural capital. Ecol. Econ. **1**, 3-15
5. Klein, A. M., Vaissiere, B. E., Cane, J. H., Steffan-Dewenter, I., Cunningham, S. A., Kremen, C. and Tscharntke, T. (2007) Importance of pollinators in changing landscapes for world crops. Proc. Biol. Sci. **274**, 303-313
6. Brown, M. J. and Paxton, R. J. (2009) The conservation of bees: A global perspective. Apidologie **40**, 410-416
7. Pettis, J. S., Lichtenberg, E. M., Andree, M., Stitzinger, J., Rose, R. and Vanengelsdorp, D. (2013) Crop pollination exposes honey bees to pesticides which alters their susceptibility to the gut pathogen *Nosema ceranae*. PLoS One **8**, e70182
8. Montesinos, E. (2007) Antimicrobial peptides and plant disease control. FEMS Microbiol. Lett. **270**, 1-11.

9. Dubos, R. J. (1939) Studies on a bactericidal agent extracted from a soil *Bacillus*: I. Preparation of the agent. Its activity *in vitro*. J. Exp. Med. **70**, 1-10

10. Dubos, R. J. and Hotchkiss, R. D. (1941) The production of bactericidal substances by aerobic sporulating *Bacilli*. J. Exp. Med. **73**, 629-640

11. Dubos, R. J. and Hotchkiss, R. (1942) Origin, nature and properties of gramicidin and tyrocidine. Trans. Coll. Physicians Phila. **10**, 11-19

12. Hotchkiss, R. D. and Dubos, R. J. (1941) The isolation of bactericidal substances from cultures of *Bacillus brevis*. J. Biol. Chem. **141**, 155-162

13. Zasloff, M. (2002) Antimicrobial peptides of multicellular organisms. Nature **415**, 389-395

14. Hancock, R. E. W. and Lehrer, R. (1998) Cationic peptides: A new source of antibiotics. Trends Biotechnol. **16**, 82-88

15. Rautenbach, M. and Hastings, J. (1999) Cationic peptides with antimicrobial activity: The new generation of antibiotics? Chimica oggi **17**, 81-89

16. Waksman, S. A. (1945) Microbial antagonisms and antibiotic substances. Soil Sci. **59**, 482

17. Pusey, P. and Wilson, C. (1984) Postharvest biological control of stone fruit brown rot by *Bacillus subtilis*. Plant Dis. **68**, 753-756

18. Pusey, P. L. (1989) Use of *Bacillus subtilis* and related organisms as biofungicides. Pestic. Sci. **27**, 133-140

19. Asaka, O. and Shoda, M. (1996) Biocontrol of *Rhizoctonia solani* damping-off of tomato with *Bacillus subtilis* RB14. Appl. Environ. Microbiol. **62**, 4081-4085

20. Chandel, S., Allan, E. J. and Woodward, S. (2010) Biological control of *Fusarium oxysporum* f. sp. *lycopersici* on tomato by *Brevibacillus brevis*. J. Phytopathol. **158**, 470-478

21. Che, J., Liu, B., Ruan, C., Tang, J. and Huang, D. (2015) Biocontrol of *Lasiodiplodia theobromae*, which causes black spot disease of harvested wax apple fruit, using a strain of *Brevibacillus brevis* FJAT-0809-GLX. Crop Prot. **67**, 178-183

22. Joo, H. J., Kim, H., Kim, L., Lee, S., Ryu, J. and Lee, T. (2015) A *Brevibacillus* sp. antagonistic to mycotoxigenic *Fusarium* spp. Biol. Control **87**, 64-70

23. Ongena, M., Jourdan, E., Adam, A., Paquot, M., Brans, A., Joris, B., Arpigny, J. and Thonart, P. (2007) Surfactin and fengycin lipopeptides of *Bacillus subtilis* as elicitors of induced systemic resistance in plants. Environ. Microbiol. **9**, 1084-1090

24. Gutiérrez-Mañero, F. J., Ramos-Solano, B., Probanza, A., Mehouachi, J., R Tadeo, F. and Talon, M. (2001) The plant-growth-promoting rhizobacteria *Bacillus pumilus* and *Bacillus licheniformis* produce high amounts of physiologically active gibberellins. Physiol. Plantarum. **111**, 206-211

25. Gueldner, R. C., Reilly, C. C., Pusey, P. L., Costello, C. E., Arrendale, R. F., Cox, R. H., Himmelsbach, D. S., Crumley, F. G. and Cutler, H. G. (1988) Isolation and identification of iturins as antifungal peptides in biological control of peach brown rot with *Bacillus subtilis*. J. Agric. Food Chem. **36**, 366-370

26. Hayat, R., Ali, S., Amara, U., Khalid, R. and Ahmed, I. (2010) Soil beneficial bacteria and their role in plant growth promotion: A review. Ann. Microbiol. **60**, 579-598

27. Compant, S., Duffy, B., Nowak, J., Clement, C. and Barka, E. A. (2005) Use of plant growth-promoting bacteria for biocontrol of plant diseases: Principles, mechanisms of action, and future prospects. Appl. Environ. Microbiol. **71**, 4951-4959

28. Bashan, Y. (1998) Inoculants of plant growth-promoting bacteria for use in agriculture. Biotechnol. Adv. **16**, 729-770

29. Loll, P. J., Upton, E. C., Nahoum, V., Economou, N. J. and Cocklin, S. (2014) The high resolution structure of tyrocidine A reveals an amphipathic dimer. BBA-Biomembranes **1838**, 1199-1207

30. Yeaman, M. R. and Yount, N. Y. (2003) Mechanisms of antimicrobial peptide action and resistance. Pharmacol. Rev. **55**, 27-55.

31. Munyuki, G., Jackson, G. E., Venter, G. A., Kövér, K. E., Szilágyi, L., Rautenbach, M., Spathelf, B. M., Bhattacharya, B. and van der Spoel, D. (2013) β-Sheet structures and dimer models of the two major tyrocidines, antimicrobial peptides from *Bacillus aneurinolyticus*. Biochemistry **2**, 7798-7806

32. Troskie, A. M. (2014) Tyrocidines, cyclic decapeptides produced by soil *Bacilli*, as potent inhibitors of fungal pathogens. Stellenbosch University, Department of Biochemistry, Stellenbosch, South Africa. **PhD. Thesis** http://hdl.handle.net/10019.1/86162

33. Seddon, B. and Fynn, G. (1973) Energetics of growth in a tyrothricin-producing strain of *Bacillus brevis*. Microbiology **74**, 305-314

34. Schazschneider, B., Ristow, H. and Kleinkauf, H. (1974) Interaction between the antibiotic tyrocidine and DNA *in vitro*. Nature **249**, 757-759

35. Bohg, A. and Ristow, H. (1987) Tyrocidine-induced modulation of the DNA conformation in *Bacillus brevis*. Eur. J. Biochem. **170**, 253-258

36. Bohg, A. and Ristow, H. (1986) DNA- supercoiling is affected *in vitro* by the peptide antibiotics tyrocidine and gramicidin. Eur. J. Biochem. **160**, 587-591

37. Park, S., Park, Y. and Hahm, K. (2011) The role of antimicrobial peptides in preventing multidrug-resistant bacterial infections and biofilm formation. Int. J. Mol. Sci. **12**, 5971-5992

38. Rammelkamp, C. H. and Weinstein, L. (1942) Toxic effects of tyrothricin, gramicidin and tyrocidine. J. Infect. Dis. **71**, 166-173

39. Robinson, H. J. and Molitor, H. (1942) Some toxicological and pharmacological properties of gramicidin, tyrocidine and tyrothricin. J. Pharmacol. Exp. Ther. **74**, 75-82

40. Herrell, W. E. and Heilman, D. (1943) Tissue culture studies on the cytotoxicity of bactericidal agents: I. Effects of gramicidin, tyrocidine and penicillin on cultures of mammalian lymph node. Am. J. Med. Sci. **205**, 157-162

41. Herrell, W. E. and Heilman, D. (1941) Experimental and clinical studies on gramicidin. J. Clin. Invest. **20**, 583-591.

42. Mann, F. C., Heilman, D. and Herrell, W. E. (1943) Effect of serum on haemolysis by gramicidin and tyrocidine. Exp. Biol. Med. **52**, 31-33

43. Rammelkamp, C. H. and Weinstein, L. (1941) Haemolytic effect of tyrothricin. Exp. Biol. Med. **48**, 211-214

44. Wigger-Alberti, W., Stauss-Grabo, M., Grigo, K., Atiye, S., Williams, R. and Korting, H. C. (2013) Efficacy of a tyrothricin-containing wound gel in an abrasive wound model for superficial wounds. Skin Pharmacol. Physiol. **26**, 52-56.

45. Henderson, J. (1946) The status of tyrothricin as an antibiotic agent for topical application. J. Am. Pharm. Assoc. **35**, 141-147

46. Goldman, L., Feldman, M. D. and Altemeier, W. A. (1948) Contact dermatitis from topical tyrothricin and associated with polyvalent hypersensitivity to various antibiotics 1. J. Invest. Dermatol. **11**, 243-244

47. Rankin, L. (1944) The use of tyrothricin in the treatment of ulcers of the skin. Am. J. Surg. **65**, 391-392

48. Weinstein, L. and Rammelkamp, C. H. (1941) A study of the effect of gramicidin administered by the oral route. Exp. Biol. Med. **48**, 147-149

49. Richards, R. M. E. and Xing, D. K. (1993) *In vitro* evaluation of the antimicrobial activities of selected lozenges. J. Pharm. Sci. **82**, 1218-1220

50. Kagan, G., Huddlestone, L. and Wolstencroft, P. (1982) Two lozenges containing benzocaine assessed in the relief of sore throat. J. Int. Med. Res. **10**, 443-446

51. Dubos, R. J. (1939) Studies on a bactericidal agent extracted from a soil *Bacillus*: II. Protective effect of the bactericidal agent against experimental *Pneumococcus* infections in mice. J. Exp. Med. **70**, 11-17

52. Troskie, A. M., Rautenbach, M., Delattin, N., Vosloo, J. A., Dathe, M., Cammue, B. P. and Thevissen, K. (2014) Synergistic activity of the tyrocidines, antimicrobial cyclodecapeptides from *Bacillus aneurinolyticus*, with amphotericin B and caspofungin against *Candida albicans* biofilms. Antimicrob. Agents Chemother. **58**, 3697-3707

53. Govan, V. A., Allsopp, M. H. and Davison, S. (1999) A PCR detection method for rapid identification of *Paenibacillus larvae*. Appl. Environ. Microbiol. **65**, 2243-2245

54. Troskie, A. M., Vlok, N. M. and Rautenbach, M. (2012) A novel 96-well gel-based assay for determining antifungal activity against filamentous fungi. J. Microbiol. Methods. **91**, 551-558.

55. Du Toit, E. and Rautenbach, M. (2000) A sensitive standardised micro-gel well diffusion assay for the determination of antimicrobial activity. J. Microbiol. Methods **42**, 159-165

56. Lehrer, R. I., Rosenman, M., Harwig, S. S. S. L., Jackson, R. and Eisenhauer, P. (1991) Ultrasensitive assays for endogenous antimicrobial polypeptides. J. Immunol. Methods **137**, 167-173

57. Rautenbach, M., Gerstner, G. D., Vlok, N. M., Kulenkampff, J. and Westerhoff, H. V. (2006) Analyses of dose-response curves to compare the antimicrobial activity of

model cationic α-helical peptides highlights the necessity for a minimum of two activity parameters. Anal. Biochem. **350**, 81-90

58. OECD (1998), Test No. 213: Honeybees, Acute Oral Toxicity Test, OECD Guidelines for the Testing of Chemicals, Section 2, OECD Publishing, Paris. http://dx.doi.org/10.1787/9789264070165-en

59. Abbott, W. (1925) A method of computing the effectiveness of an insecticide. J. Econ. Entomol. **18**, 265-267

60. Genersch, E., Forsgren, E., Pentikainen, J., Ashiralieva, A., Rauch, S., Kilwinski, J. and Fries, I. (2006) Reclassification of *Paenibacillus larvae* subsp. *pulvifaciens* and *Paenibacillus larvae* subsp. *larvae* as *Paenibacillus larvae* without subspecies differentiation. Int. J. Syst. Evol. Microbiol. **56**, 501-511.

61. Forsgren, E. (2010) European foulbrood in honey bees. J. Invertebr. Pathol. **103**, S5-S9

62. OECD (2013), Test No. 237: Honey Bee (*Apis Mellifera*) Larval Toxicity Test, Single Exposure, OECD Guidelines for the Testing of Chemicals, Section 2, OECD rearing *Apis mellifera*. B. Insectol. **57**, 107-111

64. Lüken, D. J., Janke, M., Lienau, F., von der Ohe, W. and Forster, R. (2012) Weiterentwicklung einer methode zur bienenbruthaltung unter laborbedingungen. J. Verbrauch. Lebensm. **7**, 141-145

65. Beims, H., Wittmann, J., Bunk, B., Sproer, C., Rohde, C., Gunther, G., Rohde, M., von der Ohe, W. and Steinert, M. (2015) *Paenibacillus larvae*-directed bacteriophage HB10c2 and its application in American foulbrood-affected honey bee larvae. Appl. Environ. Microbiol. **81**, 5411-5419

66. Mohr, K. I. and Tebbe, C. C. (2006) Diversity and phylotype consistency of bacteria in the guts of three bee species (*Apoidea*) at an oilseed rape field. Environ. Microbiol. **8**, 258-272

67. Spathelf, B. M. and Rautenbach, M. (2009) Anti-listerial activity and structure-activity relationships of the six major tyrocidines, cyclic decapeptides from *Bacillus aneurinolyticus*. Bioorg. Med. Chem. **17**, 5541-5548

68. Leussa, A. N. and Rautenbach, M. (2014) Detailed SAR and PCA of the tyrocidines and analogues towards leucocin A-Sensitive and leucocin A-Resistant *Listeria monocytogenes*. Chem. Biol. Drug Des. **84**, 543-557

69. Spathelf, B. M. (2010) Qualitative structure-activity relationships of the major tyrocidines, cyclic decapeptides from *Bacillus aneurinolyticus.* Stellenbosch University, Department of Biochemistry, Stellenbosch, South Africa. **PhD. Thesis** http://hdl.handle.net/10019.1/4001

70. Leussa, N. A. (2014) Characterisation of small cyclic peptides with antilisterial and antimalarial activity. Stellenbosch University, Department of Biochemistry, Stellenbosch, South Africa. **PhD. Thesis** http://hdl.handle.net/10019.1/86161

71. Ruttenberg, M. A., King, T. P. and Craig, L. C. (1965) The use of the tyrocidines for the study of conformation and aggregation behaviour. J. Am. Chem. Soc. **87**, 4196-4198

72. Stern, A., Gibbons, W. A. and Craig, L. C. (1969) Effect of association on the nuclear magnetic resonance spectra of tyrocidine B. J. Am. Chem. Soc. **91**, 2794-2796

73. Ruttenberg, M. A., King, T. P. and Craig, L. C. (1966) The chemistry of tyrocidine. VII. Studies on association behaviour and implications regarding conformation. Biochemistry **5**, 2857-2864

74. Dimick, K. P. (1951) The haemolytic action of gramicidin and tyrocidine. Proc. Soc. Exp. Biol. Med. **78**, 782-784

75. Kolmer, J. A. and Rule, A. M. (1946) Toxicity and therapeutic activity of tyrothricin by oral administration. Proc. Soc. Exp. Biol. Med. **63**, 315-317

76 Dubos, R. J. and Cattaneo, C. (1939) Studies on a bactericidal agent extracted from a soil *Bacillus*: III. Preparation and activity of a protein-free fraction. J. Exp. Med. **70**, 249

77. Jay, S. C. (1963) The development of honeybees in their cells. J. Apic. Res. **2**, 117-134

78. Genersch, E. (2010) American foulbrood in honeybees and its causative agent, *Paenibacillus larvae*. J. Invertebr. Pathol. **103**, S10-S19

79. Foley, K., Fazio, G., Jensen, A. B. and Hughes, W. O. (2012) Nutritional limitation and resistance to opportunistic *Aspergillus* parasites in honey bee larvae. J. Invertebr. Pathol. **111**, 68-73

80. Aranda, F. J. and De Kruijff, B. (1988) Interrelationships between tyrocidine and gramicidin A′ in their interaction with phospholipids in model membranes. Biochim. Biophys. Acta. **937**, 195-203

81. Van Rensburg, W. (2015) Characterization of natural antimicrobial peptides adsorbed to different matrices. Stellenbosch University, Department of Biochemistry, Stellenbosch, South Africa. **MSc. Thesis** http://hdl.handle.net/10019.1/97929

Chapter 8
Conclusions and recommendations for future studies

8.1 Introduction

The potential cyclodecapeptides produced by *Bacillus aneurinolyticus*, namely the tyrocidine and their analogues (Trcs), to target a broad range of pathogens was recognised through work performed by previous members of our group [1-4]. These cyclodecapeptides are shown to be able to target a broad range of pathogens, including the malaria virus *Plasmodium falciparum* [2,5,6]. It is their ability to efficiently target Gram-positive bacteria [3,4], and especially fungi [7-11], which makes them particularly attractive as so-called green-biocides. However, potent antimicrobial activity is found to be dependent on properties of the target cell, as well as those of the different cyclodecapeptides [1-4].

The goal of the present study was to elucidate the optimal conditions that would allow for the large scale production of target-specific subsets of these cyclodecapeptides and economical downstream purification of the peptide mixtures and single peptides (Chapters 2-4). The produced cyclodecapeptide mixtures/formulations were investigated to elucidate some parameters which may allow for optimisation to target different agricultural and/or food related pathogens/problem organisms (Chapter 5-6). Initial formulation parameters were evaluated together with the relative safety of their application within an agricultural setting by determining their *in vivo* toxicity toward honey bees, as a representative non-target insect species (Chapter 7).

8.2 Summary of findings and future work

8.2.1 Manipulation of the tyrothricin production profile

Supplementation of the growth media of the producer organism with Phe or Trp causes a shift in its antimicrobial peptide production profile. This was of particular importance as previous work by our group had illustrated variable antimicrobial activity of the different cyclodecapeptides towards different target organisms [2-7,12]. The more polar Trcs, TrcB and TrcC, containing an increased number of Trp residues together with Tyr^7 in their

structure, were more active toward Gram-positive bacteria [4,5]. Initial studies using the six major Trc analogues showed the more non-polar analogue TrcA containing Phe rich moieties had greater activity toward the human malaria parasite, *Plasmodium falciparum* [2]. Subsequent studies, using an extended peptide library of the Trcs also showed TpcC, containing Trp at all the variable aromatic amino acid positions, to also have high activity [6].

This shift in cyclodecapeptide production was first characterised by the change in aromatic amino acid occupancy of the variable dipeptide unit (position 3 and 4), while also evaluating the influence of supplementation of these two amino acids on the growth and total tyrothricin production of the producer organism (Chapter 2). Through supplementation with only Phe or Trp it was possible to shift the tyrocidine and analogue production profile between two extremes in terms of occupancy of the variable dipeptide unit producing two distinct cyclodecapeptide subsets, namely the A (Ff) and C (Ww) analogues. Supplementation using defined ratios of Phe/Trp resulted in a gradual shift in the occupancy of the variable dipeptide unit.

Subsequently the change in amino acid occupancy at position 7, occupied by Phe, Trp or Tyr, was also included in the analysis (Chapter 3). This revealed a shift in the cyclodecapeptide production profile toward the predominantly tryptocidines containing Trp^7 in Trp supplemented culture media. Co-supplementation with Phe allowed a change in the aromatic amino acid occupancy of positions 3 and 4, but not 7. Tyr occupied position 7 only at low Trp concentrations. Occupancy of position 7 by Phe only occurred at very high Phe/Trp ratios, then only contributing to about 25% of the total cyclodecapeptide production. Using these data together with kinetic parameters obtained from literature [13], a competitive binding model was constructed which eloquently described this shift in cyclodecapeptide production (Chapter 3). This model may be used to predict the cyclodecapeptides which will be produced with different Phe/Trp ratios in the culture medium, enabling the production of selected cyclodecapeptides and tailored mixtures which are aimed at targeting different pathogens.

The control of cyclodecapeptide production offered by this model may be enhanced through the use of a base media which does not contain any background amino acids that can influence the peptide production profile. The challenge the latter scenario presents would be the appreciable production in such small volumes as to allow for high throughput screening of a range of different amino acid concentrations at the same time, as was done in this study.

Current work in progress by members of our group has shown potential to expand the amino acids used to shift the cyclodecapeptide production profile to include un-natural analogues which are also incorporated into the backbone structure by the producer organism.

8.2.2 Production and purification of the tyrocidines and analogues

The use of the Trcs as green-biocides is dependent on their production being consistent and of sufficient yield and purity. Increased production was achieved in stationary flask cultures using optimised production media. Efforts to produce tyrothricin in appreciable amounts by aerated submerged culturing in bioreactors were unsuccessful and in general high growth, but low tyrothricin production was achieved. The latter was probably because the culturing did not lead the induction of tyrothricin synthesis. Tyrothricin synthesis is induced after the logarithmic growth phase [14,15,15,16] due to metabolic stress which may include a range of factors ranging from oxygen limitation to nutrient starvation [17]. It was concluded that the stress signal in flask cultures was oxygen limitation, while sufficient nutrients where still available, allowing increased tyrothricin production by the bacterial producers over an extended time. In the fast growing submerged cultures, nutrients where depleted before the producers where sufficiently induced to produce secondary metabolites. Due to the nature of the control of tyrothricin production, high production by submerged culturing is not readily achieved using growth media containing a high nutrient values and complex nitrogen sources. Successful tyrothricin production within submerged cultures, using defined minimal media containing simple nitrogen sources [18-20], is well below that observed in stationary cultures. It is thus questionable whether tyrothricin production by submerged culturing would yield sufficient product at a cost which would make it feasible for agricultural or industrial applications.

The high tyrothricin yields obtained from the flask cultures contained a proportion of co-extracted contaminants. Two purification methodologies where developed and/or optimised to purify the tyrothricin peptides from the organic solvent extracts obtained from the biomass. The first purification methodology (PM_1) involved manipulation of the solubility of the tyrothricin peptides, its main limitation was the number of arduous handling steps required to change solution. Consequently, a second purification methodology (PM_2) using column chromatography was developed with reduced number of handling steps. Both these methodologies yielded a product of increased peptide content containing ~75% (*m/m*) of

tyrocidines. These extracts where utilised successfully in *in vivo* field trials on a variety of plants by members of our group, as well as *in vivo* toxicity assays toward honey bees and their larvae in this study (Chapter 7). These studies indicated the potential of the application of these peptides in agricultural applications. Future work would entail upscaling of current production and purification methodologies so as to allow for large scale application.

Using the knowledge gained in shifting the cyclodecapeptide production profile (Chapter 2-3), greatly eased the downstream purification using selected semi-preparative HPLC methodology. Several selected culture extracts were purified further in order to obtain the major Trcs for utilisation in more detailed bio-activity and biophysical studies. After a single round of purification, more than 330 mg of peptide with purity >90% was obtained (TrcA, TrcC, TpcC); while 220 mg of peptide that was >80% enriched in one peptide was used in further purifications (TrcB, TpcA, PhcA). TpcB was the only major analogue produced in increased quantities which could not be purified due to co-elution with TrcA. Subsequent purifications of TpcB have been successful by members of our group using cultures lacking TrcA, despite greatly reduced abundance of TpcB in these cultures (personal communication W. Laubscher). This illustrated the importance of culture selection in the purification of different analogue. However, purification yields obtained in this study greatly exceeded those attained by previous members of our group using the commercial tyrocidine extract [5].

8.2.3 Structure and oligomerisation relationships of the six major cyclodecapeptides

The relationship between oligomerisation and primary structure was investigated using the six major cyclodecapeptides produced under the different culturing conditions in Chapter 5. The antibacterial activity of the Trcs is proposed to be reliant on their oligomerisation into active dimeric structures which allow for optimal interaction with membrane targets [21,22]. Differences in the primary structures of the different cyclodecapeptides, which arise due to changes in the identity of the amino acids at the three variable aromatic positions, influenced their conformation and character by altering the distribution of different amino acid side chains and thereby tweaking the backbone conformation. Ultimately, this determines the character of the monomeric peptide in relation to: amphipathicity, surface area occupied by charged residues and their ability to partake in non-covalent interactions. This will in turn

dictate the conformation of aggregates as well as the propensity to form higher order structures [5,12,23-25].

A distinct separation was observed between the characteristics of the A and C analogues containing Phe^3, Phe^4 or Trp^3, Trp^4 respectively in the variable dipeptide unit. Increased hydrophobicity was found to be associated with increased dimerization particularly by the A (Ff) analogues. TrcB with Trp^3, Phe^4 as an intermediate between the A and C analogues tended to have characteristics of both, or at times did not associate with either of the two peptide trends. This was demonstrated by the proportions of higher order structures formed, as well as the changes in backbone conformation deduced from the ellipticity ratio within different solvent environments in circular dichroism (CD) studies.

Variation of the aromatic amino acid between Tyr^7, Phe^7 or Trp^7 altered the character of the different analogues as shown by the diverse character of the three different A analogues. While the C analogues and TrcB containing Trp^3 show variable higher ordered structure formation, they exemplify a balance of the influence of the three variable aromatic amino acids acting to alter the conformation and character of different analogues.

Glucose was found to have a chaotropic effect on TrcB>PhcA>>TrcA reducing higher ordered structure formation detected by CD, which indicated a role of a conformation adopted when Phe^4 together with Tyr^7 or Phe^7. The difference in fluorescent yields of the various Trp containing Trcs in water or trifluoroethanol, as well as variable influence of glucose on the different analogues, indicates a changes in conformation that is the result of an interplay between the three variable aromatic residues. Consequently, while there are certain similarities in the structures of the different cyclodecapeptides, they each have different characteristics determined by their variable structures.

The concept of “One model fits all” for the tyrothricin-derived cyclodecapeptides, is not possible as a consequence of their structural variability. Some adjustments have to be made to, for example, the model structure and membrane interaction proposed by Loll *et al*. [22] for dimers of TrcA. Moreover, the observed higher order structure of the cyclodecapeptides in this study together with observations in literature [23,25-27] correlate with the model proposed by Munyuki *et al.* [21]. This model proposed that the Trcs can for pore structures *via* oligomerization and we recently directly observed the formation of ion-conducting pores

by the Trcs in a variety of model membranes (unpublished results in collaboration with Dr. E. Zaitseva, University of Freiburg).

8.2.4 Oligomerisation-activity relationships of the six major cyclodecapeptides

A shift in the oligomerisation pattern was observed when the single cyclodecapeptides where combined into selected co-produced pairs. In single peptides, a tendency of increased oligomerization of the more hydrophobic single peptides was observed forming predominantly dimers together with larger aggregates up to pentamers. In combinations of the co-produced peptide pairs, dimers where the predominant oligomeric species formed with trimers being the largest structure detected using ESMS. A general trend of dimer populations being composed of heterodimers of the two cyclodecapeptides was observed for all combinations; except those involving TrcB where homodimers of the more hydrophobic analogue predominated.

Antibacterial activity towards *Bacillus subtilis* was largely independent of the variable characteristics of the different analogues. This implies that the antibacterial activity could be more dependent on the conserved sequence (VOLfP) in these peptides, which coincides with the two repeating units in the analogous gramicidin S pentapeptide. In contrast, antifungal activity towards *Aspergillus fumigatus* was related to peptide structure and oligomerization. The increased antifungal activity of some of the cyclodecapeptides could also be dependent on the cell wall [1]. It was proposed that interaction with hexose moieties in the cell wall β-glucans and chitin [28] may disrupt higher order aggregates formed in an aqueous environment. Aggregation of the Trcs is proposed to decrease antimicrobial activity [24-27,29,30] and the hexose moieties could play a role in the binding and orientation of the peptide oligomers, which in turn could act as the seeding units for the active dimer structures [21,22] in the formation of pore/channels in the membrane.

The higher antifungal activity of TrcA and TrcB could be attributed to their optimal balance between hydrophobicity and target cell interaction which allowed for the increased formation of higher order pore structures in the cell membrane, after initial interaction with the carbohydrate moieties in cell wall. The lower antimicrobial activity of TpcA could be attributed to its hydrophobicity. Adopting a conformation similar to that proposed for TrcA

by Loll *et al.* [17], the steric bulk of Trp^7 may hinder optimal higher order structure formation and would account for decreased higher oligomers despite increased dimerization being observed. Alternatively, decreased antimicrobial activity may be attributed to tighter membrane binding of the indole group through hydrogen bonding to lipid carbonyl groups [27]. The TpcA peptide complex may be trapped in a conformation unable to optimally interact with other peptides to possibly form a pore/channel like structure and cause permeabilization of the cell membrane.

In order to simulate a scenario that is closer to the natural process we combined peptides that were naturally co-produced or co-produced at certain Phe/Trp ratios in the culture media. In general, an additive relationship was observed for co-produced peptides in the combinations tested. However, a slight antagonistic relationship was observed in combinations containing tryptocidines that was not beneficial to the producer organism, which is probably why TpcC is almost exclusively produced in Trp-rich media. Overt synergism was observed in combinations of TrcA:PhcA and TrcA:TrcB toward the fungal target, and TrcA:TrcB and TrcB:TrcC toward the bacterial target. This correlated with the observed characteristics of intermediate hydrophobicity and dimerization allowing for active structures which optimally interact with the fungal target cell structure. These peptide combinations formed proportions of dimeric peptides similar to those seen for the most active analogues TrcA and TrcB. Synergism observed in combinations of TrcA:PhcA toward *A. fumigatus* was possibly due to PhcA forming altered heterodimer structure together with reduced homodimers dimers which may differ in conformation.

The natural production profile of the producer organism containing increased TrcA, TrcB and TrcC (>40%) supports the synergistic activity observed, indicating an advantage in the natural production of these combinations. This study was the first to investigate the interaction and possible synergistic influence of peptide pairs from a complex of naturally produced cyclodecapeptides. Future work would entail the expansion of the library of analogues tested, as well as the range of target organisms, to allow for better correlation of activity to target cell structure.

8.2.5 Formulation of tyrothricin extracts and in vivo toxicity testing toward honey bees

The observed synergistic action found for the cyclodecapeptides produced in the natural, non-supplemented production profile supports its use in *in vivo* studies. The cyclodecapeptide mixture was obtained from culture extracts (Te) as described in Chapter 4. Due to the potential application in agricultural environments, the toxicity of Te was determined toward honey bees and their larvae as an indication of their possible influence on beneficial non-target insect species. Formulation of Te together with high purity commercial tyrocidine mixture (Tc) was evaluated in N,N-Dimethylformamide (DMF) and ethanol (EtOH), the solvents used in toxicity tests and agricultural applications respectively. The influence of glucose and sucrose, present in honey bee feeding solutions, on the aggregation and antimicrobial activity was investigated.

The size of the aggregates detected by dynamic light scattering for Te were consistently smaller than those observed for Tc, which was of high purity. The addition of sugars caused a reduction in the size of the aggregates formed by Tc in EtOH, and was particularly pronounced when dissolved in DMF. The sugars exerted a chaotropic effect on the aggregation of Tc, while a similar effect was induced by DMF on Te. The difference in aggregation was attributed to the co-extracted culture pigment in Te causing a similar disruption in aggregation. Moreover, the reduction in toxicity of Te, relative to that of Tc, toward insect cells may also allude to a role of the culture pigment. However, this aspect will be explored in future formulation of the cyclodecapeptides.

Decreased dimer populations were detected by ESMS when dissolved in EtOH. This most likely indicates a difference in conformation adopted by the cyclodecapeptides in the two solvent environments. This hypothesis was supported by the opposing influence of the two sugars, glucose and sucrose, on the antimicrobial activity of Te when dissolved in the two solvents. The addition of the sugars suppressed the antimicrobial activity of Te when dissolved in EtOH. This effect was largely relieved when dissolved in DMF, even increasing antimicrobial activity. These data supported observations of the chaotropic effect of glucose on higher order structure formation and a possible interaction with the cell wall components in fungal targets. It is highly likely that the interaction of the Trcs with glucose may depend on a balance of interaction with glucose moieties in the target structure and glucose in

solution. If too high a concentration of glucose is present in the environment, it may also result in reduced antimicrobial activity. The influence of different solvents and sugars on the Trcs is an aspect which warrants further investigation in future work.

No appreciable toxicity was observed for Te toward adult honey bees at the highest concentration we could dissolve in the 50% sucrose feeding solution after the six hours stipulated in the oral toxicity test guidelines [32]. Furthermore, there was a possible increase in survival of the Te treated adult bees in a semi-field trial environment, and potent *in vitro* activity of Te toward a broad array of pathogens causing foul brood in honey bee larvae [33,34]. Te formulations unfortunately did not show *in vivo* activity toward these bee pathogens in bee larvae curing assays, although it did significantly delay the onset of infection. It is therefore concluded that the tyrothricin peptides have a very low toxicity toward honey bees and would be extremely unlikely to cause an adverse effect toward them when applied within agricultural applications.

8.3 Last word

These cyclodecapeptides show potential for application in agriculture with appreciable high natural yields being attainable. They offer an alternate solution to conventional chemical agents to treat pathogens in the agricultural and food industries. Optimized formulation of these cyclodecapeptides would possibly enhance their potential. Due to their complex nature and production as a mixture of cyclodecapeptides, current knowledge regarding their mode(s) of antimicrobial action is limited. This is complicated further by changes in primary structure resulting in a wide range of different analogues with different properties. In order to harvest the potential of the peptides from tyrothricin, a concerted effort must be made in future investigations to gain knowledge on their mode of action, toxicity and behavior as mixtures.

8.4 References

1. Troskie, A. M. (2014) Tyrocidines, cyclic decapeptides produced by soil bacilli, as potent inhibitors of fungal pathogens. Stellenbosch University, Department of Biochemistry, Stellenbosch, South Africa. **PhD. Thesis**, http://hdl.handle.net/10019.1/86162
2. Rautenbach, M., Vlok, N. M., Stander, M. and Hoppe, H. C. (2007) Inhibition of malaria parasite blood stages by tyrocidines, membrane-active cyclic peptide antibiotics from *Bacillus brevis*. Biochim. Biophys. Acta. **1768**, 1488-1497

3. Leussa, A. N. and Rautenbach, M. (2014) Detailed SAR and PCA of the tyrocidines and analogues towards leucocin A-Sensitive and leucocin A-Resistant *Listeria monocytogenes*. Chem. Biol. Drug Des. **84**, 543-557

4. Spathelf, B. M. and Rautenbach, M. (2009) Anti-listerial activity and structure-activity relationships of the six major tyrocidines, cyclic decapeptides from *Bacillus aneurinolyticus*. Bioorg. Med. Chem. **17**, 5541-5548

5. Spathelf, B. M. (2010) Qualitative structure-activity relationships of the major tyrocidines, cyclic decapeptides from *Bacillus aneurinolyticus.* Stellenbosch University, Department of Biochemistry, Stellenbosch, South Africa. **PhD. Thesis**, http://hdl.handle.net/10019.1/4001

6. Leussa, N. A. (2014) Characterisation of small cyclic peptides with antilisterial and antimalarial activity. Stellenbosch University, Department of Biochemistry, Stellenbosch, South Africa. **PhD. Thesis**, http://hdl.handle.net/10019.1/86161

7. Troskie, A. M., de Beer, A., Vosloo, J. A., Jacobs, K. and Rautenbach, M. (2014) Inhibition of agronomically relevant fungal phytopathogens by tyrocidines, cyclic antimicrobial peptides isolated from *Bacillus aneurinolyticus*. Microbiology. **160**, 2089-20101

8. Troskie, A. M., Rautenbach, M., Delattin, N., Vosloo, J. A., Dathe, M., Cammue, B. P. and Thevissen, K. (2014) Synergistic activity of the tyrocidines, antimicrobial cyclodecapeptides from *Bacillus aneurinolyticus*, with amphotericin B and caspofungin against *Candida albicans* biofilms. Antimicrob. Agents Chemother. **58**, 3697-3707

9. Mach, B. and Slayman, C. W. (1966) Mode of action of tyrocidine on *Neurospora*. BBA-Gen. Subjects. **124**, 351-361

10. Kretschmar, M., Nichterlein, T., Nebe, C. T., Hof, H. and Burger, K. J. (1996) Fungicidal effect of tyrothricin on *Candida albicans*. Mycoses. **39**, 45-50

11. Gershenfeld, L. and Averbach, S. B. (1947) The effect of tyrothricin on fungi. Am. J. Pharm. Sci. Support. Public Health. **119**, 315-322

12. Eyeghe-Bickong, H. (2011) Role of surfactin from *Bacillus subtilis* in protection against antimicrobial peptides produced by *Bacillus* species. Stellenbosch University. **PhD. Thesis**, http://hdl.handle.net/10019.1/6773

13. Mootz, H. D. and Marahiel, M. A. (1997) The tyrocidine biosynthesis operon of *Bacillus brevis*: Complete nucleotide sequence and biochemical characterization of functional internal adenylation domains. J. Bacteriol. **179**, 6843

14. Dubos, R. J. and Hotchkiss, R. D. (1941) The production of bactericidal substances by aerobic sporulating bacilli. J. Exp. Med. **73**, 629-640

15. Dubos, R. J. (1939) Studies on a bactericidal agent extracted from a soil *Bacillus*: I. Preparation of the agent. Its activity *in vitro*. J. Exp. Med. **70**, 1-10

16. Lee, S. G., Littau, V. and Lipmann, F. (1975) The relation between sporulation and the induction of antibiotic synthesis and of amino acid uptake in *Bacillus brevis.* J. Cell Biol. **66**, 233-242

17. Marahiel, M. A., Nakano, M. M. and Zuber, P. (1993) Regulation of peptide antibiotic production in *Bacillus*. Mol. Microbiol. **7**, 631-636

18. Stokes, J. L. and Woodward, C. R. (1943) Formation of tyrothricin in submerged cultures of *Bacillus brevis*. J. Bacteriol. **46**, 83-88

19. Appleby, J., Knowles, E., Mcallister, R., Pearson, J. and White, T. (1947) The production of tyrothricin by submerged culture of *Bacillus brevis* in synthetic media. J. Gen. Microbiol. **1**, 145-157

20. Appleby, J., Knowles, E., Pearson, J. and White, T. (1947) A preliminary study of the formation, assay and stability of tyrothricin. J. Gen. Microbiol. **1**, 137-144

21. Munyuki, G., Jackson, G. E., Venter, G. A., Kövér, K. E., Szilágyi, L., Rautenbach, M., Spathelf, B. M., Bhattacharya, B. and van der Spoel, D. (2013) β-Sheet structures and dimer models of the two major tyrocidines, antimicrobial peptides from *Bacillus aneurinolyticus*. Biochemistry **52**, 7798-7806

22. Loll, P. J., Upton, E. C., Nahoum, V., Economou, N. J. and Cocklin, S. (2014) The high resolution structure of tyrocidine A reveals an amphipathic dimer. BBA-Biomembranes. **1838**, 1199-1207

23. Ruttenberg, M. A., King, T. P. and Craig, L. C. (1965) The use of the tyrocidines for the study of conformation and aggregation behaviour. J. Am. Chem. Soc. **87**, 4196-4198

24. Stern, A., Gibbons, W. A. and Craig, L. C. (1969) Effect of association on the nuclear magnetic resonance spectra of tyrocidine B. J. Am. Chem. Soc. **91**, 2794-2796

25. Ruttenberg, M. A., King, T. P. and Craig, L. C. (1966) The chemistry of tyrocidine. VII. Studies on association behaviour and implications regarding conformation. Biochemistry **5**, 2857-2864

26. Williams Jr, R. C., Yphantis, D. A. and Craig, L. C. (1972) Noncovalent association of tyrocidine B. Biochemistry **11**, 70-77

27. Paradies, H. H. (1979) Aggregation of tyrocidine in aqueous solutions. Biochem. Biophys. Res. Commun. **88**, 810-817

28. Bowman, S. M. and Free, S. J. (2006) The structure and synthesis of the fungal cell wall. Bioessays. **28**, 799-808.

29. Ruttenberg, M. A. and Mach, B. (1966) Studies on amino acid substitution in the biosynthesis of the antibiotic polypeptide tyrocidine. Biochemistry **5**, 2864-2869

30. Laiken, S., Printz, M. and Craig, L. (1971) Studies on the mode of self-assembly of tyrocidine B. Biochem. Biophys. Res. Commun. **43**, 595-600

31. Norman, K. E. and Nymeyer, H. (2006) Indole localization in lipid membranes revealed by molecular simulation. Biophys. J. **91**, 2046-2054

32. OECD. (1998) Test no. 213: Honeybees, acute oral toxicity test. Organisation for Economic Co-operation and Development

33. Beims, H., Wittmann, J., Bunk, B., Sproer, C., Rohde, C., Gunther, G., Rohde, M., von der Ohe, W. and Steinert, M. (2015) *Paenibacillus larvae*-directed bacteriophage HB10c2 and its application in American foulbrood-affected honey bee larvae. Appl. Environ. Microbiol. **81**, 5411-5419

34. Genersch, E. (2010) American foulbrood in honeybees and its causative agent, *Paenibacillus larvae*. J. Invertebr. Pathol. **103**, S10-S19